## *E. coli folate synthesis and C. elegans ageing: Investigating the effect of sulfamethoxazole on bacterial lawn morphology and metabolism*

GROOMBRIDGE, JAMES,LEE

# *E. coli* folate synthesis and *C. elegans* ageing: Investigating the effect of sulfamethoxazole on bacterial lawn morphology and metabolism

James L. Groombridge

## ABSTRACT

The gut microbiota is essential for host nutrition and may influence ageing. The nematode worm *C. elegans* provides a useful simplified model for investigating bacterial-host interactions. *E. coli* is used as a food source for *C. elegans*. Previous research has shown a decrease in *E. coli* folate synthesis results in extension of *C. elegans* lifespan. Potential detrimental effects of bacteria when producing normal amounts of folate are unlikely to be mediated by bacterial growth rate or direct effects of folate on the nematode. Potential toxicity of metabolic chemicals produced by wild type *E. coli* could explain the shorter lifespan of *C. elegans*. This thesis aims to understand the interaction between *E. coli* and *C. elegans* by investigating components that may be affected by folate synthesis and influencing lifespan.

Toxicity from bacterial formaldehyde synthesis was explored with a formaldehyde sensing lacZ reporter. A novel method was developed to quantify reporter output in a bacterial lawn. The lifespan of *C. elegans* maintained on *E. coli* constitutively expressing the formaldehyde detoxification enzymes FrmA/B was also investigated. Formaldehyde synthesis was not found to be a source of toxicity that accelerates *C. elegans* ageing. The effect of sulfamethoxazole on bacterial lawn growth, morphology and proliferation was examined and found to alter morphology, attenuate growth and impair proliferation compared to wild type and lifespan increasing mutant *E. coli*. A novel LC-MS/MS method was developed to analyse amino acids in agar. It revealed sulfamethoxazole alters bacterial amino acid metabolism associated with the serine-glycine pathway and growth. The absence of glycine in the media was also examined. It revealed changes to the exometabolome in both sulfamethoxazole treated and untreated conditions that may slow *C. elegans* ageing without altering bacterial growth.

This work developed novel methods for exploring the bacterial lawn and metabolism, providing insight into the mechanism of how sulfamethoxazole disruption of bacterial folate synthesis may influence *C. elegans* ageing.

# *E. COLI* FOLATE SYNTHESIS AND *C. ELEGANS* AGEING: INVESTIGATING THE EFFECT OF SULFAMETHOXAZOLE ON BACTERIAL LAWN MORPHOLOGY AND METABOLISM

James L. Groombridge

Submitted in accordance with the requirements for the degree of Doctor of Philosophy

Department of Biosciences
Durham University

March 2022

# CONTENTS

# LIST OF FIGURES

# LIST OF ABBREVIATIONS

| | |
|---|---|
| 1CM | one carbon metabolism |
| 1CU | one carbon units |
| ADC | 4-amino-4-deoxychorismate |
| ADH | alcohol dehydrogenase |
| AroD | 3-dehydroquinate dehydratase |
| BBB | blood brain barrier |
| BCAAs | branch chain amino acids |
| BCFAs | branch chain fatty acids |
| CA | chloramphenicol |
| CHO | carbohydrates |
| DDS | diaminodiphenyl sulfone |
| DHAP | dihydroxyacetone phosphate |
| DHF | dihydrofolate |
| DHFR | dihydrofolate reductase |
| DHNDP | 6-hydroxymethyl-7,8-dihydropterin diphosphate |
| DHP | dihydropteroate |
| DHPS | dihydropteroate synthase |
| DM | defined media |
| DM-kan | defined media supplemented with kanamycin |
| DNA | deoxyribonucleic acid |
| DR | dietary restriction |
| dTMP | thymidine monophosphate |
| FGSH | *S*-formylglutathione |
| GC-MS | gas chromatography mass spectrometry |
| GCV | glycine cleavage system |
| GFP | green fluorescent protein |
| GSH | glutathione |
| GSSG | glutathione disulphide |
| HC | homocysteine |
| HSF | heat shock factor |
| HSMGSH | *S*-hydroxymethyl-glutathione |

| | |
|---|---|
| IBD | inflammatory bowel syndrome |
| IGF-1 | insulin/insulin like growth factor |
| IIS | insulin/insulin like growth factor (IGF-1) signalling pathway |
| Kan | kanamycin |
| LB | Luria Bertani broth |
| LC-MS/MS | Ultra high performance liquid chromatography tandem mass spectrometry |
| LOD | limit of detection |
| LOQ | limit of quantification |
| LPS | lipopolysaccharide |
| Lrp | DNA-binding transcriptional dual regulator Lrp |
| MACs | microbial accessible carbohydrates |
| MG | methylglyoxal |
| mRNA | messenger ribonucleic acid |
| mTOR | Mammalian target of rapamycin |
| MTX | methotrexate |
| NGM | nematode growth media |
| NMR | nuclear magnetic resonance |
| $OD_{600}$ | optical density measured at 600 nm |
| PABA | para-aminobenzoic acid |
| PabA | aminodeoxychorismate synthase component 2 |
| PabB | aminodeoxychorismate synthase component 1 |
| PabC | aminodeoxychorismate lyase |
| PAU | peak area under the curve |
| PEP | phosphoenolpyruvate |
| RGB | Red Green Blue colour channels |
| RNAseq | ribonucleic acid sequencing |
| ROS | reactive oxygen species |
| RpoS | RNA polymerase sigma factor, RpoS |
| SAH | S-adenosylhomocysteine |
| SAM | S-adenosylmethionine |
| SCFAs | short chain fatty acids |
| SD | sulfadiazine |
| SHMT | serine-hydroxymethyltransferase |
| SKN-1 | *C. elegans* ortholog of mammalian Nrf proteins |

| | |
|---|---|
| SMX | sulfamethoxazole |
| Sub-Mic | a concentration that alters the biochemistry of the bacteria without effecting growth |
| TCA | tricarboxylic acid cycle |
| TEM | transmission electron microscopy |
| THF | tetrahydrofolate |
| TMP | trimethoprim |
| TOR | target of rapamycin |
| TORC1 | mechanistic target of rapamycin complex |
| UPLC | Ultra High Performance Liquid Chromatography |
| WTK | Kanamycin resistant strain of *E. coli* BW25113 |
| XGal | β-Galactose 5-bromo-4-chloro-3-indolyl-β-D-galactopyranoside |

# DECLARATION

I can confirm that the original research described in this thesis is my own work. In the event that work was carried out by others, appropriate credit has been given within this thesis.

The work in this thesis was supported by the Biotechnology and Biological Sciences Research Council (BBSRC).

# STATEMENT OF COPYRIGHT

# ACKNOWLEDGEMENTS

This PhD thesis would not have been possible without the help and support of so many people. First and foremost. I would like to thank my wife, Hannah. Without whom none of this would have been possible. You are my proverbial rock and the voice of reason that kept me focused on the end game. '#soulmates'. Thank you for being the best unofficial lab partner I could ask for, providing a sounding board for me to brain storm without complaint in the absence of an actual lab partner.

I do not have the words to express my gratitude for the friendship and support of David Tait and Gareth McCready. Thank you for allowing me to express my enthusiasm for all things research, nutrition and gut microbiota without complaint or mockery. Thank you for keeping me sane and motivated by providing morale in the form of belt fed wets, hoofing skran and some serious yomping. These were gems of joy amongst the pre-joy, long may they continue. NAMET 5:5 to a PhD...who knew?! Clearly not Pusser!

A massive thanks goes to my parents David and Vicki Prouse for providing endless support to Hannah and I through all my escapades. Thank you for providing the perfect writing retreat at short notice complete with emergency child care. Thank you to my sisters Erica, Lindsey and niece Evie, and my in-laws Sue and David Cranwell for taking care of Ben and Alice enabling me to write this thesis. To my Geordie family the Tait-Ray clan thank you for keeping me fed, watered and treating me like one of your own throughout my educational adventure. Thank you to Adam and Sarah Walsh for your love of science, discussion, barbeque and keeping Hannah sane.

I would like to offer my sincerest thanks to Rachael Dack. I am forever in your debt for all the endless support and help you have given me during my research. Your guidance and perseverance on developing the LC-MS/MS work was invaluable. Thank you for the added help with supporting me through the last few months, I couldn't have done it without you! Thank you to Sushmita Maitra for taking the time to teach me all the things in the lab I really needed to know and how to do them properly. I thoroughly enjoyed your 'master classes' in science. Thank you to Giulia Zavagno for the discussions and help with this work, I've really appreciated it! A huge thanks to Fraser, Karen, Oli and the

Biosciences technicians' team. You well and truly looked after me. You are the unsung heroes of science! Thank you to Joanne Robson and Christine Richardson for taking the time to answer all my questions and teach me about microscopy. Thank you to Adam Benham for your help and guidance over the last few months. Thank you to the BBSRC for providing the funding for my PhD. Thank you to David Weinkove and Durham University for giving me the opportunity to undertake my PhD.

Finally, I thank you the reader for taking the time to read this thesis. I hope you discover something new and are as awed at the amazing complexity of gut bacteria as I am.

This thesis is dedicated to my children Gracie, Ben and Alice. Set the bar high and do not fear the unknown. Comfort is an illusion, embrace challenges with determination, tenacity and a robust sense of humour. It will always propel you forwards.

This thesis is also dedicated to my Grandfather Bernard Hinc, Dad, David Prouse and my uncles Francis Hinc and Gordon Smith for teaching me to embrace hard work and that if a jobs worth doing it should be done properly.

# CHAPTER 1

# INTRODUCTION

## 1.1 Overview

The inevitability of ageing is inescapable with nearly all organisms undergoing some form of age-related physiological decline as they get older such as a loss of fertility, physical decrepitude and the vitality of youth. Accompanying these physical changes is the increased risk of age-related diseases such as cancer, cardiovascular disease, respiratory disease, diabetes and neurological dysfunction that not only hasten the advance of death but, contribute to a significantly reduced quality of life whilst creating a greater social burden in later years (Weinkove & Goljanek-Whysall, 2017). This is more poignant now than ever as rising population growth is coupled with increasing levels of chronic illness and a decline in wellbeing, paving the way for major challenges for public health globally (Naja, Makhlouf, & Chehab, 2017).

Whilst ageing research has progressed considerably in the 21$^{st}$ century to unravel the mysteries of not only how we age but why we age, it has still not been able to attribute a single specific cause that can be manipulated or controlled to slow or even stop ageing. What is clear though is the intrinsic link between the gut microbiota and the host and how ageing, diet and lifestyle influence that relationship to potentially drive dysbiosis and shift the balance away from healthy ageing (Popkes & Valenzano, 2020; Salazar et al., 2020). Advances in technology such as high throughput sequencing have allowed researchers to understand the dynamics of the microbiota and how population shifts within the gut alter with age. Unfortunately, due to high inter-individual diversity, there is still no clear definition of an 'elderly' microbiota to clearly show cause and effect in ageing (Nagpal et al., 2018; Salazar et al., 2020).

A leap forward in ageing research is the discovery of small molecule and dietary interventions that slow ageing and increase lifespan in animal models (Kennedy, 2018) including calorie restriction, metformin, sulfonamides and amino acid intake (Cabreiro et al., 2013; Catterson et al., 2018; Clark & Walker, 2018; Edwards et al., 2015; Hackmann, 1958; Y. J. Liu et al., 2019; Virk et al., 2012). Of particular interest was the revelation by

our lab that the inhibition of bacterial folate synthesis was able to slow ageing and increase the lifespan of the nematode worm *C. elegans*. A chance discovery found the *E. coli aroD* (3-dehydroquinate dehydratase) mutant was able to prolong *C. elegans* lifespan (Virk et al., 2012). The *aroD* gene encodes for an enzyme that catalyses the synthesis of chorismate a key substrate and precursor required for the synthesis of folates. This discovery was closely followed by the finding that other folate synthesis enzyme mutants were also able to confer a lifespan-extending effect (Virk et al., 2016). It was also established that the sulfonamide sulfamethoxazole that inhibits a key enzyme in the folate synthesis pathway reducing bacterial folate synthesis also caused the worms to have a significantly increased lifespan (Virk et al., 2012). The effect was found to be independent of folate availability but dependent on reduced bacterial folate synthesis although, they were not able to determine the mechanism or attribute a specific pathway for this effect (Maynard, 2017; Virk et al., 2012; Virk et al., 2016).

An important animal model in ageing research *C. elegans* is an ideal tool for investigating bacterial interactions with the host concerning health span and lifespan whereby the growth media, worm and bacteria are specifically and easily manipulated to control variables to create a model of the gut microbiota/host system. Like vertebrates, worms are unable to synthesise folates therefore, are dependent on the uptake of exogenous glutamated folates from the bacteria in their diet in the form of reduced tetrahydrofolates as co-factors to enzymes involved in one-carbon metabolism (Maynard, 2017; Virk et al., 2016). Although C. elegans and many of these models share genetic homology with higher organisms and have proven to be a considerable asset to ageing research we still do not fully understand this mechanism of ageing to the extent that we can directly translate them to humans.

This thesis aims to improve our knowledge of the mechanisms behind why reduced bacterial folate synthesis increases lifespan by focusing on the bacteria in the *C. elegans* system. Deciphering the molecular interactions between the bacteria and *C. elegans* will provide a better understanding of the gut microbiota-host relationship in higher organisms and may signpost a pathway that can be expanded upon and exploited to formulate a method to slow ageing and improve long term health in humans.

## Part 1: Using *Caenorhabditis elegans* as a model organism

1.2.1 *C. elegans*; an animal model to study ageing

Since its introduction as an animal model in 1963 by Sydney Brenner *Caenorhabditis elegans* has proven to be an excellent tool for investigating complex biological questions in a simplified system (Goldstein, 2016). *C. elegans* is a nematode worm commonly found residing in rotting vegetation and fruit (Félix & Braendle, 2010; Félix & Duveau, 2012). It is predominantly a self fertilizing hermaphrodite able to produce a large brood size of over 300 eggs within a small reproductive window (Brenner, 1974) and has a temperature dependent short lifespan and maturation time (Klass, 1977). At 25°C it develops from egg to adult in 3 days and lays up to 300 eggs in the next 3 days (figure 1.1) providing a large population of genetically uniform animals in a relatively short time. They do not require expensive and complicated methods for use and maintenance and can be maintained on easily prepared Nematode Growth Media (NGM) or defined media (DM) seeded with monoxenic bacterial lawns in Petri dishes.

There is a wide variety of bacterial strains that will sustain *C. elegans* but commonly the *E. coli* K12 strains or the B-strain OP50 are used as a nutritional source (Brenner, 1974; Goldstein, 2016; Maynard, 2017). It has a transparent cuticle allowing for easy observation of the internal organs and the fully sequenced and annotated genome provides excellent genetic tractability (Cabreiro & Gems, 2013; Kaletta & Hengartner, 2006; Yilmaz & Walhout, 2014). A key element that makes *C. elegans* a useful tool for research is its shared genetic homology of around two thirds with human genes and like humans, they have considerable variation in ageing (Kirkwood, 2005; Kirkwood & Finch, 2002) suffering the same age related progressive decline in physiological function including infertility, movement (frailty), muscle wasting (sarcopenia) and loss of integrity of the gut (Kirkwood, 2005; Klass, 1977; Son, Altintas, Kim, Kwon, & Lee, 2019; Tissenbaum, 2012).

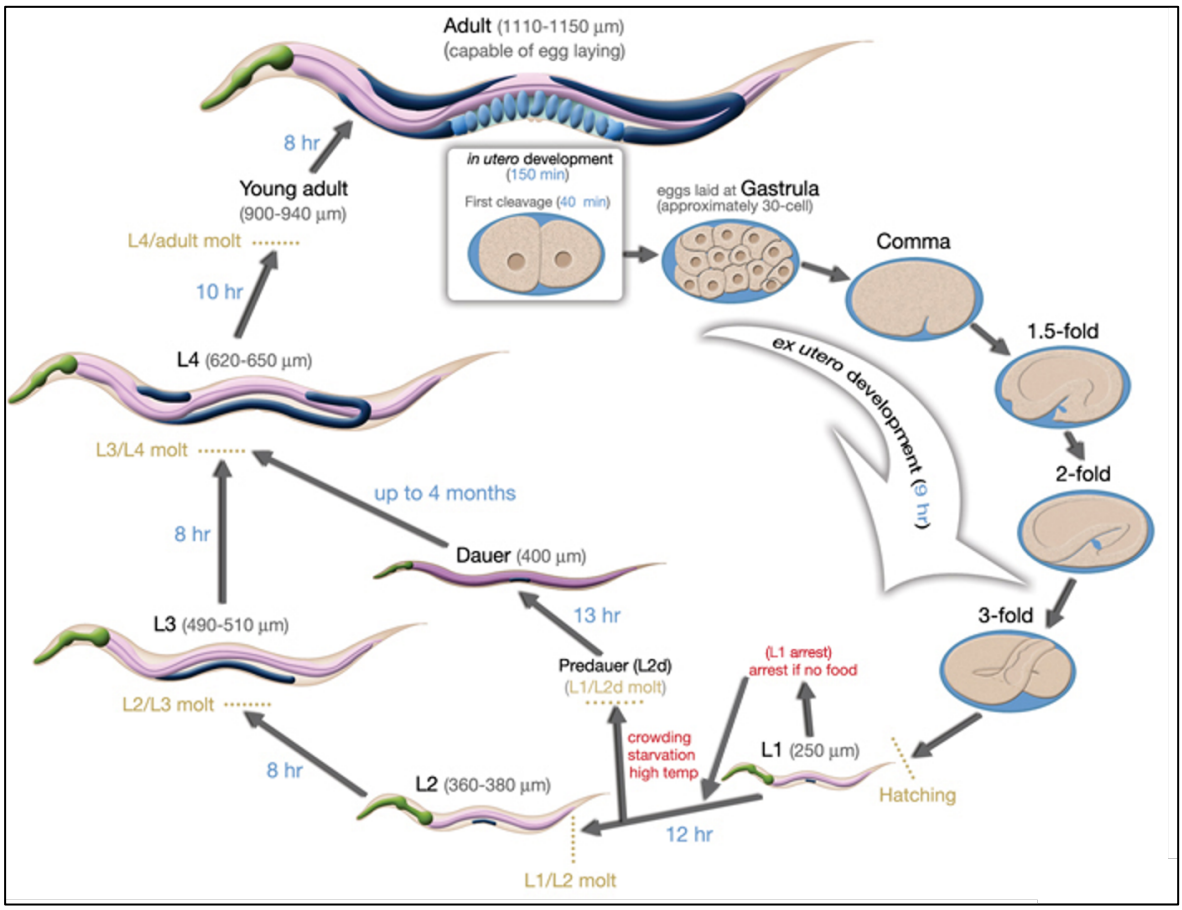


**Figure 1.1 The lifecycle of the nematode worm *Caenorhabditis elegans* at 25 °C.** At 25 °C the complete lifecycle can take around 3 days. Starting from a fertilized egg *C. elegans* develops over about 46 hours through the four larval stages of L1-L4 to become a young adult. After a further 8 hours they mature into a gravid (egg-laying) adult (hermaphrodites only). During periods of overcrowding, starvation or high temperatures the worms can enter a developmental arrest stage known as dauer formation for up to 4 months. This can occur as early in the life cycle as the L1 larval stage. When the adverse conditions are removed the worms can re-enter the L4 stage and continue with development (Maynard, 2017). Image adapted from Worm Atlas (Herndon, 2012b).

Because of its ease, simplicity and homology to humans *C. elegans* have a long history in ageing research and uncovering the molecular mechanism behind how we get old and if that can be manipulated. In 1983 the long lived *C. elegans* mutant *age-1* was identified. It was one of the first genes found that were linked to longevity pathways responsible for extending lifespan (Friedman & Johnson, 1988; Klass, 1983). It was discovered in 1993 that the *daf-2* mutant increased lifespan and is modulated by the nutrient-sensing insulin/insulin-like growth factor (IGF-1) signalling (IIS) pathway and is dependent on *daf-16* (C. Kenyon, Chang, Gensch, Rudner, & Tabtiang, 1993; Wolkow, Kimura, Lee, & Ruvkun, 2000). Together *daf-2*, *daf-16* and *age-1* form the essential components of the IIS

pathway and were the first proposed regulatory pathway of ageing that when inhibited increases stress resistance extending lifespan (Uno & Nishida, 2016). Building on this knowledge additional *daf-16* dependent pathways was found that is required to modulate ageing including, the xenobiotic response factor SKN-1 (*C. elegans* ortholog of mammalian Nrf proteins) (Blackwell, Steinbaugh, Hourihan, Ewald, & Isik, 2015), the energy and nutrient sensing AMP kinase pathway, heat shock transcription factor (HSF-1) and overexpression of the *sir-2.1* gene (C. J. Kenyon, 2010; Tissenbaum, 2012).

Intersecting the IGF-1 pathway the *C. elegans* mutant rict-1 was found to be long-lived when maintained on nutrient-rich food, *rict-1* is a component of the target of rapamycin (TOR) pathway (Soukas, Kane, Carr, Melo, & Ruvkun, 2009) which is critical to the dietary restriction (DR) mode of lifespan extension. TOR is an important nutrient and amino acid sensor (Lapierre & Hansen, 2012) and an integration centre for the regulation of growth that when inhibited extends lifespan in *C. elegans* independently of *daf-16* (Kapahi et al., 2010; C. J. Kenyon, 2010). Together these mutations and pathways modulate stress responses and nutrient sensors to adapt host physiology. The adaptation promotes longevity whilst affording protection at a cellular level.

These pathways are conserved in higher organisms from *Drosophila* to mice and humans (Blüher, Kahn, & Kahn, 2003; Clancy et al., 2001; Kapahi et al., 2004). The TOR pathway is a homolog of the mechanistic target of rapamycin complex (mTORC) in humans (Kapahi et al., 2010). Inhibition of the TOR pathway by rapamycin in mice has been shown to increase lifespan (Wilkinson et al., 2012) and polymorphisms that impaired IGF-1, variants of FOXO3A (an ortholog of daf-16) and AKT have frequently been linked to longevity in human cohorts globally (Bae et al., 2018; C. J. Kenyon, 2010; L. Sun et al., 2015; X. Sun, Chen, & Wang, 2017). Together this demonstrates the value and relevance of *C. elegans* as an excellent tool for uncovering the mysteries behind ageing in humans.

### 1.2.2 The simplified host gut-microbe model

We use *C. elegans* and *E. coli* as a simplified model to investigate gut microbiota-host interactions. In our model, the worms and bacteria are specifically and easily manipulated to control variables. We use the temperature sensitive *glp-4 (SS104) C. elegans* strain that is sterile when incubated at 25 °C allowing for reproductive control without the need for unnecessary handling or pharmacological intervention. The volume of eggs laid and the

presence of larval stage *C. elegans* are extremely difficult to separate from L4 and adult worms. Prevention of the presence of eggs and offspring in the bacterial lawn and agar prevents cross contamination when transferred between plates that can confound results within synchronised populations.

The bacteria in our model are a kanamycin resistant strain of the Keio collection parent strain BW25113 *E. coli* (WTK). The Keio collection mutants have a kanamycin resistance insert at the site of the single gene knockout allowing for easy investigation of genetic and metabolic pathways with appropriate control for comparison. Our defined media (DM) was previously developed to have precisely defined concentrations of amino acids and trace metals, be folate free and support normal *C. elegans* and *E. coli* growth whilst controlling for components that may modulate bacterial folate synthesis (Helliwell, 2013; Maynard, 2017).

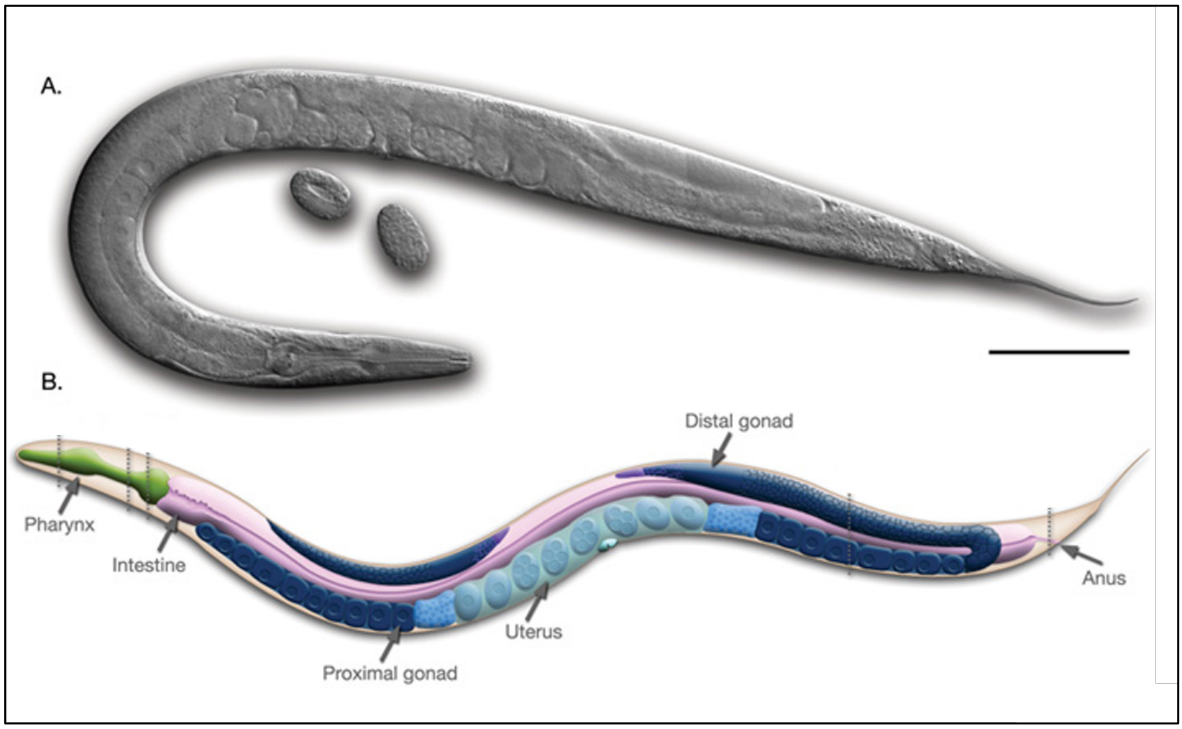


**Figure 1.2 Adult *C. elegans* hermaphrodite anatomy. A.** Differential interface contrast image of an adult hermaphrodite with eggs, the scale bar = 0.1 mm. **B**. A diagram of the worm's anatomical structures viewed laterally. Image adapted from Worm Atlas (Herndon, 2012a)

*C. elegans* is an ethical, simplified, controllable and malleable tool for investigating gut microbiota-host interactions (Backes, Martinez-Martinez, & Cabreiro, 2021). Like humans, *C. elegans* has an intestinal tube that runs from its mouth or pharynx to its anus

(figure 1.2). The pharynx that forms the oral cavity grinds and pumps ingested bacteria into the intestine, as the animal ages there is a deterioration in the pharyngeal ability to effectively function and viable intact bacteria can pass through the pharynx to the distal gut. The worm gut is formed from a non renewable epithelial monolayer with a brush border of microvilli facing into the central lumen (Brenner, 1974; McGee et al., 2011; Troemel, Félix, Whiteman, Barrière, & Ausubel, 2008) and functions in much the same way as humans providing an interface with the outside world to extract, absorb and store nutrients, excrete waste and presents the front line of defence against pathogens and environmental risk factors (Rera, Azizi, & Walker, 2013).

The worms are maintained on enterobacterial *E. coli* strains that have been adapted for use as a food source for *C. elegans* and lack pathogenicity components and the ability to colonise the *C. elegans* gut. As a product of age related impaired pharyngeal grinding bacteria are found to aggregate and colonise the worm digestive tract (Browning et al., 2013) allowing the luminal part of the gut to become populated by a bacterial population (Félix & Duveau, 2012; Garigan et al., 2002; McGee et al., 2011; Portal-Celhay, Bradley, & Blaser, 2012). It has been proposed that in the wild *C. elegans* harbours a commensal microbiota (Berg et al., 2016; Dirksen et al., 2016; Samuel, Rowedder, Braendle, Félix, & Ruvkun, 2016). Bacterial accumulation of the gut as a product of age related dysfunction does not directly constitute a synergistic gut microbiota as seen in humans and other organisms (Yilmaz & Walhout, 2014). Maintenance on a bacterial lawn provides a direct source of micro and macro nutrients made available by bacterial metabolism and specific bacterial metabolites that can modulate ageing in *C. elegans* (Cabreiro & Gems, 2013; Han et al., 2017; Hartsough et al., 2020; Pryor et al., 2019; Shin et al., 2020; Virk et al., 2016).

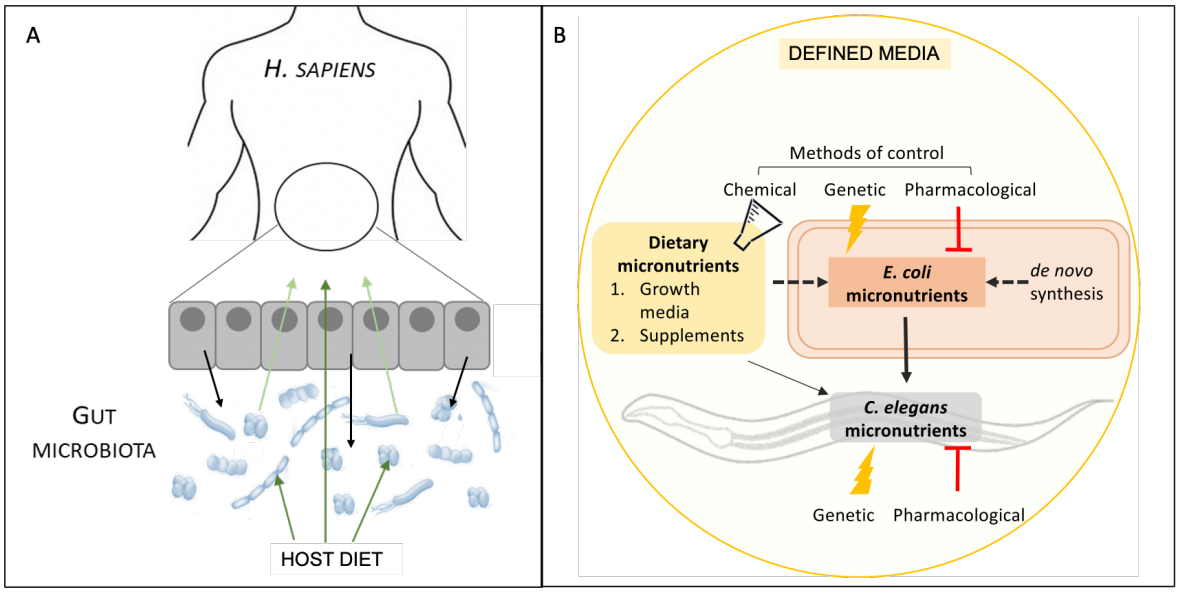


**Figure 1.3 A diagrammatic model of the *C. elegans* gut microbiota-host system. A.** The human microbiota is dependent on nutrients from the host and metabolises them synthesising secondary nutrients. The host obtains important nutrients for development and health that they could not obtain through normal digestive mechanisms or synthesise endogenously. Changes in the host environment, lifestyle and diet can positively or negatively alter the microbiota and its metabolite output. **B.** in our gut-host model the bacterial monoculture is dependent on DM for nutrition to support growth and proliferation. The bacterial monoculture provides the primary source of nutrition for *C. elegans* that is also dependent on bacterial metabolism for essential nutrients for health and development. The media-bacteria-worm association means that nutrient component alteration or pharmacological intervention to the DM and genetic manipulation of the bacteria or worms can be measured to quantify direct and indirect effects. Image adapted from (Maynard, 2017; Maynard & Weinkove, 2020).

Our model (figure 1.3) capitalises on the functional and physiological similarities between the worm and the human gut. Additionally, the presence of a pseudo-commensal bacterial population exposes *C. elegans* to direct contact with the bacteria and secreted metabolites throughout their lifetime (Maynard, 2017). This model provides a simple yet highly controllable and easily manipulated system to investigate the direct and indirect elements of the gut-microbe-host interaction (Maynard, 2017; Virk, 2013; Virk et al., 2012).

### 1.2.3 The Gut microbiota and metabolites

The gastrointestinal system of mammals and humans is the habitat of a bacterial ecosystem known collectively as the gut microbiota. This complex and diverse collection is made up of an estimated 1000 species of microorganisms from the Eukarya, Bacteria and Archea

domains (Donaldson, Lee, & Mazmanian, 2016) that number around 1:3 bacterial cells for every human cell and a collective genome (microbiome) 100 times greater than the human genome (Gilbert et al., 2018; Sender, Fuchs, & Milo, 2016; Turnbaugh et al., 2007). The population is developed and influenced by exposure to environmental, nutritional, lifestyle, diurnal, gender, lifestyle and physiological factors that begins at birth and is characterised by distinct shifts in composition and function over the lifetime of the host (Alvarez, Glotfelty, Blank, Dohnalová, & Thaiss, 2020; Kundu, Blacher, Elinav, & Pettersson, 2017).

The study of the gut microbiota has been ongoing for over 40 years with more than 15,000 papers published, of which 80 % have been within the last 7 years and represent a significant shift in the understanding of the microbiota-host relationship and how manipulation of the microbiota can modulate health and lifespan (Cani, 2018; Di Lorenzo, De Castro, Silipo, & Molinaro, 2019). This extensive body of knowledge has shown there is a mutually beneficial relationship exists between the host and the gut microbiota. The host provides an optimal environment for the bacteria to thrive in relative safety and a food source through the ready supply of carbohydrates that have escaped digestion, dietary fibre, intestinal mucus and protein from the host diet and microbes provide the commensal bacteria with a ready supply of nutrients (Jandhyala et al., 2015; Krautkramer, Fan, & Bäckhed, 2021; Thursby & Juge, 2017).

In return, the enteric bacteria interacts primarily with the host at the single epithelial layer of the mucosa (O'Hara & Shanahan, 2006) to influence physiological development, immune system optimisation, improve intestinal integrity and optimise gut function, defend from pathogens and support mucosal immunity. (Blander, Longman, Iliev, Sonnenberg, & Artis, 2017; Blaser & Dominguez-Bello, 2016; Round & Mazmanian, 2009; Sommer & Bäckhed, 2013; Thursby & Juge, 2017).

The gut microbiota also liberates previously unobtainable calories and nutrients. It synthesises a diverse array of nutrients and bioactive compounds that not only exert physiological change at a cellular level but, enter into host metabolism to promote health and development (Riccio & Rossano, 2020; Wu & Wang, 2019) where they are measurable and can be found at systemic levels higher than pharmaceutical agents (Cryan et al., 2019; Krautkramer et al., 2021).

The composition of the gut microbiota changes throughout life with considerable interindividual diversity across all age groups. There is still little understanding of what causes and regulates these variabilities over time within individuals and how that affects health and the prevention of disease (Gilbert et al., 2018). In infancy, the human gut microbiota is labile and dynamically adaptable to dietary input allowing for high variability in the microbial population.

The diversity of the gut microbiota increases with age. Interindividual variability is determined by environmental and genetic influences along with intestinal physiology, lifestyle and diet (Rinninella et al., 2019). Together they contribute to the development of a stable microbiota dominated by Firmicutes, Actinobacteria and Bacteroidetes (Rinninella et al., 2019). By the age of 3 years, the microbiota resembles an adult with only subtle shifts in composition. Followed by a period of relative stability at the age of 40 years (DeJong, Surette, & Bowdish, 2020). Beyond middle age, the uniqueness of microbial composition increases among healthy individuals (figure 1.4) (Wilmanski et al., 2021). The increasing uniqueness and a decline in core Bacteroides have been correlated with healthy ageing and longevity (Wilmanski et al., 2021). Conversely, a lack of uniqueness and retention of core taxa at high levels are associated with poor health and morbidity in the elderly (Wilmanski et al., 2021).

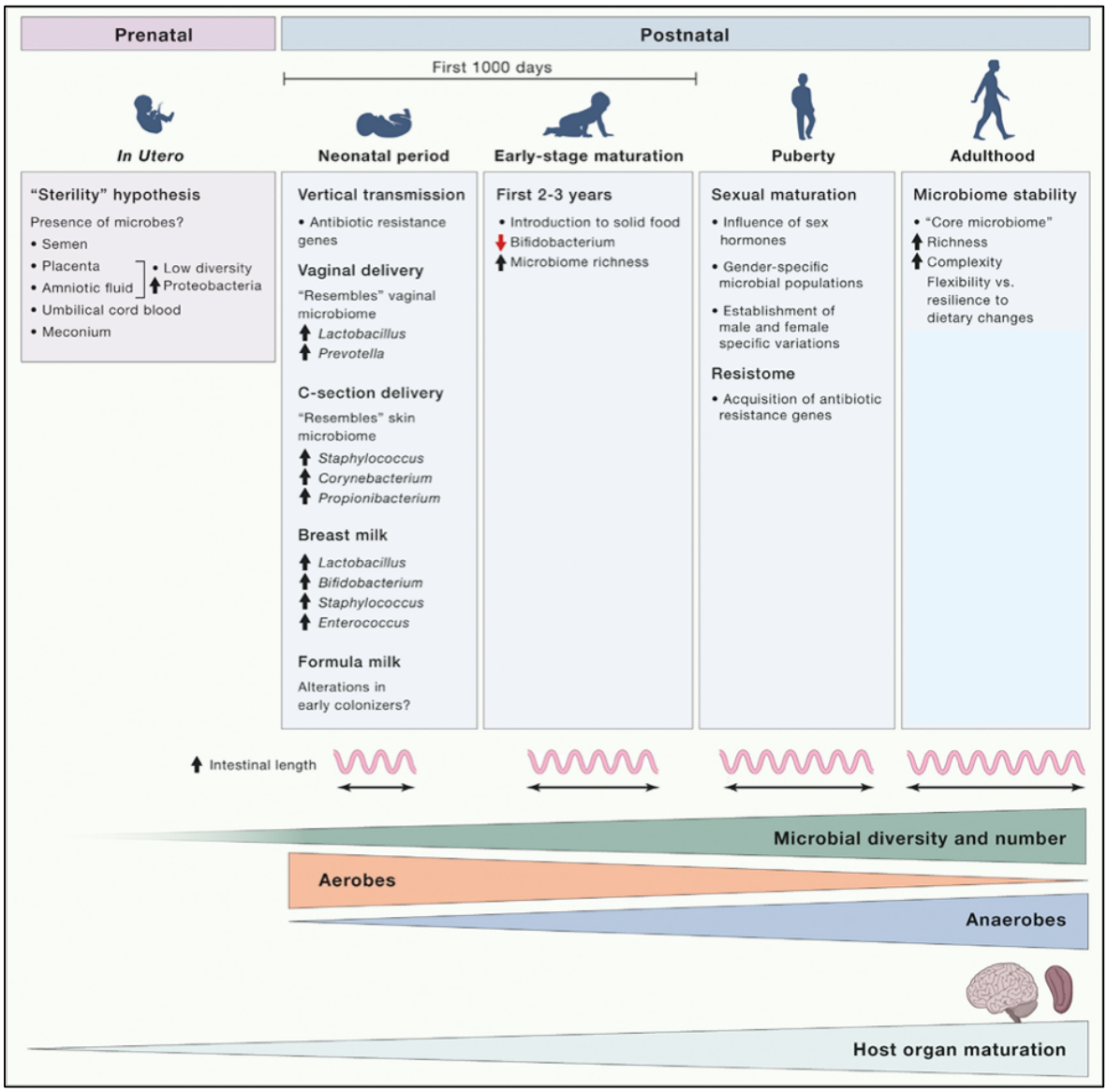


**Figure 1.4 Changes in the gut microbiota from infancy to adulthood.** Gut microbial composition alters with age and physiological development. As the host develops new niches for microbial growth and diversity are created, in adulthood the complexity and richness of the microbiota reach a plateau with the development of a core microbiome that offers resilience and flexibility to the host from intrinsic and extrinsic challenges. Adapted from (Kundu et al., 2017)

Attempts have been made to define a 'healthy' gut microbiota through the use of richness, diversity and metabolites as markers of gut health but this has proved challenging due to the vast diversity amongst healthy individuals and plasticity of the microbial population (Gentile Weir 2018). A key characteristic that has been presented as a measure of a healthy microbiota is when faced with perturbations to the microbial community through physiological, dietary and lifestyle changes the microbiota composition retains stability promoting resilience and infection resistance (Brito, 2021).

### 1.2.4 Microbial changes in ageing

A product of ageing is the decline of physiological function including loss of intestinal motility and degeneration of the mucosal barrier (Soenen, Rayner, Jones, & Horowitz, 2016). Human studies have shown changes to gastrointestinal function alter the availability of nutrients to the microbiota that in turn affects microbial composition and function (An et al., 2018). Gut function alterations influence microbiota associated enteric nervous system changes as part of the gut-brain axis, creating a characteristic low grade inflammatory state in the digestive tract (Mangiola, Nicoletti, Gasbarrini, & Ponziani, 2018). A unique and diverse bacterial population through compositional drift and depletion of core taxa, specifically Bacteroides is associated with healthy ageing in humans (Wilmanski et al., 2021). Modulation of the inflammatory state by anti-inflammatory metabolite producing bacteria as a product of the diverse microbiota may contribute to longevity and healthy ageing in humans (Wilmanski et al., 2021). Alternatively, retention of core taxa and a lack of diversity may be a driver of age related disease and dysbiosis. The lack of diversity may alter the bacterial metabolome to one that is detrimental to the host leading to negative health and ageing implications (P. E. Larsen & Dai, 2015; Soto et al., 2018; Wilmes et al., 2021)

### 1.2.5 Bacterial metabolites that influence host health and disease in higher organisms

There is a diverse, expanding repertoire of nutrients and bioactive compounds shown to, directly and indirectly, influence host health, both positively and negatively (Qi Yang et al., 2020). The gut bacteria can synthesise or liberate these metabolites by having the necessary enzymatic capabilities to exploit host dietary components that escape digestion (Mills, Stanton, Lane, Smith, & Ross, 2019).

A key source is undigested carbohydrates (CHO) encapsulated by the broad brush term dietary fibre, it predominantly consists of resistant starches, polysaccharides and oligosaccharides that transit the intestine to the distal gut providing a nutrient source for colonic bacteria (Barber, Kabisch, Pfeiffer, & Weickert, 2020). A small proportion of dietary and host protein approximating between 5 g and 12 g a day is hydrolysed by host and microbial endopeptidases and proteases to their constituent amino acids (J. Cummings & Macfarlane, 1991; E. A. Smith & G. Macfarlane, 1997).

The colonic mucosal barrier also provides an additional CHO source to bacteria. It is an inner layer that is impermeable and encapsulates the luminal epithelial wall. A viscous outer layer provides a habitat and nutrient source to commensal bacteria from the degradation of mucin enriched glycoproteins (Bhattacharya, Ghosh, & Mande, 2015; Desai et al., 2016; El Kaoutari, Armougom, Gordon, Raoult, & Henrissat, 2013; Johansson, Sjövall, & Hansson, 2013). These sources provide substrates for bacterial fermentation that yield signalling and bioactive metabolites, an array of short chain fatty acids (SCFAs). Branched chain fatty acids (BCFAs), phenols, indolic compounds, $NH_3$, sulphides and N-nitroso compounds (Kobayashi, 2018; Krautkramer et al., 2021; E. A. Smith & G. Macfarlane, 1997; Windey, De Preter, & Verbeke, 2012). A recent publication by Krautkramer et al. (2021) provides an excellent review of the current wider body of microbial metabolites and their effects on mammalian physiology. Here an overview of gut microbial metabolites known to influence host health and ageing is provided, the list is by no means exhaustive. To maintain relevance and context to this body of work this review is limited to microbial metabolites that exert a direct effect on the health or lifespan of humans, rodents and *C. elegans*.

### 1.2.6 Short Chain Fatty Acids

SCFAs are synthesised by multiple fermentation pathways of carbohydrates and protein are described in detail in figure 1.5. The most abundant in humans and mice are acetate, butyrate and propionate which comprise ≥ 95 % of the total pool synthesised by colonic bacteria in a molar ratio of 60:20:20 (Den Besten et al., 2013). They are produced by a diverse array of enteric bacteria and are a key component in the bacteria-host relationship. They have been shown to influence a wide array of immune and physiological functions and influence metabolic and neurological health and disease (Krautkramer et al., 2021).

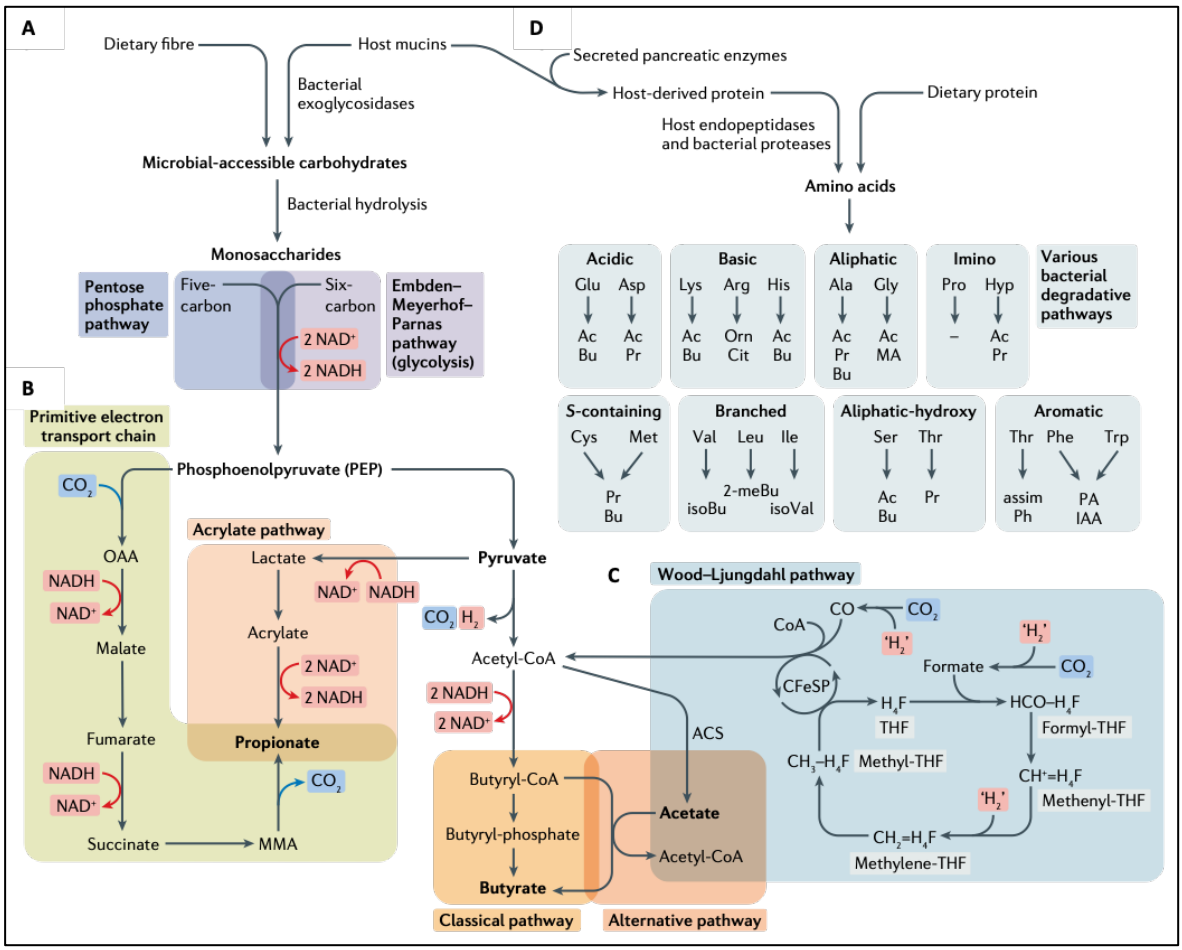


**Figure 1.5 Sources and fermentation pathways of microbially derived short chain fatty acids**. **A.** Undigested macronutrients from the host diet and the gut epithelial mucus layer provide microbial accessible carbohydrates for bacterial fermentation into short chain fatty acids. **B.** Butyrate and propionate synthesis pathways. **C.** Acetate synthesis pathways. **D.** Sources of amino acids. PEP, phosphoenolpyruvate; DHAP, dihydroxyacetone phosphate; CFeSP, corrinoid iron-sulphur protein; CoFeSO, iron-sulphur protein; MMA, methylmalonate; OAA, oxaloacetate; THF, tetrahydrofolate; Ac, acetate; Pr, propionate; Bu, butyrate; Orn, ornithine; Cit, citrulline; MA, methylamine; isoBu, isobutyrate; 2-meBu, 2-methylbutyrate; isoVal, isovalerate. . Image has been adapted from (Krautkramer et al., 2021)

Synthesis of butyrate (figure 1.5 B) occurs through the phosphotransbutyrylase/butyrate kinase pathway. It begins with pyruvate-derived acetyl-CoA providing two moieties to yield acetoacetyl-CoA followed by conversion to the intermediates β-hydroxybutyryl-CoA, crotonyl-CoA and butyryl-CoA (Pryde, Duncan, Hold, Stewart, & Flint, 2002). Butyryl-CoA is phosphorylated to butyryl-phosphate which via the action of a butyrate kinase forms butyrate (Pryde et al., 2002). Butyrate can also be synthesised via the butyryl-CoA:acetate CoA transferase pathway that sequesters exogenous acetate and

through the action of a butyryl-CoA/acetate-CoA transferase converts butyryl-CoA to butyrate and acetate to acetyl-CoA (Bai & Mansell, 2020; Diez-Gonzalez, Bond, Jennings, & Russell, 1999).

Propionate can be formed via three pathways (figure 1.5 B), two of which originate with phosphoenolpyruvate (PEP) that is converted to pyruvate and then either lactate for the acrylate pathway or oxaloacetate for the succinate pathway. The acrylate pathway begins with the reduction of lactate to lactoyl-CoA followed by dehydration to acryloyl-CoA which is reduced to propionyl-CoA and converted to propionate and acetyl-CoA (Hetzel et al., 2003; Kandasamy et al., 2013). The succinate pathway starts with the conversion of oxaloacetate to malate and then fumarate which is reduced to succinate. Succinate is reduced to succinyl-CoA before conversion to thioesters of methylmalonyl-CoA and oxidation to propionyl-CoA and finally propionate (Louis & Flint, 2017). The third route for propionate synthesis is the propanediol pathway that is downstream of deoxyhexose sugars fucose and rhamnose catabolism producing dihydroxyacetone phosphate (DHAP) and L-lactaldehyde. These can be sequestered for PEP synthesis or enter into the propanediol pathway by conversion to propane-1,2-diol then propionaldehyde which yields propanol and propionyl-CoA that is finally converted to propionate (Louis & Flint, 2017; Scott, Martin, Campbell, Mayer, & Flint, 2006).

Acetate is synthesised from acetyl-CoA from pyruvate through two one carbon metabolism (1CM) dependent pathways (figure 1.5 C). The Wood-Ljungdall pathway where $CO_2$ is reduced to formate and a methyl group added. Multiple steps form methyl-tetrahydrofolate that donates a methyl group via the cobalt and iron containing corrinoid iron-sulphur protein (CoFeSO) to yield acetyl-CoA (Svetlitchnaia, Svetlitchnyi, Meyer, & Dobbek, 2006). Or, by the carbon monoxide pathway where $CO_2$ is reduced to CO and combined with a methyl group yielding acetyl-CoA (Ragsdale & Pierce, 2008). Acetyl-CoA is further hydrolysed to form acetate for use in central metabolic pathways (Wolfe, 2005).

Dietary proteins, pancreatic enzymes and liberated host mucins provide amino acids for fermentation and dissimilatory amino acid catabolism into numerous metabolites and SCFAs including acetate, propionate, butyrate, ornithine, citrulline, methylamine, isobutyrate, 2-methylbutyrate and isovalerate (Krautkramer et al., 2021).

Of the three core SCFAs, acetate is the most abundant in the systemic circulation. The majority of acetate is taken up by the liver and utilised as an energy source and substrate for long-chain fatty acid, cholesterol, glutamine and glutamate synthesis. It is also metabolised in the heart, kidneys and adipose tissues and can cross the blood-brain barrier to influence satiety (Den Besten et al., 2013). Butyrate is found at high mM levels in the lumen of the gut where the majority is taken up by colonocytes and consumed as the primary energy source (Koh, De Vadder, Kovatcheva-Datchary, & Bäckhed, 2016). What remains is taken up and metabolised by hepatocytes preventing the systemic concentrations from becoming toxic leaving little that is detectable in the peripheral circulation (J. H. Cummings, Pomare, Branch, Naylor, & Macfarlane, 1987; Den Besten et al., 2013). Propionate has received less research attention than acetate and butyrate even though it has been noted to have distinct benefits to host health (Hosseini, Grootaert, Verstraete, & Van de Wiele, 2011).

SCFAs play a prominent role in health and disease. SCFAs appear to be intrinsically linked to host health, research is starting to reveal how modulation of bacterially derived SCFAs may provide a potential route for treatment of complex and uncurable pathologies. (Tan et al., 2014).

Increased SCFA production has been shown to be protective of colorectal cancer (Bishehsari et al., 2018). Butyrate has been found to have tumour suppressive properties by regulating cell proliferation (Bhatt, Redinbo, & Bultman, 2017). Increased intestinal acetate levels were found to enhance intestinal integrity protecting against infection (Fukuda et al., 2011) and upregulating the expression of MUC genes preserving mucosal immunity (Gaudier et al., 2004). SCFAs have also been found to influence immune cell development of memory T cells (Bachem et al., 2019).

Propionate and butyrate have been found to protect against inflammation in the gut by modulating pro-inflammatory and anti-inflammatory mechanisms by inducing the generation of anti-inflammatory immune cells (Arpaia et al., 2013) and attenuation of pro-inflammatory deacetylases, cytokines and transcription factors (Levy, Blacher, & Elinav, 2017; Parada Venegas et al., 2019).
High propionate and butyrate levels have also been positively linked to metabolic disease by enhancing energy expenditure and modulating satiety (Z. Gao et al., 2009; Heiss &

Olofsson, 2018; Lin et al., 2012). Propionate and butyrate alter gluconeogenesis and colonic motility to improve glucose homeostasis and satiety (Cherbut et al., 1998; Vallianou, Stratigou, Christodoulatos, & Dalamaga, 2019). They also activate receptor pathways in the hypothalamus to modulate the downstream signalling pathways to control appetite (De Vadder et al., 2014). Human studies support these findings, rectal infusions of SCFAs increased the concentration of circulatory satiety hormones and improved energy expenditure in overweight men (Canfora et al., 2017).

In contrast, reduced SCFA levels have been found to be a contributing factor in disease states. A decrease in butyrate producing bacteria has been found in colorectal cancer patients although any causal relationship has not been defined (Flint, Scott, Louis, & Duncan, 2012). There is a strong association between inflammatory bowel disease (IBD) and the development of colorectal cancer with IBD patients having a significantly increased risk of developing the disease (Itzkowitz & Harpaz, 2004). In addition, the loss or reduction of butyrate producing gut bacteria through dysbiosis and antibiotic treatment has been linked to type 2 diabetes mellitus and loss of insulin sensitivity (Tang, Bäckhed, Landmesser, & Hazen, 2019).

High levels of the bacterial fermentation product succinate, a substrate for butyrate and propionate synthesis, have been linked to the development of IBD (Louis & Flint, 2017). Succinate may serve as a substrate for pathogens driving overgrowth of non SCFA producing bacteria and reducing the abundance of host beneficial strains helping to drive dysbiosis and host disease (Qiuli Yang et al., 2021). Dysbiotic perturbations of the gut microbiota leading to disproportionate levels of propionate and butyrate-producing strains have also been linked to neurological disorders such as autism and depression (Adams, Johansen, Powell, Quig, & Rubin, 2011; Burokas et al., 2017; Deng et al., 2019; Wei, Melas, Wegener, Mathé, & Lavebratt, 2015).

A recent and exciting finding is the relationship between bacterial SCFA production and neurodegenerative diseases normally associated with ageing (Silva, Bernardi, & Frozza, 2020). SCFAs can cross the blood brain barrier (BBB) and have an important role in maintaining BBB integrity (Braniste et al., 2014). The loss of SCFA producing bacterial strains has been linked to the progression of Parkinson's disease through increases in bacterial derived toxins (Li et al., 2017; Unger et al., 2016). SCFAs may also be involved

in modulated Alzheimer's disease by interfering with amyloid peptides forming protein-protein interactions in the brain (Ho et al., 2018). The supplementation with acetate and butyrate has been shown to ameliorate symptoms of multiple sclerosis in a mouse model for the disease by promoting myelination of neurons and preserving spinal cord lipids (Chevalier & Rosenberger, 2017).

### 1.2.7 Amino acids and their derivatives

Bacterial fermentation of amino acids not only yields SCFAs but can produce branch chain fatty acids (BCFAs) that are exclusively derived from the branch chain amino acids leucine, isoleucine and valine to produce isobutyrate, isovalerate and 2-methylbutyrate (Krautkramer et al., 2021; E. A. Smith & G. Macfarlane, 1997; Windey et al., 2012). In addition, dissimilatory catabolic pathways of amino acids produce additional metabolites. Arginine is converted to ornithine and citrulline whilst glycine produces methylamine and acetate. The aromatic amino acids threonine, phenylalanine and tryptophan produce phenolic compounds, phenylacetate and indolic compounds (E. A. Smith & G. T. Macfarlane, 1997). Proline is the exception as it does not produce any metabolite products (figure 1.5) (Krautkramer et al., 2021). These protein-originating metabolites contribute to the wider pool of compounds able to influence host health and metabolism (Oliphant & Allen-Vercoe, 2019).

Protein-derived metabolites have been found to have a mixed impact on host health. The bacterial metabolism of tryptophan has received a lot of attention due to its characteristic potential for biochemical transformation at every atom making it a source for signalling molecules that have been linked to both neuroprotective and excitotoxic effects (Agus, Planchais, & Sokol, 2018; Alkhalaf & Ryan, 2015). Histidine decarboxylation generates histamine that has an important role in immune system regulation (Barcik, Wawrzyniak, Akdis, & O'Mahony, 2017) whilst BCFAs and histidine-derived imidazole propionate have been implicated in insulin resistance (McNabney & Henagan, 2017) and been found to be present in high levels in type 2 diabetes myelitis patients (Koh et al., 2018). Aromatic amino acid derived indolic and phenolic compounds are implicated in promoting colon cancer as genotoxic and carcinogenic tumour promoting metabolites and chronic kidney disease (Devlin et al., 2016; Nowak & Libudzisz, 2006).

The microbiota can obtain a high proportion of energy from peptides and proteins in a CHO depleted environment leading to an increase in gut pH creating a preferential environment for less dominant non SCFA producing bacteria (E. A. Smith & G. Macfarlane, 1997). An increase in protein derived metabolites that are potentially toxic to the host (E. A. Smith & Macfarlane, 1996) may drive dysbiosis and have a chronic negative effect on host health (Ratzke & Gore, 2018; E. A. Smith & Macfarlane, 1996).

### 1.2.8 Vitamins and one carbon metabolites

The gut microbiota is an important source of vitamins and 1CM metabolites that are not synthesised endogenously in higher organisms and cannot be obtained from plant, fungi or animal-derived food sources (Mischke & Plösch, 2016). Colonic bacteria produce a range of vitamins including B vitamins and vitamin K that are essential for health and development (Magnúsdóttir, Ravcheev, de Crécy-Lagard, & Thiele, 2015). Vitamins form a group of essential micronutrients that are required in all living cells to support enzyme function in cellular biochemical reactions (LeBlanc et al., 2013; J. Zhang, Holdorf, & Walhout, 2017). Importantly the enteric bacterial species Bifidobacteria are a major source of folate for 1CM along with other folate synthesising species like the proteobacteria E. coli. Vitamin B9 (folate) and its derivatives will be covered in more detail in section 1.5 of this chapter (Thursby & Juge, 2017).

### 1.2.9 Microbial metabolites that influence *C. elegans* lifespan

Researchers using *C. elegans* have revealed a considerable amount of bacterially derived molecules that beneficially affect *C. elegans* lifespan. The colonisation of the gut by butyrate-producing bacteria has been shown to rescue disrupted host proteostasis (A. C. Walker et al., 2021). Whilst exogenous butyrate has been shown to increase lifespan and improve health-span markers (C. Gao et al., 2014). Exogenous nitric oxide (NO) from *Bacillus subtillis* increased *C. elegans* lifespan (Gusarov et al., 2013). *C. elegans* does not have an increased lifespan when maintained under aerobic conditions on non-NO synthesising *E. coli* (Gusarov et al., 2013). *C. elegans* lived longer when fed on a diet of GD1 *E. coli,* a respiratory deficient strain lacking the redox active lipid coenzyme $Q_8$ (ubiquinone), the lifespan increase was due to a reduction in oxidative damage (P. L. Larsen & Clarke, 2002).

Later work found that the increase in *C. elegans* longevity was not a direct result of ubiquinone but a product of impaired bacterial respiration leading to reduced accumulation of the host gut (Gomez et al., 2012; Saiki et al., 2008). In contrast to these findings, it was proposed that as *C. elegans* synthesises endogenous coenzyme $Q_9$ a diet of *E. coli* provides ubiquinone as a supplementary antioxidant altering the worms' redox homeostasis and decreasing lifespan suggesting ubiquinone was having a direct effect on the worm as opposed to reduced bacterial respiration (Sánchez-Blanco et al., 2016).

Colanic acid is a polysaccharide normally produced by bacteria in response to stress. Several studies have found that maintaining *C. elegans* on colanic acid overproducing K12 *E. coli* mutants lived longer and had improved mitochondrial homeostasis (Gruber & Kennedy, 2017; Han et al., 2017; Hartsough et al., 2020). They also found that colanic acid supplementation was able to increase the lifespan of other nematodes divergent from *C. elegans* and improve mammalian cell mitochondrial dynamics suggesting a highly conserved colanic acid function (Han et al., 2017). The dicarbonyl bacterial metabolite methylglyoxal (MG) has been implicated in neurodegenerative diseases due to its formation of glycated end products (Thornalley, 1996), it was also shown that reduced MG synthesis or increased degradation of MG increased *C. elegans* lifespan (Shin et al., 2020).

Numerous molecules and pathways in both the host and bacteria have been proposed to increase longevity and health (Badal et al., 2020; Vernocchi, Del Chierico, & Putignani, 2016; Virk et al., 2016). *C. elegans* has been a key player in these investigations due to its simplicity and cost effectiveness. It presents a robust model for microbiota-host interactions that are easily manipulated whilst enabling a tight control on potential confounding variables as would be found in a more complex and challenging synergistic relationship in higher organisms.

### 1.2.10 Microbial metabolites friend or foe?

Influencing and manipulating these bioactive metabolites in humans and *C. elegans* to prevent and treat disease, beneficially modulate ageing and find alternatives to traditional pharmaceutical interventions is an ever expanding area of research that has garnered a lot of attention. The metabolites discussed here are only the tip of the iceberg but demonstrate quite clearly the duality of the gut microbiota, their metabolites and their intrinsic relationship with health and disease. They represent a double edged sword where they can

promote host health and prevent disease or under altered conditions feed into and drive mechanisms for illness. They have a complex role that is influenced by the availability of microbial accessible carbohydrates (MACs), lipids and proteins. Particularly the response of SCFA producing bacteria to changes in MACs where a stable microbiota can weather shifts from diet or illness but, instability such as in ageing or dysbiosis can tip the balance from host health promotion to poor health outcomes (Claesson et al., 2012; Desai et al., 2016; Krautkramer et al., 2021; Makki, Deehan, Walter, & Bäckhed, 2018).

## 1.3 Part 2: The sulfonamide Sulfamethoxazole and ageing in *C. elegans*

### 1.3.1 The history of sulfonamides

Sulfonamides or sulfa drugs are bacteriostatic antibiotics that inhibit bacterial folate synthesis and are still some of the oldest and most widely used antibacterial drugs in the world (Connor, 1998; M. I. Hutchings, Truman, & Wilkinson, 2019).

The discovery of sulfonamides as antimicrobial agents began in 1932 when the German pathologist Gerhard Domagk found the red dye 4'-sulfamyl-2,4-diaminoazobenzene was effective in treating streptococci, staphylococcal and pneumococcal infections (Domagk, 1957) as well as successfully treating a bacterial infection in his daughter's arm saving it from amputation, although it did leave her skin with a permanent red tinge (Stokstad & Jukes, 1987). Domagk reported his findings in 1935, the sulfonamide was named Prontosil and it became the first broad spectrum antibiotic discovered for clinical use saving countless lives and winning him the Nobel Prize in Physiology or Medicine in 1939 (Domagk, 1957; Stokstad & Jukes, 1987). Prontosil paved the way for the development of numerous sulfonamide antibacterial agents. These new sulfonamides were effective against multiple fatal or untreatable diseases including gonorrhoea, meningitis epidemica and pneumococcal pneumonia (Domagk, 1957).

Sulfonamides were also responsible for ushering in new legislation on drug control that still stands today, sulfanilamide caused a major drug catastrophe in 1937 killing over 100 patients (Aronson, 2015). Sulfonamides have a long history in healthcare from revolutionising the treatment of disease to improving safety regulations. They remain relevant today as treatments for malaria (Ferone, 1977), urinary tract infections (Petri, 2011), respiratory tract infections , HIV (Bussiere et al., 2020; Scozzafava, Owa,

Mastrolorenzo, & Supuran, 2003; Stranix et al., 2004) and chemotherapeutics (Bussiere et al., 2020; Scozzafava et al., 2003).

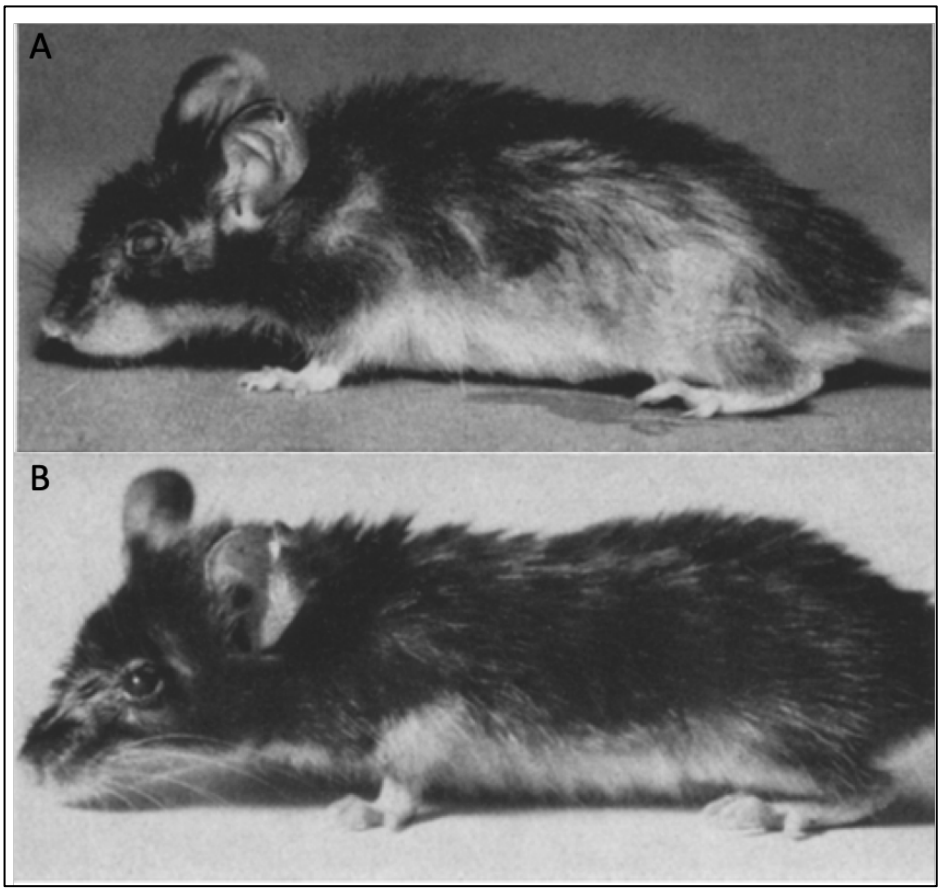


**Figure 1.6 Images of mouse 99 before and after treatment with the sulfonamide Debenal. A**. Mouse 99, a 19 month old female mouse before treatment with 0.2% Debenal. **B.** Mouse 99 6 weeks after treatment began showing improved cataracts and fur, it was also reported a normal level of activity was recovered. Image adapted from (Hackmann, 1958).

Sulfa drugs have had interesting results in early ageing research when it was found they could beneficially modify the lifespan of several organisms. In 1958 it was reported that rats and mice given the sulfonamides Debenal and methyl-Debenal lived considerably longer than control groups but also had improved physical condition, notably experiments involving aged mice treated with Debenal showed complete rejuvenation reducing all symptoms of senility (figure 1.6) It was noted by the authors though that whilst the bacteriostatic element of the drug was important the other active components of these particular sulfonamides may have also contributed to their findings (Hackmann, 1958)

1.3.2 Sulfamethoxazole and the folate synthesis pathway

Sulfamethoxazole (SMX) is a historic bacteriostatic sulfonamide drug that was introduced in the USA in 1961 (Seydel, 1968). SMX is a structural analogue for the folate precursor para-aminobenzoic acid (PABA) and prevents bacterial folate synthesis by competitively inhibiting the enzyme dihydropteroate synthase (fig 1.8) preventing the synthesis of the tetrahydrofolate (THF) intermediatory dihydrofolate (DHF) (Green & Matthews, 2007; P. A. Masters, T. A. O'Bryan, J. Zurlo, D. Q. Miller, & N. Joshi, 2003).

SMX on its blocks THF synthesis but does not prevent the utilisation of endogenous THF pools in obligate folate synthesising bacteria, allowing the bacteria to survive for multiple generations (Hitchings, 1973). To improve the bactericidal effect in a clinical setting SMX is combined with trimethoprim (TMP), a selective inhibitor of dihydrofolate reductase (Eliopoulos & Huovinen, 2001). Sequentially blockading two enzymes in the THF pathway terminates the formation of new DHF potentiating the bactericidal activity and reducing resistance (Hitchings, 1973; Philip A Masters, Thomas A O'Bryan, John Zurlo, Debra Q Miller, & Nirmal Joshi, 2003) demonstrating that on its own SMX may be an effective bactericide but it is not fast acting and the bacterial folate pathway is still able to function for some time.

SMX is used in our lab as a pharmacological intervention to extend the lifespan of *C. elegans*. Under our lifespan conditions SMX is not used in conjunction with TMP. It has been shown to effectively increase worm lifespan in a range of concentrations from 1 μg/ml to 256 μg/ml (Virk, 2013) and is typically used at 128 μg/ml. Previous work in our lab has been shown that SMX does not affect OP50 bacterial growth on NGM at our working concentrations (Maynard, 2017; Virk, 2013). This may be due to a sufficiently low enough dose of SMX to not fully inhibit bacterial folate synthesis below a level to support growth. SMX was found to reduce OP50 growth on DM, possibly due to a lack of optimisation of the media for use with SMX and the absence of residual folate precursor metabolites found in NGM. Neither medium was found to impair *C. elegans* growth, development and offspring production (fecundity) (Maynard, 2017; Virk, 2013) (figure 1.7) all of which are markers for dietary restriction which is discussed in more detail in section 1.5.7 along with the relationship between SMX, folate synthesis and *C. elegans* lifespan in section 1.5.4 of this chapter.

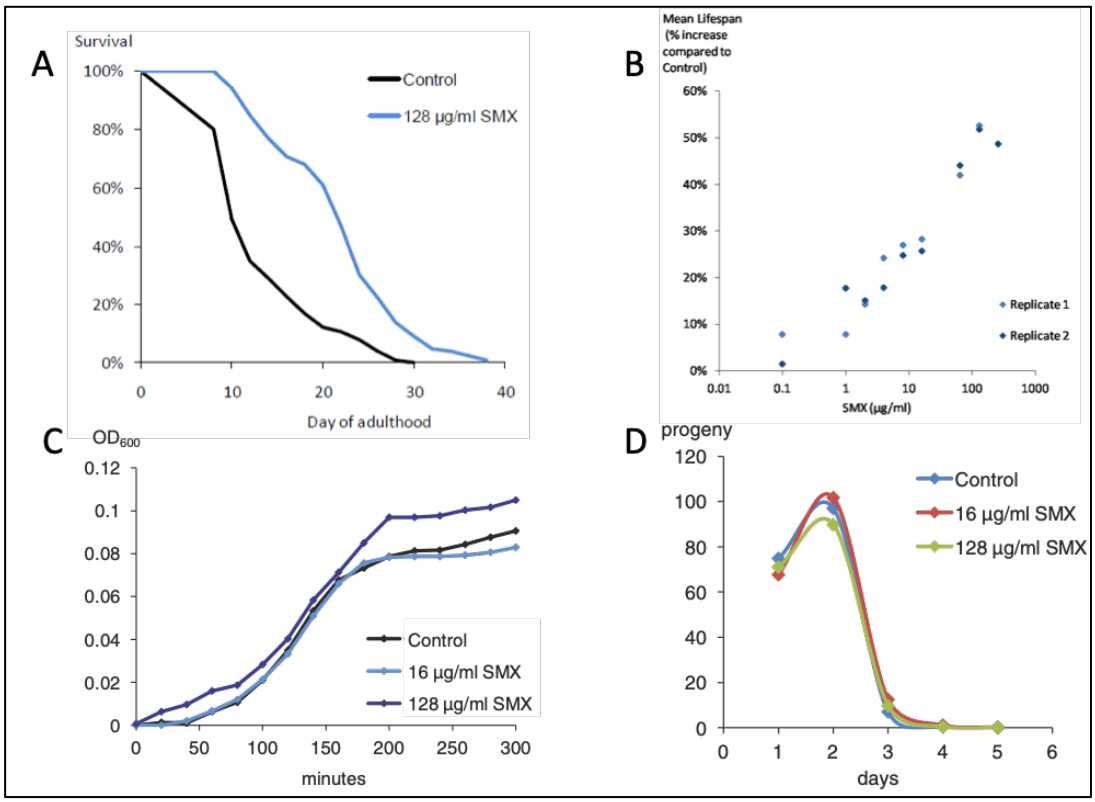


**Figure 1.7 Background work demonstrating SMX increases *C. elegans* lifespan without reducing bacterial growth or altering *C. elegans* development. A**. SMX treated OP50 increases *C. elegans* lifespan; B. SMX treated OP50 increases *C. elegans* lifespan across a range of concentrations; C. SMX does not affect exponential phase growth of OP50 in liquid culture NGM; D. SMX had no effect on *C. elegans* development time or brood size. Images adapted from (Virk et al., 2012).

### 1.3.3 Folate function, synthesis and structure

Folate is the generic name for the water soluble vitamin B9 that forms a large group of nutritionally essential compounds required to support organism development and health, whilst folic acid refers to the synthetic form that is functionally the same after reduction to the active form of folate (Naderi & House, 2018). The original discovery of bacterial folate synthesis occurred in 1941 where after the initial isolation of 'folic acid' (Mitchell, Snell, & Williams, 1941). It was found that human gut bacterial species were able to synthesise folate (B. Hutchings, Bohonos, Hegsted, Elvehjem, & Peterson, 1941; Jukes & Stokstad, 1948; Lascelles & Woods, 1952).

Folates are required by bacteria for proliferation and are a crucial component of many biosynthetic pathways. *E. coli* and many other species of bacteria including Bifidobacterium, Bacteroides, Lactobacilli and Eubacterium can synthesise folates (Rossi,

Amaretti, & Raimondi, 2011). But, are not able to take up intact folates from the environment they reside in.

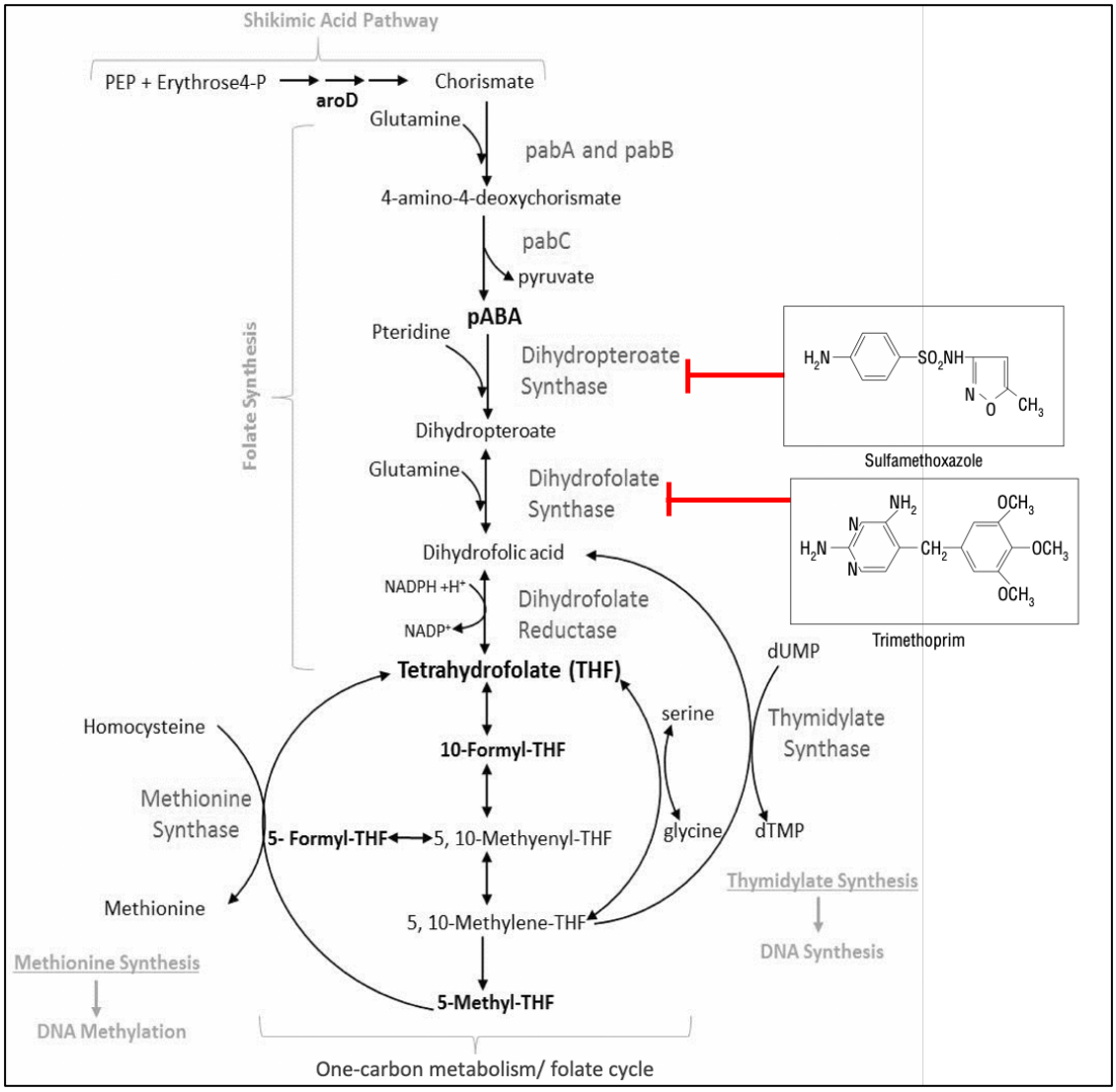


**Figure 1.8 The tetrahydrofolate synthesis and one carbon folate metabolism pathway of *E. coli.*** Derivatives of THF are created in biosynthesis and methylation reactions that transfer or remove one carbon units. Sulfamethoxazole (SMX) inhibits the THF synthesis pathway by preventing PABA from binding to dihydropteroate synthase and trimethoprim prevents the conversion of dihydropteroate to DHF through competitive inhibition. Image adapted from (P. A. Masters et al., 2003; Maynard & Weinkove, 2020).

The bacterial synthesis of folates (figure 1.8) consists of two separate substrate pathways that converge forming the main pathway of tetrahydrofolate (THF) synthesis: The chorismate-PABA pathway and the GTP/pterin pathway (Green & Matthews, 2007). Chorismate is derived from the shikimate pathway. The shikimate pathway consists of seven enzymatic steps that convert erythrose 4-phosphate and phosphoenolpyruvate (PEP)

into the aromatic precursor chorismate. Chorismate feeds into aromatic amino acid biosynthesis or it is converted to para-aminobenzoic acid (PABA) (Tzin, Galili, & Aharoni, 2012). The conversion of chorismate to PABA occurs in two steps. First, the 4-amino-4-deoxychorismate synthase enzymes PabA and PabB convert glutamine and chorismate to 4-amino-4-deoxychorismate (ADC). In the second step, ADC is aromatised by PabC an aminodeoxychorismate lyase to PABA (Green & Matthews, 2007). The GTP/pterin pathway begins with guanosine-5'-triphosphate (GTP) that is sequentially converted by enzymatic action to 6-hydroxymethyl-7,8-dihydropterin diphosphate (DHNDP). A reaction catalysed by the dihydropteroate synthase enzyme FolP condenses PABA and DHNDP to dihydropteroate. FolC a dihydrofolate synthetase conjugates the PABA moiety by an amide bond to a monoglutamate creating dihydrofolate (DHF) (Green & Matthews, 2007). DHF is reduced to its active form by a dihydrofolate reductase (FolA) to yield the final structure of tetrahydrofolate (THF) (fig 1.9) (Angier et al., 1948; Bishehsari et al., 2018; Blakely, 1987; Zheng & Cantley, 2018).

Bacteria are also able to obtain exogenous PABA to supplement endogenous PABA synthesis to enable biosynthesis of folates. The bacteria can sequester PABA from the media. PABA can be sequestered as either a PABA additive to the media or as PABA-glu, an exogenous breakdown product of folate metabolism. PABA can diffuse across the bacterial membrane, PABA-glu is transported by a para-aminobenzoyl glutamate transporter (Carter et al., 2007; Hussein, Green, & Nichols, 1998; Maynard, 2017). Inside the bacteria a carboxypeptidase protein cleaves PABA-glu to yield free PABA that along with the sequestered PABA enters into the folate synthesis pathway (figure 1.10) (Carter et al., 2007).

The glutamation of THFs improves cellular retention and increases its affinity as a cofactor for folate specific enzymes (Egan et al., 1995; Qi et al., 1999; Schirch & Strong, 1989; Turner et al., 1999). In the majority of folate dependent reactions, THF facilitates the carriage of a one carbon (1C) unit from a donor to an acceptor at the N5 or N10 atoms of the pterin moiety. The attached 1C can exist in different oxidation states yielding multiple THF species (figure 1.9) (Zheng & Cantley, 2018) that act as co-factors to enzymes integral to the synthesis of thymidylate, formate and purines, the remethylation of homocysteine to methionine, the reversible interconversion of serine to glycine (Ducker &

Rabinowitz, 2017) and biosynthesis of cellular components and downstream products (Hopkinson & Schofield, 2018).

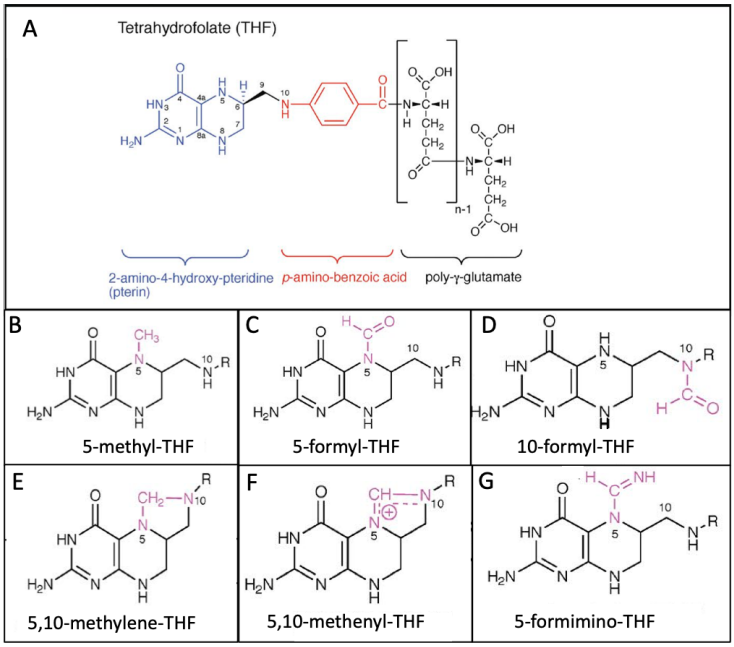


**Figure 1.9 Chemical structure of tetrahydrofolate species. A.** THF structure consisting of pterin, PABA and a glutamate with the polyglutamated tail shown. **B-G.** Structures of THF species with 1C unit attached at N5 and N10. Image adapted from (Zheng & Cantley, 2018)

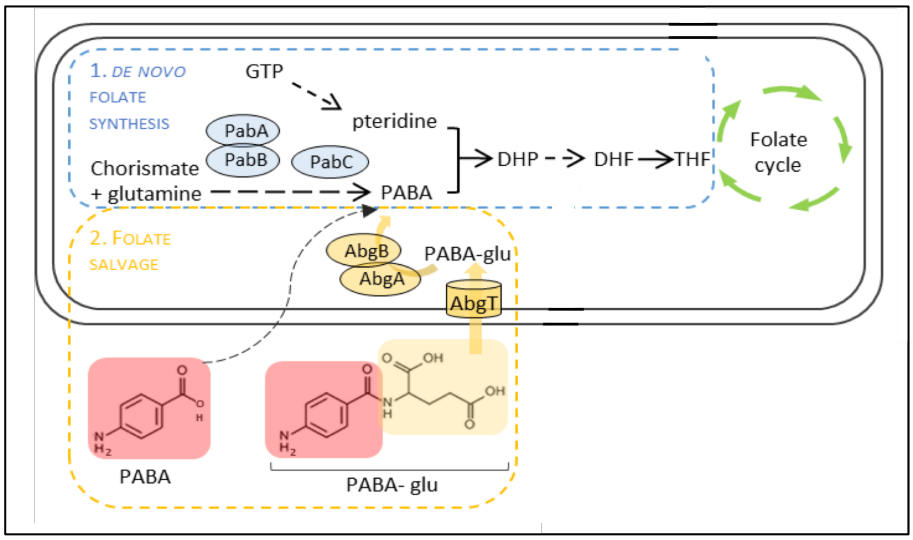


**Figure 1.10 Diagram illustrating *E. coli* bacterial folate mechanisms of substrate import and folate synthesis. 1.** De novo folate synthesis pathway**. 2.** Salvage of folate degradation products. PABA and PABA-glu. PABA, para-aminobenzoic acid; PABA-glu, PABA-glutamate; AbgT, para-aminobenzyl glutamate transporter; AbgA & AbgB, heterodimeric glutamate carboxypeptidase; PabA:PabB, heterodimeric complex 4-amino-4-deoxychorismate synthase; PabC, aminodeoxychorismate lyase; DHP, dihydropteroate; DHF, dihydrofolate; THF, tetrahydrofolate. Image adapted from (Maynard, 2017).

The wider animal kingdom has lost the ability for de novo folate synthesis making them dependent on dietary sources such as plant, animal and fermented products (Crittenden, Martinez, & Playne, 2003; Ross, Caballero, Cousins, Tucker, & Ziegler, 2012). Gut bacteria also provide a large pool of folates for host uptake (Said et al., 2000). It has been found gut bacteria produce folates beyond dietary requirements providing host organisms with a large source of bioavailable folate in excess of recommended daily intake (Denko et al., 1946; T. H. Kim, Yang, Darling, & O'Connor, 2004; Klipstein, 1967; O'Keefe et al., 2009; Rossi et al., 2011). The folate cycle of mammals and higher organisms is unable to convert PABA to THF but can reversibly interconvert sequestered THF to DHF (Bailey et al., 2015). The downstream pathways are remarkably similar to those seen in bacteria with exogenous mono and diglutamated THFs preferentially taken up by intestinal transporters (Baugh, Krumdieck, Baker, & Butterworth, 1971) and feeding into host 1CM. Folate-dependent enzymes interconvert THFs generating the numerous folate species involved as methyl carriers that can be altered for the synthesis of intermediates in multiple biological processes including DNA methylation, immune function, embryonic development and cellular differentiation (figure 1.11) (Ducker & Rabinowitz, 2017). Excessive bacterial folate synthesis may play a role in shaping the gut microbial community in health and disease but has not been shown to have direct negative effects on the host, whereas over supplementation with folic acid has been linked to oncogenesis (Strickland, Krupenko, & Krupenko, 2013) along with folate dependent pathways such as serine and glycine biosynthesis (Maddocks et al., 2017; Possemato et al., 2011).

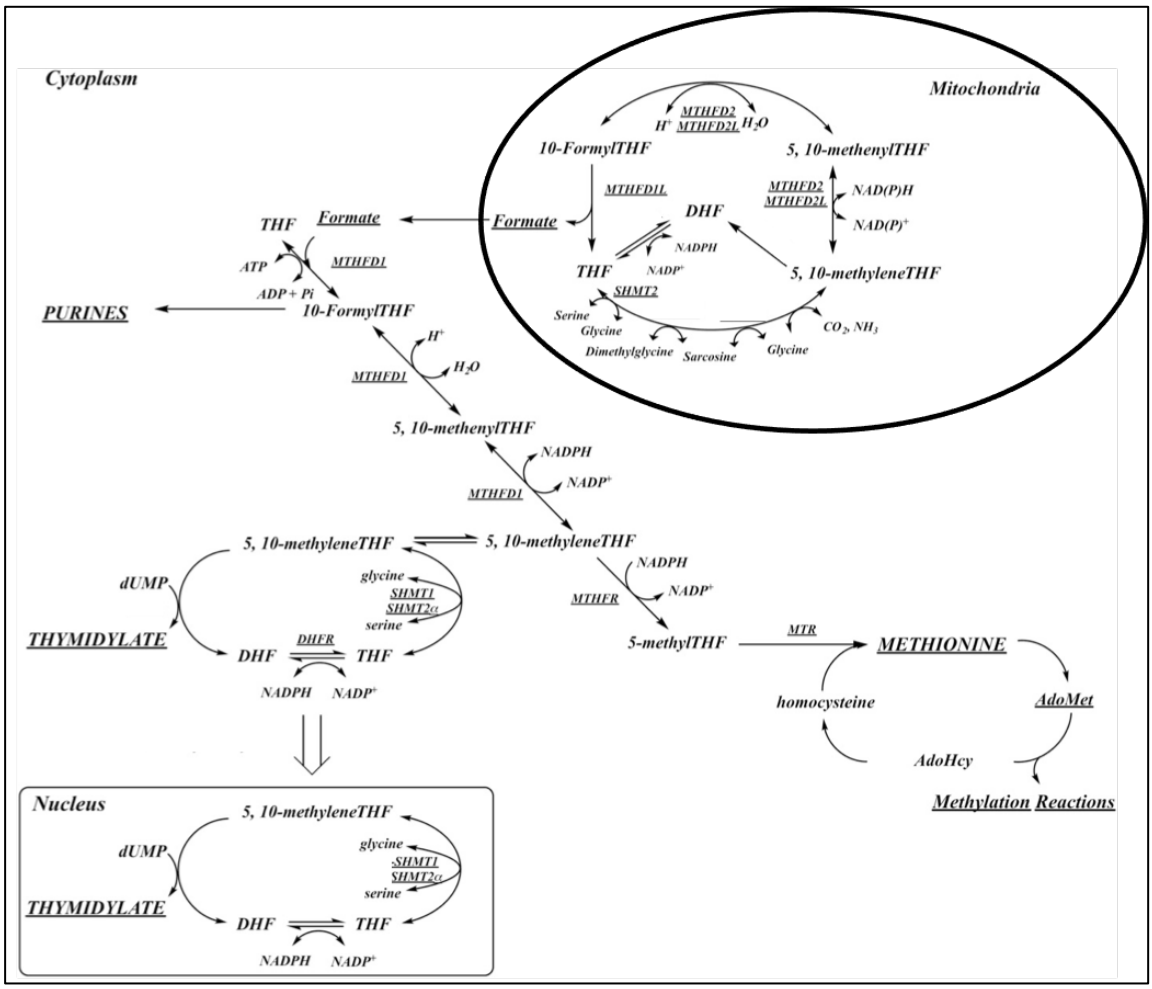


**Figure 1.11 Diagram of mammalian folate pathways and one carbon metabolism.** Folates provide methyl donors and carriers for the synthesis of methionine, thymidylate and purines. The interconversion of glycine to serine is a major source of one-carbon units through the formation of formate in the mitochondria for use in cytoplasmic 1CM. 1CM in the cytoplasm synthesises thymidylate (dTMP) and purines and homocysteine are re-methylated to methionine. In the nucleus 1CM synthesises thymidylate. Methyl donor/carriers are labelled in bold type. MTHFD, methyltetrahydrofolate dehydrogenase; MTHFR, methyltetrahydrofolate reductase; SHMT, serine hydroxymethyltransferase; DHFR, dihydrofolate reductase; AdoHcy, S-adenosylhomocysteine; AdoMet; S-adenosylmethionine; MTR, methionine synthase. Adapted from (Bailey et al., 2015)

### 1.3.4 Reduced bacterial folate synthesis extends *C. elegans* lifespan

A study by Virk et al. (2012) made the serendipitous discovery that an *E. coli aroD* mutant increased *C. elegans* lifespan. The *aroD* gene encodes 3-dehydroquinate dehydratase an enzyme that is responsible for the synthesis of the aromatic precursor chorismate (fig 1.12). Chorismate is an upstream molecule in the shikimate pathway required for endogenous synthesis of the key folate substrate PABA (Richards et al., 2006). A screen of non-essential genes that were predicted to be involved in folate synthesis revealed

deletion of *pabA* and *pabB* increased *C. elegans* lifespan (Virk et al., 2016). *pabA* and *pabB* encode for 4-amino-4-deoxychorismate synthase an essential enzyme for the conversion of chorismate into an important precursor for THF synthesis (B. P. Nichols, Seibold, & Doktor, 1989).

An independent screen of over 4000 non-essential genes reproduced the findings that *pabB* and *aroD* increased *C. elegans* lifespan (Han et al., 2017). The screen also found deletion of *aroG,* an enzyme upstream of aroD for chorismate synthesis also increased *C. elegans* lifespan. A pharmacological intervention using the sulphonamide drug SMX, a competitive inhibitor of the enzyme DHPS that utilises PABA as the substrate for folate synthesis also increased worm lifespan. SMX increased lifespan in a dose dependent response from 2 μg/ml to 256 μg/ml (Virk et al., 2012). 128 μg/ml SMX is the minimum concentration to produce the highest consistent lifespan increase (Virk et al., 2012). It remains the standard concentration in our lab for experiments investigating ageing and related mechanisms in our *C. elegans* model (fig 1.12). In both mutant and pharmacological backgrounds, disruption of the *E. coli* folate synthesis pathway increased *C. elegans* lifespan.

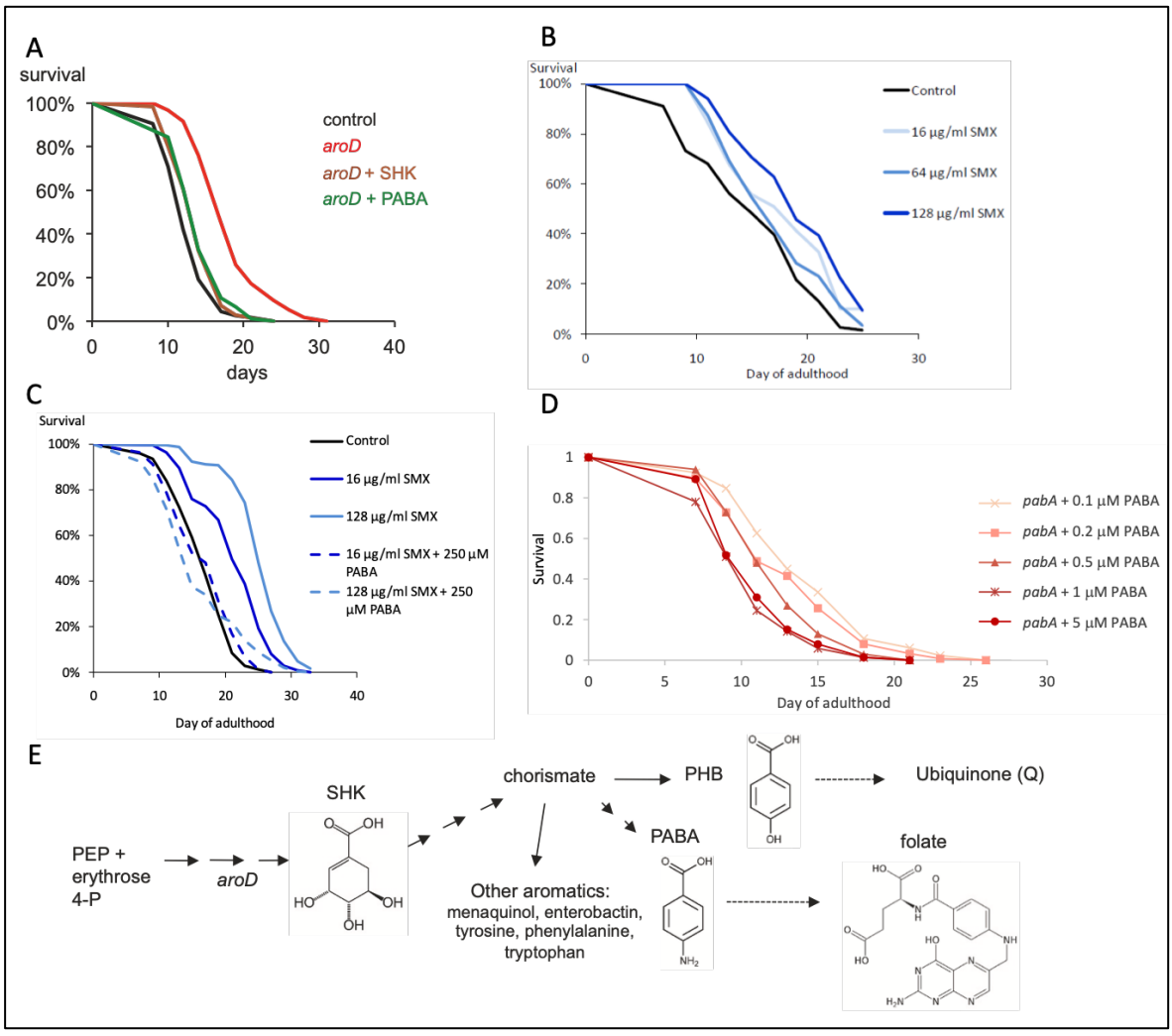


**Figure 1.12 Background work demonstrating inhibition of bacterial folate synthesis extends *C. elegans* lifespan.** **A,** The *aroD* mutant extends *C. elegans* lifespan compared to a WT control and supplementation of the media with PABA and shikimic acid reverses the lifespan effect; **B,** *C. elegans* lifespan is increased in a dose dependent response to SMX; **C,** The addition of PABA to NGM dose dependently reverses the lifespan effect; **D,**The *E. coli* mutant *pabA* increases *C. elegans* lifespan, **E**, An abbreviated schematic of the shikimate pathway and location of *aroD*. Image adapted from (Maynard, 2017; Virk, 2013; Virk et al., 2012; Virk et al., 2016)

*E. coli* lacks the transporters for folate uptake but can synthesise de novo folate through the shikimate/chorismate pathway and can utilise precursors in the media that can diffuse across the membrane or through the PABAglu uptake transporter abgT (Hussein et al., 1998). Supplementation of NGM with shikimic acid and 25 µM PABA was reported to reverse the *ΔaroD* lifespan increase in *C. elegans* (Virk et al., 2012). The enzyme AroD is a key enzyme for the synthesis of shikimate that is converted to chorismate a precursor for folate and aromatic compound synthesis (Virk et al., 2012). It was also found that reversal of the *ΔpabA* lifespan effect on *C. elegans* with PABA supplemented DM was dose

dependent, a concentration gradient of 0.2 μM - 1 μM PABA reverted worm lifespan to WT levels (Maynard, 2017). This range of concentrations was below the threshold of 100 μM PABA required to rescue bacterial growth of *ΔpabA* in liquid DM to WT levels (Helliwell, 2013; Maynard, 2017). These results demonstrated nanomolar concentrations of PABA are required to reverse any changes to *E. coli* metabolism that may be affecting worm lifespan.

Supplementation of NGM with folic acid also reversed the lifespan effect of *ΔpabA* and *ΔaroD* (Virk et al., 2012). Possibly due to the availability of folic acid breakdown products as *E. coli* cannot take up intact folic acid (J. P. Brown, Davidson, & Scott, 1974; Virk et al., 2012). This rescue was lost on the *E. coli abgT/pabA* mutant due to the loss of the bacteria's ability to sequester available PABAglu from folic acid (Maynard, 2017). The reversal of the 128 μg/ml SMX effect on *C. elegans* lifespan to WT levels was achieved with the addition of 250 μM PABA to NGM agar (Virk, 2013). 128 μg/ml SMX equates to 505 μM which is over double the concentration of PABA required for rescue.

Taken together these previous bodies of work demonstrate that SMX functions as a competitive inhibitor. It also demonstrates that the folate concentration required for normal bacterial growth and, the threshold where bacterial folate synthesis becomes detrimental to worm lifespan is at μM levels (figure 1.12) (Maynard, 2017; Virk et al., 2012).

An LC-MS/MS analysis of bacterial folate synthesis found that loss of *aroD* and *pabA* significantly reduced bacterial folate levels (Maynard, 2017; Virk et al., 2012). SMX treatment caused a dose dependent decrease in *E. coli* folate levels with a concentration of 2 μg/ml SMX rendering folate completely undetectable in the bacteria (Virk, 2013). *ΔpabB* was not investigated for folate levels but considering it encodes one half of the functional enzyme integral for PABA synthesis it would not be unreasonable to assume that deletion of this gene also decreases folate synthesis in the absence of external sources of PABA.

Together these results show that SMX targets the bacterial folate cycle and as found with folate deficient mutants, increases lifespan. Rescue of bacterial folate synthesis returns the

worm's lifespan to WT levels suggesting that decreased bacterial folate synthesis causes the increase in *C. elegans* lifespan (Virk et al., 2012; Virk et al., 2016).

### 1.3.5 Decreasing *C. elegans* folate levels does not increase lifespan

To understand if decreased endogenous worm folate levels were responsible for the increase in lifespan a *C. elegans* folate deficient mutant *gcp-2.1* was used along with the animal specific DHFR inhibitor methotrexate (MTX) and the reduced folate supplement folinic acid.

The *C. elegans* mutant *gcp-2.1* has impaired folate uptake, it cannot deconjugate poly-glutamated-THFs from the bacteria restricting the absorption of mono-glutamated-THF in the intestine (Virk et al., 2016). The mutant can obtain sufficient mono-glutamated folates from the bacterial diet for normal growth but, does not exhibit an increased lifespan phenotype (Maynard, 2017). Folinic acid is a naturally occurring reduced folate (5-formyl-THF) that is directly absorbed by *C. elegans*. It cannot be taken up by *E. coli* or provide breakdown products for the rescue of folate synthesis of *ΔpabA* or OP50 on an SMX background. Folinic acid did not reverse the *ΔpabA* or SMX increase in *C. elegans* lifespan (Maynard, 2017; Virk et al., 2016). MTX is a folate inhibitor that prevents the conversion of DHF to THF by inhibition of the dihydrofolate reductase enzyme (DHFR) in animals, not bacteria. Inhibiting *C. elegans* folate cycle with MTX did not increase the lifespan on an OP50 *E. coli* background (Maynard, 2017; Virk et al., 2016). Together these results suggest that reduced bacterial folate synthesis causes the worms to have a prolonged life. It also suggests the lifespan conferring effect is independent of worm folate status although, the mechanism for this effect is still unknown.

### 1.3.6 Reduced bacterial accumulation in the gut does not increase lifespan in the sulfamethoxazole model

A possible mechanism for the lifespan increase seen from impaired bacterial folate synthesis was reduced bacterial accumulation and proliferation in the gut of *C. elegans*. Previously it had been reported that bacterial proliferation and growth in the gut may decrease worm lifespan through accumulation causing a blockage of the intestinal tract or by some form of indirect growth related interaction with the host (Garigan et al., 2002; Portal-Celhay et al., 2012). This hypothesis was supported by the finding that respiratory

deficient *E. coli* lacking coenzyme-Q had delayed bacterial accumulation in the gut and increased *C. elegans* lifespan (Gomez et al., 2012).

A more recent study using the long-lived *C. elegans* mutants *phm-2* and *eat-2* that have a defective grinder phenotype found that accumulation of the gut by *E. coli* was key to the mechanism of longevity through a dietary restriction and innate immunity pathway. The worms were put into conditions where the pharyngeal defect allowed live non-pathogenic *E. coli* to accumulate in the gut in younger animals than WT animals that are exposed to accumulation later in life. The accumulation of live bacteria was found to upregulate genes involved in activating the innate immune response and increased bacterial avoidance behaviour inducing dietary restriction that slowed ageing (S. Kumar et al., 2019).

In the low folate model, this may not be the case. *C. elegans* maintained on SMX treated bacteria have increased lifespan and are reported to have reduced aversion behaviour. They prefer to remain within the confines of the lawn and have delayed accumulation of bacteria in the gut (Maynard, 2017; Virk et al., 2016). OP50 transformed with a plasmid to express green fluorescent protein (GFP) was used to quantify bacterial accumulation of SMX treated and control OP50 in the lumen of the *C. elegans* gut after 5 days of adulthood. The animals were separated individually into high and low accumulation groups and it was found that approximately 50 % of the recently dead untreated condition had no bacterial accumulation whereas SMX was found to only delay accumulation but not prevent it and had no significant impact on high and low accumulation across the cohorts. It was concluded that delayed accumulation of bacteria in the gut was not a cause of the lifespan increase by SMX, but more likely a product of preserved pharyngeal function as a consequence of slowed ageing (Virk et al., 2016). A similar study also found no correlation between the extended lifespan effect of *E. coli* mutants on *C. elegans* and their colonisation of the intestinal tract (Han et al., 2017).

### 1.3.7 A metabolic component of *E. coli* reduces *C. elegans* lifespan

Dietary restriction (DR) has been linked to lifespan increases in *C. elegans* through the use of impaired food intake mutants, axenic culture (absent of *E. coli*) and limiting the food source (Lenaerts, Walker, Van Hoorebeke, Gems, & Vanfleteren, 2008; Onken & Driscoll, 2010). The methods all involve reducing food intake without causing starvation to increase worm lifespan at a cost of extended development time and reduced fecundity, the

addition of live or growth arrested bacteria restored the normal short lifespan (Backes et al., 2021; Hosono, Nishimoto, & Kuno, 1989; Kaeberlein et al., 2006; Klass, 1977; G. D. Lee et al., 2006; G. Walker, Houthoofd, Vanfleteren, & Gems, 2005).

Treatment of *E. coli* bacteria with UV or antibiotics increases lifespan. Carbenicillin a bacteriostatic agent, kanamycin that inhibits bacterial translation preventing colony formation and proliferation and SMX a folate inhibitor all increase *C. elegans* lifespan. SMX does not affect bacterial proliferation whilst all four interventions are not bactericidal and have been shown to have no effect on *C. elegans* morphology or reproduction which is a marker for DR (Garigan et al., 2002; Gems & Riddle, 2000; Klass, 1977).

It has also been shown that metabolically active, as opposed to dead bacteria are required to reverse DR and that over time this component may be detrimental to lifespan (Cabreiro et al., 2013; Lenaerts et al., 2008; E. D. Smith et al., 2008). In combination, SMX and kanamycin do not have an additive effect on lifespan, even though the latter prevents bacterial growth and SMX does not in NGM. Both drugs have different targets within the bacteria but might be inhibiting a downstream shared process (Virk et al., 2016). Together this suggests that *E. coli* possess a life shortening activity that is independent of growth and proliferation, and maybe a product of metabolic pathways downstream of folate synthesis.

### 1.3.8 *C. elegans* aversion behaviour links bacterial folate synthesis to mild toxicity

A potential clue to the relationship between bacterial folate synthesis and *C. elegans* lifespan is aversion behaviour. *C. elegans* have evolved a phenotype for sensing toxicity in their environment as a product of threat avoidance in the wild from pathogenic bacteria and is termed aversion behaviour (K. Lee & Mylonakis, 2017; Melo & Ruvkun, 2012). Aversion of *C. elegans* to the bacterial lawn was found to be decreased in the lifespan extending *E. coli* mutants discovered by Virk et al. (2016). A common factor amongst these mutants is that they reduce virulence in pathogenic strains when mutated this includes the folate related genes *pabA*, *pabB* and *rpoS* (Virk et al., 2016). Interestingly *rpoS* is involved in the expression of toxins and virulence pathways in pathogenic bacteria (Bachman & Swanson, 2001; Dong, Coombes, & Schellhorn, 2009; Iriarte, Stainier, & Cornelis, 1995; Suh et al., 1999; Yildiz & Schoolnik, 1998). Folate synthesis is upregulated by *rpoS* during exponential growth and the *rpoS* mutant features

downregulated *pabA* and folate synthesis (Dong, Kirchhof, & Schellhorn, 2008; A. Ito, May, Kawata, & Okabe, 2008; Maynard, 2017; Weber, Polen, Heuveling, Wendisch, & Hengge, 2005).

As part of a wider screen of genes under regulatory control by *rpoS,* it was found that the *fic* mutant was also found to extend worm lifespan. The *fic* gene encodes for a conserved family of prokaryotic and eukaryotic toxins and when removed has reduced folate levels that could be rescued with PABA along with a reversal of the lifespan effect (Maynard, 2017). On SMX treated lawns *C. elegans* has notably reduced avoidance behaviour spending a considerable amount of time within the lawn compared to non-SMX conditions. This effect was observed on two different WT *C. elegans* strains N2 and SS104, and agar seeded with either OP50 or K12 *E. coli* both of which are common laboratory food sources for the worms and increase lifespan when treated with SMX (Maynard, 2017).

In a study investigating the *Enterobacter cloacae* B29 strain, that produces a lipopolysaccharide (LPS) endotoxin it was found that *C. elegans* maintained in this bacterium had a strong aversive reaction, reduced fecundity and shortened lifespan (Fei & Zhao, 2013). Knock out of LPS genes did not rescue these effects (Fei & Zhao, 2013). It was shown that SMX rescued the aversion behaviour, fecundity and increased lifespan (Maynard, 2017). Thus, inhibiting bacterial folate synthesis can prevent multiple toxic bacterial activities. These findings support previous work that bacterial toxicity can induce reduced progeny production (Aballay & Ausubel, 2001).

The decreased aversion seen in both SMX and mutant conditions is consistent with behaviours associated with the removal of toxicity (Melo & Ruvkun, 2012; Virk et al., 2016). This suggests that non-pathogenic *E.coli* may possess a mild yet chronic toxicity component that shortens worm lifespan. The potential toxicity effect may be dependent on an intact folate pathway that synthesises folate beyond a minimal physiological threshold to support bacterial and worm development (Maynard, 2017; Virk et al., 2016).

### 1.3.9 The sulfamethoxazole extension of lifespan is temporal

It was discovered a temporal aspect exists for increasing lifespan by reducing folate synthesis with SMX. The folate synthesis gene *pabA* was found to be maximally expressed during exponential phase of bacterial growth coinciding with the first 48 -72

hours after seeding, targeting folate synthesis with SMX during this window had an optimal effect on *C. elegans* lifespan (Maynard, 2017). In our lifespan protocol agar plates have SMX added to the media post autoclaving (day minus 3) and are seeded with bacteria 48 hours prior (day 0) to L4/young adult worms being added. On days 7 and 14 the adult worms are transferred to fresh plates that have also been seeded with bacterial lawns 48 hours before use. Throughout the entire duration of the lifespan, the bacterial lawn is subject to the effect of SMX and the worms are exposed to exponential phase bacteria in triplicate throughout their lifetime.

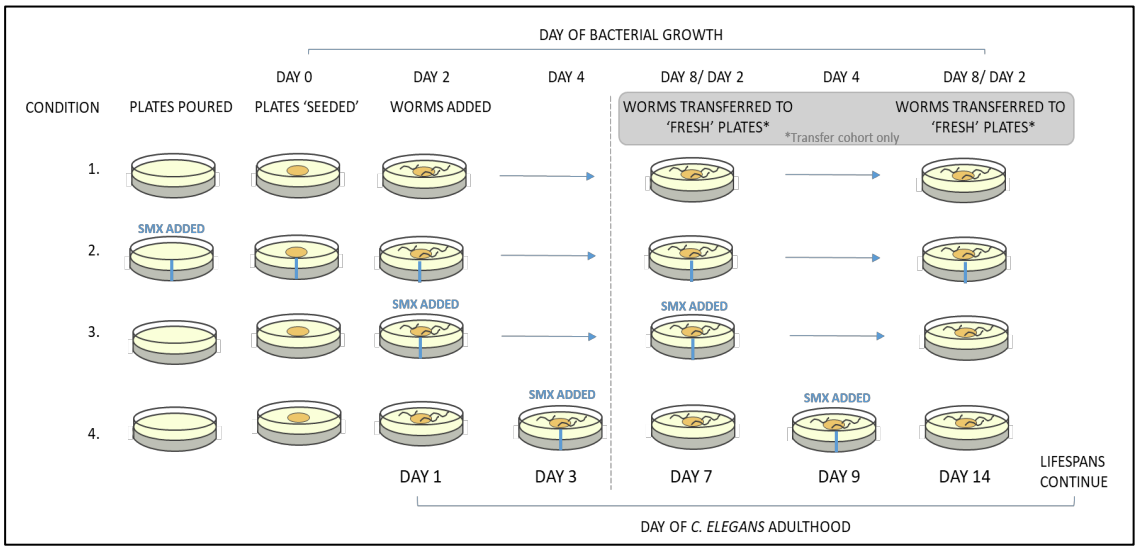


**Figure 1.13 Experimental set-up for examining the temporal aspect of how SMX affects *C. elegans* lifespan.** Plates were seeded with 100 µl E. coli culture 2 days before the addition of *C. elegans*. Condition 1. Control plates; 2. 128 µg/ml SMX added after autoclaving; 3. 128 µg/ml SMX added at day 2 of bacterial growth; 4. 128 µg/ml SMX added on day 4 of bacterial growth. *C. elegans* were added on day 2 of bacterial growth corresponding with day 1 of adulthood. On day 7 of adulthood conditions 1-4 was split into two cohorts, worms were either transferred to fresh plates or remained on the original plates giving eight experimental conditions; 1-4 Transfer and 1-4 non-transfer. The transfer cohort was transferred to fresh plates on days 7 and 14 of adulthood and the lawns had SMX added post autoclaving or were treated with SMX on either day 2 or 4 of bacterial growth as previously discussed. The non-transfer cohort remained on the same plates but either received no additional SMX treatments other than the original addition post autoclaving or

the lawns were treated with SMX on day 2 or 4 of bacterial growth. Image adapted from (Maynard, 2017).

Lifespans were conducted on bacterial lawns where synthesis of folate was inhibited at different time points by SMX. Worms were either transferred at days 7 and 14 of adulthood or, remained on the same plate (non-transfer) exposing them to the same bacterial lawn for the duration of the experiment (fig 1.13) (Maynard, 2017). It was found that non-transfer cohort worms lived longer than transfer cohort worms. Both transfer and non-transfer cohorts lived longest on *E. coli* seeded on plates treated with SMX before day 0 as opposed to day 2 of lawn growth. The results showed *C. elegans'* exposure to the first 48-72 hours of *E. coli* growth was responsible for decreasing lifespan (Maynard, 2017). Reducing bacterial folate within this window removed excess folate synthesis to optimally increase lifespan (Maynard, 2017). This temporal effect may be responsible for removing an element that is associated with bacterial folate synthesis and at its highest during exponential growth of the bacterial lawn and therefore, most detrimental or toxic to the host during this critical window (figure 1.14) (Maynard, 2017).

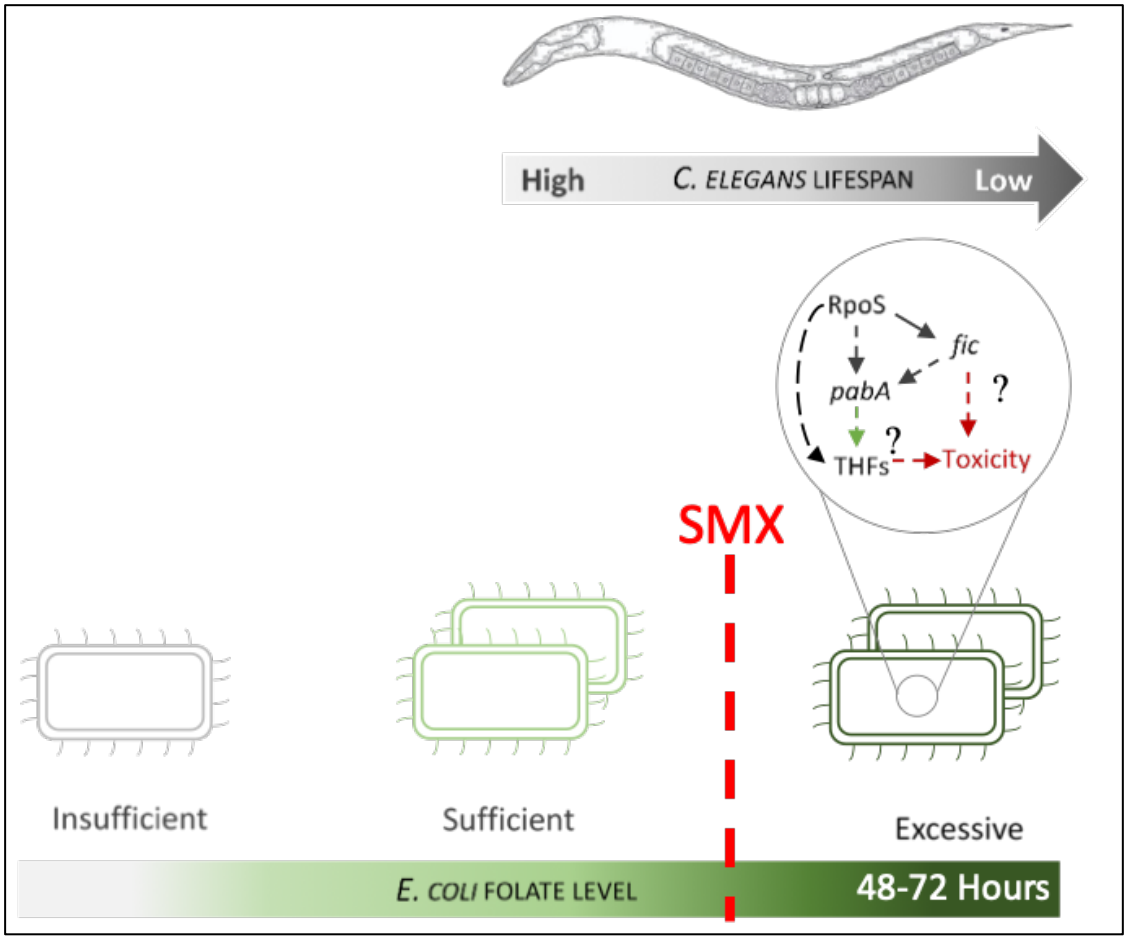

**Figure 1.14 A diagram of the model for excessive folate synthesis associated with bacterial toxicity.** During the first 48-72 hours of bacterial growth folate synthesis exceeds the threshold for normal bacteria and worm growth and development. Once beyond this threshold upregulation of downstream metabolite or pathway of folate synthesis may be associated with a toxicity that is shortening *C. elegans* lifespan. Both *pabA* and *fic* are downstream of *rpoS* which may be driving the level of folate synthesis or pathway leading to toxicity through the expression of *pabA* or indirectly through *fic*. Treatment of the bacterial lawn with 2-256 μg/ml SMX attenuates bacterial folate synthesis to a sufficient level for growth without exceeding the threshold for activation of toxicity mechanisms. Solid arrows represent direct gene regulation; dotted arrows represent indirect regulation; red arrows are possible mechanisms of toxicity; THFs, tetrahydrofolates; SMX, sulfamethoxazole. Image adapted from (Maynard, 2017).

### 1.3.10 Inhibition of folates may alter the serine-glycine and methionine pathways

Contrary to previous findings that the lifespan effect is independent of bacterial folates (Virk et al., 2016) Maynard (2017) found that there was a correlation between low levels of *E. coli* 5,10-methylene THF and the extended lifespan in *C. elegans*. 5,10-met THF is utilised as both a 1C recipient and donor during the reversible conversion of serine to glycine by the serine-hydroxymethyltransferase (SHMT) enzyme glyA and a product of the final step in the pathway the catabolism of glycine to ammonium, NADH and $CO_2$ via the glycine cleavage system (GCV) (G. Stauffer, 1996). 5,10-met THF also plays a key role in the synthesis of methionine. The methionine synthesis pathway requires the reduction of 5,10-met THF to 5-methyl THF which provides a methyl donor for the synthesis of methionine from homoserine (Shoeman et al., 1985) (figure 1.15).

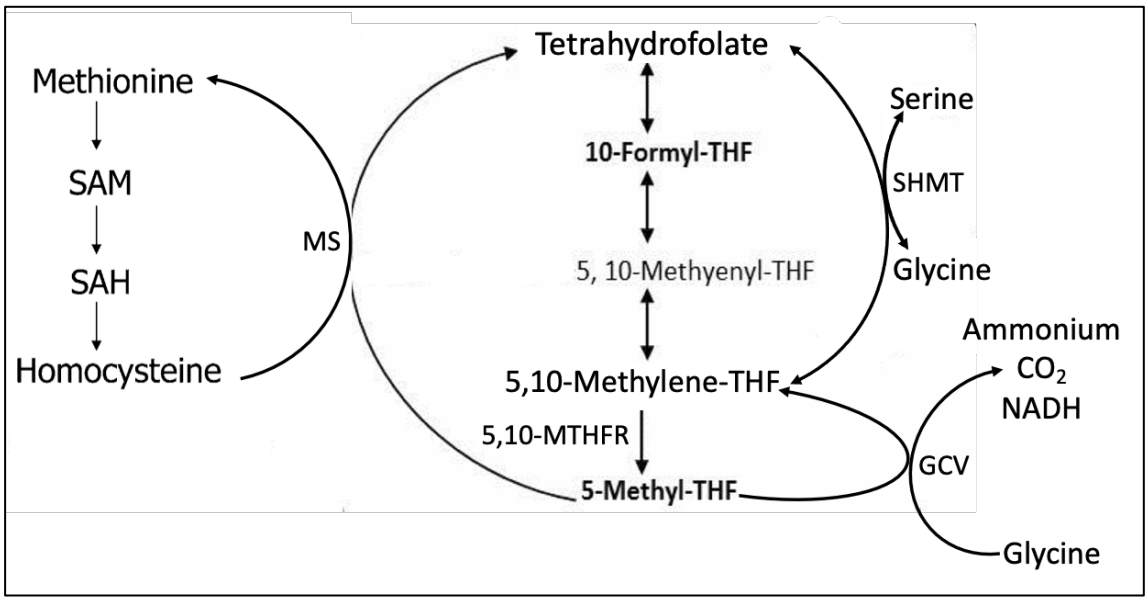


**Figure 1.15 Schematic diagram of bacterial serine-glycine and methionine synthesis pathways.** Synthesis of folate species occurs in a cyclical fashion recycling donors and acceptors of 1CM through the action of the methionine cycle and serine-glycine pathway. These pathways form part of the wider 1CM which is complex and regulated by feedback loops not shown in this diagram. SAM, S-adenosylmethionine; SAH, S-adenosylhomocysteine; MS, methionine synthase; 5,10-MTHFR, 5,10-methylenetetrahydrofolate reductase; SHMT, serine hydroxymethyltransferase; GCV, glycine cleavage system. Image adapted from (Crider, Yang, Berry, & Bailey, 2012; Riley M, 2007).

Disruption of the 5,10-met THF-methionine pathway has previously been implicated in extending *C. elegans* lifespan (Cabreiro et al., 2013). Metformin, the mitochondria complex-1 inhibitor alters methionine synthesis through the irreversible conversion of 5,10-met THF to 5-methyl THF known as the methyl trap. The methyl trap causes an accumulation of S-adenosylmethionine (SAM), S-adenosylhomocysteine (SAH), 5-methyl THF and 5,10-Met THF leading to an inhibition of folate synthesis (Cabreiro & Gems, 2013; Shane & Stokstad, 1985). Metformin used in conjunction with TMP had no additive effect on lifespan was seen suggesting a shared pathway of lifespan extension through inhibition of the folate pathway (Cabreiro et al., 2013). The lifespan extending effect of metformin was attributed to an alteration of bacterial metabolism that leads to DR in the worm rather than the removal of a folate dependent bacterial pathogenicity mechanism (Cabreiro et al., 2013).

In a more recent study, the sulfonamides diaminodiphenyl sulfone (DDS) and sulfadiazine (SD) were found to increase *C. elegans* lifespan but ultra-performance liquid

chromatography (UPLC) found no significant change between control and DDS or SD conditions of 5,10-met THF or 5-methyl THF in the bacteria. It was found that significant changes occurred in the methionine cycle intermediates SAM, homocysteine (HC) and methionine. The sulfonamide induced lifespan extension was attributed to the activation of a downstream DR pathway in the worm, *fmo-2* and suggested that sulfa drugs and metformin act by a similar microbial mediated pathway to increase *C. elegans* lifespan (H. Choi et al., 2019; H. S. Choi et al., 2021). Interestingly a metformin resistant strain of OP50 was able to increase *C. elegans* lifespan in the presence of metformin, genome sequencing revealed that this strain contained a mutation in the *glyA* gene (Cabreiro et al., 2013) that may have impaired glycine synthesis contributing to the lifespan effect (L. I. Pizer, 1965).

Previous work in our lab used nuclear magnetic resonance (NMR) to conduct a metabolic footprint of bacterial supernatant to compare the synthesis and metabolism of serine and glycine in the impaired folate synthesis mutant Δ*pabA*, Δ*pabA* with a PABA folate synthesis rescue (Δ$pabA_R$) and a WT control (CTRL). It was found that serine was rapidly consumed in all conditions although it occurred faster in Δ*pabA* than CTRL and Δ$pabA_R$. Glycine was consumed entirely by the CTRL and Δ$pabA_R$ whilst Δ*pabA* glycine consumption slowed considerably at 20 hours and remained elevated through the remaining period of the experiment. At 25 hours the Δ$pabA_R$ condition appears to have a significant reduction in glycine consumption which may be an artefact from sample preparation (figure 1.16) (Helliwell, 2013). The altered glycine consumption of Δ*pabA* was attributed to a change in preference of amino acid for carbon source whilst the early serine exhaustion was attributed to upregulation of SHMT due to serine consumption at a higher rate (Helliwell, 2013). The results in figure 1.16 by Helliwell (2013) show exogenous glycine and serine concentrations from bacterial supernatant, an inference cannot be made on endogenous glycine and serine concentrations, only that impaired folate synthesis either/or reduces glycine uptake or causes excretion.

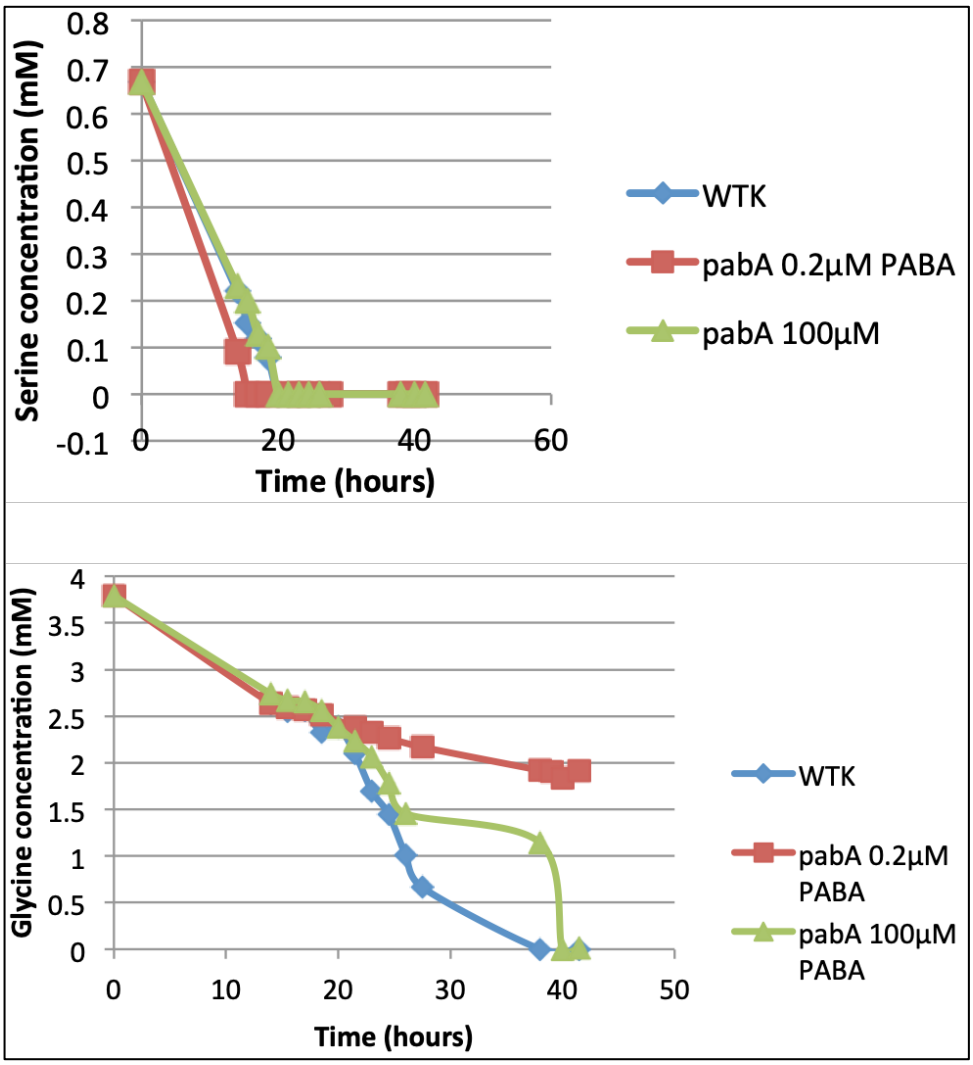


**Figure 1.16 Background work showing the effect of reduced bacterial folate synthesis on serine and glycine consumption.** Image adapted from (Helliwell, 2013).

The biosynthesis of glycine from serine represents a major pathway in bacterial metabolism as it is responsible for the downstream synthesis of an array of cellular metabolites including purines, phospholipids and methionine (G. Stauffer, 1996). The serine-glycine pathway is dependent on folate derived 1C units and provides precursor metabolites for numerous downstream amino acids and their associated metabolites (KEGG, 2021). Glycine metabolism in the bacteria per se may not be lifespan shortening. Disruption to the serine-glycine pathway through loss of folate derived 1C units may reduce the synthesis of a serine-glycine dependant metabolite or metabolites that are harmful effect to host health, subsequently shortening lifespan. In conjunction with this hypothesis elevated exogenous glycine or, endogenous glycine accumulation in the bacteria may have a lifespan promoting effect (Edwards et al., 2015) by increasing availability to the host. The perturbation to the *E. coli* serine-glycine pathway along with

the potential disruption to other downstream amino acids and metabolites may provide a compelling link to the mechanism of extended life seen in our SMX lifespan model.

1.3.11 5,10-met THF may be the source of a lifespan shortening metabolite

In the context of folate dependent bacterial toxicity, one possible mechanism proposed as a candidate for modulating lifespan is the biosynthesis of formaldehyde (Maynard, 2017). Formaldehyde is endogenously synthesised through a variety of mechanisms including repair of methylated DNA, glycine degradation and metabolic pathways involved in 1CM (K. J. Denby et al., 2016; Gonzalez et al., 2006; Ohata, Bruemmer, & Chang, 2019). Folates also provide a ubiquitous source of formaldehyde through the glycine cleavage system and the serine-glycine pathway cyclically sequestering formaldehyde and yielding 5,10-met THF which due to its intrinsic instability leads to spontaneous oxidative breakdown to produce formaldehyde (Burgos-Barragan et al., 2017; Morellato, Umansky, & Pontel, 2021). Formaldehyde is highly reactive and a toxin to both mammals and bacteria. It reacts with amino acid side chains and nucleic acid bases chemically modifying crucial cellular components causing dysfunction and genotoxicity that have been linked to disease (figure 1.16) (N. H. Chen, Djoko, Veyrier, & McEwan, 2016; K. Denby et al., 2016; Hopkinson & Schofield, 2018; Jägerstad & Jastrebova, 2014).

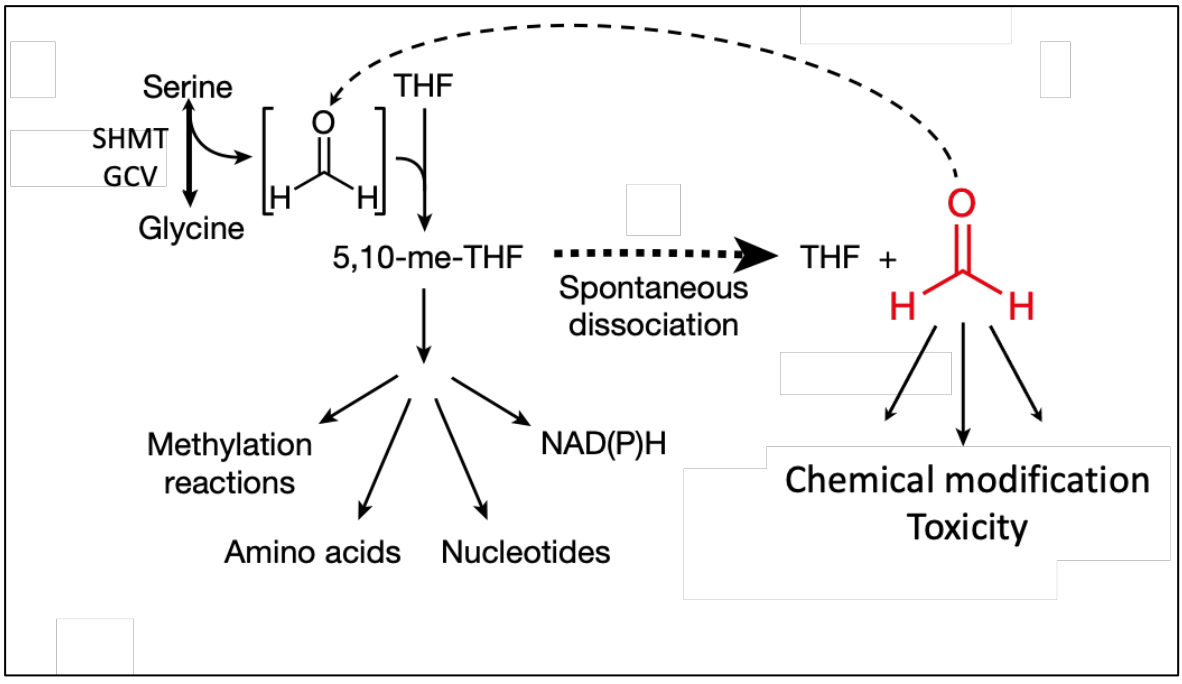


**Figure 1.17 Schematic of the cyclical sequestering of formaldehyde to generate 5,10-met THF and dissociation to yield formaldehyde.** The serine and glycine metabolic pathways sequester

formaldehyde that contributes to the pool of 5,10-met THF available for 1CM. 5,10-met THF also spontaneously degrades to yield formaldehyde that is harmful to cellular physiology but can be removed via re-uptake by the serine-glycine pathway. Image adapted from (Burgos-Barragan et al., 2017)

The detoxification of formaldehyde in an organism is critical to its survival. Mammals can prevent the build-up of toxic levels of formaldehyde through a two-tier system involving an alcohol dehydrogenase (ADH) and the Fanconi anaemia protein complex (Schug, 2018). *E. coli* contains an inducible system that consists of the *frmRAB* operon that encodes a formaldehyde sensing repressor that is inactivated in the presence of formaldehyde allowing transcription of the formaldehyde dehydrogenase *frmA* and the S-formylglutathione hydrolase *frmB* (K. Denby et al., 2016). In addition, the bacteria also have an additional S-formylglutathione hydrolase *YeiG* that is less efficient but also able to sense and detoxify formaldehyde adding a layer of redundancy (Gonzalez et al., 2006). Together this detoxification system removes potentially harmful formaldehyde to produce formate which re-enters 1CM (K. Denby et al., 2016).

Elevated folate synthesis during *E. coli* exponential phase growth may expose *C. elegans* to excess formaldehyde through digestion of the bacteria or ingestion from the bacterial lawn reducing its lifespan. Disruption of bacterial folate synthesis has been shown to reduce the level of 5,10-met THF and correlates with extended *C. elegans* lifespan (Maynard, 2017), the reduction in this folate may also be lowering formaldehyde output ameliorating a potential lifespan shortening toxicity within the bacteria.

## 1.4 Aims of Thesis

This thesis aims to provide a better understanding of the interaction between *E. coli* and *C. elegans*. Specifically, the mechanism by which SMX inhibited bacterial folate synthesis slows ageing in *C. elegans* under our lifespan conditions.

1. I aim to investigate the geography and dynamics of the bacterial lawn. There is a sparsity of literature detailing the composition and structure of *E. coli* bacterial lawns used in *C. elegans* lifespan research. Little is known about how components of the lawn are affected by bacterial folate synthesis and if they influence *C. elegans'* ageing.

2. I also aim to develop a simple and practical LC-MS/MS method to efficiently and accurately extract bacterial metabolites from the DM agar substrate. A novel method is required to conduct metabolomic analysis on the agar substrate used to maintain bacterial lawns. The method needs to be capable of extracting metabolites without altering bacterial metabolism, disturbing the agar matrix and diluting through quenching steps.
3. Finally, I aim to investigate the *E. coli* lawn exometabolome. Analysis of the exometabolome may reveal specific metabolites that underpin the mechanism of how reduced bacterial folate synthesis extends *C. elegans'* lifespan.

# Chapter 2

# Materials and Methods

## 2.1 Strains

2.1.1 *C. elegans* strains

| Strain | Genotype | Source/Origin |
|---|---|---|
| SS104 | *Glp-4(bn2)* | (Beanan & Strome, 1992) |

2.1.2 *E. coli* strains

| Strain | Genotype | Plasmid | Characteristics | Source |
|---|---|---|---|---|
| OP50 | Wild-type | n/a | $Ura^-$ | (Brenner, 1974) |
| BW25113 | Wild-type | pGreen 0029 | $kan^r$ | (Baba et al., 2006) |
| JW3323-1 | *ΔpabA* | n/a | $kan^r$ | " |
| JW5437-1 | *ΔrpoS* | n/a | $kan^r$ | " |
| JW0348-1 | *ΔfrmR* | n/a | $kan^r$ | " |
| JG1/pJI134* | WT ($P_{frmA}$-$frmR_{WT}$-*lacZ*) | PJI134† | $kan^r$, $Ca^r$ | This study |

*Derived from BW25113.

†pJI134 plasmid obtained with thanks from Peter Chivers's laboratory, Durham University.

## 2.2 General Solutions

2.2.1 Luria Bertani broth

Luria Bertani broth (LB) for bacterial cultures was prepared by thoroughly mixing 10.0 g/l Tryptone (95039, Sigma-Aldrich), 5.0g /l Yeast Extract (Y1625, Sigma Aldrich), 10.0g/l NaCl (≥99.0%. Sigma-Aldrich) in $dH_2O$. The LB was divided into 250 ml aliquots and autoclaved at 121 °C for 20 minutes.

2.2.2 Defined Media (DM-kan)

DM-kan for use with liquid bacterial cultures and LC-MS/MS analysis was prepared by dissolving 3.00 g/l NaCl (≥99.0%. Sigma-Aldrich) in $dH_2O$. The solution was then autoclaved at 121 °C for 20 minutes. It was cooled to 55 °C and in a flow cabinet the

following reagents were aseptically added: 1 ml/l of 5 mg/ml Cholesterol dissolved in ethanol (≥99.0%, Sigma-Aldrich), 1 ml/l 1M $MgSO_4$ (≥99.5%, Sigma- Aldrich), 25 ml/l 1M $KH_2PO_4$ (pH 6.0). 20.3 ml/l of stock amino acid solution¥, 0.2 ml/l trace metal solution†, 10 nM vitamin B12, 1 µl/ml of 25 mg/ml 1000x Kanamycin‡, 2 µl/ml 1 mM PABA. 1 ml/l of 128 mg/ml 100x SMX was added if being used immediately‡. DM was stored at 4 °C to be used as required (Helliwell, 2013; Studier, 2005).

2.2.3 Amino acid stock solution for defined media¥

Individual amino acids were added to distilled water and stirred until dissolved. The solution was filter sterilized and stored 4 °C to be used as required (Studier, 2005). All amino acids from Sigma Aldrich.

| **Amino Acid** | **g/750ml** |
|---|---|
| Alanine | 1.0643 |
| Arginine | 0.9698 |
| Aspartic Acid | 1.3365 |
| Cysteine | 0.0765 |
| Glutamic Acid | 2.2455 |
| Glycine | 2.5605 |
| Histidine | 0.2115 |
| Isoleucine | 0.3510 |
| Leucine | 0.6345 |
| Lysine | 0.6930 |
| Methionine | 0.1643 |
| Phenylalanine | 0.4118 |
| Proline | 1.5480 |
| Serine | 0.6323 |
| Threonine | 0.4005 |
| Tryptophan | 0.0428 |
| Tyrosine | 0.2385 |
| Valine | 0.47025 |

2.2.4 Trace metal stock solution for defined media†

2000x trace metal solution was produced from individual metal stock solutions. Stock solutions were prepared in distilled water and filter sterilised and stored at 4 °C (Studier, 2005). All trace metals from Sigma Aldrich.

| **2000x Trace Metals** | | | | |
|---|---|---|---|---|
| **Volume** | **Stock M** | **Metal** | **MW** | **1 x Conc.** |
| 36 ml $dH_2O$ | | | | |
| 50 ml | 0.1 M | $FeCl_3$ in ~0.12 M HCl | 270.3 | 50 μM Fe |
| 2 ml | 1 M | $CaCl_2$ | 110.99 | 20 μM Ca |
| 1 ml | 1 M | $MnCl_2$-$4H_2O$ | 197.91 | 10 μM Mn |
| 1 ml | 1 M | $ZnSO_4$-$7H_2O$ | 287.56 | 10 μM Zn |
| 1 ml | 0.2 M | $CoCl_2$-$6H_2O$ | 237.95 | 2 μM Co |
| 2 ml | 0.1 M | $CuCl_2$-$2H_2O$ | 170.486 | 2 μM Cu |
| 1 ml | 0.2 M | $NiCl_2$-$6H_2O$ | 237.72 | 2 μM Ni |
| 2 ml | 0.1 M | $Na_2MoO_4$-$2H_2O$ | 241.98 | 2 μM Mo |
| 2 ml | 0.1 M | $Na_2SeO_3$-$5H_2O$ | 263.03 | 2 μM Se |
| 2 ml | 0.1 M | $H_3BO_3$ | 61.83 | 2 μM B |

2.2.5 M9 Buffer

M9 buffer for use with bacterial lawn extraction for growth curves was prepared by dissolving 7.37 g/l $Na_2HPO_4.2H_2O$ (≥99.0%, Sigma-Aldrich), 3.0 g/l $KH_2PO_4$ (≥99.0%, Sigma-Aldrich) and 5.0 g/l NaCl (≥99.0%, Sigma-Aldrich) in $dH_2O$. The solution was separated into aliquots of 250 ml autoclaved at 121 °C for 20 minutes.

## 2.3 Antibiotic, para-aminobenzoic acid and β-Galactose 5-bromo-4-chloro-3-indolyl-β-D-galactopyranoside solutions‡

2.3.1 100x Sulfamethoxazole Antibiotic, PABA and X-Gal solutions

SMX (S7507, Sigma Aldrich) was prepared for immediate use in a sterile labelled 10 ml Falcon tube with 128 mg SMX added to 8 ml $dH_2O$ and 300 μl 4M NaOH (S5881, Sigma Aldrich). It was vortexed until no solute particles could be seen then topped up to 10 ml with $dH_2O$ and vortexed until no solute particles could be seen then the tube was covered in foil to protect from light.

2.3.2 1000x kanamycin (kan)

Kanamycin (25 mg/ml 1000x stock) (K0126, Melford Laboratories Ltd) was prepared in advance and stored in 1 ml aliquots at -20 °C. It was prepared in a 50 ml sterile Falcon tube with 0.5 g kanamycin mixed with 15 ml $dH_2O$. It was vortexed until no solute particles could be seen, topped up to 20 ml with $dH_2O$ and filter sterilised and aliquot into 1.5 ml labelled centrifuge tubes and stored at 20 °C.

2.3.3 100x chloramphenicol (CA)

Chloramphenicol (100x stock) (C0378-5G, Sigma Aldrich) was prepared in a sterile 10 ml Falcon tube by adding 350 mg chloramphenicol into 10 ml 100% ethanol and vortexed until no solute particles seen then filter sterilized. It was then aliquot in 1 ml labeled centrifuge tubed (25 mg/ml 100x CA) and stored at -20°C. It was used at 1:1000 dilution in LB or DM (Biotechnology, 2021).

2.3.4 β-Galactose 5-bromo-4-chloro-3-indolyl-β-D-galactopyranoside (X-Gal)

X-Gal stock solution was prepared by adding 200 mg of X-Gal (X-Gal, GoldBio Catalog # X4281, CAS 7240-90-6, MW = 408.63 g/mol) into a sterile 15 ml Falcon tube with 10 mL of Dimethylformamide (DMF). It was vortexed until X-Gal dissolved. Store at -20 °C with the tube wrapped in aluminum foil to protect from light (Biotechnology, 2021).

2.3.5 1000x para-aminobenzoic acid (PABA)

For 1000x 1 mM PABA (A9878, Sigma Aldrich) solution 2150 µl 4M NaOH and 30 ml $dH_2O$ was added to a 50 ml sterile Falcon tube with 7.0 mg PABA and vortexed until all solutes were dissolved. It was then topped up to 50 ml, vortexed and filter sterilized and diluted into 1 ml aliquots in labeled centrifuge tubes and stored at 20 °C. It was added to DM or DM-agar at 1 µl/ml for 0.1 µM, 2 µl/ml for 0.2 µM.

For a 1000x 250 µM PABA stock 335.0 mg PABA was added to 550 µl 4M NaOH and 8 ml $dH_2O$ in a sterile Falcon tube and vortexed until all solutes had dissolved. It was then topped up to 10 ml and vortexed then filter sterilized and aliquoted into 1 ml centrifuge tubes and stored at -20 °C.

## 2.4 Plate preparation

2.4.1 Nematode Growth Media (NGM) plate preparation

NGM plates were made by adding 3.0 g/l NaCl, 2.5 g/l Peptone (70171, Sigma- Aldrich) and 20.0 g/l Agar (05038, Sigma Aldrich) to $dH_2O$. The media was sterilised by autoclaving at 121 °C for 20 minutes. After cooling to 55 °C and in a flow cabinet the following reagents were aseptically added: 1 ml/l of 5 mg/ml Cholesterol dissolved in ethanol (≥99.0%, Sigma-Aldrich), 1 ml/l of 1M $CaCl_2$ (≥96.0%, Sigma-Aldrich), 1 ml/l of 1M $MgSO_4$ (≥99.5%, Sigma-Aldrich), 25 ml/l of 1M $KH_2PO_4$ (pH 6.0) and 25 µg/ml 100x Kanamycin‡ and 1 ml/l of 128 mg/ml 100x SMX‡ if required. The NGM was aliquoted into sterile 60 mm plates to a volume of 15 ml and allowed to set. Plates were stored at 4 °C or used the following day once set. For use with OP50 kanamycin was omitted. For use with the pJI134 plasmid 25 µl/ml X-Gal, and 25µg/ml 1000x Chloramphenicol (CA) were added with the main reagents.

2.4.2 Defined media plate preparation

Defined Media (DM) agar plates were prepared by dissolving 3.0 g/l NaCl (≥99.0%. Sigma-Aldrich) and 18.0 g/l high-purity agar (56763, Sigma Aldrich) in $dH_2O$. The solution was then autoclaved at 121 °C for 20 minutes. It was cooled to 55 °C prior to the following reagents being aseptically added in a fume cupboard: 1 ml/l of 5 mg/ml Cholesterol dissolved in ethanol (≥99.0%, Sigma-Aldrich), 1 ml/l 1M $MgSO_4$ (≥99.5%, Sigma- Aldrich), 25 ml/l 1M $KH_2PO_4$ (pH 6.0). 20.3 ml/l of stock amino acid solution¥, 0.2 ml/l trace metal solution†, 10 nM vitamin B12, 1 µl/ml of 25 mg/ml 1000x Kanamycin‡, 1 µl/ml 1 mM PABA. 1 ml/l of 128 mg/ml 100x SMX‡ if required. The DM-agar was aliquoted into sterile 60 mm plates to a volume of 15 ml and allowed to set. Plates were stored at 4 °C or used the following day.

## 2.5 Preparation of bacterial cultures and bacterial lawns

2.5.1 Luriea Bertani Overnight cultures

Luria Bertani (LB) overnight cultures were prepared by aseptically pipetting 5 ml of sterile LB into 10 ml labelled sterile falcon tube with 10 µl of 25 mg/ml 1000x Kanamycin‡. The LB was seeded by using a sterile pipette tip to add *E. coli* from stock cultures kept at -80 °C. The tubes were incubated for 18 hours at 37 °C in an orbital shaker set to 220 rpm

(Stuart SL1 Lab-scale orbital shaker) and stored at 4 °C before use. For use with OP50 *E. coli* kanamycin was omitted.

2.5.2 Defined media overnight cultures

The LB culture was used to seed DM-kan overnight cultures by aseptically pipetting 90 µl of LB overnight culture into 20 ml of sterile DM-kan in a 50 ml labelled sterile Falcon tube. The tubes were incubated for 18 hours at 37 °C in an orbital shaker set to 220 rpm (Stuart SL1 Lab-scale orbital shaker) or until an $OD_{600}$ of 1.0 was reached. Cultures were used immediately to seed DM agar plates.

2.5.3 Seeding nematode growth media and defined media-kan plates with *E. coli*

NGM and DM-kan agar plates were seeded by using a sterile repeat pipette dispenser to aseptically add 100 µl of bacterial culture to the center of the plate. The plates were incubated for 48 hours at 25 °C before use for lifespan assays or *C. elegans* maintenance.

2.5.4 Seeding and imaging *E. coli* mini lawns

For the mini lawn assay, NGM plates were seeded with 100 µl O/N culture and incubated for 48 hours at 25 °C. At $OD_{600}$ lawns were removed with a scraper and 1 ml of sterile M9. Diluted cultures were removed from plates by pipette to 1 ml Eppendorf tubes and homogenized by shaker. +/- 100 µl of O/N bacterial culture was added to the center of the plate and 5 x 2 µl of diluted bacterial culture was added at equidistant points around the perimeter of the plate ensuring the mini lawn was at least 5 mm from plate edge.

2.5.5 Measuring bacterial growth

For measuring bacterial growth on NGM plates LB cultures were prepared as described in section 2.4.1. For bacterial growth on DM-kan plates DM cultures were prepared as described in section 2.4.2. Plates were prepared as described in section 2.3. Bacterial cultures were grown to $OD_{600}$ 1.0 before seeding. 3-5 plates were used per time point for each condition. Plates were incubated at 25 °C with each timepoint batch removed for measurement. Samples were taken every 24 hours unless specified otherwise in chapter 5. Each sample was obtained from individual plates by adding 1.5 ml of M9 to a plate. At later timepoints, 2 ml of M9 was used due to the agar splitting and becoming more porous to compensate for loss and ensure accurate recovery of the bacterial lawn. After adding

the M9 a clean glass scraper was used to agitate the lawn from the agar surface by tilting the plate at an angle to allow collection at the plate edge. The M9-bacteria mixture was quickly removed using multiple pipettes to a labelled centrifuge tube. The volume removed was recorded. This process was repeated for each plate. The centrifuge tubes were vortexed until a homogenized mixture was achieved. A 200 µl aliquot of each sample was added to a cuvette with 800 µl of M9 and analysed at 600 nm in a spectrophotometer and $OD_{600}$ was recorded. The liquid in the cuvettes was disposed of and the cuvettes were cleaned in $dH_2O$ for reuse. Bacterial growth was calculated by: (volume extracted*$OD_{600}$) *dilution factor.

## 2.6 Transformation of *E. coli* with the pJI134 plasmid

### 2.6.1 Transformation method

A plasmid insert was used to transform the kanamycin resistant wild-type genotype *E.coli* BW25113 (WTK) (Baba et al., 2006): PJI134; formaldehyde responsive $P_{frmA}$-$frmR_{WT}$-*lacZ.*

The plasmid was kindly donated by Dr Peter Chivers (Dept. of Biosciences, Durham University). The plasmid contains a promoter ($P_{frmA}$), a formaldehyde sensitive repressor (*frmR)* that has been retained as WT and the β-Galactosidase reporter gene *lacZ* in place of the *S*-formylglutathione hydrolase *frmB* and a chloramphenicol resistance cassette. Construction of the plasmid is described in K. Denby et al. (2016). 5 ml of sterile LB-Kan was pipetted aseptically into a sterile 10 ml falcon tube. A sterile pipette tip was used to inoculate the LB with WTK *E. coli* from a stock culture stored at -80 °C. Tubes were incubated overnight at 37 °C in an orbital shaker (Stuart SSL1 Lab-scale orbital shaker) at 220 rpm. The overnight culture was then transformed using the method described by Pope and Kent, (1996) and streaked onto a 90 mm master plate containing 60 ml NGM-Kan-CA and incubated overnight at 37 °C.

### 2.6.2 Strain validation

Suitable colonies were selected from the overnight master plates and used to aseptically seed 5 ml of sterile LB-Kan-CA as previously described. After overnight culture 1 ml aliquots were spun down on a bench centrifuge at 13,000 rpm. The supernatant was discarded and the pellet retained for miniprep (GenElute Plasmid Miniprep kit, Sigma-Aldrich) and restriction digest using an EcoRI digest to cleave the plasmid at two

restriction sites (1.9 kb, 5.4 kb) as predicted on the plasmid map. After the miniprep and digest the plasmid DNA was analysed for quantity using a Nanodrop (NanoDrop 1000 Spectrophotometer) and gel electrophoresis to confirm the transformation. A suitable culture was then selected as the working culture for the duration of the experiment.

2.6.3 Diagnostic PCR

All *E. coli* strains used were validated by PCR (Techne TC-5000) to ensure the correct strains were being used. A 1 ml aliquot of overnight culture was centrifuged to produce a pellet. The supernatant was discarded and the pellet was retained for miniprep (QIAprep® Spin Miniprep Kit, Qiagen). 40 µl reactions were prepared and PCR reactions were conducted as follows:

| **Component** | **Volume** | **Final Concentration** |
|---|---|---|
| $dH_2O$ | 16.4 µl | - |
| Dream Taq DNA Polymerase | 20 µl | 2x |
| Forward primer | 0.8 µl | 400 nM |
| Reverse primer | 0.8 µl | 400 nM |
| Sample | 2 µl | - |

| **Step** | **Temperature** | **Time** | **Cycles** |
|---|---|---|---|
| Initial Denaturing | 94 °C | 2 min | 1 |
| Denaturing | 94 °C | 25 secs | 35 |
| Annealing | Dependent on primers | 30 secs | |
| Elongation | 72 °C | 30 secs | |
| Final Extension | 72 °C | 10 mins | |
| Hold | 4 °C | ∞ | |

2.6.4 PCR primers

The ApE – A Plasmid Editor Version 3.08 was used to design primers. PCR product was dependent on gene of interest size. Keio collection single gene knock out mutants that contain the kanamycin resistant gene will give a PCR product of ~891-1025 bp.

| Primer | Sequence 5'-3' | Tm °C |
|---|---|---|
| K2 fwd | CGGTGCCCTGAATGAACTGC | 61.4 |
| pJI Plasmid fwd | CGACGGCCAGTGAATCC | 57.6 |
| *frmA* rev | CAGCCGCCAAAGCTGAC | 61.4 |
| *frmR* rev | CCGACTTCAACCACAACGCC | 61.4 |
| *pabA* rev | CAATGGCCCAACGCCGTAAC | 57.0 |
| *rpoS* rev | GTGCGTATTGGTGACGCTGG | 56.0 |

2.6.5 Gel electrophoresis

Analysis of PCR products and miniprep-digest products were conducted using gel-electrophoresis. Samples were loaded at a volume of 10 µl into a 1% agarose gel (MB1200, Melford) prepared with ethidium bromide in a TAE buffer and run at 110 V for 20 minutes.

## 2.7 *C. elegans* maintenance

Maintenance of *C. elegans* was conducted to ensure sufficient animals were available for Lifespan. Populations were incubated at 15 °C on NGM agar plates seeded with 100 µl OP50 *E. coli*. After the lawn has been fully consumed regions of the agar containing worms 1 $cm^3$ cubes are removed and placed onto fresh plates containing OP50 lawns. The worms are able to enter fresh cycles of growth, development and reproduction (Stiernagle, 1999).

## 2.8 Synchronising *C. elegans* populations

2.8.1 Bleaching

To obtain a sterile and synchronised population of eggs gravid unstarved worms undergo a process of bleaching (Stiernagle, 1999). Each plate containing worms was washed with 2.5 ml M9 (for 90 mm plate) or 1-2 ml (for 60 mm plates) to remove the worms. The M9 containing the worms was carefully pipetted into a 1.5 ml Eppendorf. Worms were allowed to settle for 5 minutes and the M9 was pipetted out to leave approximately 200 µl at the bottom of the tube. 125 µl of cold bleach solution (7:8 sodium hypochlorite, 425044, Sigma Aldrich) was added to each tube. The tubes were manually shaken continuously for 4-5 minutes and monitored by eye to observe for loss of worm

definition and cloudiness. The time was dependent on laboratory temperature, freshness of bleach and number of worms. The tubes were immediately filled with M9 and centrifuged for 1.5 min @ 3000 rpm. The supernatant was removed with a pipette leaving 50 µl and the tube refilled with 1 ml of M9. The pellet was dissociated pellet with vigorous shaking and the centrifuge step was repeated. The supernatant was removed and the pellet suspended in M9. The clean eggs were pipetted onto fresh NGM agar plates (2 plates for each lifespan being set up) seeded with WTK. Plates were then placed in the 15 °C incubator until the worms have developed into gravid, unstarved adults.

2.8.2 Overnight egg lay on DM-kan plates

For a lifespan assay egg lays were set up in late afternoon. 4-5 fresh DM-kan plates per condition were seeded 48 hours prior with the *E. coli* strains for each replicate. 3-5 gravid worms were transferred from the egg bleaching population to each replicate plate. Plates were incubated overnight at 15 °C and gravid worms removed once a sufficient quantity of eggs had been laid. Plates were stored at 15 °C until worms had developed to L4 ready for shifting to 25 °C and transfer of worms to lifespan plates.

## 2.9 Analysis of *C. elegans* lifespan

2.9.1 Lifespan assay

The lifespan protocol for this thesis used the temperature sensitive glp-4(bn2) SS104 *C. elegans* strain. This strain is sterile at 25 °C reducing the need for transfer every 1-2 day by eliminating the presence of offspring that may confound results and impair accurate analysis of the worm population. Figure 2.1 details the full procedure the includes the bleaching and synchronization protocols detailed in sections 2.8.1 and 2.8.2 of this chapter. DM-kan agar plates were used for each condition. 5 plates were used with 25 worms on each plate to give n~ 125 per condition. For the duration of the lifespan plates were incubated at 25°C and the worms were transferred to fresh plates (seeded with respective bacteria 48 hours prior) at days 7 and 14 to ensure starvation did not occur. The first count was conducted on day 7 of adulthood and then every other day thereafter with worms being recorded as either alive, dead or censored. If contamination was observed worms were censored. The analysis continued until all worms for each condition were recorded as dead.

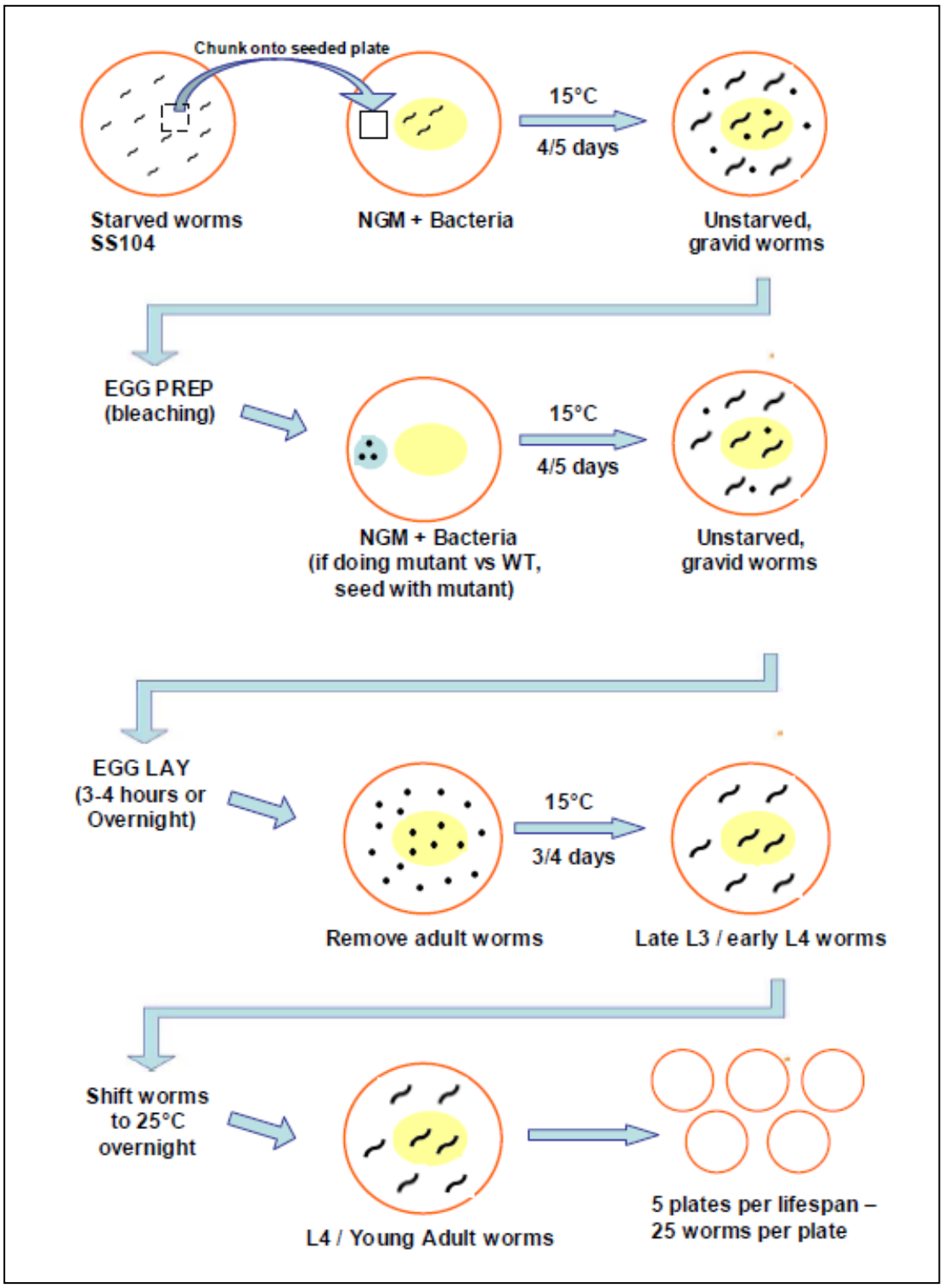


**Figure 2.1 Diagram describing the *C. elegans* lifespan protocol.** Lines represent worms, dots represent eggs, blue dot containing black dots represents eggs from bleaching. Adapted from Maynard (2017).

2.9.2 Healthspan provided by Magnitude Biosciences Ltd

The protocol described in this section for the healthspan experiment was provided by Giulia Zavagno of Magnitude Bioscience Ltd and adapted for this chapter. An Egg lay of

30 plates of 20 SS104 gravid *C. Elegans* was conducted and worms were maintained at 15 °C. A culture of OP50 E. coli was prepared from -20 °C. 20 ml of LB was seeded with 7 µL of OP50 and incubated for 18 hours at 37 °C. Amino acid stocks were prepared to a final volume of 187.5 ml to the concentrations specified in section 2.2.3. One stock had glycine omitted. DM-kan agar plates were prepared as described in section 2.2.2 with the exception of the omission of kanamycin and the addition of 2 µl/ml uracil. The plates contained +/- 128 µg/ml SMX and +/- glycine relevant to each condition. A synchronised population of *C. elegans* was made by bleaching and an egg lay as described in section 2.8. Once worms had reached L4 of development 30 worms were added to each plate before being placed in the Healthspan machine for analysis over 7 days.

## 2.10 Image analysis of bacterial lawns

2.10.1 Image analysis of LacZ output and bacterial lawn morphology

Images were viewed using a Leica M165 FC fluorescent stereo microscope at 12x magnification and acquired with Leica Application Suite v4, exposure settings were 65% brightness, 1.30 saturation, 0.60 gamma and the white auto balance was set with a control plate. Image analysis was conducted using Fiji v2 software. A straight line was plotted from the edge of the lawn to the edge of the image and the brightness of RGB and each colour channel was measured. The RGB values were used to measure LacZ output and produce a plot of the lawns topography as described in detail in chapter 3.

2.10.2 Image analysis of mini lawns

A detailed description of the mini lawn method is described in section 3.3.7 of chapter 3. Images were viewed using a Leica M165 FC fluorescent stereo microscope at 1.25x magnification and acquired with Leica Application Suite v4, exposure settings were 100 % brightness, 0.6 gamma, exposure 1.3 ms and the white auto balance was set with a control plate. Image analysis was conducted using Fiji v2 software. Each mini lawn was measured by manually plotting the outside edge of the lawn and measuring the area.

2.10.3 Transmission Electron microscopy (TEM)

Mica discs were carbon coated and prepared for glow discharge (Cressington 308UHR) to remove contaminants and make the grid hydrophilic by Mrs Christine Richardson, Dept of Biosciences, Durham University. The sample preparation protocol for TEM was adapted

from Monson, Foulds, Foweraker, Welch, and Salmond (2011) and Lane, Simms, and Mobley (2007). A detailed description of sample preparation is provided in section 3.6iii of chapter 3. Grids were coated in poly-l-lysine and allowed to air dry. Bacterial cells were attached by light touching a 5 µl dot of diluted bacterial lawn. Unattached cells were washed off by dipping the grid into a 5 µl dot of $dH_2O$ and immediately blotted on filter paper. This step was repeated 3 times. Samples were then stained by dipping into a 5 µl dot of 1% sodium phosphotungstic acid (pH 5.8, HT152, Sigma Aldrich ) for 30 seconds and then allowed to dry. Samples were examined and imaged at 100 kV using TEM (Hitachi H7600 TEM, EMSIS Xarosa 20 megapixel bottom-mount CMOS camera, Max resolution 3.5 Å with 120 kV tungsten filament).

## 2.11 Formaldehyde protocol

Bacterial cultures containing WTK *E. coli* or the WTK-pJI134 transformed strain were prepared in LB as described in section 2.4.1. Cultures containing the WTK-pJI134 strain also had the addition of chloramphenicol exception of the addition of 25 µg/ml 1000x Chloramphenicol. NGM agar plates (n3 per condition) were prepared as described in section 2.3.1 and 100 µl of each culture was added as described in section 2.4.2. Plates were incubated at 25 °C. β-Galactosidase activity was measured every 24 hours for seven days from seeding as described in section 2.8.1.

## 2.12 Tandem liquid chromatography-mass spectrometry (LC-MS/MS) analysis

Chapter 4 provides a detailed explanation of the sample extraction and preparation methods. All TEM parameters and conditions were optimised and provided by Dr Rachael Dack in the Durham University Biosciences Dept. LC-MS/MS analysis was conducted on a Shimadzu Nexera X2 Chromatography system consisting of binary pumps, on-line degassing unit, autosampler, and a column oven (Shimadzu Corporation, Kyoto, Japan). These were coupled with an AB Sciex 6500 QTRAP mass spectrometer consisting of an electrospray ionization (ESI) source (AB SCIEX, Framingham, MA, USA). Chromatographic separation of amino acids was achieved on a Waters Acquity UPLC BEH Amide column (1.7 µm 1.0 x 100 mm) with an Acquity BEH amide guard column held at 40 °C at a flow rate of 0.2 mL/min. The mobile phases consisted of Solvent A (85% MeCN + 10 mM ammonium formate and 0.15% formic acid) and Solvent B (85:15 H2O:MeCN + 10 mM ammonium formate and 0.15% formic acid). A gradient elution was optimized for

the separation of individual AAs: 0-6.0 minutes, 100% Solvent A; 6.0-10.0 minutes, 100%-0% solvent A; 10-12 minutes, 0% solvent A; 12.1 minutes, 100 % solvent A; 12.1-18 minutes, 100 % solvent A. The ion source was operated in positive mode under optimal conditions: curtain gas, 40 psi; GS1, 50 psi; GS2, 50 psi; ion spray voltage, 5500 V; and temperature 500 °C. Optimal multiple-reaction monitoring (MRM) transitions were identified and are detailed in Table 2.1. Data acquisition and analysis were all performed with Analyst 1.7.1 software (AB SCIEX).

**Table 2.1 Table detailing MRM transitions.** Provided by R. Dack (personal communication, February 2022).

| Q1 mass | Q3 mass | Time ms | Name | DP | EP | CE | CXP |
|---|---|---|---|---|---|---|---|
| 205.1 | 146.1 | 50 | Tryptophan | 36 | 10 | 23 | 12 |
| 166.1 | 120.1 | 50 | Phenylalanine | 30 | 10 | 15 | 12 |
| 132.1 | 86.1 | 50 | Leucine | 30 | 10 | 15 | 12 |
| 132.1 | 86.1 | 50 | Isoleucine | 30 | 10 | 15 | 12 |
| 150 | 104 | 50 | Methionine | 30 | 10 | 15 | 12 |
| 136 | 90 | 50 | Homocysteine | 30 | 10 | 15 | 12 |
| 118.1 | 72.1 | 50 | Valine | 30 | 10 | 15 | 12 |
| 116 | 70.1 | 50 | Proline | 30 | 10 | 15 | 12 |
| 182.1 | 136.1 | 50 | Tyrosine | 30 | 10 | 15 | 12 |
| 122 | 76 | 50 | Cysteine | 30 | 10 | 15 | 12 |
| 90.1 | 44.1 | 50 | Alanine | 30 | 10 | 10 | 12 |
| 120 | 74.1 | 50 | Threonine | 30 | 10 | 15 | 12 |
| 76 | 30.1 | 50 | Glycine | 30 | 10 | 20 | 12 |
| 147.1 | 84.1 | 50 | Glutamine | 30 | 10 | 15 | 12 |
| 106 | 60 | 50 | Serine | 30 | 10 | 10 | 12 |
| 133 | 74 | 50 | Asparagine | 30 | 10 | 25 | 12 |
| 148 | 84 | 50 | Glutamate | 30 | 10 | 15 | 12 |
| 134 | 74 | 50 | Aspartate | 30 | 10 | 15 | 12 |
| 156 | 110.1 | 50 | Histidine | 30 | 10 | 15 | 12 |
| 175.1 | 70.1 | 50 | Arginine | 30 | 10 | 15 | 12 |
| 147.1 | 84.1 | 50 | Lysine | 30 | 10 | 15 | 12 |
| 240.9 | 74 | 50 | Cysteine | 30 | 10 | 15 | 12 |

## 2.13 Statistical Analysis

Statistical analysis of the lifespan assays was conducted using the JMP Pro 14.1 software and survival function was estimated with the Kaplan-Meier estimator that allows for censoring when worms are withdrawn. Data analysis was conducted using the Data Analysis package for Microsoft Excel v15.38 software. All data used for statistical analysis was checked for normal distribution using Descriptive Statistics and any data with a skew and kurtosis between -2 and 2 was deemed as normal, the students t-Test: Two-

Sample Assuming Equal Variances was used to determine statistical significance ($P<0.05$). Healthspan data was provided by Magnitude Biosciences Ltd. Data analysis was conducted using the analyse package of Prism 9 v9.3.1 (350) software. The data was checked for normal distribution and analysed by a one-way ANOVA Kruskal-Wallis test to determine statistical significance ($P<0.05$).

# Chapter 3

# Investigating The Bacterial Lawn to Explain Why Inhibiting Bacterial Folate Synthesis Slows Ageing in *C. Elegans*

## 3.1 Introduction

As previously discussed in chapter 1.3.4 our research group found that inhibiting bacterial folate synthesis increases lifespan in *C. elegans*. SMX has been used to pharmacologically inhibit folate synthesis in *E. coli* to increase *C. elegans* lifespan with a dose dependent relationship between lifespan and SMX from 2 μg/ml to 256 μg/ml (Virk et al., 2012; Virk et al., 2016). A key finding was a temporal aspect of the lifespan effect by SMX that is discussed in detail in chapter 1.3.9. It was found that expression of folate synthesis enzymes peaked during the first 48-72 hours of early exponential bacterial growth (Maynard, 2017). This corresponded with elevated folate levels and that inhibition of folate synthesis in this window with SMX maximally extended lifespan (Maynard, 2017). These results demonstrated that temporally the bacteria have a folate dependant mechanism that may be at its most toxic to *C. elegans* during the exponential growth phase and may be responsible for reducing lifespan (Maynard, 2017).

The role of bacterial growth and proliferation concerning lifespan has been studied in the context of accumulation within the *C. elegans* gut and is discussed in chapter 1.3.6. Previous work suggested that as *C. elegans* ages bacteria can colonise and accumulate in the gut as a product of age-related frailty of pharyngeal grinding and pumping. These accumulations were proposed to correlate with an indirect interaction with the host and a constipation related early death (Garigan et al., 2002; Portal-Celhay et al., 2012). Work within our lab showed that SMX did not affect OP50 growth and did not impair *C. elegans* development and fecundity which are markers for a calorific or dietary restricted induced state of prolonged lifespan ruling out this mode as the potential cause for the lifespan increase (Virk et al., 2012). Our lab also found that bacterial lawns treated with SMX decreased accumulation of bacteria in the gut of *C. elegans* but did not correlate with an increased lifespan effect (Virk et al., 2016). It was proposed that a component of bacterial

exponential growth phase that is attenuated through folate inhibition by SMX may be responsible for reducing lifespan (Maynard, 2017).

### 3.1.1 Investigating formaldehyde toxicity

A mechanism proposed as a potential candidate for modulating lifespan in the context of folate is the biosynthesis of formaldehyde (Maynard, 2017). It was found that bacterial folate levels were highest during the first 48 -72 hours post seeding and these levels were reduced after treatment with SMX in particular 5,10-met THF (Maynard, 2017). 5,10-met THF is a key component as a methyl donor and acceptor for the serine-glycine pathway. The pathway yields formaldehyde and it has been shown to spontaneously degrade into formaldehyde along with the other folates DHF and THF (Burgos-Barragan et al., 2017; K. Denby et al., 2016; Gonzalez et al., 2006; Morellato et al., 2021; Ohata et al., 2019) and explained in more detail in chapter 1.3.11.

*C. elegans* consume the bacterial lawn, transit through it and reside in it which may expose them to excess formaldehyde endogenously and exogenously through digestion and direct contact. Due to its highly reactive properties formaldehyde may cause damaging chemical modification to proteins, cellular components and DNA (K. J. Denby et al., 2016). This may contribute to overwhelming the worms stress response if its presence in the gut lumen are elevated beyond the maximal capacity of endogenous detoxification pathways. SMX may reduce the presence of formaldehyde at its source preventing saturation of host and bacterial detoxification mechanisms to increase lifespan. A starting point to explore the toxicity hypothesis was investigating bacterial formaldehyde output under lifespan conditions. A formaldehyde sensitive *lacZ* reporter was used to measure metabolite output and if those changes influenced lifespan.

### 3.1.3 The effect of sulfamethoxazole on lawn morphology and bacterial motility

Our lab observed a difference between SMX and non-SMX lawns. There is an absence of bacterial transfer to the wider agar environment and a distinctive sharp edge to the SMX lawns. This may be linked to a loss of a folate dependant mechanism for proliferation. Whilst it was observed that bacteria are transferred away from the main lawn and seeded by the worms, it was limited to the *E. coli* OP50 strain and did not fully establish if they were able to grow and proliferate in competition with the parent lawn.

The mini lawn protocol developed by Pefani (2019) was adapted as a method for measuring lawn expansion in relation to proliferation across the agar. The method was used to observe the effect of the presence of the main bacterial lawn and the influence it may have on influencing satellite lawn growth. The unexpected by-product from the use of the reporter fusion plasmid was an opportunity to compare lawn morphology both temporally and spatially. To support this work, transmission electron microscopy (TEM) was conducted to provide a simple but effective means of observing morphological differences.

## 3.2 Chapter Aims

1. To investigate whether decreased formaldehyde levels could explain why decreased bacterial folate synthesis extends lifespan.
2. Investigate the effect of decreased folate synthesis on lawn morphology as a possible explanation for an extended lifespan.

## 3.3 Results

### 3.3.1 Measuring pJI134 formaldehyde sensing plasmid output

Endogenous formaldehyde rapidly degrades and is highly unstable. It was not viable to utilise common methods of measurement for biological metabolites such as LC-MS/MS to measure formaldehyde levels in the bacterial lawn. An alternative method was devised utilising *E. coli* strains transformed with a plasmid reporter fusion of the $P_{frm}$-*frmR*-*lacZ* (pJI134) plasmid kindly donated by Dr Peter Chivers of Durham University. The pJI134 plasmid insert contains the *frmRAB* promoter ($P_{frm}$) and the formaldehyde sensitive transcription regulator *frmR* that is ligated to the β-Galactosidase reporter *lacZ*. In the absence of formaldehyde, the plasmid functions by *frmR* remaining bound to $P_{frm}$ repressing the expression of *lacZ*. In the presence of formaldehyde, FrmR induces expression of the *lacZ* enzyme that hydrolyses β-Galactose 5-bromo-4-chloro-3-indolyl-β-D-galactopyranoside (Xgal) to release a substituted indole giving a product that is an intense blue (Juers, Matthews, & Huber, 2012) as an output of enzyme activity in response to endogenous formaldehyde.

The activity of the pJI134 $P_{frm}$-*frmR*-*lacZ* plasmid in response to endogenous formaldehyde turns the bacterial lawn blue. The brightness of the blue is relative to bacterial density so the output is inversely proportional, the higher the pixel brightness the fewer bacteria in a particular region and relative formaldehyde synthesis. Although the output from lacZ activity produces a darker image over time the spatiality of the lawn remains as activity is still quantitively localised relative to bacterial density. The mean grey scale brightness along the images X-axis data of each conditions replicates was used to produce a spatial output graph or 'morphology plot'. The lawn edges were aligned to create a consistent reference point for comparison and quantified as proximal to distal distance from the lawn interior (in arbitrary units) (figure 3.1A).

Under normal lifespan conditions *C. elegans* is introduced to *E. coli* at 48 hours of bacterial growth and plates are incubated at 25 °C. Considerable data and imagery was obtained and analysed for the three time points investigated. The experiment was allowed to run for 144 hours. Past this time point plasmid conditions became too saturated in blue to provide reasonable data for critical analysis (figure 3.1). This time point is 24 hours less than the worm transfer point of 168 hours. 72 hours is the mid-point of the experimental timeline for analysis and is also the maximum timepoint of the window for exponential growth that was found to decrease the lifespan of *C. elegans* (Maynard, 2017). Non-plasmid conditions provided a negative control and a baseline of endogenous lacZ output. Due to the lack of identifiable blue output of the negative control meant a statistical comparison was not made between DM and NGM plasmid and non-plasmid conditions.

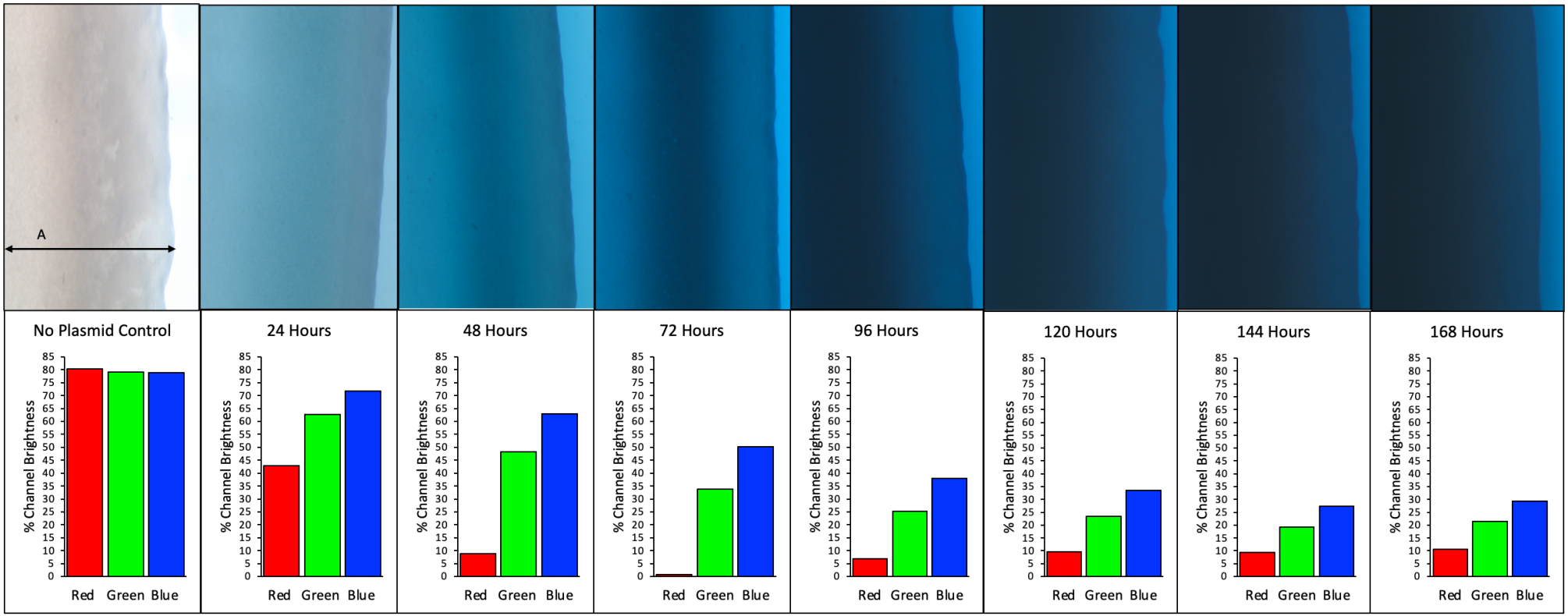


**Figure 3.1 Images of a WTK bacterial lawn over 7 days constitutively expressing the pJI135 *$P_{frm}$-$frmR_{STOP}$-lacZ plasmid*.** WTK bacteria was transformed with the plasmid *$P_{frm}$-$frmR_{STOP}$-lacZ* that constitutively expresses the *lacZ* enzyme. The plates (n= 5 plates per condition) were incubated at 25 °C for 168 hours to observe the long-term effect of lacZ output on the image analysis of blue**. A.** represents the line of measurement used to generate an average of Red, Green and Blue channel brightness from the images edge to the lawn edge. A 144 hours WTK no plasmid control has been included to demonstrate the colour channel output. The graphs show each time point and % brightness of each colour channel.

### 3.3.2 Quantification and Analysis of Images: What Makes Blue 'Blue'?

Because *lacZ* expression leads to a blue colour it was intuitive to measure the amount of total blue as a marker for this activity. Unfortunately measuring the blue output in relation to the background media proved to be problematic for several reasons. Firstly, the software tools used were developed for measuring GFP and localised staining. They require clear lines of demarcation to differentiate the border between a blue and non-blue region, enabling automated isolation of the area for quantification. Secondly, the image contained a wide distribution of multiple shades and concentrations of blue that merged within the lawn and background agar. They lacked any clear lines of separation between regions of high and low output. Thirdly, how humans view an image in its totality is not the same as how a computer views an image and returns its visual output via pixel brightness. The human eye interprets images as a product of reflected light in the form of a range of wavelengths within the visible spectrum of about 390 to 700 nanometres (Gomes & Preto, 2015). This is also subjective from an analytical point of view as individually our perception of an image is variable depending on light and visual impairments such as red-green colour blindness (Gomes & Preto, 2015). The image output from a computer processor is a multi-component representation based upon the product of the channels red, green and blue (RGB) (Goesele, 2004; T. Kumar & Verma, 2010). Each pixel is a sample of the original image and the intensity of the component RGB channels forms the representative colour output (Goesele, 2004).

To overcome this problem each component channel (RGB), hue, saturation and brightness (HSB) were explored to observe how they changed as the image increased in blue concentration. The software output of numerical data was a product of RGB brightness per pixel. The image was deconstructed into its greyscale components to determine where the changes in the image were occurring concerning the increased plasmid output generating a darker blue over time. Figure 3.1 shows that 'blue' in an image is a product of ratios of red and green in relation to the pixel brightness of blue. If red and green brightness decrease in a greater proportion to blue then the image is a more obvious 'blue' in colour. In this case, LacZ output from the pJI134 plasmid generates a darker shade of blue over time due to an increase in enzyme output in response to the presence of formaldehyde, i.e., the darker the blue the more formaldehyde is present, this is interpreted by the processor as a reduction in red and green brightness.

The interpretation of colour output cannot be changed between the experimental conditions. The image will always be a product of RGB (Red, Green, Blue) brightness, white will always have a maximal pixel brightness of Red = 255, Green = 255 and Blue = 255, and black will always be the opposite with Red = 0, Green = 0 and Blue = 0. Blue will always be a product of Red + Green + Blue with Red + Green determining how 'blue' the image appears and Blue dictating the shade and all three combined determining the overall brightness (T. Kumar & Verma, 2010). By understanding these relationships within the context of the images it was possible to inversely quantify the visual output for comparison. A flaw in this method was that beyond 144 hours the image became saturated and the Blue channel brightness increases altering the ability to accurately measure blueness at subsequent time points (figure 3.1). It is an inherent limitation but still provided a means to quantitively measure and compare conditions at up to and beyond 72 hours to sufficiently observe formaldehyde output for comparison.

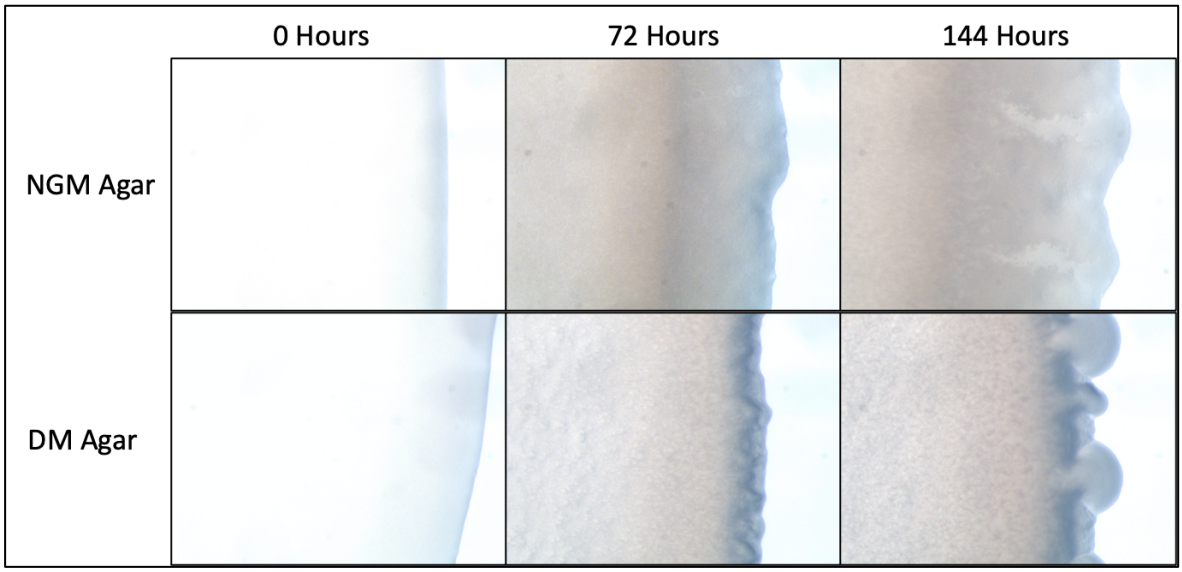


**Figure 3.2 Images of lawn section used for analysis showing endogenous LacZ activity.** Each image represents a single biological replicate for a section of 100 µl WTK non-plasmid bacterial lawn seeded on NGM or DM agar treated with Xgal. Images were taken at 0 hours (6 hours after seeding), 72 hours and 144 hours. Background *lacZ* activity can be observed as a blue output from the bacteria.

The non-plasmid conditions in figure 3.2 share the colour channel pattern of output but in their case, the blue is a residual output of endogenous lacZ in the background that changes very little and dissipates over time. The image composition consists of all three colour planes remaining high in relation to each other as the dominant colour seen is not 'blue'

but a ‘beige’ with a blue hue. This makes it very difficult to quantify and track endogenous *lacZ* output in these conditions or, use it as a basis for normalising plasmid output data. If endogenous LacZ was synthesising increased blue product then the image would still have to reflect this with the appropriate RGB output to generate a ‘blue’ image, thus by tracking the Red/Green ratio to blue gives a quantifiable output of LacZ irrespective of the addition of the plasmid. The rule for blueness still applies whereby the relationship of channel brightness is inverse to total blue but accuracy of this output is affected by the processer’s interpretation of the wider lawn image and the colour it presents.

3.3.4 Effect of sulfamethoxazole on formaldehyde synthesis in bacterial lawns

To investigate whether SMX inhibition of bacterial folate synthesis influences formaldehyde synthesis in bacterial lawns seeded on NGM and DM agar WTK bacteria was transformed with the pJI134 plasmid and the cultures seeded on to +/- SMX plates under lifespan conditions along with non-plasmid controls. Figures 3.3 and 3.4 show a comparison of all NGM and DM conditions respectively. The sample images demonstrate that the lawn sample area became increasingly bluer in colour over time. Accurate visual differentiation between SMX and non-SMX conditions is difficult due to individual subjectivity and the distribution of blue within the image. This may skew any interpretation of the visual data so analysis of the quantification of the blueness of the images was relied upon. The requirement of a different brightness of back light between NGM and DM agar to obtain accurate images made any kind of direct statistical comparison between the two media unachievable

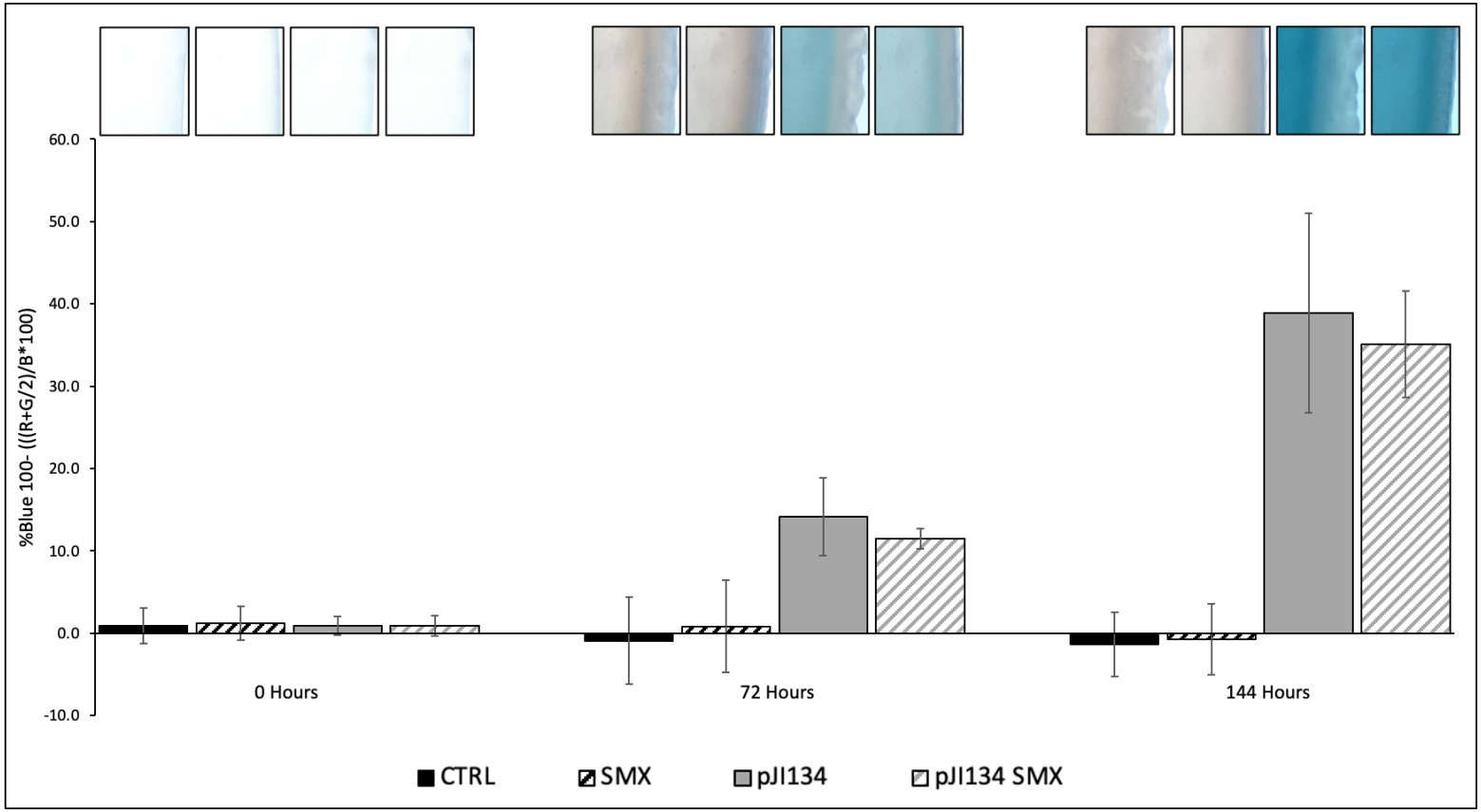


**Figure 3.3 Percentage blue of NGM agar seeded with 100 µl bacteria transformed with the pJI134 plasmid.** Transformed and non-transformed WTK were seeded onto NGM agar treated with Xgal +/- 128 µg/ml SMX and incubated at 25 °C (n= 3 plates per condition). **CTRL**. WTK; **SMX**. WTK + 128 µg/ml SMX; **pJI134**. WTK-pJI134 plasmid; **pJI134 SMX**. WTK-pJI134 plasmid + 128 µg/ml SMX. Images were taken at 0 hours (6 hours after seeding), 72 hours and 144 hours. Thumbnail images of the samples used have been included as a visual reference to the change in blue output over time. The blue level is expressed as an inverse percentage of pixel brightness. Error bars represent SD over 3 biological replicates. Statistical analysis was conducted using Student's t-Test Two-Sample Assuming Unequal Variances.

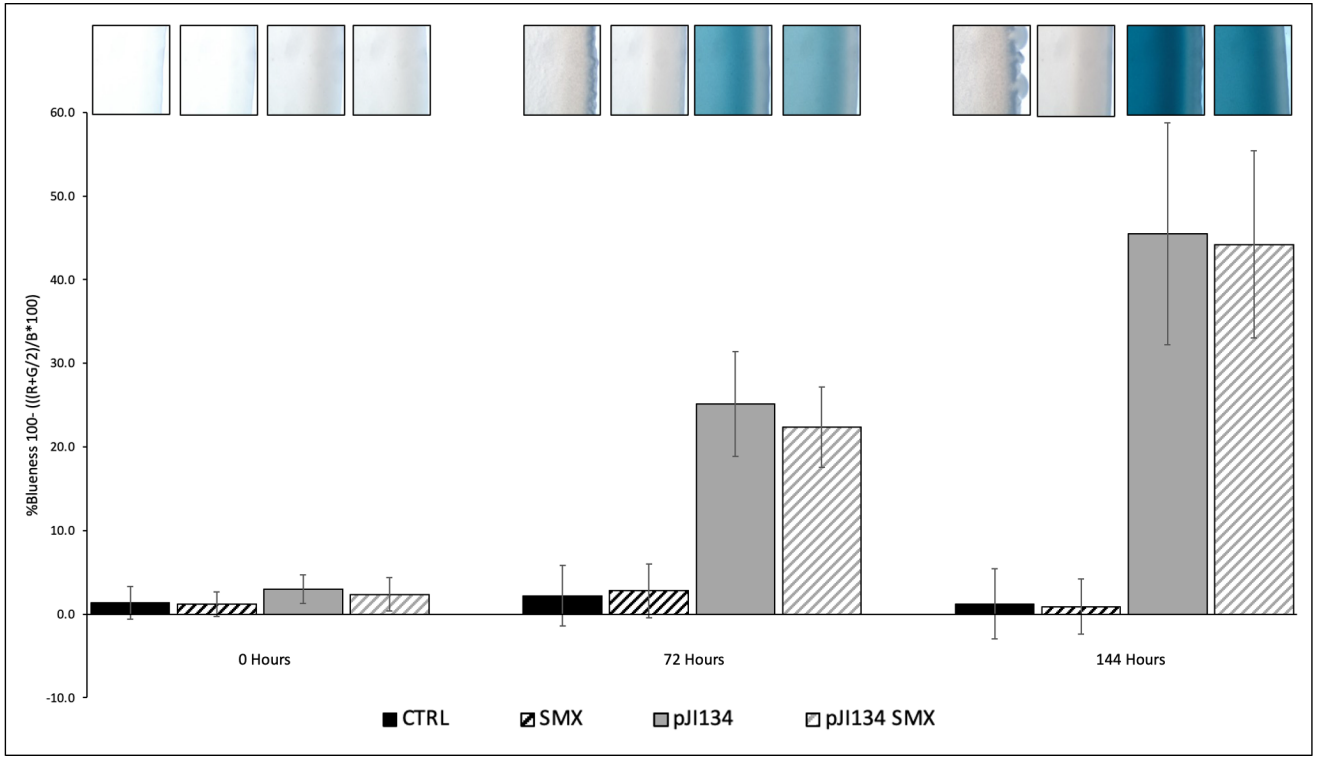


**Figure 3.4 Percentage blue of DM agar seeded with 100 µl bacteria transformed with the pJI134 plasmid.** Transformed and non-transformed WTK were seeded onto DM agar treated with Xgal, +/- 128 µg/ml SMX and incubated at 25 °C (n= 3 plates per condition). **CTRL**. WTK; **SMX**. WTK + 128 µg/ml SMX; **pJI134**. WTK-pJI134 plasmid; **pJI134 SMX**. WTK-pJI134 plasmid + 128 µg/ml SMX. Images were taken at 0 hours (6 hours after seeding), 72 hours and 144 hours. Thumbnail images of the samples used have been included as a visual reference to the change in blue output over time. The blue level is expressed as an inverse percentage of pixel brightness. Error bars represent SD over 3 biological replicates. Statistical analysis was conducted using Student's t-Test Two-Sample Assuming Unequal Variances.

To investigate the formaldehyde synthesis of bacteria on NGM the blue output of LacZ bacterial lawns seeded on NGM agar was measured (figure 3.3). It revealed that at 72 hours and 144 hours the pJI134 conditions have an increased blue output compared to the non plasmid conditions demonstrating that the pJI134 plasmid is functioning. The pJI134 conditions appear to have a difference in formaldehyde synthesis at 72 hours and 144 hours with SMX reducing output compared to non-SMX conditions although this difference is not significant (figure 3.3).

To understand the difference in formaldehyde synthesis on DM the experiment was repeated using DM agar as the substrate for the bacterial lawns (figure 3.4). It showed that the pJI134 conditions have a higher blue output than the non-pJI134 conditions again demonstrating the plasmid is functioning. At 72 hours and 144 hours, the pJI134 conditions have an increased amount of blue compared to pJI134-SMX which is slightly reduced although the difference is not significant (figure 3.3). A decrease in blueness on DM and NGM agar plates for the SMX plasmid conditions indicates a decrease in LacZ enzyme activity in response to endogenous formaldehyde. This suggests formaldehyde synthesis of a bacterial lawn treated with SMX may be mildly reduced compared to non-SMX treated lawns. The lack of statistical significance between the two conditions indicates that SMX does not reduce endogenous bacterial formaldehyde synthesis in lawns maintained on either NGM agar or DM agar.

To determine if non-pJI134 transformed bacteria have an endogenous LacZ output as part of normal metabolism that may skew the plasmid data and if SMX affected that output non-pJI134 lawns were investigated under the same lifespan conditions on both media (figures 3.3 & 3.4). It showed that bacterial lawns got progressively darker on both DM agar and NGM agar due to bacterial growth. It also showed that the lawns and agar retain a blue tinge as a result of background endogenous LacZ activity. The endogenous LacZ activity of non-pJI134 bacteria appear to decrease over time for both NGM and DM conditions. There is no significant difference in blueness between SMX and non-SMX conditions suggesting that SMX does not impair endogenous *lacZ* expression (figures 3.3 & 3.4). Although the differences in expression are small and non-significant it suggests that the endogenous LacZ product is not sufficient to produce an output that may contribute to a positive bias of plasmid activity on either media. The lack of non-pJI134

blue output may be attributed to it either not accumulating through reduced enzyme activity or the LacZ product being metabolised by the bacteria.

It should be noted that blue is not the dominant colour in the non-pJI134 images and from a statistical stand point there is no difference between the conditions. Non-pJI134 conditions contain only one copy of the gene for lacZ whilst the pJI134 conditions contain multiple copies of the enzyme enabling the bacteria to produce a considerably increased blue output in response to formaldehyde independently of the endogenous enzymes normal metabolic activity (Lodish et al., 2000).

The lack of quantified differences in formaldehyde synthesis for both NGM (figure 3.3) and DM (figure 3.4) could be attributed to several causes; a decrease in enzyme transcription or increase in enzyme degradation. A decrease in enzyme production due to decreased gene transcription of the plasmid. Decreased gene transcription due to decreased promoter activity and decreased promoter activity due to a decrease in endogenous formaldehyde synthesis. Previous work by Y. K. Kwon, M. B. Higgins, and J. D. Rabinowitz (2010) showed that inhibition of folate synthesis by the sulfonamide TMP significantly depleted bacterial glycine and purine levels triggering a starvation response in the bacteria that leads to inhibition of protein biosynthesis. The evidence here is not relevant to a conclusion about a bacterial stress response but it may allude to a reduction in gene transcription and decreased enzyme production. SMX may be having a similar effect by reducing the availability of folate species that degrade to formaldehyde folates. Maynard, Cummins, Green, and Weinkove (2018) showed that impaired folate biosynthesis levels of all folate species were significantly reduced although 5,10-met THF which is key folate upstream of purine synthesis and source of formaldehyde remained at a slightly higher level than the other species present. It may be a source of formaldehyde under these conditions that is maintaining the *frmR* response of pJI134 at similar levels to the non-SMX condition.

An alternative explanation to the change in blue output between time points and pJI134 conditions that may skew the data is that it could be a product of colour saturation or β-Galactose leakage. The lawn is a three-dimensional structure with a surface, circumferential edge and varying depth of lawn across its diameter. The increased levels of blue across the sample could be deemed as a readout of colour spread through

accumulation not bacterial activity. This is misleading visually as the differences in blue can be viewed but limitations within the analysis may not accurately represent the biological activity.

3.3.5 formaldehyde detoxification and *C. elegans* lifespan

To investigate if increased formaldehyde biosynthesis had a direct impact on *C. elegans* a lifespan assay was conducted using the Keio collection *E. coli* mutant *ΔfrmR*. This mutant lacks the formaldehyde sensing regulator *frmR* which is a negative repressor of the formaldehyde detoxification enzymes *frmAB* and discussed in more detail in chapter 1.3.11. The removal of this regulator causes constitutive expression of the *frmRAB* enzymes (K. J. Denby et al., 2016). Upregulating of the formaldehyde scavenging enzymes may be an important link to slowing *C. elegans* ageing and increasing lifespan through the removal of a potential source of toxicity.

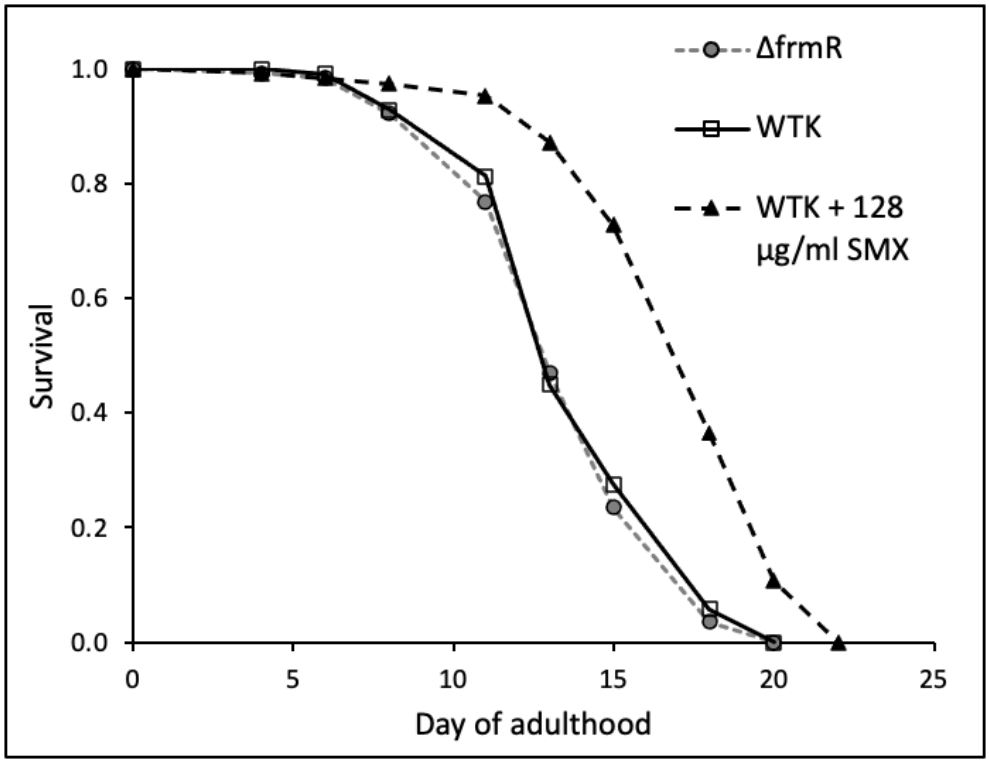


**Figure 3.5 Lifespan analysis of the *E. coli ΔfrmR* strain reveals constitutive expression of formaldehyde detoxification enzymes does not increase *C. elegans* lifespan.** *C.* elegans (n=120) were transferred at L4 stage onto NGM agar plates supplemented with +/- 128 µg/ml SMX and seeded with Δ*frmR* or WTK and incubated at 25 °C. The lifespan analysis was conducted using the Kaplan-Meier survival curve and JMP software. See thesis chapter 2.9 for full detail of conditions.

To investigate if increased expression of formaldehyde detoxification enzymes improved *C. elegans* longevity a lifespan assay with the *E. coli ΔfrmR* mutant was conducted. WTK + 128 μg/ml SMX was used as a positive control. The results show that constitutive expression of the formaldehyde detoxification enzymes *frmRAB* did not extend lifespan further than the WT condition (figure 3.5) suggesting that under normal folate synthesis conditions formaldehyde detoxification does not have a role in SMX mediated longevity.

### 3.3.6 Morphological differences of the bacterial lawn

To better understand if SMX induced differences in the bacterial lawn morphology that may have an influence on *C. elegans* lifespan the images obtained for the pJI134 plasmid investigation were used to create a montage. Each condition was imaged to provide a visual comparison of the lawn geography and the spatial arrangement of the bacteria within it. The RGB data obtained from each image was used to create a graphical representation of the lawn geography, referred to as morphology plots (figure 3.6). It can be clearly seen that the pJI134 plasmid conditions have a distinct morphological characteristic. They show an accumulation of bacteria in specific regions of the lawn area that is visually amplified due to the blue output. An absence of the plasmid still reveals the same spatial and morphological differences. These can be seen across all conditions suggesting the lawn retains regions of high and low metabolically active bacteria.

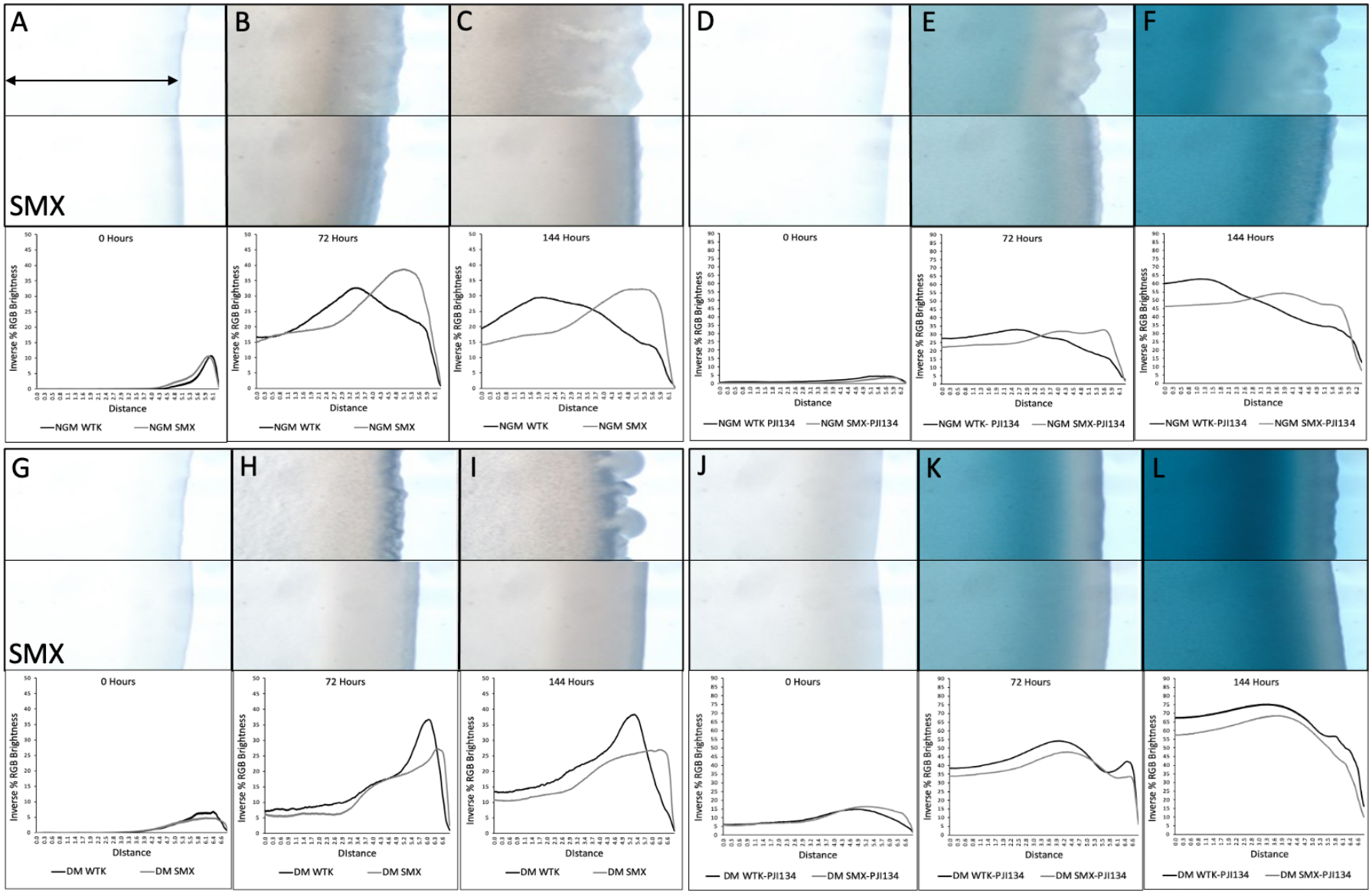
A
B
C
D
E
F
SMX
0 Hours
72 Hours
144 Hours
0 Hours
72 Hours
144 Hours
Inverse % RGB Brightness
Distance
NGM WTK
NGM SMX
NGM WTK PJI134
NGM SMX-PJI134
NGM WTK- PJI134
NGM WTK-PJI134
G
H
I
J
K
L
SMX
0 Hours
72 Hours
144 Hours
0 Hours
72 Hours
144 Hours
Inverse % RGB Brightness
DIstance
DM WTK
DM SMX
DM WTK-PJI134
DM SMX-PJI134

**Figure 3.6 Plots of bacterial lawn images using the inverse of percentage RGB brightness to produce a graphical representation of the lawn's topography.** As LacZ output increases the blue becomes darker indicating higher enzyme activity and regions of bacterial density. The graphs represent this change by an increase in the % value of the data for each time point (n= 3 plates per condition) as can be seen when comparing the peaks of the graph with the darker regions of the lawn images. The lawn edges were aligned for analysis to allow an equidistant measurement across samples. Due to this the location of the lawn edge is not spatially representative nor is the output quantitative. **A-C**. NGM agar +/128 μg/ml SMX no plasmid; **D-F**. NGM agar +/128 μg/ml SMX pJI134 plasmid; **G-I**. DM agar +/128 μg/ml SMX no plasmid; **J-L**. DM agar +/128 μg/ml SMX pJI134 plasmid. Images were restricted to a section of lawn edge due to the overall lawn size being too large to image. The double ended arrow represents the line of measurement that was used to plot the graph of the lawn topography for comparison.

To investigate if reduced bacterial folate synthesis alters the observed morphology the images of pJI134 and non-pJI134 SMX samples from both DM and NGM agar were analysed. It can be seen that DM agar bacteria treated with SMX have a smooth defined lawn perimeter that is less distinct but still present in the NGM conditions. The defined edge feature also occurs earlier in the timeline for DM agar. It is less pronounced between SMX and non-SMX conditions than NGM agar. The perimeter of non-SMX conditions does not share the feature of a defined edge. They appear to have an irregular and protuberant structure radiating peripherally. This suggests the bacteria may be expanding the footprint of the lawn although this appears to be attenuated by pJI134. Both NGM and DM agar have a dark band of bacterial aggregation distal to the lawn edge. The location of the band differs between conditions. It is more proximal to the lawn edge in the plasmid and SMX conditions suggesting these are regions of higher bacterial density. The edge regions may be influenced by the nutrient availability to the lawn or, metabolic demand of the lawn (figure 3.6).

It may be possible that the plasmid and its increased enzyme biosynthesis is putting the bacteria under further metabolic stress. Increased transcription and translation of the additional lacZ enzymes in the presence of a formaldehyde stimulus elicits an increase in demand for protein synthesis components which are downstream products of the folate cycle, such as purines and amino acids (Diaz Ricci & Hernández, 2000). This high demand state may further compromise bacterial metabolism beyond its capability to effectively proliferate in a nutrient controlled or low nutrient environment, this may also be the reason why on DM agar the lawn appears to have specific regions of bacteria distal to the perimeter as opposed to the NGM conditions where it appears more diffuse and more widely spread.

The property of each media may also contribute to morphological differences. DM is a chemically defined nutrient source that does not contain peptone but instead has a specific concentration of free amino acids, metals and vitamin B12. 0.1 μM PABA that is added to DM. The addition of these components compensate for the absence of folates and associated folate components available for metabolism by the bacteria (Helliwell, 2013). DM was specifically created to allow for a more controlled nutrient profile that supported growth at the same level as NGM but absent of folate breakdown products (Helliwell, 2013). NGM contains a proprietary peptone complex of vitamins, minerals, metals, amino

acids and peptides that provides all nutrients in abundance (Guide, 2019). NGM may have a higher concentration of folate precursor metabolites such as PABA which can compete with SMX enabling the bacteria to synthesise folates, subsequently activating downstream mechanisms enabling continued growth of the lawn to extend out into the agar (Maynard et al., 2018).

3.3.6i Morphology continued: Motility characteristics of the bacterial lawn

To determine if SMX removed a component of bacterial proliferation the images of the mini lawns from the original mini lawn protocol developed by Pefani (2019) were used to visually compare and contrast morphological differences between *E. coli* lawns with and without treatment with SMX.

Conveniently the images produced for analysis allowed for a more distanced analysis of the lawn area, the surface area covered by a 100 μl lawn made it impossible to image the entire lawn. Initial observations revealed that the 2 μl min lawns shared the same morphological characteristics as the significantly larger lawns allowing for a more detailed context to the commentary. These characteristics included the protuberant leading edge of the lawn perimeter and regions of bacterial accumulation internally distal from the perimeter as described in section 3.3.6 of this chapter.

The image analysis of the mini lawns showed that the regions of circumferential projection form a diffuse cloud like structure is clear to see in figure 3.7A. A darker band of bacterial accumulation adjacent to the lawn edge can also be seen in all images analysed (figures 3.6, 3.7B, 3.7E). The band of accumulation appears slightly different between the media due to different lighting conditions used to obtain the images and the size of the overall lawn alters its geographical position. The darker band of aggregation at the lawn edge suggests a region of higher bacterial density that can clearly be seen in figure 3.8B. Treatment of 128 μg/ml SMX produced a thin but darker leading edge to the lawns in figure 3.6 and this characteristic is easily observable in figure 3.7D.

The inner region of the lawn distally from the lawn edge in all conditions appears more diffuse suggesting an area of lower bacterial density (figures 3.6, 3.7C). The distribution of density within the bacterial lawn may be driven by nutrient availability. The leading edge

of the lawn retains the highest concentration of cells as they are in the region with the highest nutrient availability as the main body of the lawn consumes nutrients from the agar beneath it and in the immediate vicinity of its region of contact with the base substrate. The capacity to exploit the environment and obtain nutrients from the wider agar may be impaired by SMX. It may be attenuating nutrient sequestering and metabolism leading to a distinct region of low density within the lawn area and a narrow band of aggregation at the lawn edge of live but non-proliferating bacteria .

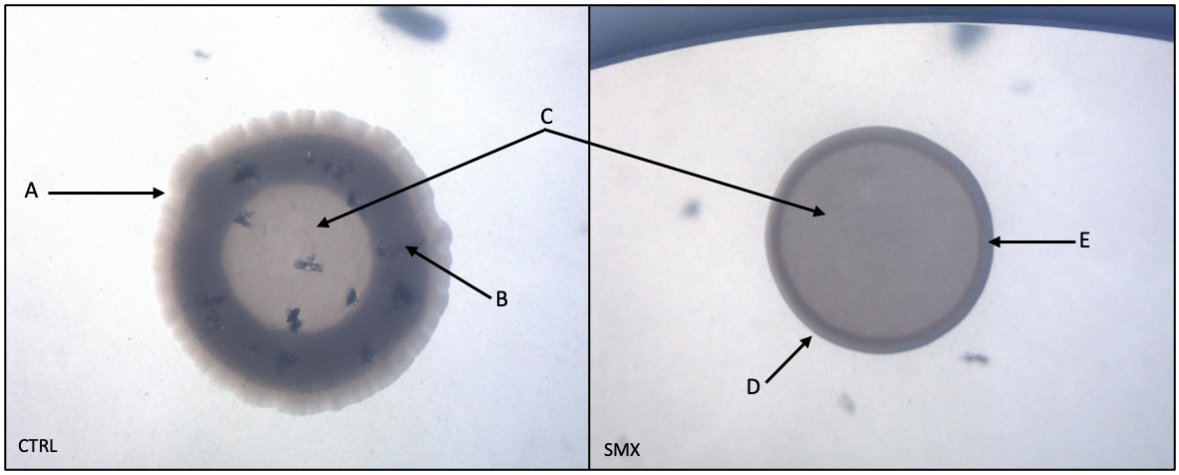


**Figure 3.7 Use of mini lawns show distinct morphological differences of bacteria treated with 128 µg/ml SMX.** Images are of mini lawns 9 days after seeding. WTK was cultured overnight in LB at 37 °C and used to seed 2 µl mini lawns in the presence or absence of a 100 µl parent lawn on NGM agar +/- 128 µg/ml SMX and incubated for 9 days at 25 °C. These experiments were limited to the use of NGM agar and LB cultures. The labelled arrows represent: **A**. Protuberant lawn edge of non- SMX conditions; **B**. Region of high bacterial accumulation in non-SMX conditions; **C**. Region of low bacterial accumulation in all conditions; **D**. SMX induced defined leading edge; **E**. Region of high bacterial accumulation in SMX conditions. CTRL, WTK no SMX.

The interior of the lawn (figure 3.8C) may represent a region of low bacterial density. Either through bacterial migration to the periphery over time or, loss of population through death. The central lawn region may also represent an area of low nutrient content. As the nutrients in the agar within the lawn footprint are consumed the population may enter a stationary phase (Kolter, Siegele, & Tormo, 1993) or, a growth assisted stationary phase (GASP) (Allocati, Masulli, Di Ilio, & De Laurenzi, 2015). GASP releases nutrients as a product of programmed bacterial cell death, supporting the wider population during periods of stress (Allocati et al., 2015; Pletnev, Osterman, Sergiev, Bogdanov, & Dontsova, 2015). Alternatively, as a product of overall lawn growth and nutrient demand

(figure 3.8) the bacteria may move concentrically to the periphery. The population accumulates and consolidates to form a region of higher bacterial density adjacent to the lawn edge (figures 3.7B, 3.7E) (J A Shapiro, 1987).

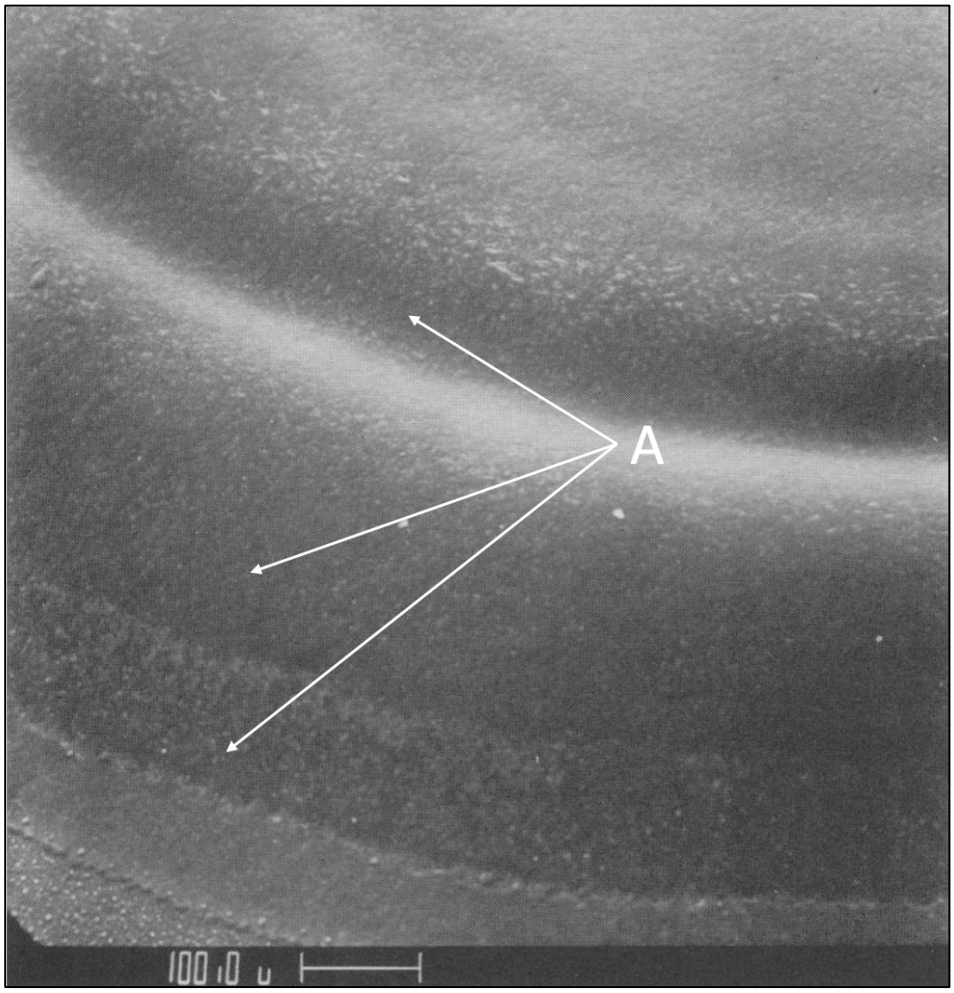


**Figure 3.8 Image demonstrating radial concentric growth ring formation by *E. coli*.** Low magnification scanning electron microscopy (SEM) was used to image growth bands of 1 µl bacterial culture inoculation spots on agar. **A**. Arrows denote concentric growth rings. Image adapted from (J A Shapiro, 1987)

The differing width of the aggregation band seen in figure 3.8 may be due to differences in overall population or the ability to exploit the nutrient content of the agar either through competitiveness, metabolic capacity or physical ability to respond to nutrient depletion within the environment. Section 3.3.7 of this chapter will discuss the competitive and nutrient gradient aspect and 3.3.8 will explore growth.

At the periphery of the lawn (figure 3.7A) cells may be in a more motile state with the lawn edge representing a region of motility referred to as the swarming zone (figure 3.9). Differentiation of vegetative cells in this region may be driven by a chemotaxic response to signals within the substrate such as nutrient concentration enabling exploitation of the environment to out compete competitors for resources and support population growth (G. M. Fraser & Hughes, 1999; Freilich et al., 2011; Sourjik & Wingreen, 2012). Differentiation to a motile state generates highly filamented cells adept at swarming that are able to migrate rapidly away from the main body of the lawn until they cease movement and revert by cell division to a vegetative state known as consolidation (Allison & Hughes, 1991; G. M. Fraser & Hughes, 1999).

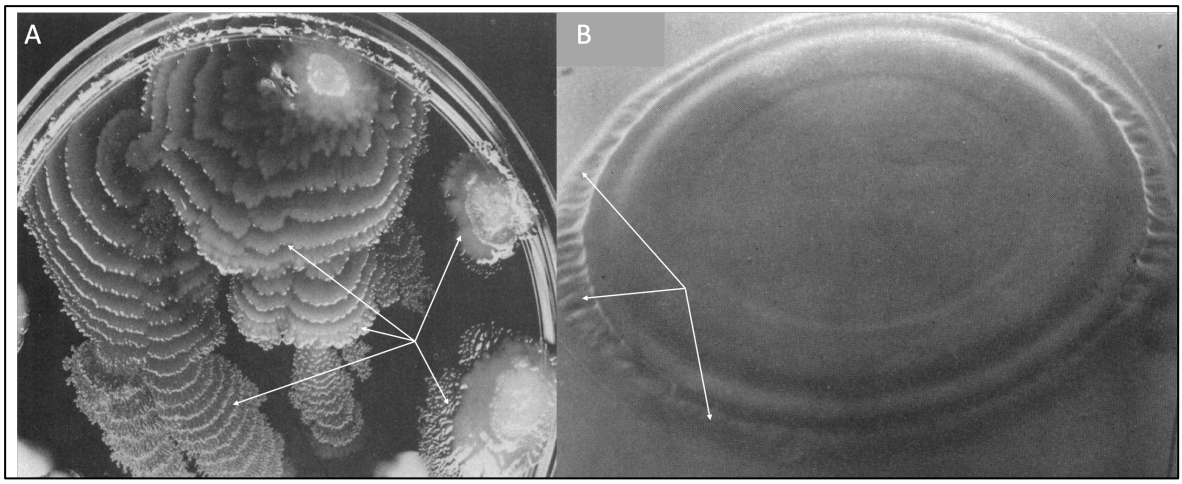


**Figure 3.9 Images of bacterial colony swarming zones.** **A**. *P. mirabilis* swarming over tryptone-yeast agar; **B**. Low magnification SEM image of a 48 hour spot inoculation of *E. coli* on agar. Arrows denote regions of swarming. Image adapted from (J A Shapiro, 1987)

Extracellular secretions form the liquid like edge of the lawn boundary (figure 3.7A) as a component of the swarming zone. Surfactants and lipopolysaccharides (LPS) act as wetting agents by extracting water from the agar creating a sufficiently fluid environment for motility (Inoue et al., 2007). LPS is considered to be crucial for swarming motility, in particular the O-antigen polysaccharide component confers a hydrophilic state to the bacterial cells alleviating friction and surface tension with the agar (Inoue et al., 2007).

The *E. coli* K-12 strain lacks the ability to express the O-antigen. It has previously been reported by Inoue et al. (2007) as being '*extremely fastidious'* about the correct environment for swarming. It will not swarm on agar concentrations above 1 % (our DM

and NGM agars are 2 %) requiring Eiken or LB-glucose-Difco agar to rescue this phenotype (Gómez-Gómez, Manfredi, Alonso, & Blázquez, 2007; Harshey, 2003). Swarming is contingent on surface moisture conditions and the expression of the O-antigen thus leading to the consensus that K-12 *E. coli* is poorly motile and incapable of swarming (Ambagaspitiye et al., 2019; Harshey, 2003; Inoue et al., 2007). Contrary to this it was reported by Allison and Hughes (1991) and Parker, Demetci, and Li (2019) that swarming can occur by non-swarming bacteria and poorly motile strains can adapt to their environment to become motile (Parker et al., 2019).

A definitive conclusion cannot be drawn from the images in figures 3.6 and 3.7 as to whether WTK is able to adopt a swarming phenotype. It does demonstrate a morphology that has similarities to the previously described swarming zone (figure 3.9) suggesting that even in the absence of the O-antigen the bacterial lawns are able to adopt a motile phenotype to promote lawn growth.

The effect of SMX on the lawn edge alters the motile morphology described previously to produce the characteristic defined lawn edge by mechanisms as yet undetermined. The physiological consequence of the pharmaceutical interference of the folate pathway is disruption of downstream products including amino acids, pyrimidines and purines (Burchall, 1973; Hitchings, 1973). It has previously been demonstrated that SMX does not impair bacterial growth in liquid culture (Virk et al., 2012) suggesting that the 1CM pathways involved in growth are sustained in the presence of SMX . Seeding bacteria directly onto the agar may limit nutrient accessibility or require increased endogenous synthesis of amino acids and other metabolites required for growth.

In an environment where nutrients are sparse or depleted *E. coli* are able to sense single amino acid starvation resulting in a stress response known as the stringent response (Magnusson, Farewell, & Nyström, 2005). The stringent response alters gene expression in preference of survival over growth by decreasing metabolism and increasing cell resistance to elicit a pro-stress and scavenging phenotype (Magnusson et al., 2005; Matin, Auger, Blum, & Schultz, 1989; Traxler et al., 2008). The product of the stringent response to nutrient starvation is down regulation of protein and purine synthesis and the physical structure and shape of the cell capsule changes to become a spherical structure with a large periplasmic space (D. E. Chang, Smalley, & Conway, 2002; K. Liu, Bittner, & Wang,

2015; Navarro Llorens, Tormo, & Martínez-García, 2010). In an amino acid deprivation model of serine depletion, it has previously been seen that chemotactic and motility metabolic pathways are downregulated (Durfee, Hansen, Zhi, Blattner, & Jin, 2008). Flagellum expression is reduced by repression of the gene *FlhDC,* a transcription factor responsible for regulating biogenesis of flagellum and swarming migration (Claret & Hughes, 2002; Durfee et al., 2008; Stafford, Ogi, & Hughes, 2005).

Another possible mechanism for the loss of a motile region in SMX treated *E. coli* is the disruption of the chemotaxis pathways which modulate bacterial responses to nutrient signals. *E. coli* can sense chemical signals in its environment and react by moving towards or away from that signal based on favourability (Colin & Sourjik, 2017). the array of sensors responsible for this sensing mechanism is composed of methyl-accepting chemotaxis proteins (MCP) (Colin & Sourjik, 2017). The MCP transmembrane receptors activate intracellular signalling pathways that control flagella motors enabling the bacteria to respond and adapt to its environment (Clausznitzer, Oleksiuk, Løvdok, Sourjik, & Endres, 2010; Parkinson, Hazelbauer, & Falke, 2015).

A key component to this signalling pathway is the cytosolic *S*-adenosylmethionine-dependant methyltransferase CheR and the deamidase/methylesterase CheB (Parkinson et al., 2015). The enzyme CheR utilises the carbon donor SAM to methylate the MCPs into an 'on-state' driving the flagellar motor response (Parkinson et al., 2015). The 'off-state' is driven by demethylation of the MCPs by CheB which together with CheR act in a feedback loop enabling adaptation to external stimuli (Parkinson et al., 2015). Inhibition of folate synthesis by SMX may interfere with the MCP pathway. SAM synthesis is dependent on the folate pathway product 5-methyl THF (H. S. Choi et al., 2021; Marriott, Birt, Stalling, & Yates, 2020). Maynard (2017) showed that OP50 *E. coli* treated with 128 μg/ml SMX ceased to synthesise 5-methyl THF. It has previously been shown that inhibition of bacterial folate synthesis with sulfonamides effects SAM levels that drive a feedback to further impair folate synthesis (H. Choi et al., 2019; H. S. Choi et al., 2021). The downstream effect may be a reduction or loss of SAM leading to inactivation of the MCP sensing network preventing bacterial lawn differentiation into a motile state and reducing proliferation.

3.3.7 Electron microscopy to observe if impaired folate synthesis alters flagella expression

In order to observe if motility components were present in *E. coli* treated with SMX transmission electron microscopy (TEM) was used to image bacteria extracted from the lawn. Flagella are fragile and easily damaged from direct physical contact such as removing lawns by scraping so a method was developed in an attempt to preserve the integrity of expressed motility components.

The lawn removal method involved removing a 1 $cm^3$ chunk of the agar incorporating as much of the lawn perimeter without damaging it with the scalpel and placing it in a 6-well plate. A Pasteur pipette was used to wash the lawn from the chunk with 1-2 ml of M9. Once the lawn was removed from the slice the agar was discarded and the bacteria could be extracted. Due to the fragility of the flagella and risk of damage from a narrow aperture tip of standard 1000 µl pipette a Pasteur pipette was used to isolate the bacteria for sample preparation. This provided an improved technique for preserving physical components of the bacteria but detrimentally the lawns were diluted and partially homogenised preventing accurate identification of sample location within the lawn. The bacteria observed in figure 3.10 could have originated from any region proximal or distal to the lawn edge within the area of the extracted lawn as demonstrated by figures 3.7A and 3.7B.

The TEM images revealed that numerous flagella were present in the non-SMX condition (figures 3.10A-C) whilst in the SMX condition none were present except for what appears to be a clump of tangled and aggregated flagella or flagella components (figures 3.10D-E). The images do suggest that SMX may reduce flagella expression or disrupt flagella synthesis to produce a non-motile phenotype through damaged or improperly constructed flagella as seen in figure 3.10F.

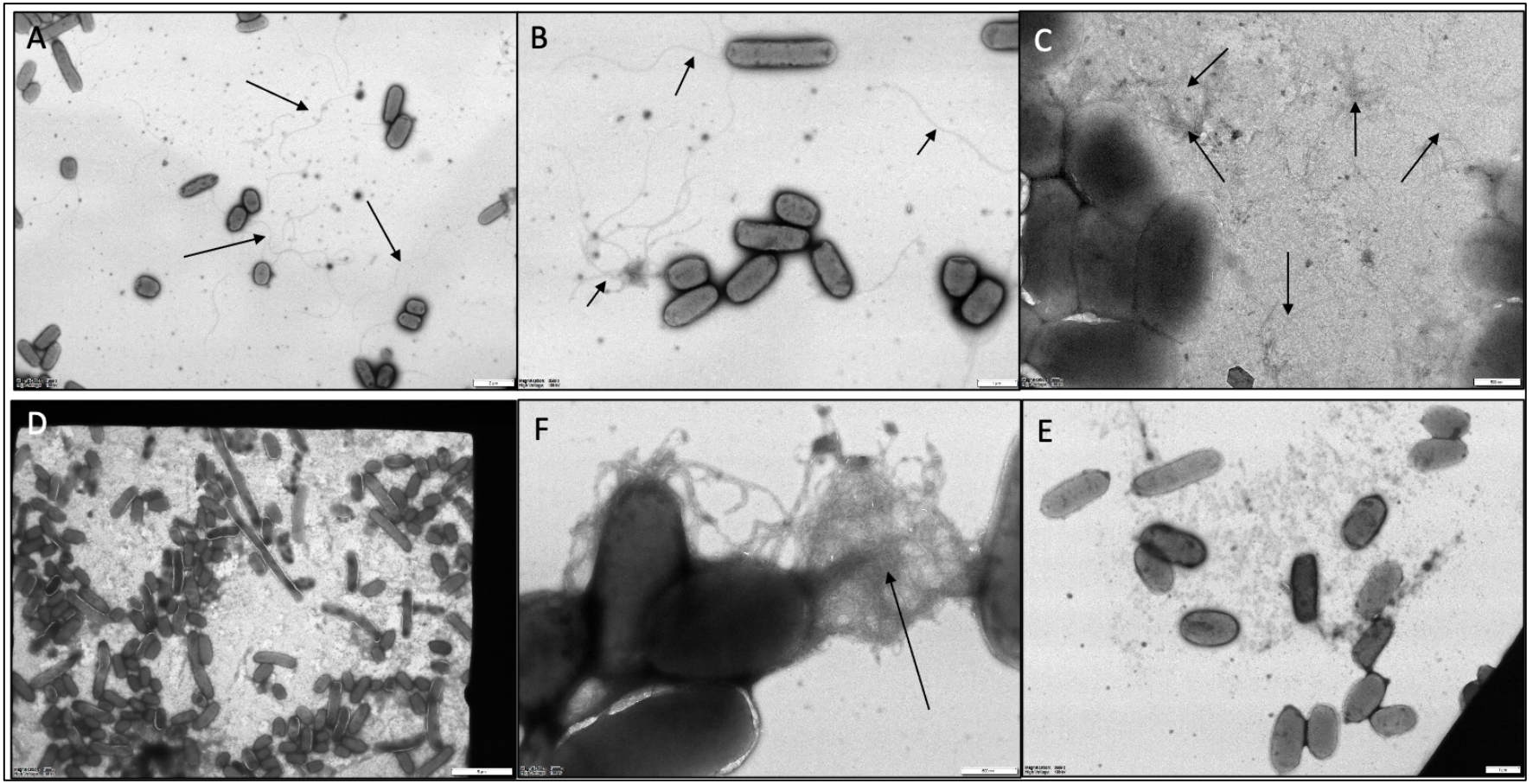


**Figure 3.10 TEM images of samples taken from 100 µl *E. coli* lawns at increasing magnification show 128 µg/ml SMX alters expression of flagella.**

Samples were obtained from the edge of a single bacterial lawn, 100 µl LB WTK cultures were seeded on NGM agar +/- 128 µg/ml SMX and incubated at 25 °C for 48 hours. Arrows denote flagella, **A**, WTK no SMX 1800x magnification**; B**, WTK no SMX 3500x magnification; C, WTK no SMX 8000x magnification; D, WTK + 128 µg/ml SMX 1000x magnification; E, WTK + 128 µg/ml SMX 3000x magnification; F, WTK + 128 µg/ml SMX 10000x magnification.

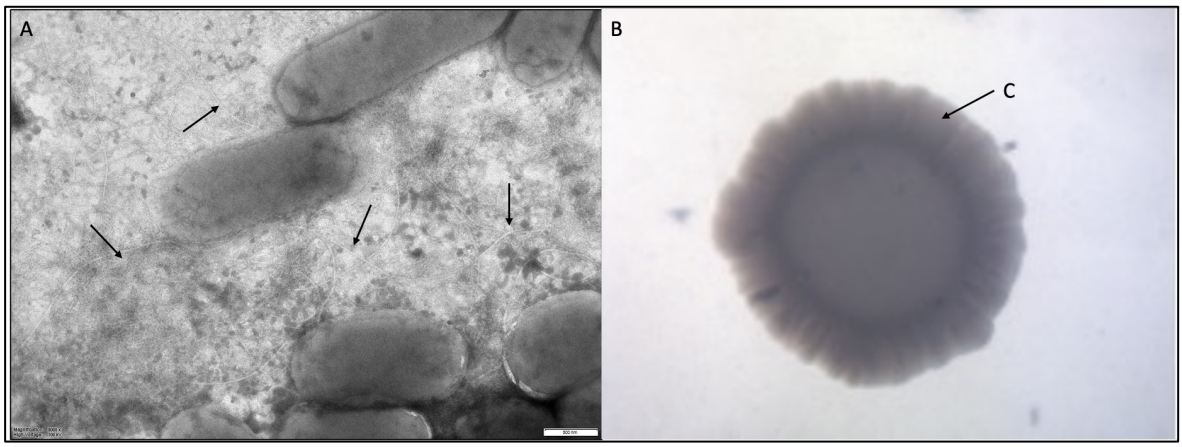


**Figure 3.11 TEM and mini lawn image of the reduced folate synthesis *E. coli ΔrpoS* mutant demonstrating the absence of motility components does not correlate with *C. elegans* lifespan.** **A**. TEM image of *ΔrpoS* bacteria recovered from a 100 µl lawn with arrows to denote flagella; **B**. Image of *ΔrpoS* mini lawn; **C**. Motility region.

To observe if flagella expression was impaired in other low folate extended lifespan models the *ΔrpoS E. coli* mutant that has been shown to robustly increase the lifespan of *C. elegans* and has reduced folate synthesis (Virk et al., 2016) was imaged. The TEM image showed that *ΔrpoS* has flagella expressed in abundance and can be seen in large quantities surrounding the bacteria (figure 3.11A). It was not possible to determine from the images whether the aggregation of the flagella was a product of impaired flagella assembly or a product of the extraction and fixing method. Images were also taken of mini lawns of *ΔrpoS*. These were not used for any quantitative analysis under the context of proliferation but purely to observe if the motility zone morphology is abolished or conserved in correlation with a lifespan increasing bacterial strain. It can be seen in figure 3.13B that the motility zone morphology (figure 3.11C) is retained suggesting flagella expression and mechanisms of motility remains intact.

Here it can be seen that in the low folate mutant *ΔrpoS* the components and motility morphology are intact. This suggests that the absence of flagella or components associated with motility as seen in SMX treated *E. coli* may not correlate with the increased lifespan of *C. elegans* in a low folate model.

### 3.3.8 Exploiting the agar, nutrient gradients and competitive growth

An observation seen in our lifespans is that the worms are able to transfer and seed bacteria around the wider agar as a product of their roaming activities. This phenomenon is not

seen on plates treated with SMX with little to no transfer occurring across the 9 day duration of a plates use. The absence of these lawns or bacterial spreading in the presence of SMX was originally investigated by Pefani (2019) and is discussed in more detail in chapter 1.3.6. The experimental protocol involved seeding <5 µl diluted bacterial cultures (mini lawns) on NGM agar to replicate bacteria transfer from a parent lawn by *C. elegans* over the course of a lifespan experiment. The NGM agar substrate was either non-treated or treated with 16 µg/ml, 32 µg/ml or 128 µg/ml of SMX. The mini lawns were then imaged and visually analysed for growth differences.

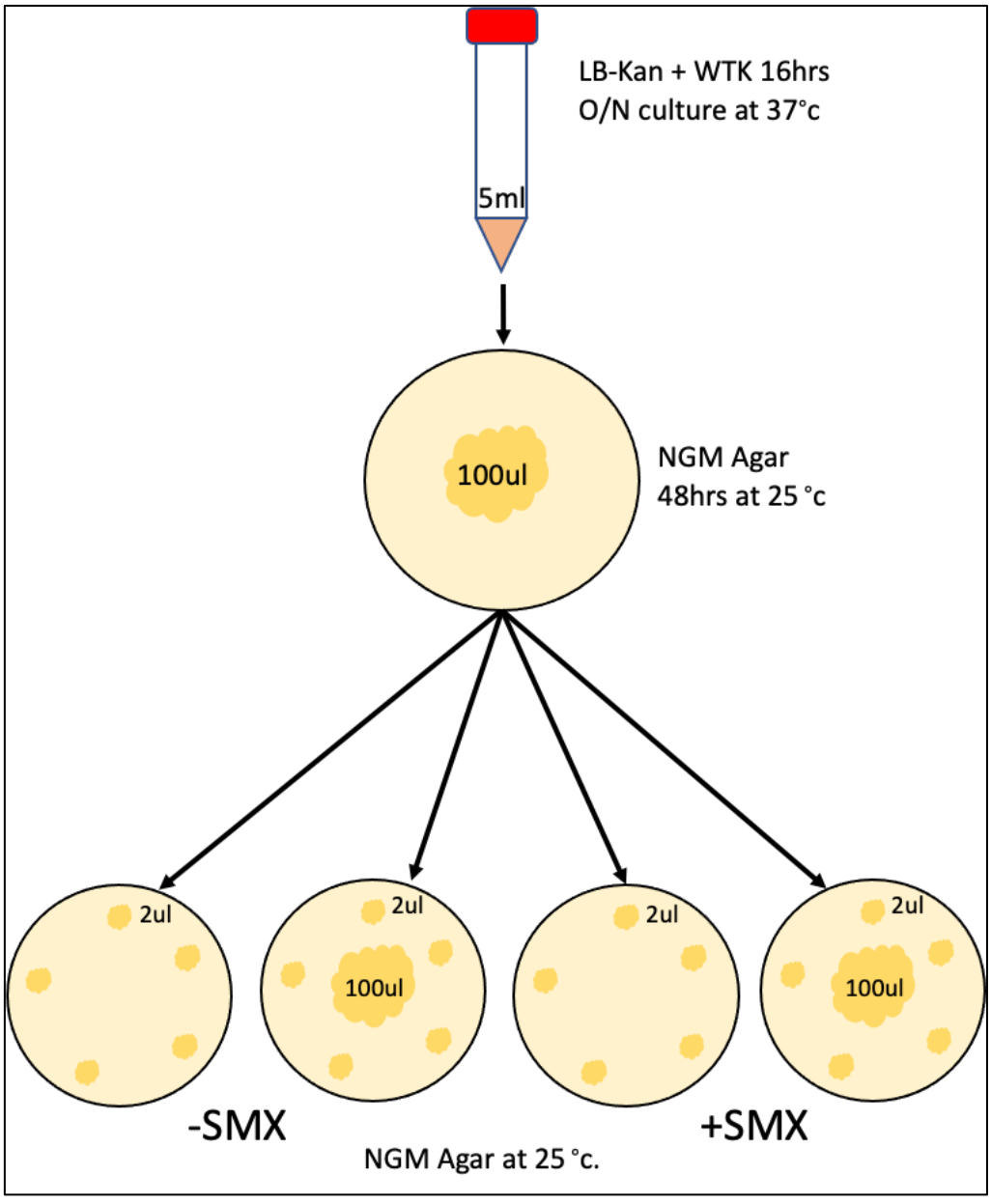


**Figure 3.12 Schematic of the mini lawn protocol.**

I adapted this protocol to explore if SMX prevented bacterial proliferation when isolated in low cell numbers through either a loss in motility to exploit the environment or if a competition exists from the parent lawn that attenuates growth. The adaptation involved seeding 2 µl mini lawns in the absence or presence of a 100 µl parent lawn onto SMX treated and non- treated NGM agar (figure 3.12). The mini lawns were imaged and the perimeter measured daily over the duration of 9 days enabling me to quantify and measure differences in bacterial proliferation. 2 µl was found to be the smallest volume that could be accurately pipetted onto agar to form a spherical lawn without damaging the surface of the substrate. It should also be noted that 2 µl of bacterial culture contains considerably more cells than a single worm will transport from the parent lawn. A limitation was the use of NGM as opposed to DM as larger than 5 µl mini lawns were required to guarantee sufficient growth which proved problematic for image capture over time. As both DM and NGM share the same lawn edge characteristics this was deemed an acceptable trade off.

The mini lawn data showed that in CTRL versus SMX conditions there was a significant difference between mini lawn surface area in both the absence and presence of a parent lawn ($P=<0.001$). The surface area of the CTRL mini lawns is increasing and the SMX mini lawns have decreased over time, visually it can be seen the lawns have been able to grow (figure 3.7). Without corroborating $OD_{600}$ data a comparison cannot be made. The data does suggest that any motile ability to expand the lawns periphery is absent in the SMX conditions. Growth curves have shown SMX lawns are considerably smaller in biomass than WTK lawns (discussed in detail in section 5.3 - 5.3.4 of chapter 5). The assumption here would be that mini lawns share the same population characteristic although, this may not be a true reflection of a larger lawns capacity to expand due to significantly lower cell numbers from culture dilution as part of the protocol.

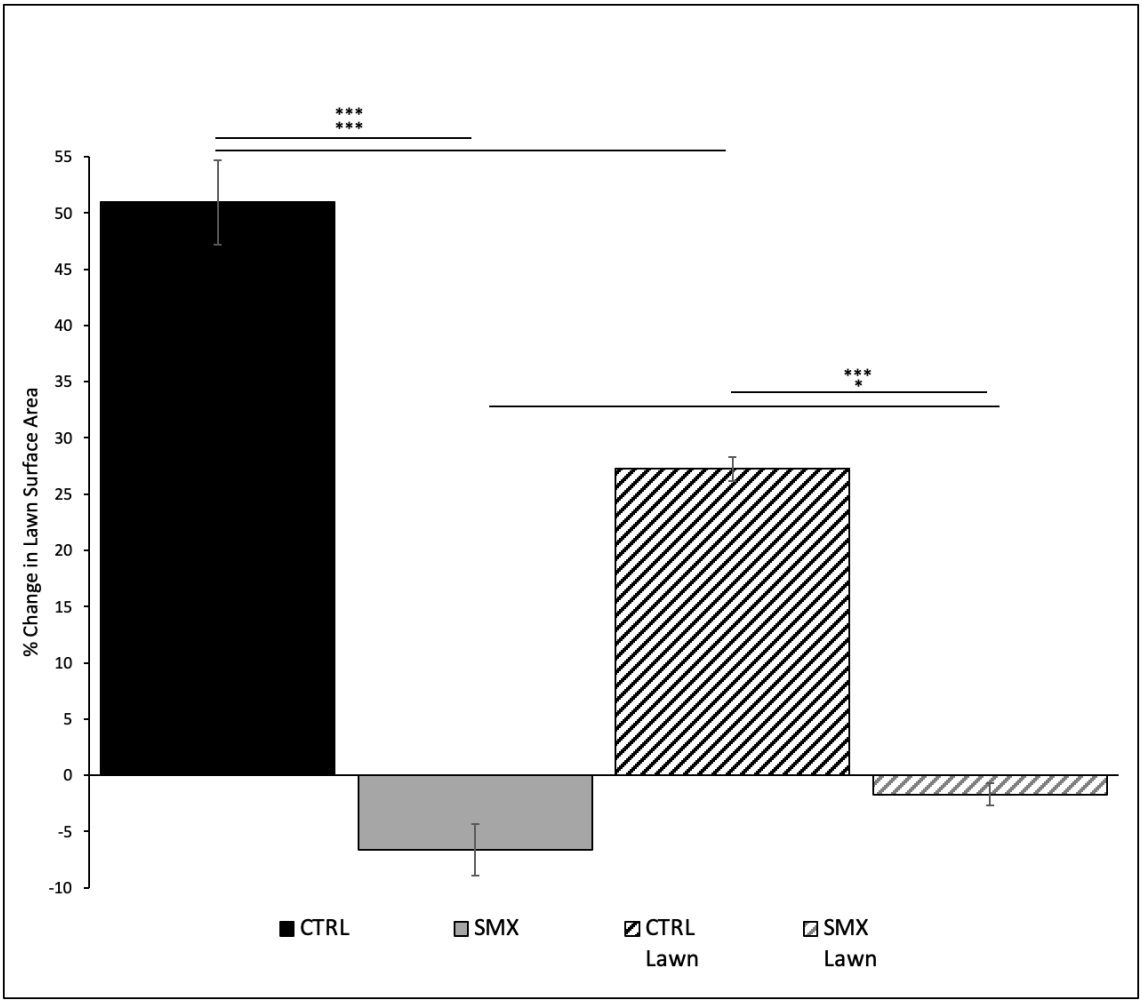


**Figure 3.13 Analysis of WTK mini lawn surface area in the presence or absence of a competing lawn and 128 μg/ml SMX.** Images were taken at 16 hours (T0) and 9 days (T9) after seeding. Images were analysed by measuring the lawn perimeter at T0 and T9, change was calculated by ((T9-T0)/T9)*100 %. Error bars represent SD over 15 biological replicates. Asterisks represent the results of Student's t-Test Two-Sample Assuming Unequal Variances, ***=P<0.001, **=P<0.005, *=P<0.05.

The presence of the parent lawn may be a significant competitor to the mini lawns. The non-parent lawn CTRL mini lawns grew by 51 % compared to the parent lawn exposed CTRL mini lawns that had a gain of 27 %, an almost 50 % difference (P=<0.001) (figure 3.13). The parent lawn has a considerably higher biomass to the mini lawns creating a higher demand for the agar nutrients whilst having the capacity to harvest them. It may have outcompeted the mini lawns including scavenging of its own metabolites obtaining the majority share of nutrients to create a larger gradient in the agar (Gude et al., 2020; Koch, 1999; Wolfe & Berg, 1989). Nutrients may move down a gradient as the parent lawn utilises them at a higher rate than the surrounding mini lawns creating an

asymmetrical gradient in detriment to the mini lawns (figure 3.14A). The growth of the mini lawns is unable to keep up as supply is unable to match demand attenuating proliferation across the agar to expand their footprint (Inoue et al., 2007; Limoli et al., 2019).

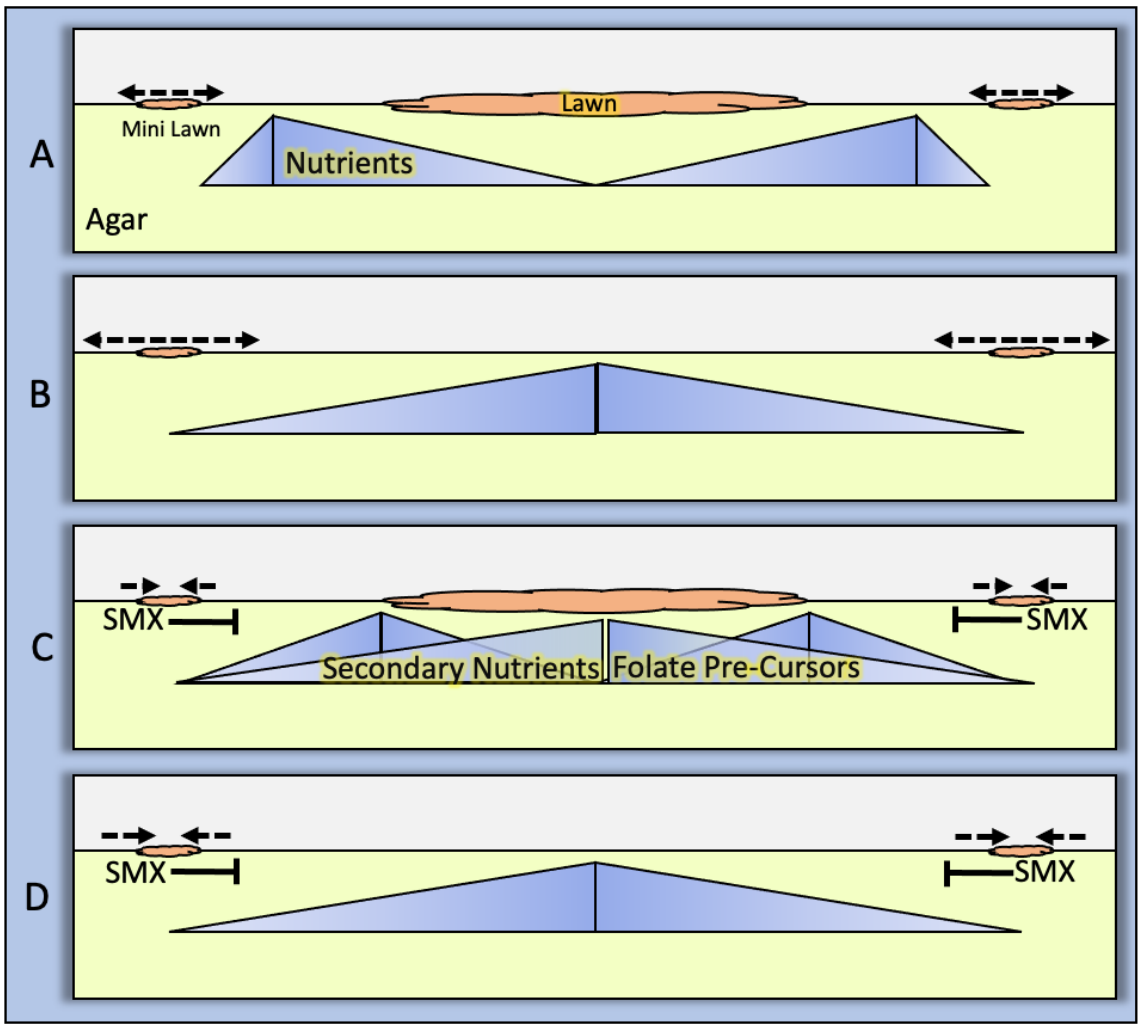


**Figure 3.14 Model of proposed nutrient gradients in agar and the effect on WTK mini lawn surface area growth in the presence or absence of a competing lawn.** A, NGM agar nutrient gradient in the presence of mini lawns and parent lawn; B, NGM agar nutrient gradient with mini lawns only; C, NGM agar + 128 μg/ml SMX nutrient gradient and opposing lawn derived nutrient and folate pre-cursor gradients from parent lawn with mini lawns; D, NGM agar + 128 μg/ml SMX nutrient gradient with mini lawns only. Triangles denote concentration gradient; Dotted arrows denote growth or shrinkage of the mini lawn; T bar denotes inhibition of 1CM.

The absence of a parent lawn revealed non-parent lawn mini lawns increased their footprint considerably more than the parent lawn conditions (figure 3.13). The lack of

competitive pressure effectively provided unhindered access to the nutrient reservoir in the agar to drive and sustain growth (Gude et al., 2020) (figure 3.14A).

The SMX mini lawns area decreases irrespective of the presence of a parent lawn (figure 3.13). The reduction in mini lawn area is significantly different between parent and non-parent lawn conditions ($P = <0.05$). The SMX parent lawn condition revealed the SMX mini-lawns shrank less than the non-parent lawn SMX mini lawn condition (figure 3.13). This suggests NGM agar lacks sufficient folate pre-cursor substrates to rescue SMX impaired mini-lawn growth. The presence of a parent lawn may provide additional nutrients and folate pre-cursor metabolites to partially recover growth or, have an increased uptake of SMX, decreasing concentration in the agar. The parent lawn may sequester a larger proportion of SMX than the mini lawn and the bacterial turn-over within the parent lawn may be excreting metabolites, including folate pre-cursors (figure 3.14C).

The presence of a secondary gradient and increased uptake of SMX by the parent lawn may rescue the effect of SMX on mini lawns, but not reverse that effect in its entirety. In the parent lawn SMX condition, both the parent lawn and the mini lawns are subject to the effects of impaired folate synthesis by SMX. This may hinder the separate bacterial population's ability to exploit the NGM nutrient content. (figure 3.14C, 3.14D). The hindering of nutrient exploitation may be a product of impaired 1CM potentially creating a more evenly balanced nutrient gradient. The secondary nutrient gradient is in an opposing direction to the existing NGM nutrient gradient. The secondary gradient potentially maintains the mini lawns by enabling access to a larger proportion of available nutrients whilst providing folate rescue metabolites preventing shrinkage at the same level as seen with its non-parent lawn counterpart.

Counterintuitively, the absence of a parent lawn increased the regression of the non-parent lawn condition SMX mini lawns compared to non-parent lawn SMX mini lawns (figure 3.13). The absence of a parent lawn may remove a large bacterial population that may sequester a higher proportion of SMX and provide growth rescue metabolites to the mini lawns. The SMX mini lawns are then exposed to the full effect of SMX severely inhibiting growth (figure 3.14D). This is compounded by a loss of bacterial proliferation mechanisms through disruption to 1CM preventing uptake and utilisation of available nutrients (Ducker & Rabinowitz, 2017; Shetty & Varshney, 2021).

Here in both SMX parent lawn and non-parent lawn conditions mini lawn growth wasn't abolished as the original seeded culture produced the T9 mini lawn (figure 3.7). The results suggest the 2 µl dilute cultures contained sufficient bacteria to establish a surviving bacterial population. Growth of the seeded population was above a minimum growth threshold in the presence of a sub-mic (a concentration that alters the biochemistry of the bacteria without effecting growth) dose of SMX.

SMX may induce a transition to stationary phase by the mini lawn bacteria causing the observed lawn to shrink. During periods of insult such as starvation or nutrient deprivation bacteria can enter stationary phase (Kolter et al., 1993). Stationary phase is commonly referred to as the point post growth phase where cell division and cell death is at equilibrium (Kolter et al., 1993; Navarro Llorens et al., 2010). It is not a period of stasis, but a reversible transitioning point ensuring bacterial viability and a descriptive term that does not discern if cell metabolism and division are active (Kolter et al., 1993). When subjected to the insult of SMX the bacteria may be discarding motility machinery and deactivating transcription machinery involved in environmental or resource utilisation (Aurelia Battesti, Majdalani, & Gottesman, 2011; Ferreira et al., 2019). The adaptive response may prevent the mini-lawns from becoming more established and increasing their footprint in the agar.

The lawn edge may represent a region of high value to the bacteria for the proliferation of the population. Because the non-SMX condition can fully utilise 1CM pathways it is still able to exploit its environment even as a mini lawn in competition with the parent lawn. The SMX condition may induce an increase in demand for exogenous metabolic substrates to drive 1CM and subsequently growth and proliferation. The absence of folates may prevent proper uptake and utilisation of these to drive lawn expansion and growth, even with the potential rescue effect of parent lawn metabolites. SMX may prevent proliferation of bacteria beyond the parent lawn by disruption of nutrient sensing and adaptation mechanisms that drive a stress response. In isolation, very low cell numbers may result in a total failure to establish and grow through the absence of communal nutrient rescue or the collective ability to override the limiting effect of SMX on folate synthesis and 1CM.

## 3.4 Discussion

3.4.1 Sulfamethoxazole is unlikely to decrease bacterial formaldehyde levels

The investigation into the mechanism of SMX extended lifespan began by testing the original hypothesis of Maynard (2017) that formaldehyde as a downstream metabolite of the folate pathway may be a source of toxicity to *C. elegans* that reduces its lifespan. The first part of this chapter made use of a formaldehyde sensing *lacZ* reporter that converted Xgal to a blue indole as a marker for endogenous formaldehyde with output relative to formaldehyde levels in the bacteria

The quantification of output by a *lacZ* reporter in a bacterial lawn has not previously been reported in the literature. This work developed a novel way to convert a visual image as seen by the naked eye into a quantifiable image as 'seen' by an image processor to quantify the colour blue as a product of LacZ enzyme activity. It was found that the ratio of green and red pixel channel brightness in relation to the blue pixel brightness produced quantifiable data up until the 144 hour timepoint that was termed 'blueness'. This is an arbitrary label to describe a quantified perception of the processor's output of the colour blue and its respective shades. To consolidate the formaldehyde output data the *E. coli ΔfrmR* strain that constitutively expresses the formaldehyde detoxification enzyme FrmA/B was used to determine if the presence of increased or decreased endogenous bacterial formaldehyde decreased or increased lifespan in *C. elegans.*

This method of analysis had limitations. After 144 hours the numerical output ceased to be representative of the changes visually seen in the sample images. The relative changes in the colour channels no longer matched the visual output in relation to the parameters of the calculation, skewing the data. Another limitation was the formaldehyde sensing reporter fusion lacked enough sensitivity to detect low levels of formaldehyde. Use of a standard curve for the plasmid output may have provided more clarity on the sensitivity and output relative to conversion of Xgal for a more accurate analysis. It may also be possible that when *E. coli* is masticated *by C. elegans's* pharyngeal grinder or digested, increased formaldehyde is released causing higher concentrations in the worm gut.

The evidence indicated SMX did not significantly reduce formaldehyde in the bacterial lawn. Neither NGM nor DM agars had a significant difference in blueness at each

timepoint irrespective of treatment with SMX. If formaldehyde is a source of toxicity the permanent expression of detoxification enzymes by loss of *frmR* would increase *C. elegans* lifespan. Increased systemic clearance of formaldehyde would remove any potential toxicity towards *C. elegans* and potentially extend lifespan. The data revealed this did not occur. *C. elegans* maintained on *ΔfrmR* had a survival rate no different from the WT control.

Together this suggests that prolonged exposure to formaldehyde from its food source and the immediate environment does not decrease lifespan and an increased detoxification capacity in *E. coli* does not contribute to an increase in lifespan. Both *C. elegans* and *E. coli* contain detoxification pathways for removing formaldehyde. A spontaneous reaction between glutathione (GSH) and formaldehyde forms *S*-hydroxymethylglutathione (HMGS), an alcohol dehydrogenase (ADH5 in *C. elegans*) and *S*-hydroxymethylglutathione dehydrogenase (*frmA* in *E. coli*) oxidises HMGS to *S*-formylglutathione (FGSH). FGSH is hydrolysed by an *S*-formylglutathione hydrolase (FrmB and YeiG in *E. coli*) that is yet to be documented in *C. elegans* to GSH and formate that feeds back into 1CM (Burgos-Barragan et al., 2017; N. H. Chen et al., 2016; K. J. Denby et al., 2016; Dingler et al., 2020; Gonzalez et al., 2006).

Given that both organisms have effective detoxification pathways and that *E. coli* has the added redundancy of the YeiG enzyme it is unlikely that even under wild type conditions of folate synthesis formaldehyde is able to saturate detoxification enzymes to a point that negatively influences lifespan. This does not rule out the theory that a low-level bacterial toxicity to the host exists but, in this case, formaldehyde from folate may not be a component of the mechanism of SMX increased lifespan.

### 3.4.2 Sulfamethoxazole alters the morphology of a bacterial lawn

An unexpected by-product of the formaldehyde sensing *lacZ* reporter was the improved observation of differences in bacterial lawn morphology and the ability to produce a graphical representation of the topography from the data. This was named a ‘morphology plot’. The morphology plots represent the spatial arrangement of the bacterial lawn based upon the density of bacteria and the subsequently reduced brightness of those regions. Because the pixel brightness of the combined colour channels RGB was used to plot the data the previously discussed method for quantifying blue was not applicable. The plots

could be produced using individual channels but the most reproducible and robust representation was the use of RGB brightness as a percentage of maximum brightness. The data was also trimmed to allow for a point of reference to align the lawn edges for comparison although this did not provide a method of comparison for actual size. The plots are not suitable for statistical analysis. They provide a simplified but superficial model of the bacterial distribution within the lawn for comparison as seen through a confocal microscope.

The morphology results showed that lawns grown on either DM or NGM agar had differences in regions of bacterial accumulation, possibly due to the differences in the nutrient profile of the agars. In the non-SMX conditions, the bacteria are still able to expand the lawn outwards sharing what appears to be a swarming phenotype. Suggesting the bacteria are proliferating peripherally into the agar. The SMX conditions produce the appearance of a sharp lawn edge and a loss of the swarming morphology. This characteristic difference maybe the product of a bacterial stress response to low nutrient availability.

### 3.4.3 The presence of a competitive lawn and Sulfamethoxazole alters growth of satellite colonies

Continuing on from the initial morphology plot observations 2 µl mini lawns were used to observe a bacterial lawn in its entirety although on a much smaller scale. Even with a much-reduced bacterial population, the morphology differences between conditions could be clearly seen. In particular the striking clearly defined edge of a an SMX lawn and the cloud like swarming morphology in the absence of SMX.

There have been almost no previous studies of the dynamics and geography of the bacterial lawn. However, there are morphological similarities between biofilms and bacterial lawns used for lifespan studies. O'Toole, Kaplan, and Kolter (2000) define biofilms as *'communities of microorganisms that are attached to a surface'*, although within this broad definition it should be noted that typically biofilms are made up of a consortium of multiple species and formed from the adherence of single cells to a solid surface (O'Toole et al., 2000; P. Stoodley, K. Sauer, D. G. Davies, & Costerton, 2002). In the context of our *E.* coli lawns like a biofilm they are attached to a semi-solid surface (agar) and may be a region of biological stability represented by a spatially organised population of cells. The

spatial organisation of the lawn may relate to differing states of differentiation dependent on their geographic location, metabolic requirements, response to environmental and external stimuli (J A Shapiro, 1987; James A Shapiro, 1998; Stubbendieck, Vargas-Bautista, & Straight, 2016).

The bacterial lawn is often thought of as a simple layer of bacterial cells that are morphologically static and lacking in any real structure. The lawns appear to be a three-dimensional structure with a complex dynamic morphology that is able to interact with its environment. Much like a biofilm the lawn bacteria may have an advantage for growth and survival by the potential to optimize strategies to access nutrients externally or through esoteric population control (Stubbendieck et al., 2016). They may also be able to better defend from antagonists such as SMX by a collective sharing of the burden of the insult (James A Shapiro, 1998). They may also have a dynamic interaction with the agar that enables environmental signal detection, detection of other bacteria and secretion of polysaccharides to promote adhesion and movement for survival (Harshey, 2003; James A Shapiro, 1998).

Disrupting folate synthesis with SMX may cause the loss of a key sensory and adaptation mechanism to exploit the environment. This may have a wider impact preventing proliferation external to the lawn rather than a direct impact on lifespan. This feature may result in transiently spread bacteria failing to survive externally to the lawn environment and correlate with a reduced capacity to establish growth in the ageing *C. elegans* gut as seen in the SMX long lived phenotype.

### 3.4.4 Flagella expression does not correspond with reduced lifespan

The relationship between bacterial growth and host lifespan has been explored from the context of accumulation in the gut of *C. elegans*. SMX has been shown to cause a delay in bacterial accumulation as the worms age but has not been attributed to causation of extended lifespan. A mechanism proposed here for the observed SMX morphology is the absence of flagella as a product of impaired bacterial folate synthesis. This also corresponds with a toxicity hypothesis whereby flagella are known to be immunogenic to the host (Barnhart & Chapman, 2006) and therefore pose a potential source of toxicity reducing the lifespan of *C. elegans*.

The *E. coli* mutant *ΔrpoS* has loss of a regulatory gene reducing folate synthesis and has previously been shown to increase *C. elegans* lifespan (Maynard, 2017). This strain was used to compare bacterial morphology between lifespan promoting bacteria, WTK and SMX treated bacteria. Supplementary TEM was also to image and analyse bacteria treated with SMX under lifespan conditions. It was found that the morphology of the lifespan increasing mutant *ΔrpoS* correlated with the WTK morphology, flagella were present in abundance. Conversely, SMX had no obvious flagella suggesting the mechanism of SMX increased lifespan was not through inhibited expression of motility components but, it may play a role in delayed gut accumulation. Further work will be needed to develop a suitable protocol to specifically extract the bacteria from the lawns whilst preserving external bacterial components. Gut accumulation experiments using the *ΔrpoS* mutant and other extended lifespan phenotype mutants with flagella expression may reveal if this phenotype alters accumulation in comparison to WTK and SMX treated bacteria. This will further add to the current knowledge that bacterial growth and proliferation in the low folate model is independent of the lifespan effect.

### 3.4.5 Sulfamethoxazole prevents exploitation of nutrients in the agar

The original mini lawn concept was developed to represent a proxy for bacteria transported from the parent lawn to the wider media. The use of 2 µl mini lawns allowed for the highest volume that could effectively be accurately observed and measured from the earliest possible timepoint. Surface area measurements were taken throughout the time period of a lifespan protocol to analyse the effect of SMX on lawn expansion in the context of proliferation. The absence or presence of a 100 µl parent lawn provided secondary data to investigate if competitive element influences bacterial growth external to the lawn under lifespan conditions. The results showed that small colonies in the presence of large populations of bacteria may be in competition for nutrients and metabolites in the agar. The presence of a parent lawn has competitive dominance over the outlying colonies but bacteria are still able to proliferate in the absence of SMX. Blockading folate synthesis with SMX prevents any proliferation causing the mini lawn area to shrink. This shrinkage is to a lesser extent in the presence of a parent lawn, which may be contributing rescue nutrients and greater clearance of SMX.

These results support the previous data that SMX treated bacteria are unable to adapt to and exploit the environment around them causing a loss of proliferation that may lead to a failure to survive once removed from the security of the larger lawn. Additional analysis with $OD_{600}$ may establish if the population is in decline or still growing and the use of further diluted mini lawn cultures may provide a more realistic model of bacterial transfer by *C. elegans*.

# Chapter 4

# Development of an LC-MS/MS Protocol to extract and analyse metabolites in the agar from the *E. coli* bacteria lawn

## 4.1 Introduction

Bacterial metabolism can be directly altered by pharmacological intervention or by the use of single gene knockouts to target specific enzymatic pathways. Inhibition or attenuation of enzymatic activity can result in direct and indirect downstream changes to associated metabolic pathways. The metabolite profile of an organism is known as the metabolome, changes to metabolic pathways subsequently affect the metabolome whether that is through enzymatic disruption or alterations to nutritional input (Sébédio, 2017). The metabolome can be analysed and compared between conditions through the use of metabolomics (A. Zhang, Sun, Wang, Han, & Wang, 2012). It can be used to observe similarities and differences of the metabolome between wildtype strains, mutant strains and pharmacologically treated bacteria (M. Ito, Baba, Mori, & Mori, 2005; Y. K. Kwon et al., 2010; R. J. Nichols et al., 2011).

To better understand if SMX affects metabolism downstream of the folate pathway a targeted analysis of the bacterial exometabolome using ultra high-performance liquid chromatography mass spectrometry (LC-MS/MS) was undertaken. The use of metabolomics allows identification and quantification of small molecules that are derived from bacterial metabolism (Luan, Wang, & Cai, 2019). The metabolomic profile represents the outcome of metabolic activity revealing detailed information about the biological system being investigated (X. Liu & Locasale, 2017).

The *E. coli* metabolome is extremely complex. Whilst a shotgun approach to metabolomics may provide a broader overview of the changes in the metabolome it was not feasible within the time constraints of this thesis. Based on previous work from our lab it was decided to undertake a footprint analysis focusing on changes in the amino acid profile. Previous work has been limited to NMR analysis of liquid bacterial culture and endometabolomic analysis of bacterial folates using LC-MS/MS (Helliwell, 2013;

Maynard, 2017). These studies did not directly focus on the relationship between the lawn and the agar substrate over the duration of a lifespan assay. Focusing on the bacterial lawn provides a more representative analysis of *E. coli* metabolism under conditions of our lifespan protocol and the metabolomic changes that occur which may be influencing worm ageing. DM has a defined nutrient content with a known amino acid profile that may provide a baseline to measure changes under different conditions.

4.1.1 Previous metabolic foot printing in our lab

Our lab has previously investigated the effect of impaired bacterial folate synthesis on the amino acids serine and glycine by nuclear magnetic resonance (NMR), which is discussed in more detail in chapter 1.3.10. The study conducted metabolic foot printing on the *E. coli* mutant Δ*pabA* and found serine was rapidly depleted whilst glycine remained elevated throughout the time span of the experiment (Helliwell, 2013). There were some limitations to the original study. Potential ethanol contamination due to the NMR protocol, the use of liquid culture and the study duration was limited to 40 hours (Helliwell, 2013). Conducting a study of bacterial lawns on solid agar for 7 -9 days reflects a lifespan assay more accurately. The worms are exposed to the bacterial lawn on DM agar for 7 days and there is 9 days of bacterial growth before the transfer of animals to fresh plates.

The use of Δ*rpoS* is relevant to this work due to its role as a transcription regulator of folate synthesis genes and use in previous work by our lab. The σ factor *rpoS* is a major regulator of *E. coli* stress responses (Gottesman, 2019). Knockout of this gene has previously been shown to attenuate expression of *pabA,* a key folate synthesis enzyme (Maynard, 2017). Attenution *of* pabA reduced endogenous bacterial folate even in the presence of a PABA rescue protocol (Maynard, 2017). The use of Δ*pabA* is also relevant to this work as the mutation is in a folate synthesis enzyme upstream of the site of activity by SMX where both reduce bacterial folates increasing *C. elegans* lifespan (Maynard, 2017). Δ*pabA* has a single gene knockout for the DNA sequence encoding a sub-unit of the aminodeoxychorismate synthase complex (ADCS) (Roux & Walsh, 1992). ADCS forms a part of the upstream pathway for the conversion of chorismite into the folate precursor PABA (Roux & Walsh, 1992). SMX acts downstream of ADCS to competitively inhibit the enzyme dihydropteroate synthase, preventing the amalgamation of PABA and pterin forming a key precursor metabolite for THF synthesis (Richey &

Brown, 1969; Swedberg, Fermér, & Sköld, 1993; Vedantam, Guay, Austria, Doktor, & Nichols, 1998).

SMX treated bacteria and Δ*pabA* are also able to utilise exogenous PABA for de-novo folate synthesis (Maynard, 2017). The bacteria retain an ability to grow on both NGM and DM to sufficiently support *C. elegans* growth and development (Maynard, 2017; Virk et al., 2016). The bacteria provide the worms sole source of nutrients whilst extending its lifespan (Helliwell, 2013; Maynard, 2017; Virk et al., 2016).

The similarities between the mode of action by SMX and Δ*pabA* may also be shared in changes to bacterial amino acid metabolism. Understanding these changes may provide a further understanding of the mechanism of how decreased bacterial folate synthesis extends *C. elegans* lifespan. Due to the findings by Helliwell (2013) I decided to develop a protocol extract amino acids from agar for LC-MS/MS metabolomic analysis. The protocol would be used to investigate amino acid metabolism by the bacterial lawn.

### 4.1.2 The use of LC-MS/MS for metabolic foot printing

Both LC-MS/MS and gas chromatography mass spectrometry (GC-MS) provide suitable platforms for the analysis of bacterial metabolites (Perez et al., 2016). GC-MS is limited to volatile compounds only, any non-volatile compounds must be derivatised to be analysed effectively (Perez et al., 2016). The advantage of this is a stable fragmentation of metabolites, the reproducibility of separation and a high resolution for accurate analysis. Conversely, LC-MS/MS samples do not require any derivatisation due to the mobile phase being liquid rather than gas (Perez et al., 2016). In some cases, the samples only require dilution and can be added directly to the platform increasing sample throughput (Roman Perez et al., 2016).

Depending on the source of the sample and target metabolites both methods require multiple steps before analysis through the chosen platform (Winder et al., 2008). For bacterial samples, this usually consists of some form of halting metabolic activity (quenching) with a sub-zero mixture of ethanol and water or glycerol (Smart, Aggio, Van Houtte, & Villas-Bôas, 2010). Extraction by filtration or a suitable solvent, solid or liquid phase separation, the addition of standards, solvent removal or washing and a concentration step (Gamon et al., 2020; P. Gao & Xu, 2015; Hounoum, Blasco, Emond, &

Mavel, 2016; W. Lu et al., 2017; Mashego et al., 2007; Nemkov, D'Alessandro, & Hansen, 2015; C.-H. Park et al., 2011; Perez et al., 2016; Smart et al., 2010; Taymaz-Nikerel et al., 2009; X. Wang et al., 2014; Winder et al., 2008).

To the best of our knowledge, there are no examples in the literature of analysing metabolites from solid agar plates. This is likely due to the number of unique challenges extracting metabolites from this medium presents. Firstly, the quenching of the bacterial lawn before removal may dilute or removing key metabolites before extraction (Bolten, Kiefer, Letisse, Portais, & Wittmann, 2007). Quenching may also stimulate a stress response in the bacteria due to the extreme negative temperatures needed for this step to be effective (Smart et al., 2010). This could lead to loss of low abundance metabolites and changes to the metabolite profile (Bolten et al., 2007; M.-m. Chen et al., 2014). The second problem was how to effectively and reproducibly extract the metabolites from the agar. Simply using heat to dissolve the agar before filtration would not have sufficed. The increased temperature would also act as a stressor on the bacteria potentially altering metabolism (Chung, Bang, & Drake, 2006). Dissolving the agar with agarase was also excluded as an option as this may contaminate the sample whilst impairing filtration due to viscosity and cooling. It is also important to ensure all samples for analysis are free of any particles that could negatively affect instrumentation.

Finally, larger liquid cultures are typically used for this kind of analysis. A 100 µl bacterial lawn on agar has a considerably lower biomass compared to larger volume liquid cultures. This risks a low recovery yield of the specific metabolites under investigation from the agar (Patejko, Jacyna, & Markuszewski, 2017). Multiple steps used in sample preparation could reduce metabolite concentration below the limit of detection (Patejko et al., 2017). It was therefore decided that the steps required for GC-MS were too complex and presented too many limitations. LC-MS/MS would be more suitable due to its ability to separate metabolites without the need for as many pre-analytical steps (Vernocchi et al., 2016). An in-house method for the analysis of non-derivatized amino acids by LC-MS was also in place. This made the platform the appropriate tool to develop a novel method for the extraction and isolation of bacterial amino acids from solid agar media.

4.1.3 Protocol Development

To develop this protocol and subsequent further analysis of the bacterial exometabolome in DM agar I was gratefully assisted by Dr Rachael Dack who provided invaluable support with the ultra-high performance liquid chromatography QTRAP mass spectrometry service of the Bioanalytic facility of Durham University. The parameters and settings of the LC-MS/MS used are detailed in section 2.9 of chapter 2 and were originally developed by Dr Ian Cummins of Durham University as part of a method to analyse non-derivatised amino acids by multiple reaction monitoring. The LC-MS/MS system can measure mass-to-charge ratio (m/z) of ions formed from the analyte of interest. Using multiple reaction monitoring specific precursor ions are fragmented into product ions providing a highly sensitive and selective methodology to detect compounds at picomole levels (figure 4.1) (Maynard, 2017; McMaster, 2005).

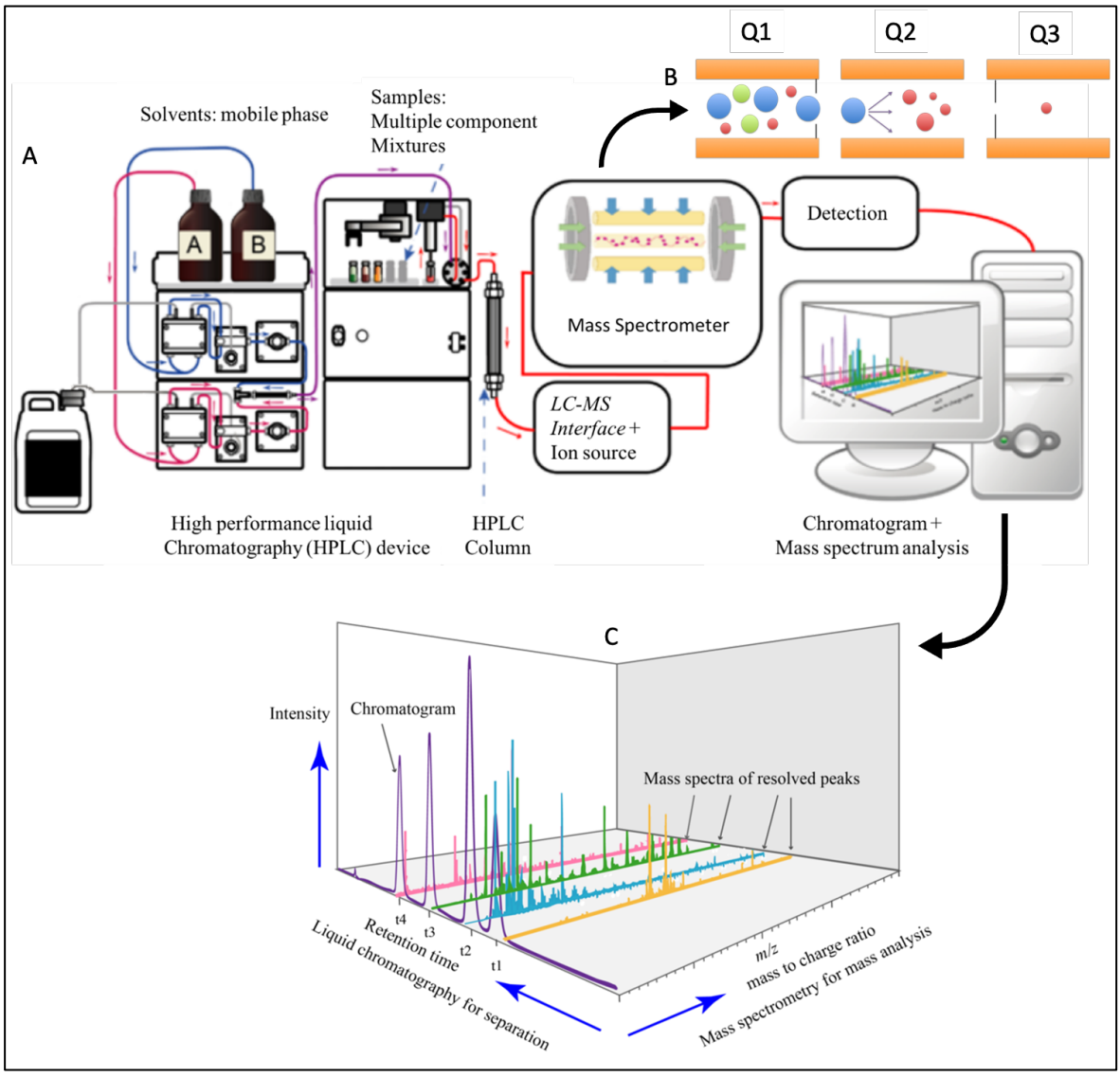

**Figure 4.1 Schematic diagram of the LC-MS/MS QTRAP system.** **A**. The LC-MS/MS system consists of a HPLC pump system, injector and HPLC column connected to an evaporative ionizing interface that feeds into a hybrid quad/trap mass spectrometer (QTRAP). All of which is linked to a computer system that controls and manages the HPLC system (McMaster, 2005); **B**. The QTRAP has three quadropoles that can selectively fragment ions through a process called multiple reaction monitoring. Q1 selects a specific precursor ion that enters Q2 where it is fragmented, selected product ions enter Q3 for detection. **C**. Ion abundance is measured and plotted to display peak intensity of the analyte ion versus retention time through the column with each peak corresponding to a mass spectrum (m/z). Image adapted from (Kailasam, 2021; Maynard, 2017).

The lifespan protocol used in our lab relies on a bacterial lawn on a solid agar plate that forms the backbone of the overall model of the host/microbiota interaction. *C. elegans* resides in and feeds on the bacterial lawn as part of its experimental habitat (Stiernagle, 1999). The worms consume bacterial metabolites endogenously within the gut as part of digested *E. coli* and exogenously due to bacterial excretions and secretions forming a ubiquitous part of the food source melange (Yilmaz & Walhout, 2014). Isolating the exometabolome from the agar whilst removing the bacterial lawn without diluting or contaminating it would require a specific method.

A search of the literature was conducted for protocols that were suitable for analysis of bacterial metabolites in agar. A considerable body of work exists but none were found reporting protocols that dealt directly with analysing metabolites from solid agar or that catered for the removal of a bacterial lawn without the need for the addition of reagents that could negatively influence metabolite concentrations. Protocols predominantly used liquid bacterial cultures vastly exceeding the volume of a 100µl lawn, where quenching and separation involved addition of larger volumes of extremely low temperature liquid reagents, vacuum filtration or both combined (Bordag et al., 2016; Dudzik, Barbas-Bernardos, García, & Barbas, 2018; Link, Anselment, & Weuster-Botz, 2008; Smart et al., 2010; Taymaz-Nikerel et al., 2009; Van Gulik, 2010; Winder et al., 2008). Due to the absence of a suitable protocol to meet our metabolomics needs it was deemed that the appropriate route was to develop my own to meet my research needs.

## 4.2 Chapter Aims

1. Develop a simple refined method of amino acid extraction from DM agar for LC-MS/MS analysis.
2. Develop a protocol with the least number of preparatory steps to preserve metabolite integrity and provide accurate analysis between conditions.
3. The protocol must allow for the limitation of metabolite extraction from a small population of bacteria on semi-solid substrate rather than liquid culture for optimum sample recovery.

## 4.3 Results

4.3.1 A reproducible agar extraction method

To access the agar beneath the lawn footprint and extract a suitable sample that could be practically processed meant devising a reproducible method without the need for quenching or removal methods that could dilute or compromise recovery of metabolites.

The 100 µl bacterial lawn covers an area of approximately 3 $cm^2$ to a depth of about 1-2 mm. For accuracy before removal of the bacterial lawn the base of the petri dish was marked in the centre of the the lawn. This allowed for an extraction reference point that was within the perimeter of the lawn area. The most efficient way to gain access to the agar beneath was by removal with a sterile glass scraper. This involved firmly but gently scraping the lawn from the agar in one single clean stroke leaving minimal bacterial residue (figure 4.2). Care had to be taken not to put excessive downward pressure on the scraper to prevent damage to the agar. The technique proved successful in rapidly removing the lawn without the need for quenching with a liquid reagent at -20 °C to -30 °C. Once the agar beneath the lawn is exposed a sample can be extracted.

To maintain continuity the sample being removed needed to be cut to the full depth of the agar to produce the same $cm^3$ size sample. The sample had to fit easily into a 1.5 ml Eppendorf tube with four times the mass in volume of extraction reagent. It was found that removal of a circular 8 mm diameter core section produced on average a 225 mg sample. The sample could be handled efficiently and fitted within the Eppendorf tube with space for the addition of reagents to extract the amino acids. The agar sample was sliced horizontally and laterally to expose the maximum surface area to the extraction reagent .

Once placed inside the Eppendorf its mass was calculated by subtracting the tube weight from the total weight of the sample and the tube. HCl was then added to the tube at a ratio of 1:4 (figure 4.2).

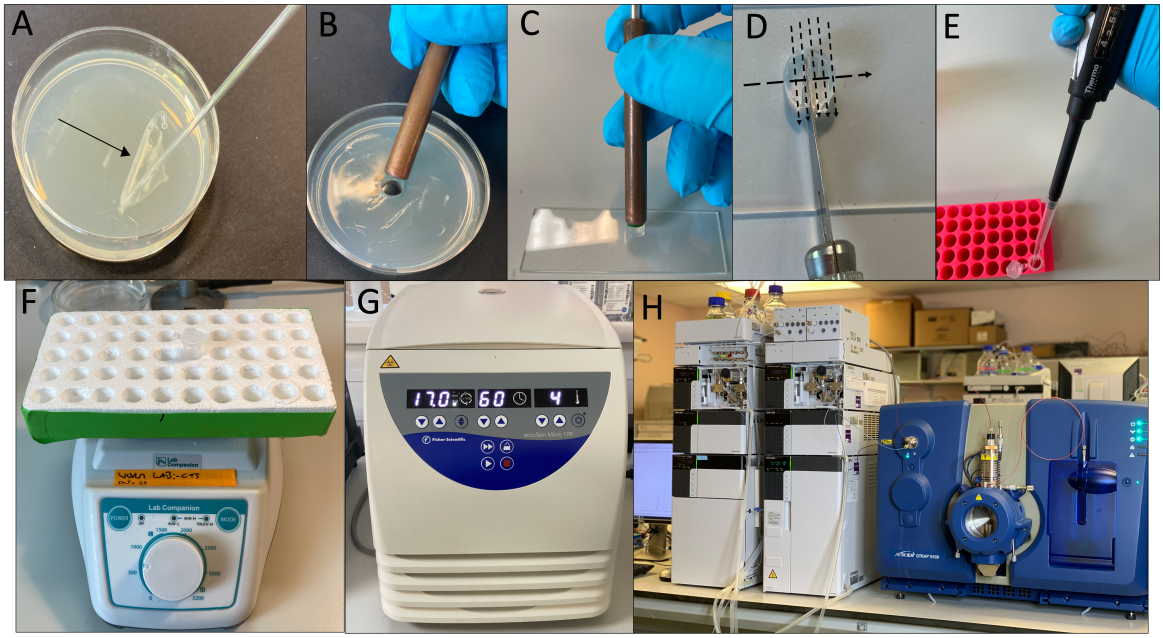


**Figure 4.2 Images demonstrating the extraction and preparation of an agar sample using the finalised protocol.** **A.** For the purpose of clarity the image shows removal of a 300 µl lawn. Typically, when removing a 100 µl lawn there is significantly less residue that us retained by the scraper. Arrow denotes direction of scraping method; **B**. The sample is extracted with a sharpened 8 mm diameter tube that is placed centrally to the centre of lawn mark and pressed firmly down wards. The tube is rotated several times to ensure a clean and full extraction upon removal from the agar; **C**. The agar sample is pushed out of the tube with a blunt metal rod and placed on a clean glass slide; **D**. The sample is sliced laterally and horizontally with a scalpel before being place into a pre-chilled Eppendorf tube with tweezers; **E**. Chilled solvent is added to the sample tube in µl at a ratio of 4 times the agar mass; **F**. The sample tubes are placed into a purpose made shaker at 500 rpm and incubated at 4 °C for 60 mins; **G**. On completion of incubation samples were placed in a chilled centrifuge and spun for 60 mins; **H**. at the end of the centrifuge step 250 µl of each sample was aliquoted into pre-chilled Eppendorf tubes and was ready for LC-MS/MS pre- analysis preparation.

### 4.3.2 Extraction of amino acids from the agar

Isolating amino acids from the agar for analysis required a suitable solvent. The solvent would allow optimal extraction of all amino acids in the agar whilst catering for a range of solubility characteristics. This would remove the need for ethanol mixtures that have been

previously used. The side chain properties of amino acids can interact with ethanol in water-ethanol mixtures altering solubility (Bowden, Sanders, & Bruins, 2018). In some cases, the addition of heat is required to optimise to improve solubilisation which may be detrimental in preserving the wider exometabolome (Bowden et al., 2018; Mo, Dang, & Wei, 2011; Zhou et al., 2012). Previous work has found that 0.1N HCl has improved solubility of amino acids compared to $H_2O$ with an optimum extraction time of 60 minutes although these findings were restricted to plant matter (Del Campo et al., 2009; Moldoveanu, Zhu, & Qian, 2015).

To examine if this method was suitable for extracting amino acids from semi-solid agar a comparison was conducted between 0.01N HCl, 0.1N HCl and $H_2O$ on agar samples prepared as described in section 4.3.1 of this chapter. Each solvent was added at a volume 5-fold the calculated mass of the agar. The sample was then incubated for 60 mins at 4 °C followed by centrifuging at 17,000 x G for 60 mins at 4 °C. 250 µl of the supernatant of each sample was aliquoted to a fresh Eppendorf tube and stored at -80 °C. Prior to analysis each sample was vortexed and diluted 1 in 20 with HILIC A buffer.

It was found that all solvents were able to recover the basic amino acids arginine and lysine. The aliphatic non-polar amino acids glycine; alanine; leucine; isoleucine; methionine; proline and valine. The aromatic amino acids tyrosine; phenylalanine and tryptophan. The acidic amnio acids aspartic acid and glutamic acid and the polar amino acids serine and threonine. Recovery of alanine, isoleucine, leucine, proline, valine and glutamic acid by 0.01N HCl was not as efficient as $dH_2O$ and 0.1N HCl which had similar recovery levels for all the amino acids with the exception of tryptophan which had limited extraction by $dH_2O$ (figure 4.3).

To understand if amino acid recovery was influenced by the agar an analysis was conducted to compare extraction of amino acids from liquid DM and DM agar. Both were prepared simultaneously and samples obtained as per the protocol described above. The results show that there was limited difference in recovery between the media. Tyrosine had increased recovery from DM and isoleucine had increased recovery from agar but both results had considerable variance that may be skewing the data. Overall, the results

suggested that the agar does not impede solubility and extraction of amino acids using 0.1N HCl (figure 4.4).

Next, to understand if SMX used in our attenuated folate model alters the ability of 0.1N HCl to solubilise amino acids from the DM agar a comparison was conducted between DM agar plates treated with 128 μg/ml SMX and non-SMX treated DM agar plates. It was found that SMX did not alter recovery of the amino acids suggesting that it did not have a negative interaction with amino acids (figure 4.5).

In neutral pH aqueous solutions amino acids exist as zwitterionic molecules due to the amino and carboxyl groups of the amino acid becoming ionised with an equal positive (cationic) and negative (anionic) charge (Pradhan & Vera, 1998). The use of $dH_2O$ as a solvent act as both an acid and a base retaining amino acids in a zwitterionic state which may impair solubility at low temperatures (Palecz, Piekarski, & Romanowski, 2000; Xu, Nilles, & Bowen Jr, 2003) and specifically, reduce dissociation from the agar of the aromatic amino acid tryptophan. The addition of HCl decreases the pH providing a hydrogen ion to the anionic carboxyl group forming cationic amino acids that are more easily solubilised and may disassociate from the agar more easily (Pradhan & Vera, 1998). Our findings support the work of Del Campo et al. (2009) that showed the use of 0.1N HCl provided a reproducible method for the extraction of amino acids. It was therefore decided that 0.1N HCl was the appropriate solvent for the analysis of the exometabolome in this study.

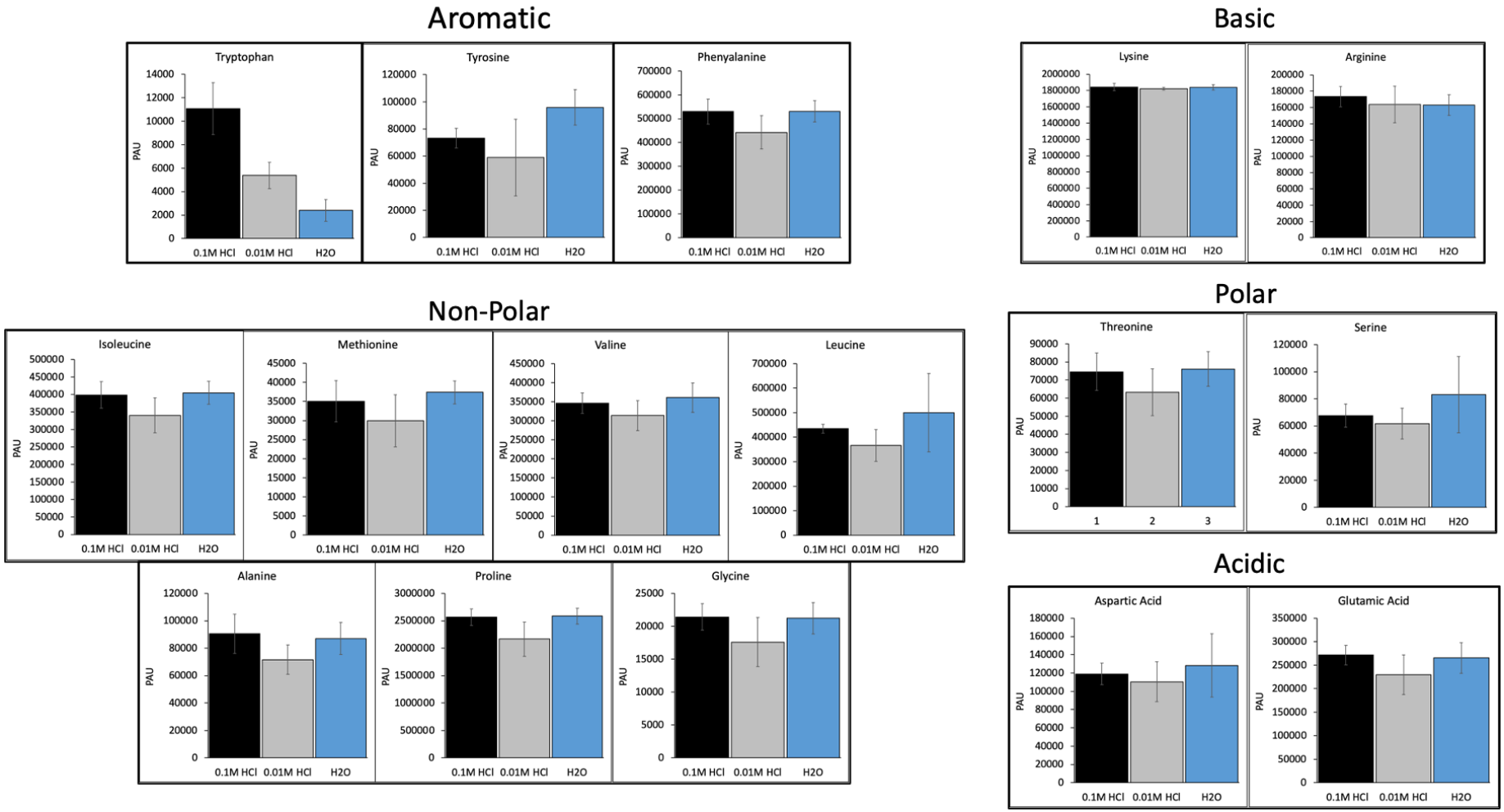


**Figure 4.3 Extraction of amino acids from semi-solid agar using 0.01N HCL, 0.1N HCl and dH$_2$O.** Samples (n=3 per condition) were obtained from semi-solid DM agar prepared 48 hours prior to extraction. PAU is specific to each amino acid and not scaled for inter amino acid comparison. Error bars represent SD; PAU, peak area under the curve; HCl, Hydrochloric acid; H2O, H$_2$O.

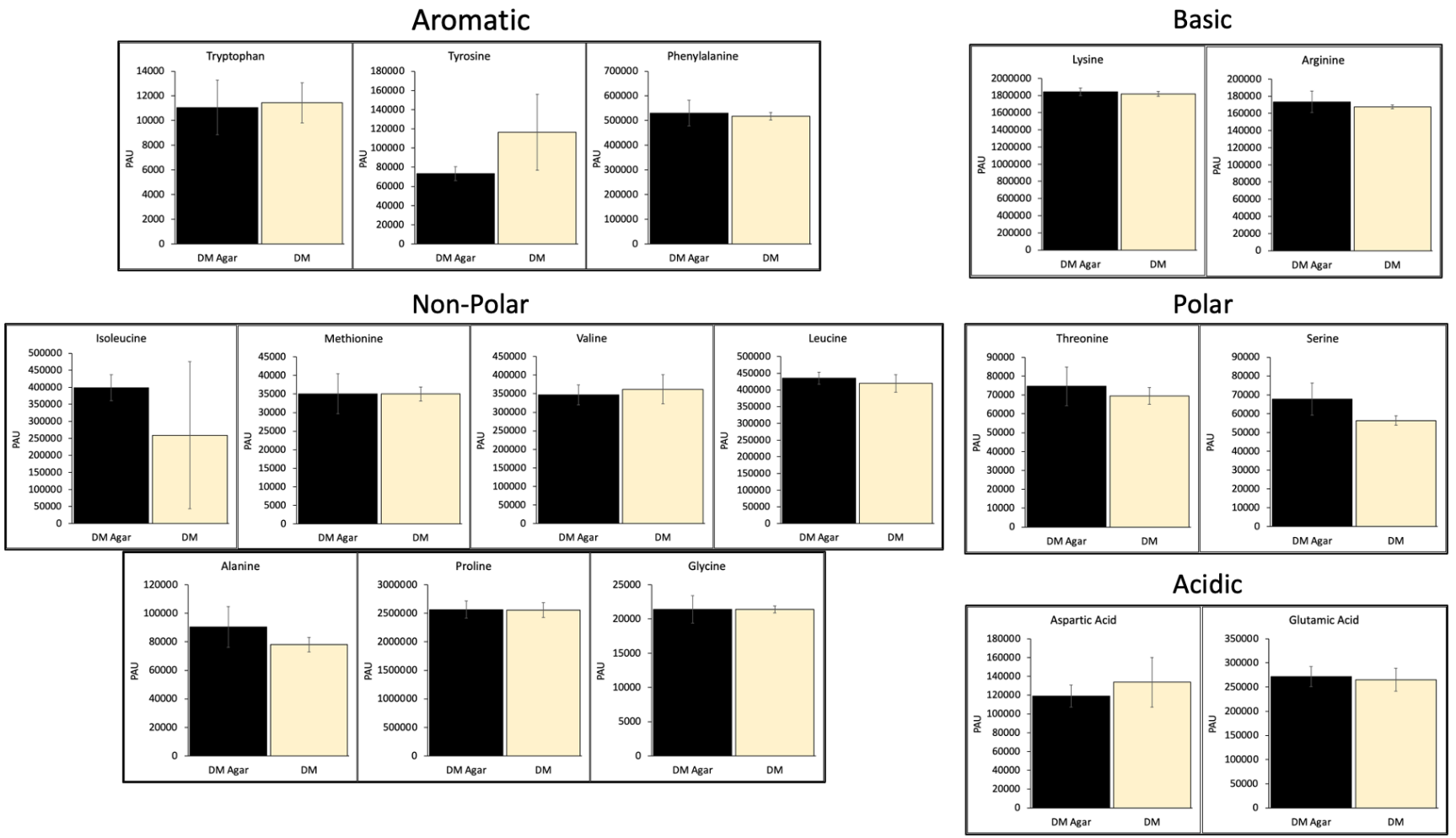


**Figure 4.4 Results of LC-MS/MS analysis of amino acids demonstrating agar does not impede recovery.** Samples (n=3 per condition) were obtained from liquid DM and DM-agar prepared 48 hours prior to extraction. PAU is specific to each amino acid and not scaled for inter amino acid comparison. Error bars represent SD; PAU, peak area under the curve; HCl, Hydrochloric acid; H2O, $H_2O$.

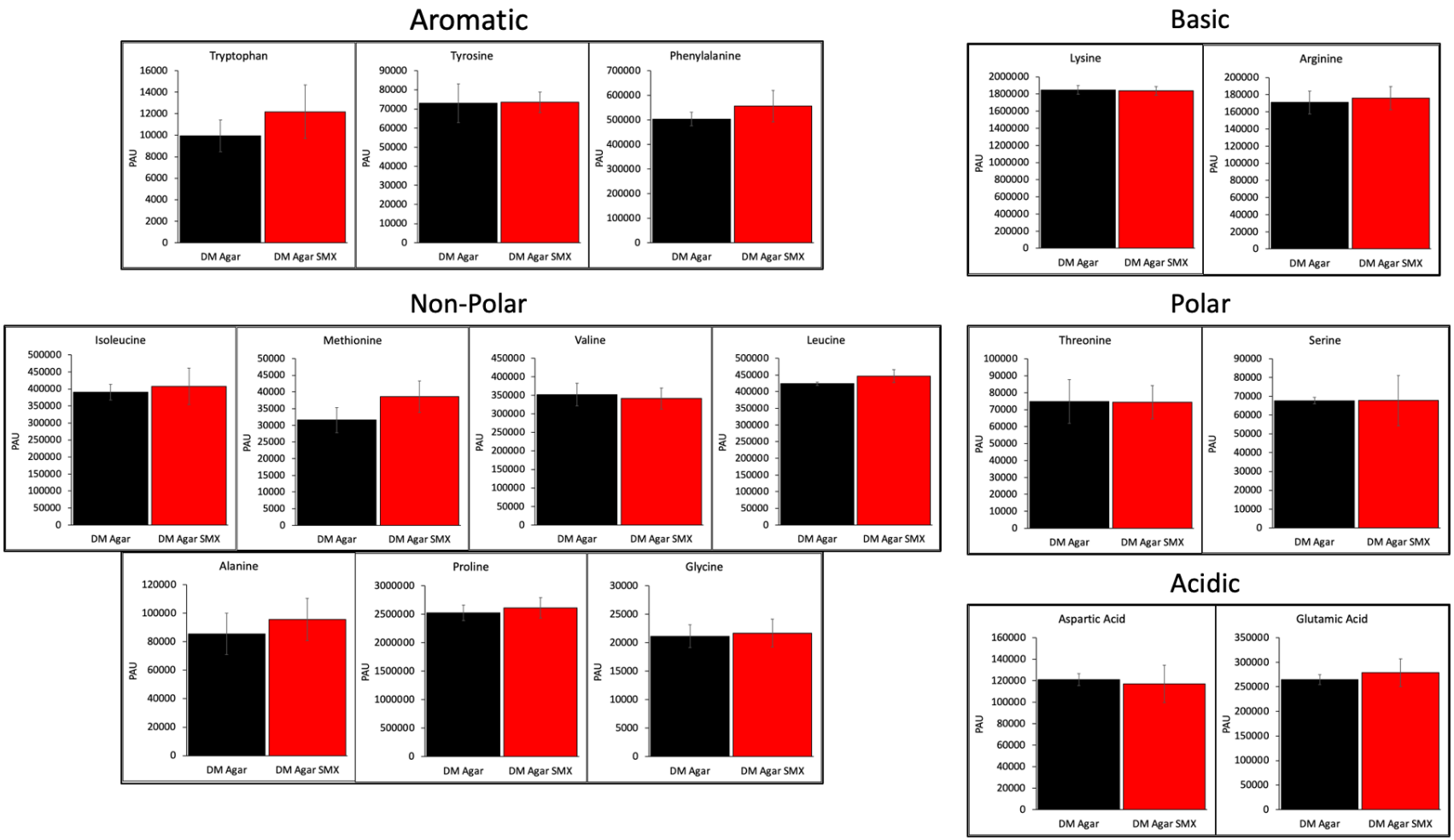


**Figure 4.5 Results of LC-MS/MS analysis demonstrating SMX does not impede amino acid recovery.** Samples (n=3 per condition) were obtained from DM-agar prepared 48 hours prior to extraction +/- 128 µg/ml SMX. PAU is specific to each amino acid and not scaled for inter amino acid comparison. Error bars represent SD; PAU, peak area under the curve; HCl, Hydrochloric acid; H2O, $H_2O$.

4.3.3 LC-MS/MS method development and validation

The existing LC-MS/MS method was further validated for linearity, sensitivity, and matrix effect by Dr Rachael Dack of Durham University. The limit of detection (LOD) and limit of quantification (LOQ) were calculated according to ICH guidelines, (LOD = 3.3*(σ/m) and LOQ = 10*(σ/m)) (R. Dack, personal communication, November 20, 2020). Tryptophan and Cysteine which are added to DM at low concentrations were found to be below the LOD in samples following sample preparation and were excluded from subsequent analysis (R. Dack, personal communication, November 20, 2020).

Linearity was assessed by linear regression shown in table 4.2. It was important to produce a calibration curve that covered the concentration range of amino acids present in the DM media at time point zero. Linear regression analysis showed that across this range the data was heteroscedastic thus 1x-weighting was applied to the calibration curves (R. Dack, personal communication, November 20, 2020). To test the effect of the matrix on ionisation efficiency, standards of amino acids were prepared in DM media or dd$H_2O$ and diluted with HILIC A (R. Dack, personal communication, November 20, 2020). The calibration curves showed no significant difference in the slope (R. Dack, personal communication, November 20, 2020).

**Table 4.1 Linear regression of amino acids. LOD, limit of detection; LOQ, limit of quantification.** Data provided by R. Dack, (personal communication, November 20, 2020).

| | LOD (µM) | LOQ (µM) | Linearity |
|---|---|---|---|
| Phenylalanine | 0.09 | 0.29 | 0.993 |
| Leucine/Isoleucine | 0.45 | 1.38 | 0.991 |
| Methionine | 0.11 | 0.35 | 0.997 |
| Valine | 0.36 | 1.08 | 0.996 |
| Proline | 0.30 | 0.90 | 0.995 |
| Tyrosine | 1.05 | 3.18 | 0.994 |
| Alanine | 0.33 | 0.99 | 0.994 |
| Threonine | 0.46 | 1.39 | 0.992 |
| Glycine | 0.33 | 1.01 | 0.997 |
| Serine | 0.64 | 1.95 | 0.994 |
| Aspartate | 0.37 | 1.13 | 0.994 |
| Histidine | 0.50 | 1.52 | 0.993 |
| Arginine | 0.48 | 1.44 | 0.993 |
| Lysine | 0.74 | 2.23 | 0.983 |

4.3.4 Quantification of amino acids by LC-MS/MS from agar

During this preliminary phase of analysis, the ability to observe relative changes in the amino acid profile between conditions was of greater importance than absolute quantification. Thus, amino acids were quantified by external calibration curve. The use of labelled standards would provide a more accurate method of quantification. Due to the number of amino acids of interest and range of physiochemical properties it was deemed too expensive at this stage. Based on initial matrix effect experiments which showed no significant difference stock solutions were prepared in 0.1N HCl and diluted with HILIC A.

The data allowed a comparison of the measured amino acid concentration in 15 ml of DM agar compared to the known baseline of stock concentration of amino acids added during plate preparation. This was achieved by comparing peak area under the curve (PAU) to amino acid standards of a known concentration (How et al., 2014). Table 4.1 shows the calculated concentration of each amino acid per 15 ml agar in a 6 cm petri dish and the calculated concentration after a 100-fold dilution from the addition of 0.1N HCL and HILIC A.

**Table 4.2 Concentration of amino acids per 15ml DM agar and after 100 fold dilution from sample preparation.**

| Amino Acids | µM/15 ml Agar Plate | 100 fold dilution µM |
|---|---|---|
| Tryptophan | 5.69 | 0.06 |
| Cysteine | 17.18 | 0.17 |
| Methionine | 29.72 | 0.30 |
| Tyrosine | 35.66 | 0.36 |
| Histidine | 36.94 | 0.37 |
| Phenylalanine | 67.43 | 0.67 |
| Isoleucine | 72.35 | 0.72 |
| Threonine | 91.02 | 0.91 |
| Valine | 108.47 | 1.08 |
| Lysine | 128.17 | 1.28 |
| Leucine | 130.89 | 1.31 |
| Arginine | 150.55 | 1.51 |
| Serine | 162.60 | 1.63 |
| Aspartic Acid | 271.57 | 2.72 |
| Alanine | 322.90 | 3.23 |
| Proline | 363.53 | 3.64 |
| Glutamic Acid | 412.73 | 4.13 |
| Glycine | 922.36 | 9.22 |

Attempts to quantify the amino acids extracted from the agar revealed that the concentration was considerably higher than the expected baseline concentration (figure 4.6). Despite initial matrix effect experiments, this anomaly was consistently observed in repeat runs. It was hypothesised that an element within the media or, stock amino acid solution was potentially causing an amplification of the analyte signal.

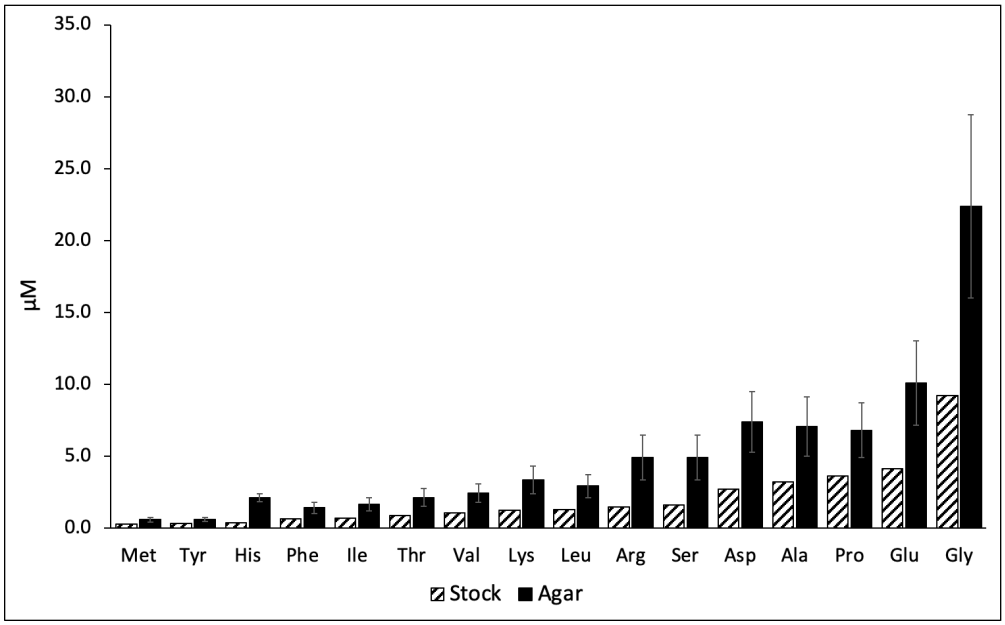


**Figure 4.6 Quantification of amino acids extracted from 15 ml DM agar.** Samples (n=40) were extracted at a ratio of 1:5 0.1N HCl and diluted 20-fold with HILIC A prior to analysis. Error bars represent SD.

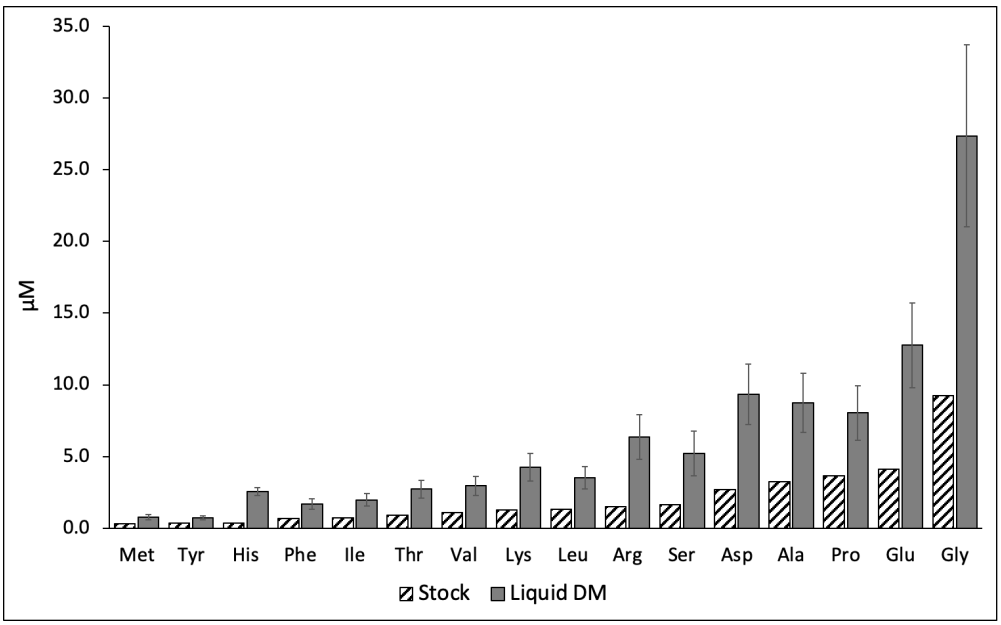


**Figure 4.7 Quantification of amino acids extracted from 15 ml liquid DM.** Samples (n=40) were extracted at a ratio of 1:5 0.1N HCl and diluted 20-fold with HILIC A prior to analysis. Error bars represent SD.

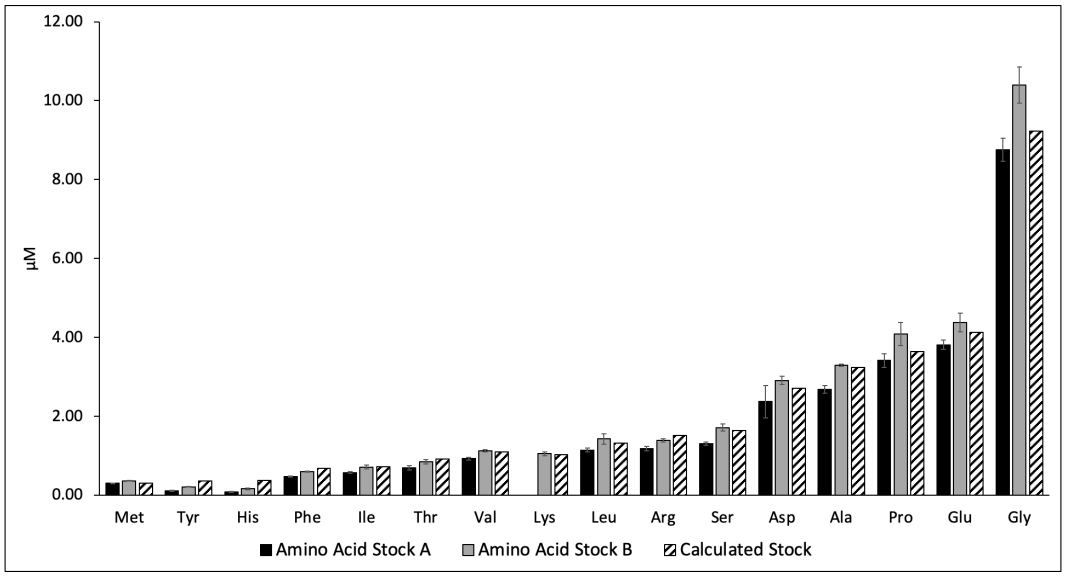


**Figure 4.8 Quantification of amino acids extracted from two separate batches of amino acid stock.** Samples (n=3 per condition) were extracted at a ratio of 1:5 0.1N HCl and diluted 20-fold with HILIC A prior to analysis. Error bars represent SD.

Initial matrix effect experiments utilised liquid DM media rather than agar plates. To determine if the agar in the media was causing the increase of the amino acid concentration in liquid DM was analysed. Figure 4.7 shows that the absence of agar did not reverse the amplified concentration in comparison to the calculated stock concentration of amino acids. These results suggest that agar or agar detritus in the samples are not responsible for the increased amino acid concentrations.

To validate the accuracy of the amino acid stock solution the preparation *of* two independently prepared solutions was analysed. One was prepared in house and one was prepared by Giulia Zavagno in the laboratory of Magnitude Biosciences. Samples were diluted at the same ratio as used in DM preparation with either dd$H_2O$ or liquid DM without amino acids. Samples were then diluted 1:5 with 0.1N HCl and 1:20 with HILIC A buffer to replicate samples. Figure 4.8 reveals that the amino acid stocks did not produce an amplified amino acid concentration as previously seen. The results show that the quantification is close to the calculated stock concentrations with an average recovery of 95.2% across all amino acids. This suggests that it is possible to accurately quantify amino acids using this method. Amino acid stock A is consistently less than the calculated stock. Amino acid stock B appears to be elevated compared to amino acid stock A and for several amino acids of the calculated stock. The variability may be due to individual preparation differences between laboratories and reagent quality. This suggests that the

amino acids in the stock are not interacting with each other to produce an amplification or matrix effect but may be interacting with a component of the agar.

### 4.3.5 Peak area under the curve as a means of analysing relative change in exometabolomic amino acid profile between conditions

Despite initial results showing a disparity between the expected concentration of amino acids in the agar plates and measured value, a reproducible change in PAU relative to μM concentration was observed. To observe if the pattern of PAU corresponded with changes in amino acid profile previously observed by our group an experiment was conducted using bacteria lawns as per the lifespan assay protocol described in section 2.9 of chapter 2. Briefly, samples were collected at 48 hours from bacterial lawns seeded with impaired folate synthesis mutants that are known to increase *C. elegans* lifespan (Han et al., 2017; Maynard, 2017; Virk et al., 2016). The aim was twofold. Firstly, to observe if metabolomic changes can be observed between conditions and secondly, if exometabolomic amino acid changes of lifespan increasing mutants correlated with the SMX condition.

Figure 4.9 and figure 4.10 demonstrates that amino acid changes can be observed and analysed using the PAU output of LC-MS/MS. The pattern of output for PAU matches that of μM for all the amino acids recovered. The μM data revealed concentration enhancement of signal as previously seen for amino acids when compared to calculated stock levels in the agar.

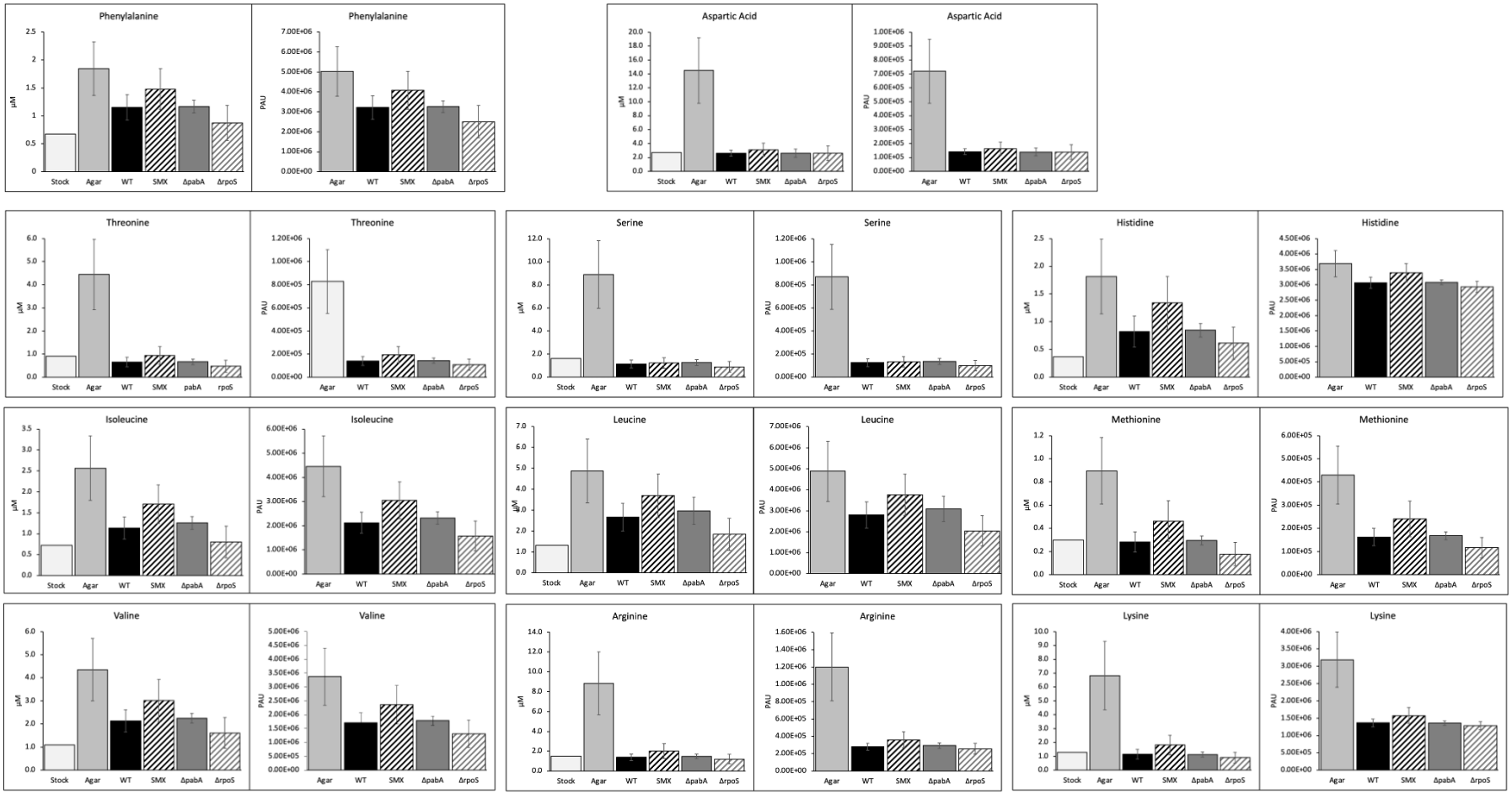


**Figure 4.9 PAU corresponds with amino acid concentration changes in DM agar.** The pattern of change seen in µM is reproduced using PAU allowing for observation and analysis of exometabolomic amino acid changes from bacterial lawns on DM agar. Error bars represent SD calculated from n=10 replicates per condition. Statistical analysis was conducted using Student's t-Test Two-Sample Assuming Unequal Variances.

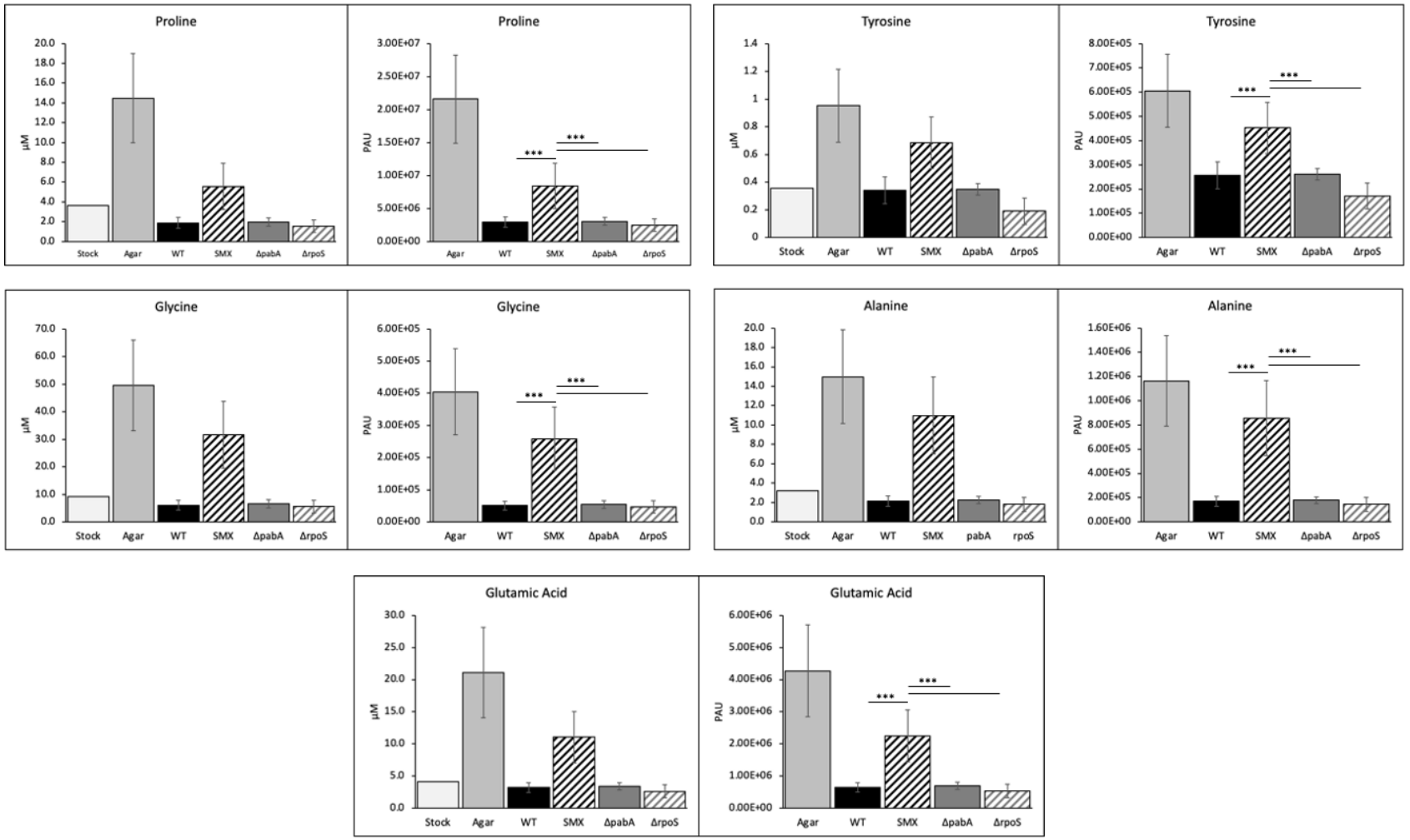


**Figure 4.10 Graphs showing PAU corresponds with amino acid concentration changes in DM agar and exometabolomic amino acids significantly changed by WTK lawns treated with 128 µg/ml SMX.** Error bars represent SD calculated from n=10 replicates per condition. PAU, peak area under the curve. Asterisks represent the results of Student's t-Test Two-Sample Assuming Unequal Variances. ***=P<0.001.

Quantification can be achieved by the use of internal standards of a known concentration prepared in a matched matrix to the sample. This allows for a calculation of amino acid concentration based on PAU against a linear standard curve. This method was ruled out due to the prohibitive cost of purchasing a labelled standard for each amino acid. PAU is directly proportional to the amount of analyte within the sample (Cantin, 2010; X. Liu & Locasale, 2017). It was found that it was possible to observe differences in the amino acid profile between conditions although this is limited to qualitative analysis as opposed to quantitative analysis this preliminary data will help shape future research questions.

4.3.6 Folate synthesis impaired *E. coli* mutants' amino acid exometabolome

LC-MS/MS was used to investigate the amino acid exometabolome of known decreased folate *E. coli* mutants that have been found to increase *C. elegans* lifespan. The aim was to understand if these mutants have a different exometabolome to the WTK condition samples after 48 hours from bacterial seeding. The results did not show a difference in the exometabolomic amino acid profile between the mutants and WTK condition (figures 4.9 and 4.10).

Previous work investigating the loss of *rpoS* has been found to alter amino acid uptake (Lacour & Landini, 2004) and metabolism (Vijayakumar, Kirchhof, Patten, & Schellhorn, 2004). Genes involved in amino acid metabolism of valine, isoleucine, serine, asparagine, methionine and arginine were found to be down regulated whilst genes involved in metabolism of histidine, alanine, leucine, threonine, cysteine, lysine and glutamate were upregulated (Rahman, Hasan, Oba, & Shimizu, 2006). Although these results was found in early stationary phase and restricted to growth in an LB broth at 37 °C. Here I did not see any alterations to *ΔrpoS* amino acid uptake or evidence of an altered exometabolome compared to WTK (figure 4.11A). This may be due to samples being obtained during growth phase at 48 hours from DM agar and the incubation temperature of 25 °C may not be an optimal temperature for*ΔrpoS* amino acid metabolism. There may also be sufficient PABA available to rescue folate synthesis to a level that does not significantly alter metabolism.

Knockout of *pabA* a constitutively expressed key enzyme in folate synthesis has also been shown to have impaired endogenous folate synthesis (Maynard, 2017). The relationship

between impaired bacterial folate synthesis and amino acid uptake and excretion in DM agar has not previously been reported. I found that compared to the WTK control *ΔpabA* did not have altered amino acid uptake and exometabolome (figure 4.11A). The *ΔpabA* mutant is still able to sequester PABA exogenously for folate synthesis (Maynard, 2017). DM agar has PABA added to a final concentration of 0.1 µM which has been found to be sufficient to rescue folate synthesis and bacterial growth without reversing the lifespan effect (Maynard, 2017). The previous work in our lab by Helliwell (2013) using NMR to investigate *ΔpabA* had reported a significant difference in glycine uptake that is not reproduced here (figure 4.11).

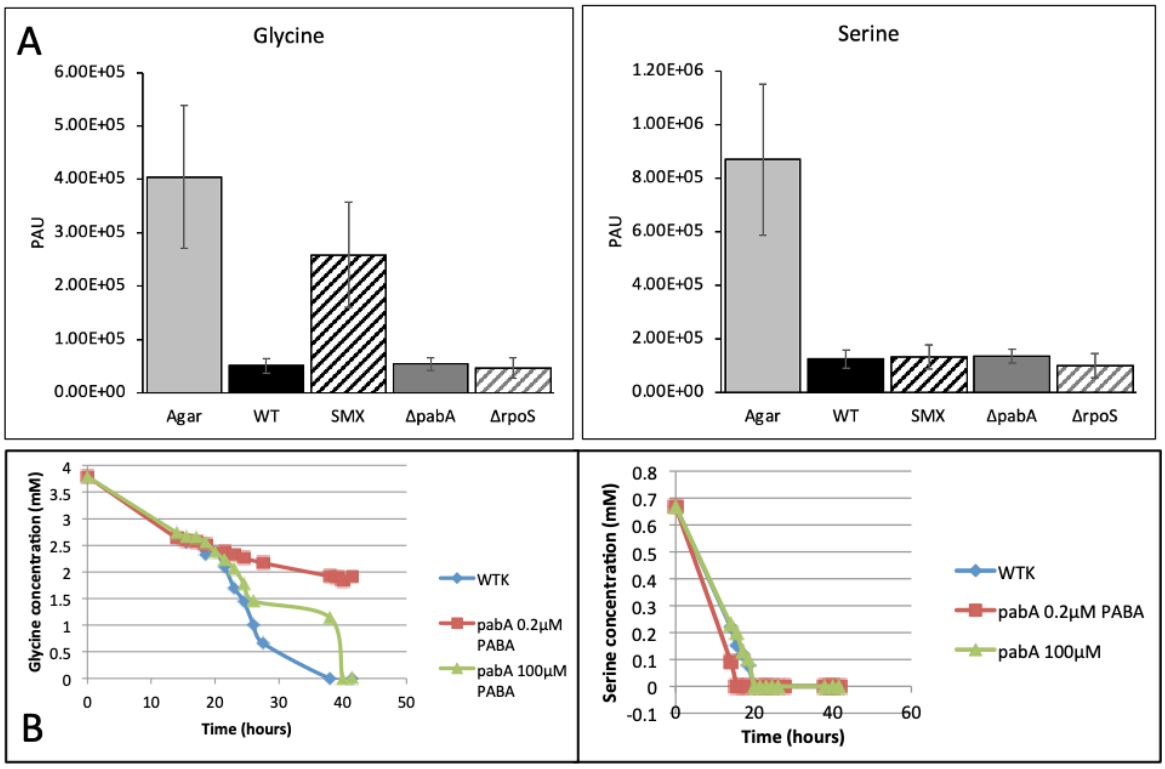


**Figure 4.11 Comparison of NMR and LC-MS/MS data for exometabolomic glycine and serine in DM. A.** LC/MS qualitative data for serine and glycine obtained from DM agar seeded with WTK, *ΔpabA*, *ΔrpoS* or WTK +128 µg/ml SMX and incubated for 48 hours at 25 °C. Agar condition was lawn free and provides a baseline for comparison. **B.** NMR quantitative data of serine and glycine obtained from liquid DM seeded with WT and *ΔpabA* and incubated for 40 hours at 25 °C from a study by Helliwell (2013). PAU, peak are under the curve.

Graph B in figure 4.11 shows the start of the glycine plateau for *ΔpabA* and 0.2 µM PABA at around 20 hours. This suggests that in liquid culture PABA levels have been sufficiently depleted to inhibit 1CM and SHMT/GCV/CycA activity. At around 25 hours

the *ΔpabA* and 100 μM PABA condition also appears to reach a glycine plateau, this may correspond with an exponential growth of bacteria during the time period creating an exponential demand for PABA and inhibiting 1CM.

Together the results suggest that impaired bacterial folate synthesis in either an *ΔrpoS* or *ΔpabA* model does not alter amino acid uptake or excretion compared to WTK. The bacteria are still able to sufficiently synthesise folates for 1CM to maintain metabolism of amino acids, in particular methionine, serine and glycine which are downstream products of the folate cycle (Y. K. Kwon et al., 2010; R. J. Nichols et al., 2011).

4.3.7 The effect of sulfamethoxazole on the bacterial amino acid exometabolome

To understand if 128 μg/ml SMX alters the *E. coli* amino acid exometabolome a comparison of the SMX condition against WTK and the mutant strains was made using the previously developed LC-MS/MS protocol. It revealed no significant differences in the amino acid exometabolome for phenylalanine, aspartate, threonine, histidine, serine, isoleucine, leucine, methionine, valine, lysine and arginine (figure 4.10). A significant difference was seen for tyrosine, proline, glycine, alanine, glutamate and glycine (figure 4.11).

Tyrosine is an aromatic amino acid and a downstream product of the shikimic acid pathway that is not dependant on 1CM for endogenous synthesis (Walsh, Liu, Rusnak, & Sakaitani, 1990). Uptake is dependent on the general aromatic transporter system AroP (K. D. Brown, 1970) and the tyrosine specific permease TyrP (Andrews, Lawley, & Pittard, 1991). Expression of the uptake pathways are regulated by intracellular levels of tyrosine, phenylalanine and tryptophan and if levels of any one of these aromatic amino acids is high the uptake pathways are depressed (James Pittard & Yang, 2008; Wookey, Pittard, Forrest, & Davidson, 1984). The data in figure 4.10 reveals phenylalanine uptake for SMX is decreased but not significantly compared to the non-SMX conditions. It suggests that SMX may be reducing catabolism of the aromatic amino acids or, increasing synthesis endogenously leading to decreased uptake. Further method development to detect tryptophan in levels within these samples would be required to fully assess this hypothesis.

The significantly elevated proline, alanine and glutamic acid levels in the agar SMX condition (figure 4.10) suggests exogenous uptake is decreased and there is sufficient endogenous synthesis or decreased catabolism within the bacteria.

Proline is synthesised through the chemical reduction of glutamate (Csonka & Leisinger, 2007) whilst uptake of proline is dependent on the transporter PutP that is down regulated by the repressor PutP in response to high endogenous levels of proline (Wood, 1988). Glutamate is added to the amino acid stock solution in its ionic form glutamic acid and uptake is via a glutamate/aspartate transport system (Booth, Kleppang, & Kempsell, 1989; Schellenberg & Furlong, 1977). Here we can see in figure 4.11 that the exogenous level in the agar is significantly higher in the SMX condition than WTK. The decreased sequestering of exogenous glutamic acid may be linked due to elevated endogenous proline negating the need for exogenous glutamate to drive proline synthesis.

Uptake of alanine is via the D-serine/glycine/alanine proton symporter CycA and is inhibited by high levels of endogenous glycine and the branch chain amino acids (BCAAs) leucine, isoleucine and valine (Robbins & Oxender, 1973). Figure 4.9 shows that the BCAA levels in the agar for the SMX condition are elevated (but not significantly) compared to WTK and figure 4.10 shows that the glycine level is significantly higher than the WTK condition suggesting intracellular levels of the BCAAs and glycine may be sufficient to inhibit uptake of alanine.

Alanine, proline and glutamate are carbon sources for multiple metabolic pathways that can be used to endogenously synthesise substrates for rapid aerobic growth (figure 4.12) (Franklin & Venables, 1976; Marcus & Halpern, 1969; Wood, 1988). The elevated levels in the SMX agar may also be a product of decreased bacterial metabolism. This corresponds with the finding that *E. coli* treated with 128 μg/ml SMX has attenuated growth compared to WTK which is discussed in detail in sections 5.3.1-5.3.4 of chapter 5 of this thesis. The attenuation of bacterial growth by SMX may reduce the overall demand for carbon sources from the amino acids proline, alanine and glutamate subsequently maintaining higher endogenous levels and reducing uptake from the agar.

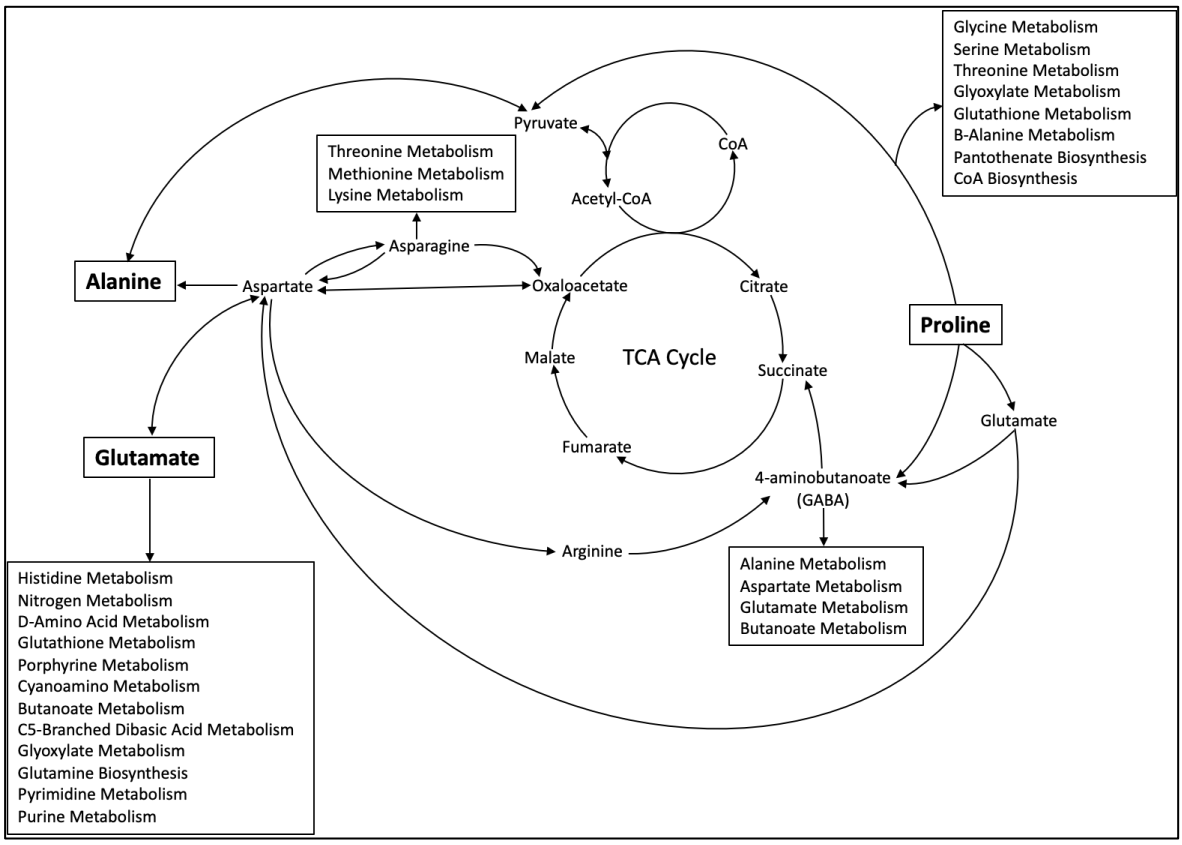


**Figure 4.12 Simplified schematic of *E. coli* pathways of glutamate, proline and alanine metabolism.** Exogenous derived glutamate, proline and alanine provide substrates for numerous pathways required for bacterial growth and energy synthesis including their respective de-novo synthesis. Amino acids in bold represent exogenously derived substrates. Adapted from (KEGG, 2021; Keseler, 2021)

Glycine in the SMX condition was found to be significantly higher than in the WTK and mutant conditions (figure 4.11). The major source of 1C units and glycine biosynthesis occurs through the reversible interconversion of serine to glycine by the *glyA* gene product SHMT (G. Stauffer, 1996). It is dependent on THF for the transfer and receipt of a 1C unit yielding 5,10-met THF (Ghrist & Stauffer, 1995; Y. K. Kwon et al., 2010; G. Stauffer, 1996; G. V. Stauffer & Stewart, 2004). A secondary 1CM independent pathway catabolises threonine in two steps to synthesise acetyl CoA and glycine (J. Fraser & Newman, 1975; G. Stauffer, 1996; G. V. Stauffer & Stewart, 2004). Together these pathways provide de-novo endogenous glycine whilst the SHMT pathway can provide both glycine and serine to the bacteria.

In the absence of sufficient THFs the SHMT pathway may be unable to convert serine to glycine or vice versa due to the lack of THF and 5,10-metTHF. In addition, oxidative

cleavage of glycine by the glycine cleavage system (GCV) pathway is also dependent on THF to produce 5,10-met THF, $CO_2$ and $NH_3$ (G. Stauffer, 1996; G. V. Stauffer & Stewart, 2004). Sulfa drugs have previously been shown to down regulate expression of GCV genes thus, further reducing 1C unit availability and facilitating an increase in endogenous glycine levels (R. J. Nichols et al., 2011). A contributing factor to the potential accumulation of endogenous glycine is repression of *glyA* Elevated levels of internal and external glycine has been shown to downregulate the expression of *glyA* and its gene product SHMT. (B. Miller & Newman, 1974; G. V. Stauffer & Stewart, 2004; X. Zhang, El-Hajj, & Newman, 2010). The loss of this enzyme may contribute to the internal glycine pool but may also contribute further to the starvation of 1C units that drive these mechanisms.

Inhibition of glycine uptake by bacterial negative feedback mechanisms may cause the observed elevated glycine levels in the DM compared to the WTK and mutant conditions. The WTK and mutant conditions may have sufficient 1CM to degrade glycine below the threshold for transporter inhibition. Loss of functional 1CM in the SMX condition may also be having a wider effect by preventing uptake of exogenous glycine. A major route for glycine uptake is through the membrane transporter CycA a serine/alanine/glycine:$H^+$ symporter (Robbins & Oxender, 1973; G. V. Stauffer & Stewart, 2004). It is negatively regulated by expression of sRNA encoded by the gene *gcvB* (G. V. Stauffer & Stewart, 2004; Urbanowski, Stauffer, & Stauffer, 2000). High intracellular levels of glycine activates transcription of *gcvB* that targets *cycA* mRNA preventing translation by blocking ribosome binding to down regulate expression of the *cycA* glycine uptake pathway (Pulvermacher, Stauffer, & Stauffer, 2009; G. V. Stauffer & Stewart, 2004; Urbanowski et al., 2000). A combination of the endogenous supply of threonine derived glycine and the loss of key glycine degradation pathways may be causing an accumulation of endogenous glycine. This may be inhibiting uptake of glycine from the DM and having a wider effect by reducing alanine uptake via the *cycA* pathway

The differences between the WTK, mutant and SMX conditions may be attributed to the respective conditions ability to alleviate diminished 1CM through sequestering of available PABA in DM. The addition of 0.1 μM PABA to DM has been shown to recover *ΔpabA* and *ΔrpoS* bacterial growth to WT levels suggesting that 1CM remains intact to sufficiently support the serine-glycine pathway (Maynard, 2017). Growth data discussed

in chapter 5 reveals that 0.1 μM PABA does not fully recover growth of *E. coli* treated with 128 μg/ml SMX. This may correlate with disruption to the SHMT and GCV pathways and a wider impact on metabolism. Without an appropriate method of quantifing the exometabolomic data it is impossible to determine if elevated glycine, proline, tyrosine, alanine and glutamic acid in the agar is a product of excretion or a product of decreased uptake from imapaired 1CM by SMX.

Together the data does not show a correlation between the mutant and SMX amino acid exometabolome. SMX has a noticeable impact on *E. coli* amino acid metabolism, unlike the mutants that remain relatively indistinguishable from WTK. This suggests that 1CM in folate deficient mutants is preserved at a level to maintain normal metabolism. And that the associated amino acid metabolic pathways may not be the source of the observed lifespan increase in *C. elegans*.

## 4.4 Discussion

### 4.4.1 Development of a LC-MS/MS protocol to investigate *E. coli* amino acid exometabolome

Of specific interest to this work are changes to amino acid metabolism in *E. coli* from decreased bacterial folate synthesis. Specifically, the downstream products of folate synthesis that may slow the ageing of *C. elegans*. Previously work established that disruption of the folate synthesis pathway by either drug or, single gene knockout mutant increases worm lifespan independently of folates and not as a product of dietary restriction (Virk et al., 2012 & 2016).

Folates have numerous and diverse roles in bacterial metabolism (Dawadi, Kordus, Baughn, & Aldrich, 2017). It was proposed that the disruption of the folate cycle would have an effect on multiple downstream pathways. Rather than one individual bacterial component that may be responsible for the phenotype. The respective collective metabolites of these pathways may yield a metabolome that elicits the lifespan increasing response in the host.

To investigate this potential mechanism, a novel protocol was devised to extract amino acids from media the *E. coli* lawns and *C. elegans* are maintained on and analyse them

using LC-MS/MS. A comparison was made against a baseline of known amino acid concentration within the agar. The protocol was found to be successful in extracting the amino acids and providing a comparison between patterns of change between conditions. However, it was not possible to accurately quantify the amino acids relative to the expected concentration in the DM stock. This observation appeared to be independent of the agar, amino acid stock solution, and SMX.

Interactions between reagents may cause a matrix effect where ionization efficiency is altered by coeluting analytes adversely affecting sensitivity and limits of quantification (Taylor, 2005). Suppression of ionisation is a much more common matrix effect phenomenon than analyte enhancement (Furey, Moriarty, Bane, Kinsella, & Lehane, 2013). Quantification of amino acids above expected baseline concentration was observed across all amino acids with varying physiochemical properties spanning the full gradient. The over quantification was not seen in preliminary matrix effect experiments comparing water and DM. Nor was it seen in the amino acid stock solution, suggesting there was no error in the preparation of the stock used for media preparation.

It is possible an interaction causing a matrix effect may be occurring between the DM reagents potassium phosphate, $MgSO_4$, cholesterol, trace metal and B12 solutions. No significant difference was observed in the slope between the DM and $H_2O$ conditions, suggesting that the DM itself may not be the cause.

The possibility of a dehydration concentration effect whilst in incubation has been considered but ruled out. Over estimation of amino acids was seen in both liquid DM and DM agar. Liquid DM is incubated in a sealed falcon tube. Whilst some loss of $H_2O$ from the agar occurs over time the mass loss to the sample is compensated by the ratio of 0.1N HCl to sample mass for extraction. Meaning dilution is relative to mass and negating any concentration effect.

The observed over quantification as a product of the extraction protocol, as opposed to a matrix effect from the media or reagents has also been ruled out. The equipment used to extract agar samples is not used for obtaining liquid DM samples which relies on sterile pipetting and filter sterilisation. In addition, sample preparation in separate laboratories by different people using independently provided equipment and reagents did not prevent

signal amplification. A common denominator may be the use of Eppendorf tubes that may be inadvertently interacting with the samples causing artifacts that are confounding the results (Chanotiya, Pragadhessh, & Uniyal, 2013; Grzeskowiak & Eppendorf).

Further work will be needed to determine why the quantification of amino acids does not correlate with expected baseline levels in the media. Improvements to explore include the use of solid phase extraction (SPE) to remove potential matrix interference. And the use of standard addition for quantification or the use of labelled internal standards. The time constraints of the project meant SPE or standard addition experiments were unfeasible due to large increase in injections per sample required to generate the standard curves. Another alternative would be to use labelled standards that can be spiked into samples. Due to the varying physiochemical properties of the amino acids one standard per amino acid would be best practice. The cost of purchasing these standards was not appropriate at this time. A number of amino acids that appear to be altered between the SMX and WTK conditions were identified. This preliminary data could be used to filter the list of candidates in the first instance.

Due to the previously discussed amplification anomaly, the protocol and analysis method was deemed insufficiently accurate to quantitively measure *E. coli* exometabolomic changes. Without an accurate measurement of concentration, it was not possible to determine if differences seen between conditions were a product of bacterial uptake of amino acids from the DM or, changes in excretion. Because both uptake and excretion is likely to be occurring simultaneously, endometabolomic data and the use of labelled substrates to identify metabolites would be needed to properly evaluate amino acid flux. By focusing on the PAU data, the protocol did provide a suitable method to observe and compare relative changes in the levels of amino acids between conditions. Differences in ionisation efficiency are relative to the analyte's respective standards. The sensitivity of individual amino acids may limit quantification and comparison amongst the wider pool of amino acids but, differences can be observed within the thresholds of sensitivity of detection. The use of a non-lawn DM agar plate provides a suitable baseline for comparison as this too is subjected to the same amplification anomaly negating the positive bias.

4.4.2 LC-MS/MS analysis of the bacterial lawn amino acid exometabolome

The qualitative analysis of the amino acid exometabolome of known folate deficient *E. coli* mutants that increase *C. elegans* lifespan; *ΔrpoS* and *ΔpabA* revealed no significant differences between the WT condition. The data also showed no correlation between the amino acid exometabolome of the mutants and *E. coli* treated with 128 μg/ml SMX. The SMX condition showed significant differences between the WTK and mutant conditions for the 1CM associated amino acids serine and glycine, the aromatic amino acid tyrosine and the amino acids glutamic acid, proline and alanine.

Glutamic acid, proline and alanine are utilised as carbon sources by *E. coli* (Franklin & Venables, 1976; Marcus & Halpern, 1969; Wood, 1988). The elevated levels in the SMX-DM agar condition may be attributed to decreased metabolic demand that correlates with attenuated bacterial growth, including in the presence of sufficient PABA to support WTK and mutant growth. The elevated alanine levels may also be a product of disrupted glycine metabolism from the loss of sufficient 1CM causing down regulation of alanine uptake pathways.

4.4.3 The LC-MS/MS glycine/serine data reproduces previous nuclear magnetic resonance analysis data

Strikingly the data for serine and glycine revealed a similar pattern as previously seen with the *E. coli* strain *ΔpabA* in an investigation using NMR in our lab by Helliwell (2013). Both experiments revealed the complete uptake of serine by all conditions by the 40 hour and 48 hour time points. This corroborates with previously documented findings that *E.coli* preferentially utilises serine during exponential growth and is rapidly taken up before other amino acids (Kriner & Subramaniam, 2020; Prüss, Nelms, Park, & Wolfe, 1994; Selvarasu et al., 2009; X. Zhang et al., 2010). No further similarities were seen between conditions. Nor did I reproduce the findings by Helliwell (2013) that *ΔpabA* had elevated glycine at 48 hours. In this study this was only seen in the SMX condition (figure 4.12). The reason for this lack of reproducibility may be due to the effectiveness of PABA in rescuing 1CM of *ΔpabA* in liquid culture compared to DM agar. Bacterial growth in liquid culture may be optimised due to the availability of nutrients in free media as opposed to an agar matrix which may be dictated by nutrient gradients in the agar (discussed in detail in chapter 5).

In the current LC-MS/MS data this pattern of glycine consumption was not seen in the *ΔpabA* condition. The bacterial lawn consists of 100 µl of bacterial culture on the surface of DM agar as opposed to immersed in 250 ml of liquid DM. Growth will not be relative between the two. The lawn can only obtain nutrients and PABA available at the interface between the bacteria and the agar whereas the liquid culture is surrounded by its nutrient source and that nutrient source is not bound in an agar matrix limiting accessibility that in turn modulates growth and subsequent 1CM demand. A comparison of final $OD_{600}$ for bacterial growth between the two experiments may reveal these differences in growth dynamic between conditions.

Another confounding factor to comparison is differences in analytical methods as opposed to biological differences. The NMR study reported on glycine concentration in mM, unlike this study which is restricted to analysis of analyte changes measured by PAU. This prevents a direct comparison between the two experiments. Also, the previous NMR study was conducted using liquid DM culture and *ΔpabA* supplemented with 0.2 µM or 100 µM PABA and restricted to 40 hours. Samples were obtained through centrifugation and concerns were raised about potential ethanol contamination in tubes skewing the data (Helliwell, 2013). This study used LC-MS/MS to analyse DM agar supplemented with 0.1 µM PABA. It relied on a novel extraction method that did not use ethanol to recover metabolites from a bacterial lawn after 48 hours of incubation.

Overall, the attempts to quantify the amino acids yielded levels above the expected baseline amount preventing accurate quantification of the exometabolomic data, This made it difficult to determine if the elevated amino acids seen in the agar are a product of excretion or decreased uptake due to impairment of 1CM by SMX. Comparison with the non-lawn agar condition (timepoint 0 hours), provides a baseline from which we can infer bacterial uptake from the agar based on and changes in individual amino acids. A further complication of adopting this methodology is unlike liquid cultures where repeat sampling is possible, each agar plate representing different timepoints is an indepenent culture. Despite these limitations some significant differences in the amino acid profile of the SMX and WTK conditions have been observed that aligns with previous findings from our group. Further work to refine the protocol and improve the quality of the data have been outlined.

# Chapter 5

# Investigating The *E. coli* Exometabolome in Defined Media Agar Over Time to Understand If Changes in Amino Acids by Sulfamethoxazole Alters Lawn Growth and Slow Ageing in *C. elegans*

## 5.1 Introduction

Researchers using the *C. elegans* model have revealed a considerable amount of bacterially derived molecules that can beneficially affect *C. elegans* lifespan. These are discussed in detail in chapter 1, sections 1.2.11 and 1.2.12 of this thesis. Amongst these metabolites, amino acids have been found to influence the lifespan of *C. elegans* (Canfield & Bradshaw, 2019; Edwards et al., 2015; Le Couteur et al., 2020; Mansfeld et al., 2015). Except for phenylalanine nineteen of the common amino acids when supplemented exogenously were found to increase lifespan in a range of concentrations from 1 mM to 10 mM (Canfield & Bradshaw, 2019; Edwards et al., 2015). It was also found that branch chain amino acid (BCAA) catabolism when inhibited in *C. elegans* increased lifespan and supplementation with individual BCAA's also promoted the health and lifespan of the worm (Le Couteur et al., 2020; Mansfeld et al., 2015).

### 5.1.1 The wider effect of sulfamethoxazole on bacterial growth

The effect of SMX on growth of the kanamycin resistant strain of BW25113 *E. coli* (WTK) and its effect on bacteria grown on defined media has not previously been investigated. Defined media (DM) controls for the availability of folate precursors and other nutrients. WTK serves as an appropriate control when compared to Keio mutants (they have a Kanamycin resistance insert at the site of the single gene knockout).

As part of our lifespan protocol, a pre-starvation step during bacterial culture was included. This removed excess folate breakdown products that are carried over from the parent Luria Bertani (LB) culture. The DM for the agar plates are supplemented with 0.1 μM para-aminobenzoic acid (PABA). Development work conducted by Helliwell (2013); Maynard

(2017) reported 0.1 μM PABA is the minimum concentration required for bacterial lawn growth on DM agar without reversing the lifespan effect of *ΔpabA*. *C. elegans* maintained on *ΔpabA* have significantly longer lifespans compared to worms maintenance on WT and WTK *E. coli (Maynard, 2017)*. It was also found that supplementing agar with 250 μM PABA reverses the extended lifespan phenotype of *C. elegans* maintained on 128 μg/ml SMX treated *E. coli* to control levels (Virk, 2013).

The effect on lawn growth has not previously been measured to observe if the lawn returns to control levels in correlation with lifespan under the 250 μM PABA conditions. *C. elegans* maintained on SMX treated lawns do not have reduced fecundity suggesting dietary restriction (DR) is not the cause of the increased lifespan observed with SMX (Virk et al., 2016). The effect of SMX on lawn proliferation, growth and its relationship to lifespan is not fully understood. The observed increase in *C. elegans* lifespan may be a product of altered metabolic pathways downstream of 1CM, including amino acid metabolism that has been previously shown to influence lifespan. Understanding the relationship between lifespan and lawn growth during bacterial folate synthesis inhibition may provide further insight into the correlation between proliferation and lifespan.

### 5.1.2 Investigating the temporal aspect of the amino acid exometabolome and the effects of those changes on the healthspan of *C. elegans*

Chapter 4 found that *E. coli* treated with 128 μg/ml SMX had an altered amino acid exometabolome compared to WTK and folate deficient mutants that extend *C. elegans* lifespan. Of particular interest was changes to glycine uptake similar to previous findings by Helliwell (2013) who used NMR to explore the Δ*pabA* exometabolome. A major source of 1C units is the serine-glycine pathway that produces the key folate 5,10-met THF through the interconversion of serine to glycine by SHMT (G. Stauffer, 1996). Disruption of the folate synthesis pathway by SMX and Δ*pabA* reduces bacterial levels of 5,10-met THF (Maynard, 2017). Low levels of 5,10-met THF was found to correlate with extended lifespan in *C. elegans* maintained on the SHMT null mutant *ΔglyA* (Maynard, 2017; Virk et al., 2016).

Other bodies of work have implicated disruption of the serine-glycine pathway in increasing *C. elegans* lifespan through its intrinsic relationship with the methionine

synthesis pathway. The use of metformin, TMP and the sulfonamides DDS and SD were found to induce the DR pathways of the worm through disruption of the methionine synthesis intermediates SAM and SAH, possibly via inhibition of glycine synthesis (Cabreiro et al., 2013; H. Choi et al., 2019; H. S. Choi et al., 2021).

The change to exogenous glycine by SMX may be through folate and 1C unit depletion preventing SHMT from interconverting serine to glycine and vice versa halting the reaction. GCV may also be unable to degrade glycine into new 1C units to feed back into this cycle and support wider metabolism. The endogenous glycine level is maintained by the conversion of threonine to glycine. Glycine may remain above a threshold inhibiting the uptake of external glycine and downregulating SHMT and GCV, compounding the negative feedback loop. Elevated endogenous glycine levels may be directly or indirectly toxic to *E. coli* whilst having the downstream effect of making the bacteria less toxic to *C. elegans*.

Exploring the temporal aspect of the amino acid exometabolome of *E. coli* over the duration of a lifespan may expand our understanding of how SMX effects bacterial amino acid metabolism.

## 5.2 Chapter Aims

1. To test the hypothesis that bacterial growth influences ageing by investigating bacterial lawn growth over the timeframe of a lifespan experiment and how growth is influenced by reduced folate synthesis.
2. Investigate the temporal effect of SMX on the *E. coli* amino acid exometabolome over a longer timespan using the previously developed LC-MS/MS protocol.
3. Investigate if changes to the *E. coli* exometabolome influence *C. elegans* ageing.

## 5.3 Results

5.3.1 Sulfamethoxazole and its effect on bacterial growth over the duration of a lifespan

Lifespan assays have previously been conducted using NGM a common peptone based media that cannot be controlled for micro and macro nutrient content and DM, a

chemically defined folate free media that now remains as the standard within our lab (Maynard, 2017; Virk et al., 2012; Virk et al., 2016). They found that SMX treated *OP50* had a dose dependent increase on *C. elegans* lifespan (Virk et al., 2012) and that the *C. elegans* lifespan increase between NGM and DM was remarkably similar (Helliwell, 2013; Maynard, 2017; Virk, 2013).

It has previously been established that bacterial lawn growth does not correlate with *C. elegans* lifespan in the context of DR and SMX does not affect the growth of WTK on the more widely used NGM agar (Helliwell, 2013; Maynard, 2017; Virk et al., 2016). These studies were limited to a shorter duration than a typical lifespan assay and did not investigate the effect of SMX on bacterial lawn growth (Helliwell, 2013; Maynard, 2017; Virk et al., 2016). Bacteria seeded on DM has only been explored with SMX added but not with a concentration of PABA that rescues lifespan (Helliwell, 2013; Maynard, 2017; Virk et al., 2016).

Maynard (2017) discovered a temporal effect of SMX on lifespan in the reduced bacterial folate model that the amount of *C. elegans* exposure to exponential phase bacteria negatively influenced lifespan. A thorough analysis of the temporal effect of SMX on *E. coli* lawn growth has not been previously conducted within the context of its relationship to lifespan. It may provide further insight into the relationship between bacterial growth and *C. elegans* lifespan.

The method for lawn growth analysis is described in detail in section 2.5.5 of chapter 2 in this thesis. The process is simple but extremely time consuming that can lead to considerable delays in sample recovery between plates and conditions that may skew the data. Limiting plate numbers for each condition and reducing the time points allowed for accurate recovery of robust and reproducible data. It also prevented an unmanageable workload or increased extraction times that could affect sample quality and consistency.

### 5.3.2 A comparison of the growth curves between nematode growth media agar and defined media agar

A similar lifespan increase is seen in *C. elegans* maintained on DM or NGM treated with 128 μg/ml SMX (Maynard, 2017; Virk et al., 2016). A direct comparison between bacterial lawn growth of WTK seeded on DM and NGM has not previously been

conducted. To investigate if growth correlates with the observed lifespan effect growth curves were conducted.

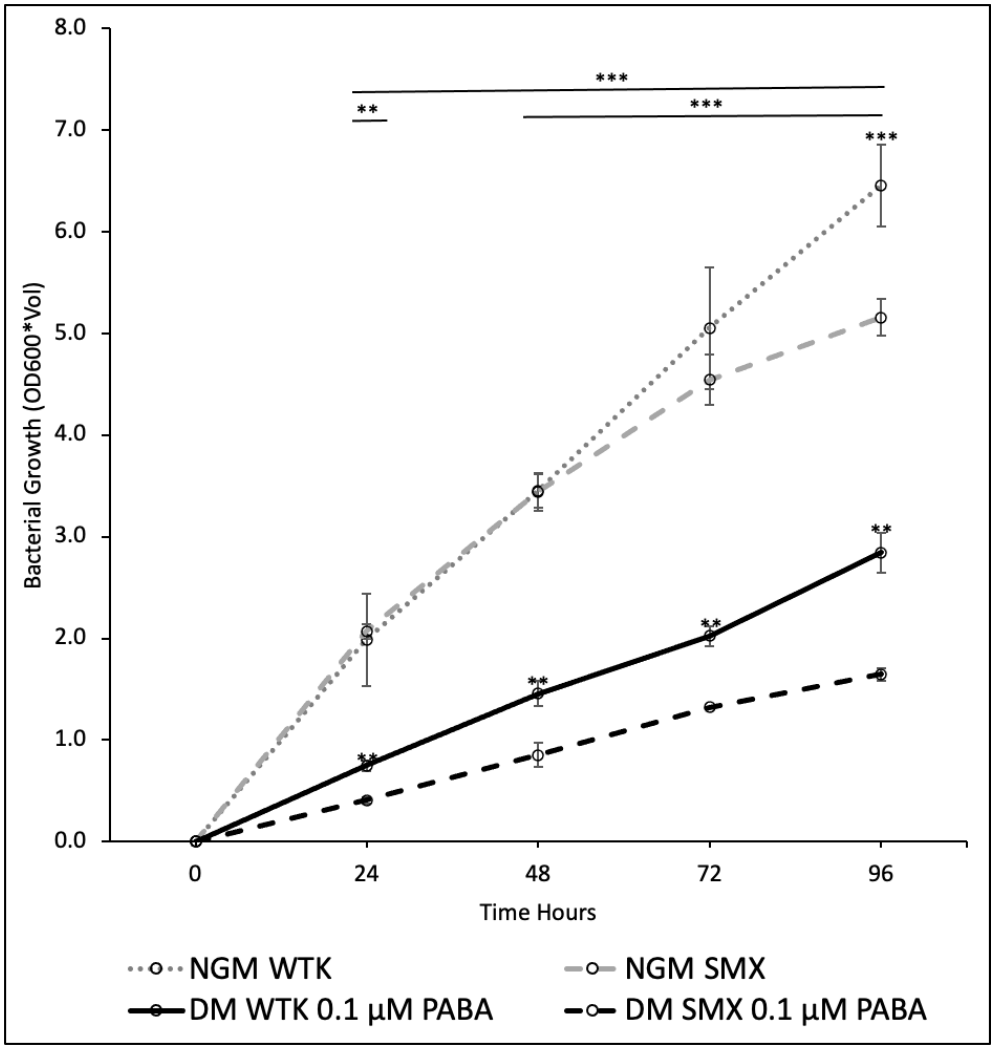


**Figure 5.1 Growth curves of NGM and DM agar +/- 128 µg/ml SMX showing differences in bacterial lawn growth over 96 hours.** Data was obtained from a separate DM and NGM runs (n=5 per condition, per timepoint), solid agar plates +/- 128 µg/ml SMX were seeded with 100 µl WTK cultured in either LB (NGM) or DM + 0.2µM PABA (DM) and incubated at 25 °C. Error bars represent SD. Asterisks represent the results of Student's t-Test Two-Sample Assuming Unequal Variances, ***=P<0.001, **=P<0.005, *=P<0.05, top row of lined asterisks represents NGM WTK v NGM SMX, bottom row represents DM WTK v DM SMX.

Figure 5.1 shows that 128 µg/ml SMX treated NGM agar at 25°C does not affect WTK growth until 72 hours. A small but non-significant reduction in the SMX conditions appears at 72 hours before significantly diverging at 96 hours. These results do not corroborate the results previously reported by Virk (2013) that 128 µg/ml SMX does not

affect bacterial growth although this work used OP50 *E. coli* in liquid NGM at 37 °C and was limited to only 5 hours.

Peptone based media is a rich source of nutrients for the bacterial lawn. It may contain considerable folate pre-cursor metabolites (section 3.3.6i of chapter 3 in this thesis) that may rescue the growth of SMX treated bacteria. After 48 hours these metabolites may have been depleted causing the significantly different divergence in growth. In contrast bacterial lawns grown on DM agar have significantly decreased growth compared to NGM and the DM-SMX lawn growth is significantly reduced compared to DM-WTK at all time points.

DM lacks the nutrient dense profile of NGM. It was originally optimised during development by Helliwell (2013) to provide the essentials for bacterial growth to match NGM, without the inconsistencies or potential abundance of growth promoting metabolites. It also has strictly controlled concentrations of the folate precursor PABA to maintain growth but retain folate levels beneath a threshold that reverses *C. elegans* lifespan. Proprietary blends of peptone can have up to 20% carbohydrates (CHO) and 55% of peptides and amino acids (Guide, 2019). The presence of CHO as an additional carbon source to the already abundant amino acids may promote rapid and increased bacterial growth compared to DM (Bayne-Jones, 1936). NGM also contains trace levels of folates. Exogenous folates provide breakdown products for bacterial folate synthesis and 1CM that may improve growth compared to DM and provide a small rescue to SMX (Helliwell, 2013; Maser, Peebo, Vilu, & Nahku, 2020; Zampieri, Hörl, Hotz, Müller, & Sauer, 2019).

The results suggest that there is no correlation between bacterial growth and *C. elegans* lifespan between either media as bacterial growth on DM is significantly reduced. It can also be seen from these results that the nutrient profile of DM does not maintain bacterial growth at the same level as NGM. For the purposes of the remainder of this chapter the focus will remain on DM agar. DM agar is the current medium used in all lifespan protocols and is relevant to the wider body of work presented here.

5.3.3 Effect of defined media agar on the growth of the low folate *E. coli* mutant *ΔpabA*

To investigate if growth of the *E. coli* mutant *ΔpabA* correlates with SMX treated bacterial growth on DM growth curves were conducted. *C. elegans* maintained on DM agar seeded with *ΔpabA* have a long-lived phenotype. The mutant is also dependent on exogenous PABA to recover growth on DM agar with concentrations >0.1 µM PABA sufficient to reverse the lifespan effect on *C. elegans* (Maynard, 2017). The SMX lifespan extension of *C. elegans* can also be reversed with 250 µM PABA (Virk, 2013) which will be explored further in section 5.4.3 of this chapter. The effect of PABA on *ΔpabA* growth has not been investigated over the duration of a lifespan of 168 hours. This is time from seeding to the first transfer of animals to fresh plates and lawns. A comparison was made with SMX treated bacteria to observe if the two long life promoting bacterial conditions shared growth characteristics.

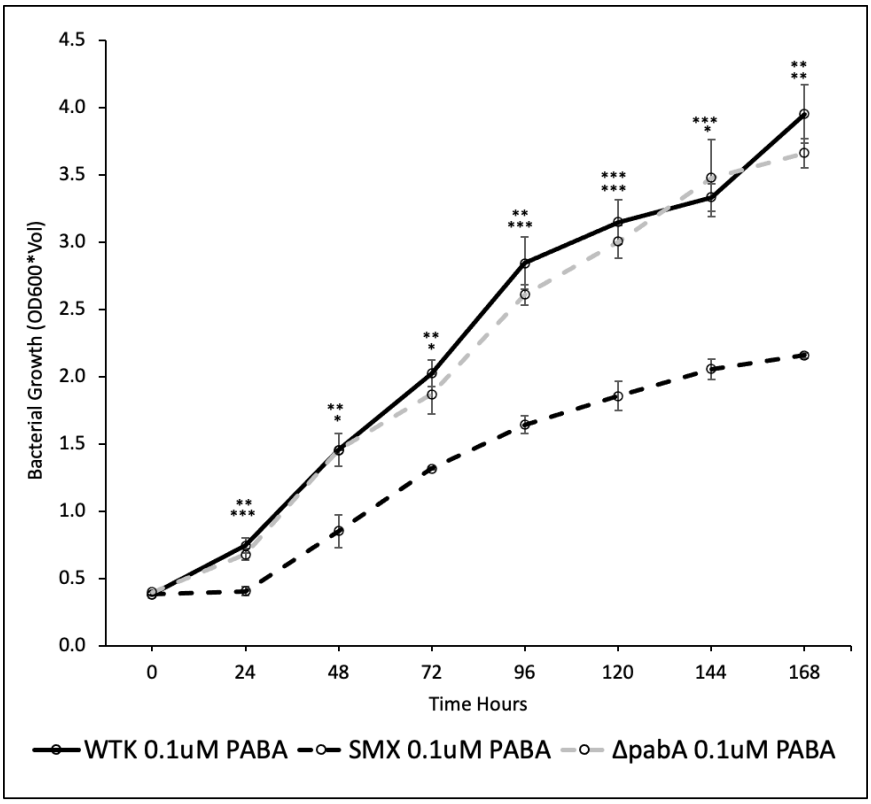


**Figure 5.2 Growth curves of *ΔpabA* and WTK +/- 128 µg/ml SMX on DM over the duration of a lifespan.** DM solid agar plates (n=5 per condition, per timepoint) supplemented with 0.1 µM PABA were seeded with 100 µl WTK or *ΔpabA* cultured in DM + 0.2µM PABA and incubated at 25 °C. Error bars represent SD over 3 biological replicates. Asterisks represent the results of Student's t-Test Two-Sample Assuming Unequal Variances, ***=P<0.001, **=P<0.005, *=P<0.05, top row of asterisks represents WTK v SMX, the bottom row represents *ΔpabA* v SMX.

Comparing the growth of *ΔpabA* to SMX treated WTK during *C. elegans* lifespan conditions showed that the mutant had no significant difference in growth than WTK and was significantly higher than the SMX condition (figure 5.2). As a competitive inhibitor 128 μg/ml SMX has a more severe effect on growth than the partial loss of an enzyme. *ΔpabA* can utilise the PABA without competition. Not having to compete with SMX for the enzyme allows for much lower concentrations of PABA to rescue the folate synthesis pathway and recover growth to WTK levels. Unlike SMX conditions that requiring high concentrations of PABA for rescue to outcompete the drug at the site of action. Interestingly the morphology of this strain is remarkably similar to WTK shown in figure 3.9F of chapter 3 in this thesis. Suggesting there is no correlation between bacterial proliferation mechanisms and lifespan in the reduced folate model.

### 5.3.4 Recovery of the sulfamethoxazole bacterial lawn with 250 μM para-aminobenzoic acid

Included in the original work by Virk (2013) was an analysis of the effect of PABA as a rescue to 128 μg/ml SMX (505 μM). It showed that a concentration of 250 μM PABA fully rescued the increased lifespan of *C. elegans* to WT control levels (Virk, 2013). It did not show if it also rescued bacterial growth to WTK levels. A growth curve was conducted to investigate if reversal of *C. elegans* lifespan by SMX rescued bacterial growth. Measurements were limited to the following points along the lifespan timeline; 48 hours, the timepoint animals are added to the plate; 168 hours, the time of first transfer of worms to a new plate; 96 hours, An appropriate mid-point for continuity.

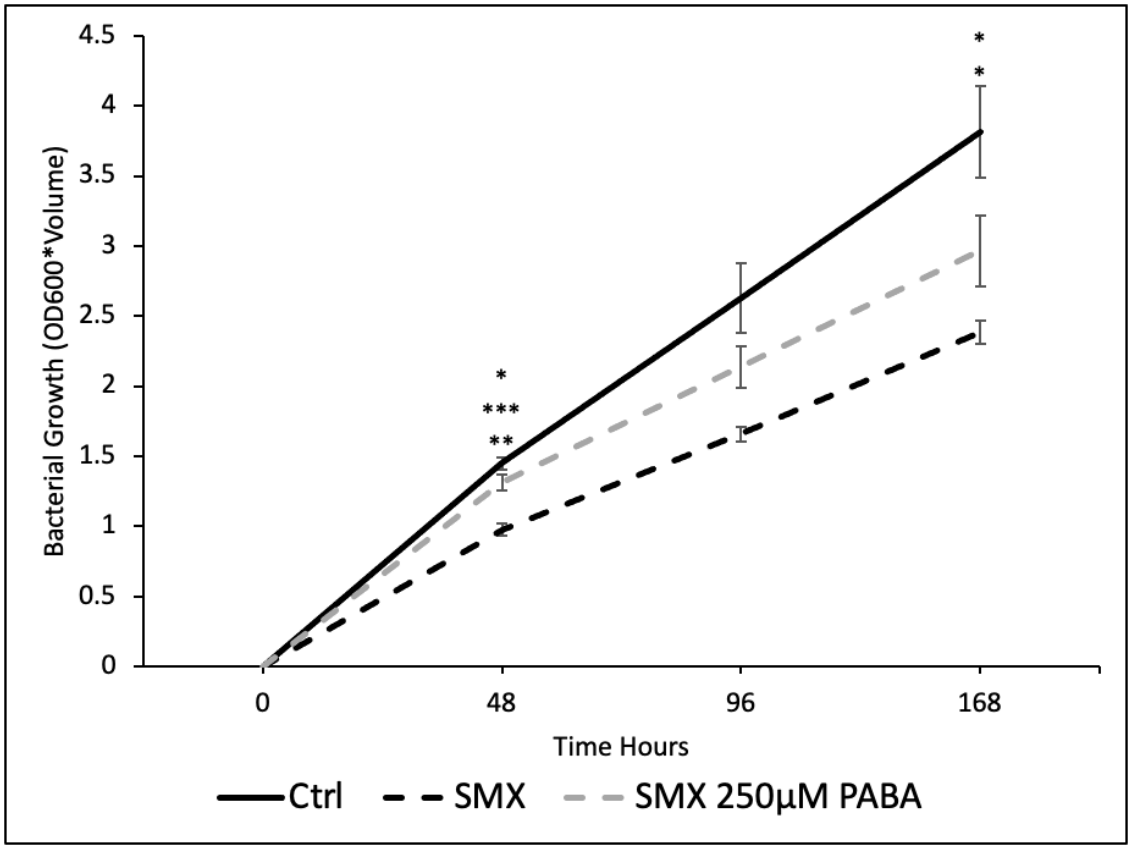


**Figure 5.3 Growth curves of WTK and WTK + 128 µg/ml SMX +/- 250 µM PABA at select points over the duration of a lifespan.** DM solid agar plates (n=5 per condition, per timepoint) supplemented with 0.1 µM PABA or 250 µM PABA were seeded with 100 µl WTK cultured in DM + 0.2µM PABA and incubated at 25 °C. Error bars represent SD over 3 biological replicates. Asterisks represent the results of Student's t-Test Two-Sample Assuming Unequal Variances, ***=P<0.001, **=P<0.005, *=P<0.05, top row of asterisks represents WTK v SMX 250 µM PABA, middle row represents WTK v SMX and bottom row represents SMX 250 µM PABA v SMX.

The growth curve in figure 5.3 shows that 250 µM PABA led to a partial recovery of lawn growth in the SMX condition but did not return it to WTK levels. The concentration of SMX in a lifespan assay is 505 µM. The addition of 250 µM PABA may not be enough to completely abolish the effect of SMX by outcompeting it at the enzyme. Thus, being unable to synthesise folates to the minimum threshold required to rescue lawn growth to match WTK growth on DM media. Growth is only partially recovered by 250 µM PABA. It cannot outcompete SMX but was able to fully reverse the lifespan effect, at least on NGM. This suggests that the *C. elegans* increase in lifespan seen with SMX treated bacteria is independent of bacterial growth. Downstream mechanisms involved in

reducing host lifespan may only require low levels of folates to be reinstated to a level of functionality that reduces *C. elegans* lifespan.

Together these results show SMX does result in lawns with less bacteria at timepoints that had not been measured previously and slows bacterial growth in the long term. Bacterial growth and proliferation may not correlating with or, be the causative factor in lifespan. Rather, it may be the disruption or, upregulation of metabolites downstream from folate synthesis that are key to the mechanism of how sub-mic doses of SMX are able to increase *C. elegans* longevity.

5.3.5 Effect of sulfamethoxazole on the amino acid exometabolome over time

The use of a novel method to extract and analyse the *E. coli* exometabolome from DM revealed significant differences when bacterial lawns were treated with 128 μg/ml SMX. In SMX treated bacteria the non-polar amino acids glycine, alanine and proline, the aromatic amino acid tyrosine and the acidic amino acid glutamic acid all showed a significantly reduced uptake compared to the WTK control at 48 hours. This time corresponds with the point in a lifespan assay when *C. elegans* is added to the lawn on the agar plate. This also corresponds with previous work by Maynard (2017) that showed a temporal window exists for maximal lifespan increase on SMX treated lawns, reviewed in detail in chapter 1.3.9 of this thesis.

To understand if the observed changes at 48 hours persisted over time a temporal assay was conducted using the LC-MS/MS method described in chapters 2 and 4 of this thesis. In a lifespan assay the worms are added to their respective lawns at 48 hours from bacterial seeding of the agar and maintained on the lawn for a maximum of 7 days.

It was found to be impractical for accurate sample handling and too large for LC-MS/MS analysis to obtain 9 days of agar samples with sufficient biological replicates (3-5 replicates). Attempts to run a high volume of samples through the LC-MS/MS had a detrimental impact on elution times and caused widespread variation amongst the data. The timepoints for review were limited to a maximum of 120 hours with samples being obtained every 24 hours. This allowed for sufficient sample analysis on either side of 48 hours to observe any changes to the exometabolome within the agar.

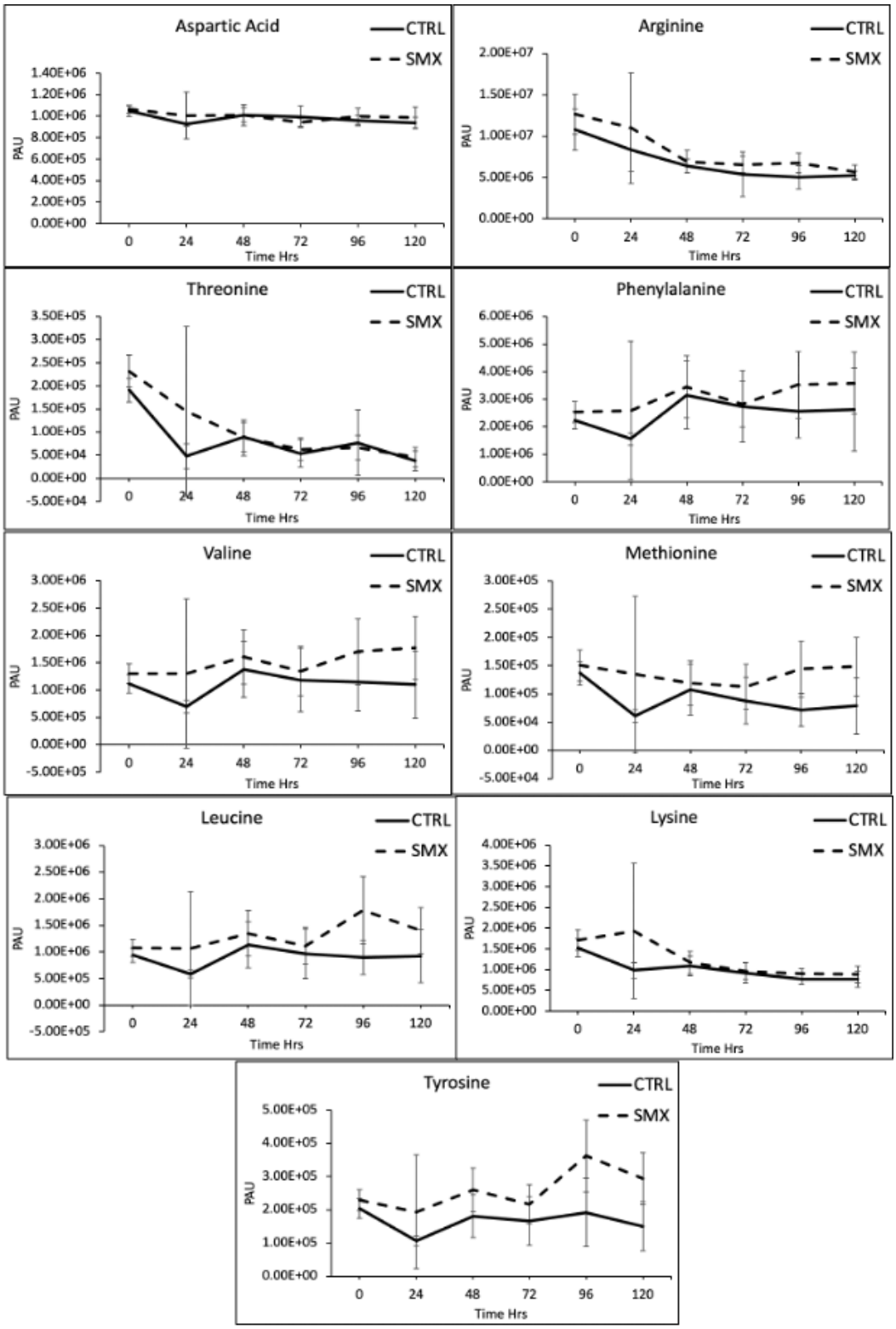


**Figure 5.4 Graphs showing LC-MS/MS analysis of *E. coli* amino acid exometabolome in DM agar over 120 hours that did not reveal any significant changes.** Samples (n=5 per condition, per timepoint) were obtained from the full depth of the agar beneath the centre of bacterial lawns seeded on DM agar and incubated at 25 °C. PAU, peak area under the curve. Error bars represent SD. Statistical analysis was conducted with Student's t-Test Two-Sample Assuming Unequal Variances.

The results in figure 5.4 show no significant differences were observed over the duration of the analysis for aspartic acid, arginine, threonine, phenylalanine, valine, methionine, leucine, serine, tyrosine and lysine. Cysteine, histidine, isoleucine and tryptophan were omitted from the results due to overly short or long elution times causing significant inaccuracies in detection. The amino acids in figure 5.4 have previously been discussed in detail in section 4.3.7 of chapter 4. There is considerable variation seen within the samples for each amino acid due to the presence of outliers within the data as can clearly be seen at 24 hours which may be negatively skewing the results. The additional data obtained from multiple time points that show amino acid PAU increasing from below 0 hours levels to the same or above 0 hours may suggest excretion is occurring.

The lack of significant differences seen between amino acids in the conditions corresponds with the 48 hour data in chapter 4 of this thesis. In the SMX condition tyrosine levels are higher but not statistically significant than the WTK control at all time points. Valine, phenylalanine, methionine and leucine all show a non-significant increase compared to the WTK control at 72, 96 and 120 hours and share a similar pattern of change over the duration of the experiment. Analysis of data from multiple repeats (data presented in appendix A) suggests the elevated levels seen in the SMX condition for tyrosine, valine, phenylalanine, methionine and leucine may not be excretion but a reduced uptake from the DM.

Methionine uptake is via the ABC MetNIQ high affinity transporter system (Kadaba, Kaiser, Johnson, Lee, & Rees, 2008). It is regulated by the MetJ repressor that is expressed in relation to the pool size of intracellular methionine as part of a negative feedback loop (Weissbach & Brot, 1991). where expression of the ABC transport system is upregulated when intracellular methionine levels fall below 150 μM (Bennett et al., 2009; R. J. Kadner, 1974; R J Kadner, 1977; J. G. Yang & Rees, 2015). De-novo synthesis of methionine is energy expensive for E. coli. The presence of extracellular methionine preferentially drives uptake as it is energetically more efficient (J. G. Yang & Rees, 2015). The preference for external supply may also reduce the demand for intracellular 1C units through attenuation of biosynthesis of methionine from homoserine (Ferla & Patrick, 2014) mediating the impact of SMX on 1CM.

Phenylalanine has multiple pathways for entry into the cell. The constitutively expressed high affinity transporter PheP (Cosgriff et al., 2000; Whipp & Pittard, 1977) exclusively transports phenylalanine in conjunction the aromatic amino acid transporter AroP that facilitates transport of phenylalanine, tryptophan and tyrosine (James Pittard & Yang, 2008). Tyrosine is also transported by AroP but can also be taken up by its specific transporter TyrP (Wookey et al., 1984). High intracellular levels of the aromatic amino acids can individually inhibit expression of transport pathways through the activity of the repressor/activator protein TyrR (Camakaris & Pittard, 1982; J. Pittard, Camakaris, & Yang, 2005). Tyrosine and phenylalanine can also be transported into the cell by the branched chain amino acid high affinity transport system LIV-I (Koyanagi, Katayama, Suzuki, & Kumagai, 2004).

Valine and leucine transport is by the high affinity LIV-I and low affinity branched chain amino acid LIV-II transport systems leucine is also transported by the high affinity LS system (Haney, Platko, Oxender, & Calvo, 1992; Koyanagi et al., 2004; Rahmanian, Claus, & Oxender, 1973). The BCAA transport systems are regulated by the Lrp (DNA-binding transcriptional dual regulator Lrp) protein (Calvo & Matthews, 1994; Haney et al., 1992). Lrp functions as a nutrient sensor to regulate their expression and the expression of other genes involved in metabolism at times of feast or famine by responding to leucine levels (Calvo & Matthews, 1994; Haney et al., 1992).

Together the MetNIQ, AroP, PheP, TyrP, Liv-I, LIV-II and LS transport systems supply proteinogenic amino acids to the bacteria (Aledo, 2019; Calvo & Matthews, 1994; J. Pittard et al., 2005). They modulate bacterial metabolism to support bacterial growth through their respective regulatory pathways by Lrp and TyrR independently of 1C unit availability (Aledo, 2019; Calvo & Matthews, 1994; James Pittard, Yang, & Stewart, 2008). Sections 5.3.4 and figure 5.3 of this chapter demonstrates SMX significantly attenuates growth of *E. coli*. Attenuated growth may reduce metabolic demand for protein synthesis and cell division substrates. The elevated levels of phenylalanine, methionine, valine, leucine and tyrosine reported in the SMX condition of figure 3.4 may not be from a direct effect of SMX on uptake and metabolism. It may be a product of reduced bacterial growth from impaired 1CM reducing demand for these amino acids.

5.3.6 Sulfamethoxazole alters *E. coli* amino acid exometabolome as a product or reduced bacterial growth

It was reported in section 4.4.3 of chapter 4 of this thesis that *E. coli* treated with 128 μg/ml SMX significantly changed glycine, glutamic acid, proline and alanine levels in DM agar. To investigate is these changes were reproducible and persistent over time data from the LC-MS/MS temporal assays described in section 5.3.5 of this chapter was analysed. The data reveals variation amongst samples appears to be high and may be skewing the results, in particular at 24 hours which has been previously discussed in section 5.3.5 of this chapter.

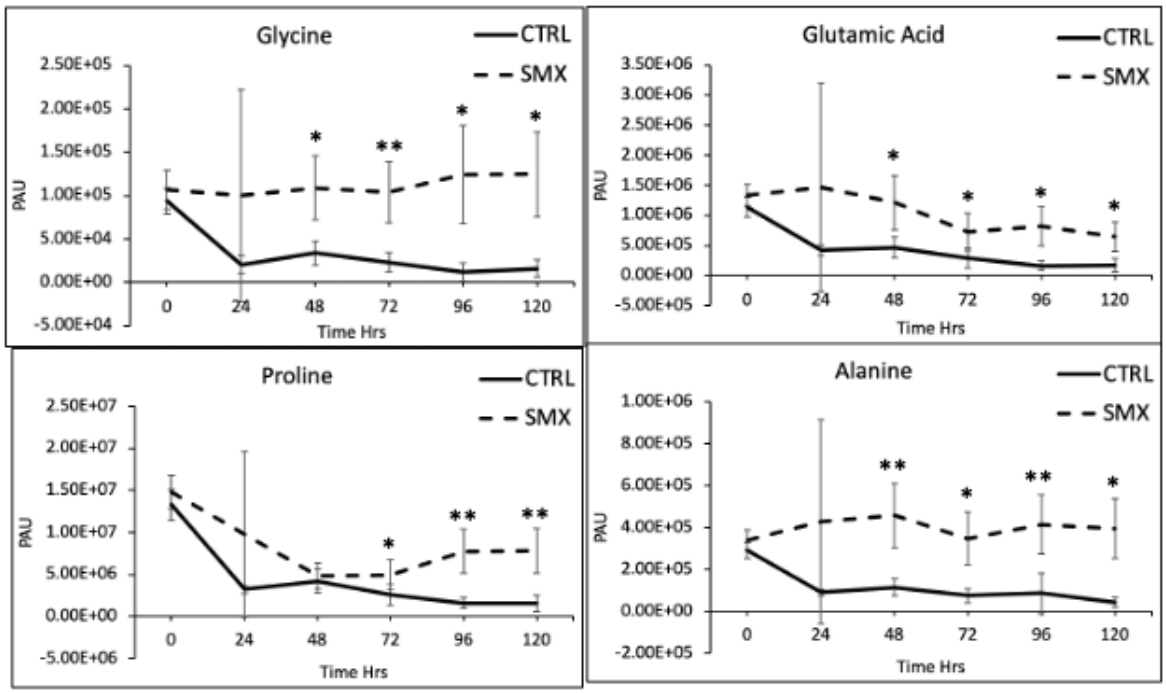


**Figure 5.5 Graphs showing LC-MS/MS analysis of *E. coli* amino acid exometabolome in DM agar over 120 hours with significant differences.** Samples (n=5 per condition, per timepoint) were obtained from the full depth of the agar beneath the centre of bacterial lawns seeded on DM agar and incubated at 25 °C. CTRL = WTK; SMX = WTK + 128 μg/ml SMX. PAU, peak area under the curve. Error bars represent SD. Asterisks represent the results of Student's t-Test Two-Sample Assuming Unequal Variances. *=P<0.05; **=P<0.005.

The results in figure 5.5 show that glycine, alanine and glutamic acid levels in the SMX condition were significantly different to the WTK control as previously seen at 48 hours in figure 4.11 of chapter 4 in this thesis. Proline did not show the previously reported significantly different increased level compared to WTK control. Further analysis of

temporal assay repeats revealed the lack of change was reproducible (Appendix A). The results suggest the initial report in chapter 4 may not be an accurate representation of proline in the exometabolome.

The data revealed across the timeline that glycine, proline, glutamic acid and alanine in the DM reproducibly retained higher levels in the SMX condition than the WTK. The pattern of change has some variance in the temporal assay repeats. The amino acids showed rapid uptake, followed by what appears to be excretion elevating levels in the DM agar over time. Or, a short period of modest uptake before maintaining a steady state over time (Appendix A). It is unclear whether the increase in these amino acids is a product of bacterial excretion or reduced uptake. Without an accurate method for quantification and comparison to the known baseline level in the media, it is not possible to determine if excretion is occurring. Further work will be needed to improve the LC-MS/MS protocol and investigate this proposed mechanism of amino acid change.

The effect of impaired 1CM by SMX on these amino acids has been discussed in detail in section 4.3.7 of chapter 4 in this thesis. Except for glycine which will be discussed in the next section alanine, proline and glutamate are carbon sources that can be utilised to support bacterial growth (Franklin & Venables, 1976; Marcus & Halpern, 1969; Wood, 1988). The consistently elevated levels of proline, glutamic acid and alanine in the SMX condition may correspond with the SMX attenuated bacterial growth reported in section 5.3.3 of this chapter. This suggests that SMX is reducing bacterial amino acid uptake as a product of attenuated growth.

### 5.3.7 A model for glycine metabolism inhibition by sulfamethoxazole

A finding that is consistent with the results reported in chapter 4 of this thesis is the almost complete uptake of serine by 48 hours and an elevated level of glycine in the SMX condition compared to the WTK control. Figure 5.6 shows that in multiple repeats of the temporal LC-MS/MS assay these results are consistently reproducible. There does appear to be considerable differences in variation between timepoints and experimental repeats. These may be skewing the results and the statistical difference between each condition. In the SMX condition, the elevated glycine beyond 48 hours and almost fully depleted serine post 24 hours for both conditions remain remarkably similar across each repeat. The results correspond with the previously reported results in section 4.3.7 of chapter 4.

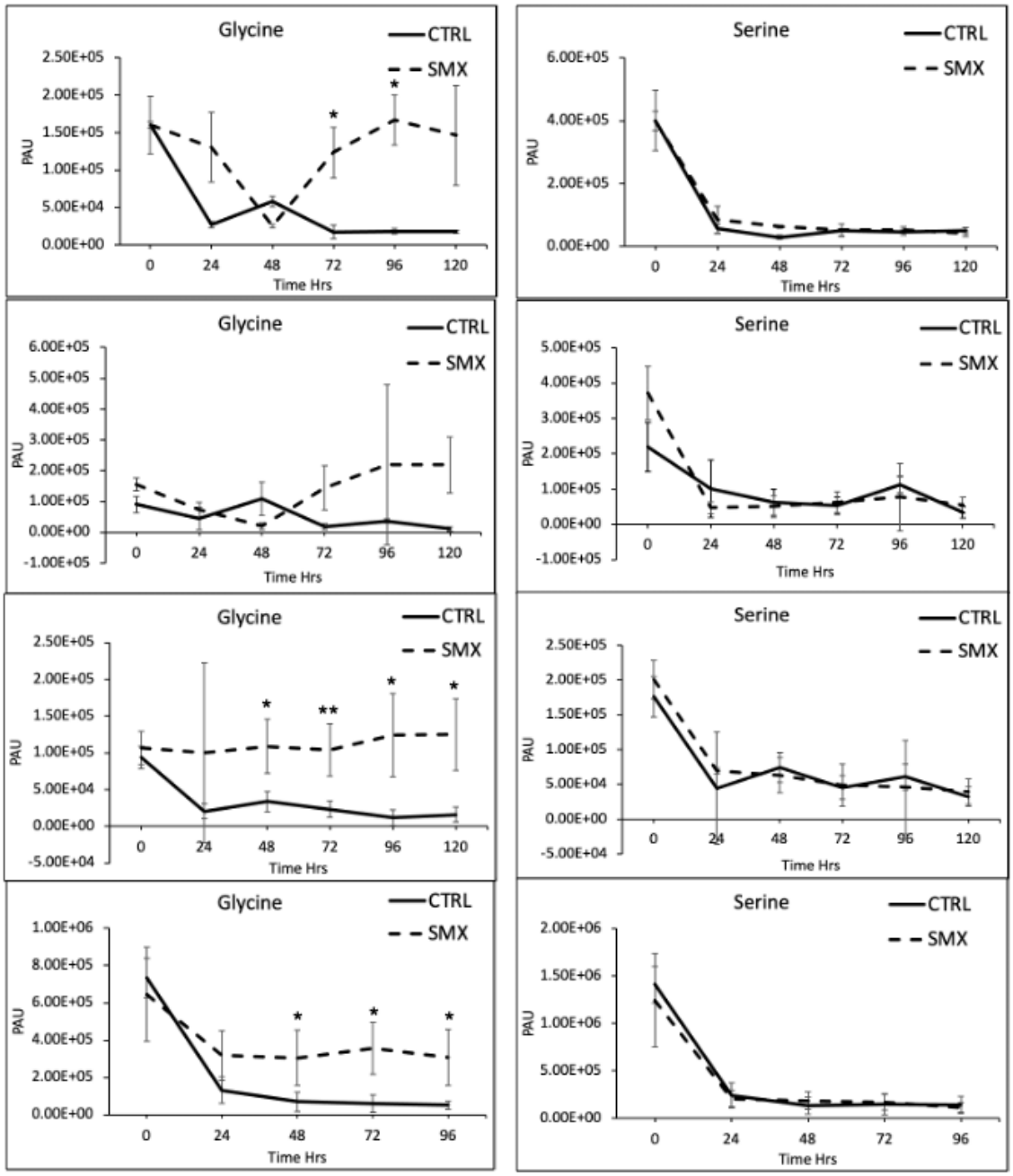


**Figure 5.6 Graphs showing repeat results of LC-MS/MS temporal analysis of serine and glycine in DM agar after from *E. coli* +/- 128 μg/ml SMX.** Samples (n=5 per condition, per timepoint) were obtained from the full depth of the agar beneath the centre of bacterial lawns seeded on DM agar and incubated at 25 °C. CTRL = WTK; SMX = WTK + 128 μg/ml SMX. PAU, peak area under the curve. Error bars represent SD. Asterisks represent the results of Student's t-Test Two-Sample Assuming Unequal Variances. *=P<0.05; **=P<0.005.

The attenuation of 1CM in *E. coli* by SMX may contribute to elevated exogenous glycine through a self-inhibitory negative feedback pathway. It further depletes available 1C units to maintain high endogenous glycine and prevent further uptake externally. Figure 5.7 provides a schematic of the proposed pathway

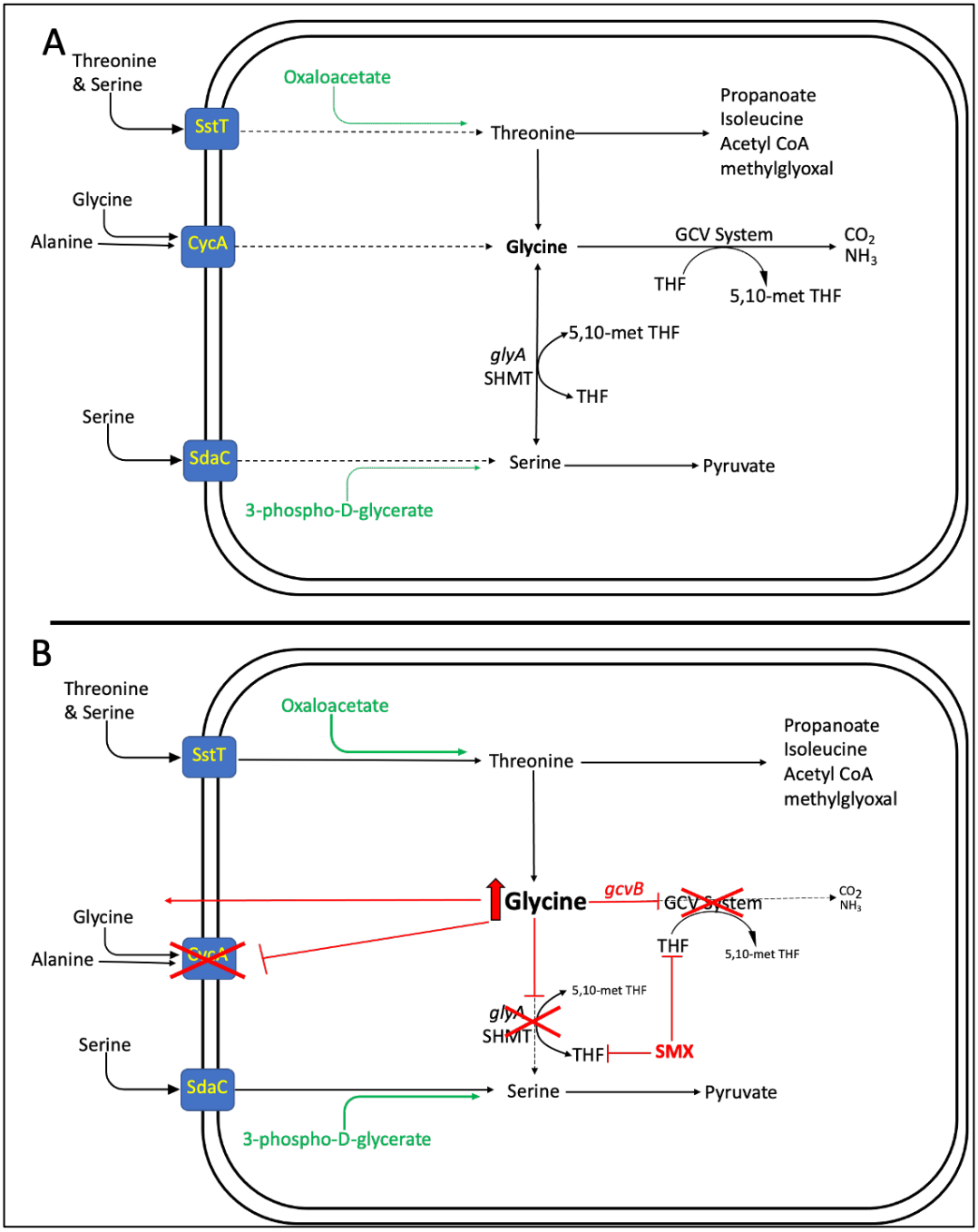


**Figure 5.7 Schematic of proposed *E. coli* serine/glycine metabolic pathways disrupted by SMX. A.** Diagram representing uptake pathways and normal metabolism of serine, glycine and associated amino acids in *E.coli*. **B.** Diagram representing the effect of 128 μg/ml SMX on 1CM and the uptake and metabolism of serine, glycine and associated amino acids in *E. coli*. Red cross denotes enzymes with reduced or loss of function; Red arrow represents excretion of glycine; Metabolites marked in green with green arrow represent substrates for the synthesis of associated molecule; SstT: serine/threonine:$Na^+$ symporter; CycA: D-serine/alanine/glycine/:$H^+$ symporter; SdaC: L-serine:$H^+$ symporter; GCV System: Glycine cleavage system; gcvB: Small regulatory RNA; glyA: Gene encoding the serine hydroxymethyltransferase SHMT; THF: tetrahydrofolate; 5,10-met THF: 5,10-methylene tetrahydrofolate.

Under normal metabolic conditions (figure 5.7A) the 1CM pathways remain intact allowing the serine/glycine pathway and GCV pathway that have been described in detail in section 4.3.7 of chapter 4 to function normally. Serine is preferentially taken up as a carbon source and for de-novo glycine synthesis (Lewis I. Pizer, 1965; Selvarasu et al., 2009). Exogenous glycine is also taken up as seen by the almost complete consumption from the DM by 48 hrs (figures 5.4 and 5.6). Glycine is degraded via the GCV and SHMT pathways to yield 5,10-met THF, a major source of 1C units to the wider bacterial physiology (Ghrist & Stauffer, 1995). Exogenous threonine also contributes to the glycine pool that feeds into the GCV and SHMT pathways (Ghrist & Stauffer, 1995; G. Stauffer, 1996; G. V. Stauffer & Stewart, 2004). Having several independent pathways of uptake and synthesis may supply 1C units during time of high metabolic demand and add a layer of redundancy during times of metabolic stress.

Figure 5.7B shows the proposed pathways after treatment of the bacterial lawn with SMX. SMX disrupts 1CM by significantly impairing THF synthesis (Maynard, 2017; Virk, 2013) that may deny SHMT and GCV of 1C units preventing both de-novo glycine synthesis and degradation. The endogenous levels of glycine may begin to accumulate as the threonine pathway continues to contribute to de-novo glycine synthesis. The SHMT and GCV pathways are no longer able to reduce endogenous levels of glycine. The increased endogenous glycine may activate the GcvB negative feedback pathways to inhibit uptake of exogenous glycine via CycA (Pulvermacher et al., 2009). The loss of this transporter does not prevent uptake of serine as this is still able to enter the cell via the membrane transporters SstT (Y.-M. Kim et al., 2002) and SdaC (Kriner & Subramaniam, 2020) and is almost completely consumed from the DM in both WTK, mutants and SMX conditions (figure 5.6).

These pathways may not be completely inhibited as the bacteria is still able to use limited 1C units from exogenous and endogenously synthesised PABA (Maynard et al., 2018). The PABA may feed into 1CM through competition with SMX. It may not be sufficient to manage glycine/serine homeostasis thus, maintaining reduced availability of 1C units and elevated intracellular glycine driving the CycA repression. Loss of enzymatic capacity to synthesise glycine from serine or, the availability of 1C units from the GCV pathway has also been shown to cause excretion of glycine (G. V. Stauffer & Stewart, 2004). This may also be a contributing factor to the elevated exogenous glycine levels seen in the SMX

condition. Although, the results in figure 5.6 suggests a cessation of uptake rather than excretion.

An alternative explanation for consistently elevated glycine is the relationship of amino acid demand for bacterial growth discussed in section 5.3.6 of this chapter. Glycine is a key substrate for the synthesis of purines and 1C units central to normal physiological function in the cell (G. Stauffer, 1996). Demand for these metabolites may be reduced under conditions of low growth or, in this case the lack of synthesis due to impaired 1CM may be attenuating bacterial growth.

5.3.8 Effect of exogenous glycine on the bacterial growth

Previously, it was shown that WTK treated with 128 μg/ml SMX attenuates bacterial growth (section 5.3.1 of this thesis). It was shown to alter the amino acid exometabolome with a significantly reduced uptake of glycine from DM compared to WTK (section 5.3.7 of this thesis). To understand if reduced glycine metabolism attenuates bacterial growth, glycine free DM was used to produce growth curves for analysis. It was hypothesised that the absence of a source of exogenous glycine would replicate the SMX condition at the 48 hour time point where glycine uptake ceased.

Removal of an external source of glycine meant the bacteria was solely dependent on endogenous de-novo synthesis to meet glycine demand for metabolism. Glycine degradation is a major source of 5,10-met THF required for 1CM (Ducker & Rabinowitz, 2017). Perturbations to this pathway may attenuate bacterial growth in WTK corelating with the reduced growth seen in SMX treated *E. coli*.

Figure 5.8 shows that omission of glycine from the media had a statistically significant effect on the bacterial growth in both conditions. The differences increase after 48 hours suggesting glycine metabolism may have insufficient capacity to meet demand for growth over a prolonged period. This suggests WTK and SMX treated bacteria retain the ability to synthesise endogenous glycine and maintain sufficient metabolic capacity to support growth. Although, it is at a reduced capacity over time as wider substrate availability from nutrients is exhausted.

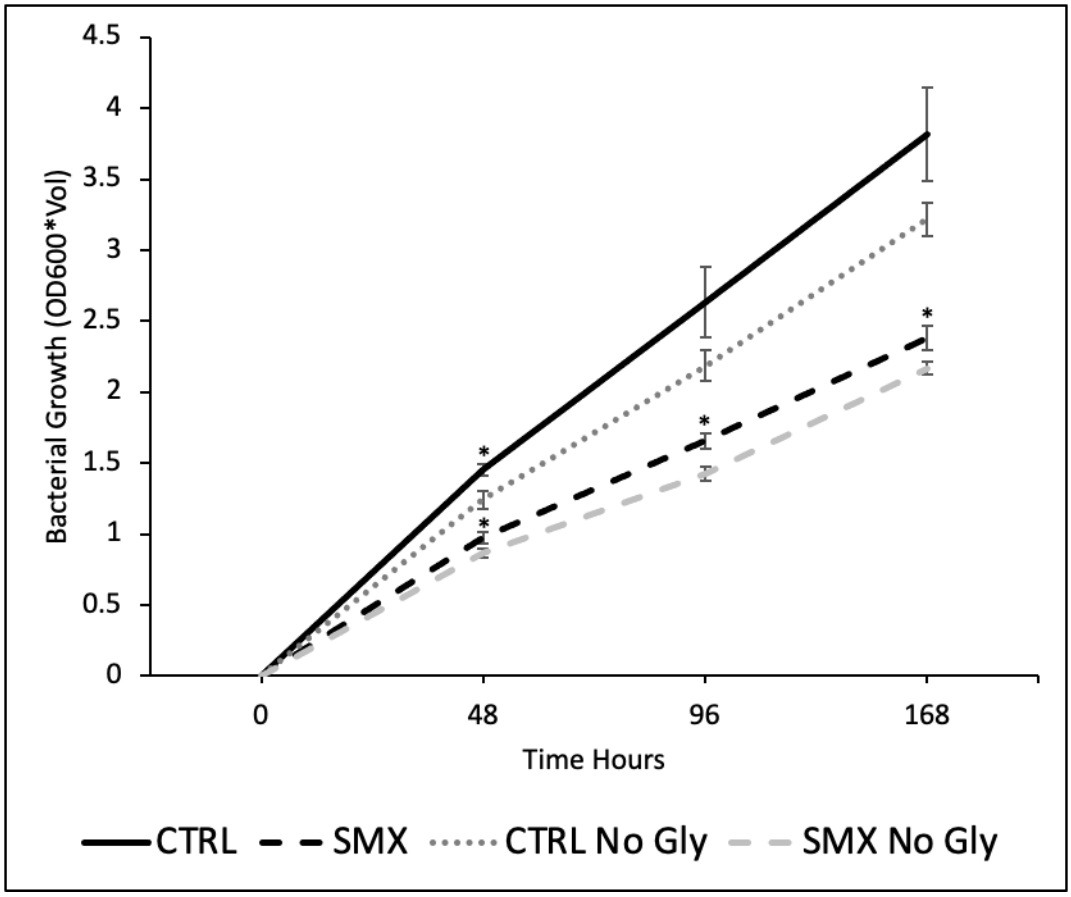


**Figure 5.8 Graph showing removal of exogenous glycine reduces bacterial growth.** DM solid agar plates (n=5 per condition, per timepoint) supplemented with 0.1 μM PABA and +/- 128 μg/ml SMX were seeded with 100 μl WTK cultured in DM + 0.2μM PABA and incubated at 25 °C overnight. Bacterial lawns were removed by washing and scraping with 2 ml sterile M9. Measurements were taken at 48 hours, 96 hours and 168 hours and analysed by spectrophotometer where bacterial growth = $OD_{600}$*volume. CTRL, WTK; SMX, WTK +128 μg/ml SMX; No Gly, DM plates made without glycine. Error bars represent SD over 3 biological replicates. Asterisks represent the results of Student's t-Test Two-Sample Assuming Unequal Variances *=P<0.05.

In the absence of exogenous glycine de-novo synthesis occurs through the conversion of serine to glycine as part of 1CM or, independent of folates by catabolism of threonine as described in section 5.3.7 of this chapter. It is not known here if de-novo endogenous glycine synthesis is occurring as a product of a functioning serine-glycine pathway or independent of 1CM through the threonine pathway.

5.3.9 Effect of exogenous glycine on the bacterial amino acid exometabolome

To understand if reduced exogenous glycine availability alters the WTK amino acid exometabolome similar to SMX treated bacteria a temporal LC-MS/MS analysis of

bacteria maintained on glycine free DM was conducted. Previous LC-MS/MS analysis of SMX treated bacteria showed that there is a difference in amino acid concentration in the DM that suggests demand for external supply is attenuated.

It is not known if these changes are a direct product of impaired 1CM or, as a result of changes to the serine-glycine pathway that is responsible for generating the physiologically important folate 5,10-met THF. After a short period of uptake exogenous glycine ceases to be sequestered from the media by the bacteria at 24 hours. The attenuation of external glycine uptake may be due to the loss of sufficient THF by SMX to metabolise glycine inhibiting transport pathways (Ghrist & Stauffer, 1995). The wider effect is a metabolic change to the organism as seen by changes to the amino acid exometabolome and growth curves of SMX treated bacteria.

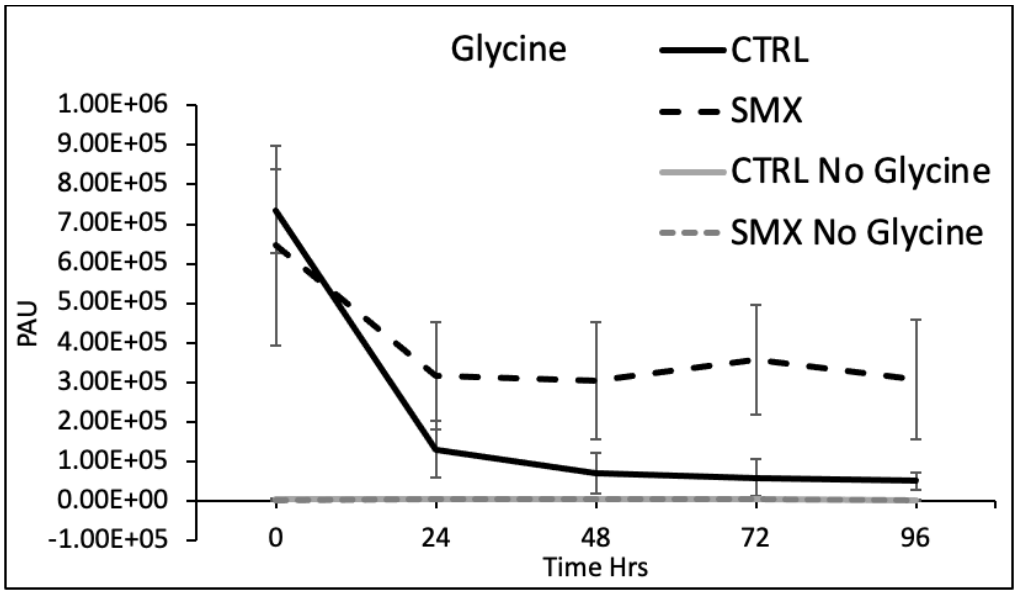


**Figure 5.9 Graph showing LC-MS/MS analysis of glycine in DM that reveals excretion does not occur in the absence of exogenous glycine.** Samples (n=5 per condition, per timepoint) were obtained from the full depth of the agar beneath the centre of bacterial lawns seeded on DM agar +/- 11.53 μg glycine and +/- 128 μg/ml SMX. Plates were incubated at 25 °C. CTRL = WTK; SMX = WTK + 128 μg/ml SMX. PAU, peak area under the curve. Error bars represent SD. Statistical analysis was conducted with Student's t-Test Two-Sample Assuming Unequal Variances.

In the previous section, it was suggested that a reduction in available folates by SMX prevents degradation of glycine causing an accumulation in the cell. High internal levels of glycine may downregulate uptake and may also cause excretion adding to the exogenous pool in the DM. Figure 5.9 demonstrates that there does not appear to be any glycine excreted by the bacteria in all conditions. This may be due to no excretion occurring as the PAU does not increase beyond the lowest levels seen at 0 hours for the no-glycine conditions and 24 hrs for the CTRL and SMX conditions. The presence of excreted glycine may be below the threshold for detection or, that synthesis and degradation pathways maintain internal levels below a threshold for excretion.

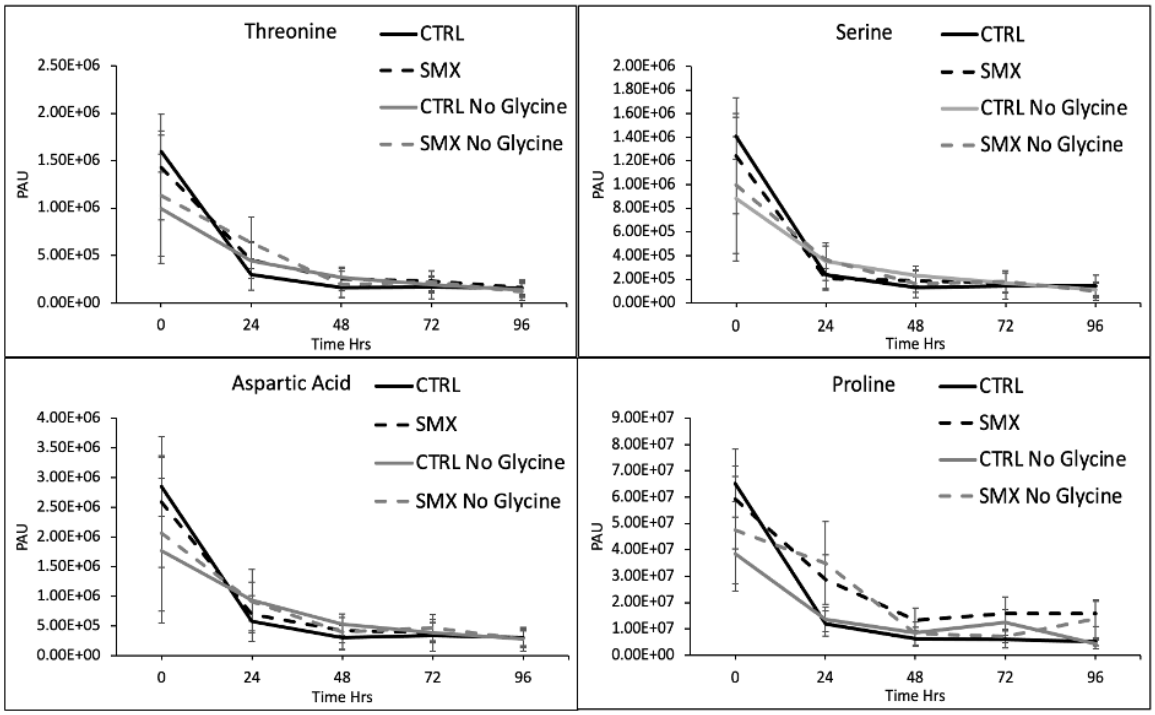


**Figure 5.10 Graph showing the absence of exogenous glycine in DM does not alter the amino acid exometabolome of threonine, aspartic acid, serine and proline in WTK +/- SMX.** Samples (n=5 per condition, per timepoint) were obtained from the full depth of the agar beneath the centre of bacterial lawns seeded on DM agar +/- 11.53 μg glycine and +/- 128 μg/ml SMX. Plates were incubated at 25 °C. CTRL = WTK; SMX = WTK + 128 μg/ml SMX. PAU, peak area under the curve. Error bars represent SD. Statistical analysis was conducted with Student's t-Test Two-Sample Assuming Unequal Variances.

The absence of exogenous glycine does not alter the exometabolome of threonine, aspartic acid, serine and proline seen in Figure 5.10. They are all important upstream substrates that provide both nitrogen and carbon sources for energy production and bacterial growth

through multiple metabolic pathways (Frank & Ranhand, 1964; Franklin & Venables, 1976; Ghrist & Stauffer, 1995; Reitzer, 2003; Sawers, 1998; Schneider, Kiupakis, & Reitzer, 1998; Schubert et al., 2021; Simanshu, Chittori, Savithri, & Murthy, 2007). External transport of these amino acids is not regulated by glycine levels (Mellies, Wise, & Villarejo, 1995; Nakao, Yamato, & Anraku, 1988; F. Z. M. Rashid, Chaurasiya, Brocken, & Dame, 2021). The no-glycine WTK control condition retains a similar pattern of uptake as the WTK control condition. Suggesting metabolism of these amino acids is not affected by exogenous glycine and uptake does not appear to be impaired or demand reduced.

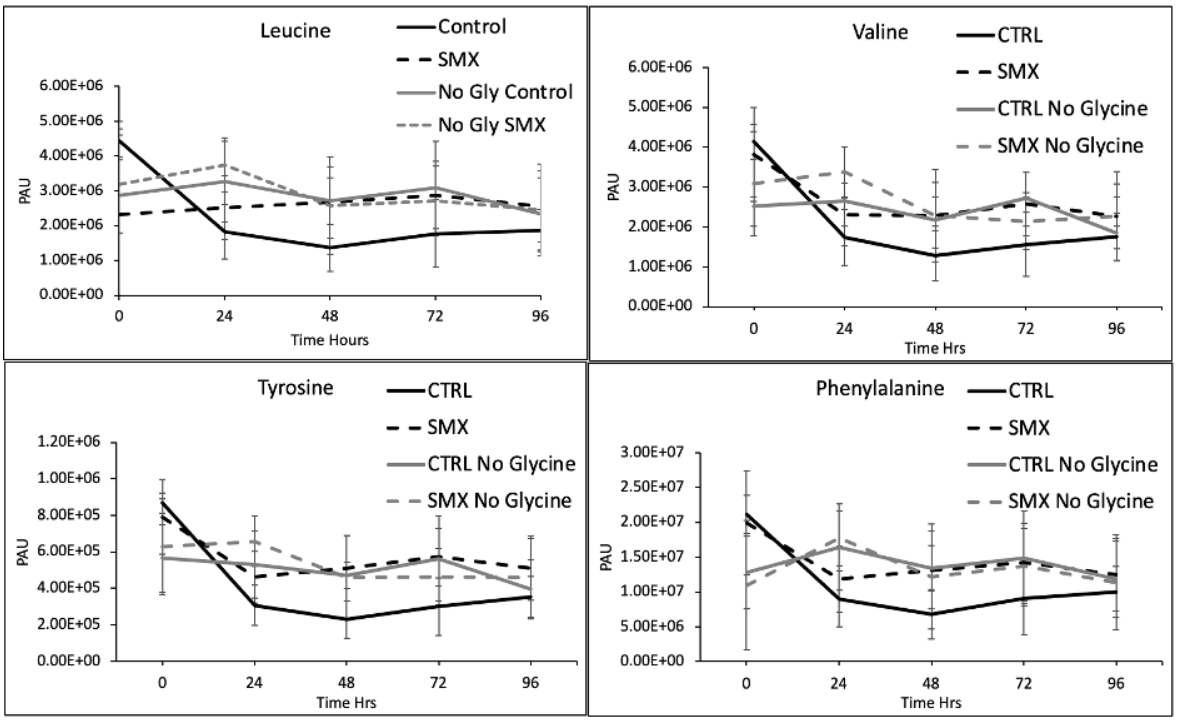


**Figure 5.11 Graph showing the absence of exogenous glycine in DM changes the amino acid exometabolome of leucine, valine, tyrosine and phenylalanine of WTK but not WTK + SMX.** Samples (n=5 per condition, per timepoint) were obtained from the full depth of the agar beneath the centre of bacterial lawns seeded on DM agar +/- 11.53 µg glycine and +/- 128 µg/ml SMX. Plates were incubated at 25 °C. CTRL, WTK; SMX, WTK + 128 µg/ml SMX. PAU, peak area under the curve. Error bars represent SD. Statistical analysis was conducted with Student's t-Test Two-Sample Assuming Unequal Variances.

Figure 5.11 shows that in the absence of external glycine WTK had a decrease in uptake for leucine, valine, tyrosine and phenylalanine although these changes were not statistically significant. There appear to be similarities in the pattern of uptake in all conditions over time that may relate to changes in metabolic demand.

Leucine, valine and phenylalanine share the LIV-II transport pathway (Koyanagi et al., 2004) and tyrosine uptake is through TyrP (Wookey et al., 1984). Regulation of these pathways is interconnected through the global regulator Lrp. A key regulator of metabolism, Lrp responds to nutrient abundance by interacting with other global regulators to repress or upregulate the biosynthesis of amino acids during growth (Kroner, Wolfe, Freddolino, & DiRita, 2019). The regulatory activity of Lrp has been found to not be solely dependent on leucine levels (Kroner et al., 2019). The effect of SMX may be activating Lrp in response to the intracellular changes to 1C units and the associated pathways whilst the absence of exogenous glycine upregulates Lrp in the no SMX WTK condition. In both cases Lrp may be repressing the TyrP and LIV transport pathways as part of a bacterial stress response.

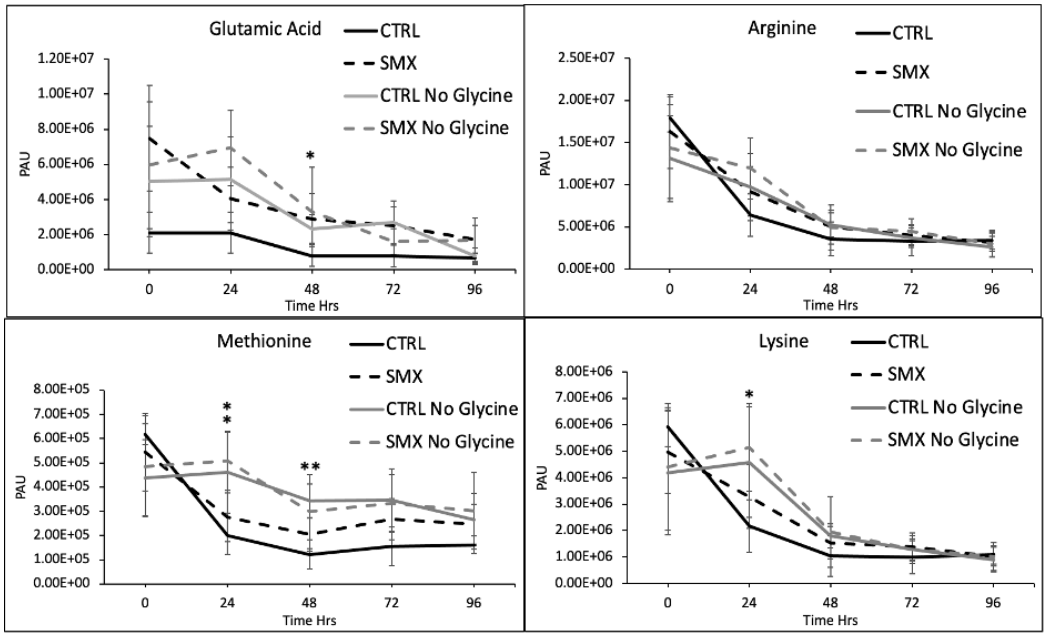


**Figure 5.12 Graph showing the absence of exogenous glycine in DM changes the amino acid exometabolome of glutamic acid, arginine, methionine and lysine of WTK and WTK + SMX.** Samples (n=5 per condition, per timepoint) were obtained from the full depth of the agar beneath the centre of bacterial lawns seeded on DM agar +/- 11.53 µg glycine and +/- 128 µg/ml SMX. Plates were incubated at 25 °C. CTRL = WTK; SMX = WTK + 128 µg/ml SMX. Glutamic acid shows a significant difference between SMX and CTRL at 48 hours. Lysine has a significant difference between no glycine SMX and CTRL at 24 hours and methionine has significant differences between no glycine SMX and CTRL at 24 hours, no glycine CTRL and CTRL at 24 and 48 hours. PAU, peak area under the curve. Error bars represent SD. Asterisks represent the results of Student's t-Test Two-Sample Assuming Unequal Variances. *=P<0.05; **=P<0.005; ***=P<0.001.

The bacterial WTK control and WTK +SMX conditions both appear to have a change in uptake when maintained on glycine free DM. Figure 5.12 reveals glutamic acid, arginine, methionine and lysine have a similar pattern whereby uptake is decreased up to 24 hours before increasing along the remainder of the time line. The decrease at 24 hours may be a result of the lower PAU for the no glycine conditions, suggesting glycine may have a small matrix effect amplifying analyte signal. It may also be a product of the high variance seen amongst the samples. The absence of this effect may have revealed a more linear increase in uptake possibly correlating with demand for bacterial growth as the bacterial lawn population increases over time.

Lysine, arginine and glutamate are important components of acid resistance pathways that protect the bacteria from low pH conditions (Castanie-Cornet, Penfound, Smith, Elliott, & Foster, 1999; Diez-Gonzalez & Karaibrahimoglu, 2004; H. T. Richard & Foster, 2003; Waterman & Small, 2003). In addition to the acid response function these amino acids play a central role in *E. coli* metabolism (Chiang, Lin, Hu, & Chao, 2021; C.-D. Lu, 2006; Schilling et al., 2019). Lysine is required for post translational modification of proteins (Nakayasu et al., 2017) and as a source of succinate for the TCA cycle (Knorr et al., 2018). Arginine is also precursor for glutamate synthesis and metabolised into succinate to provide substrate for energy synthesis (Schneider et al., 1998). Glutamate is a major nitrogen donor, carbon source and component of proteins (Marcus & Halpern, 1969; Reitzer, 2004). It is also a precursor metabolite for de-novo biosynthesis of numerous amino acids (Charlier & Glansdorff, 2004; Csonka & Leisinger, 2007; B. Shapiro & Stadtman, 1970).

Transport for lysine and arginine uptake is shared through the HisPMQArgT ATP-Binding Cassette (ABC) transporter and the lysine specific transporter LysP (Rosen, 1971). Glutamate uptake has four separate pathways for uptake including the pH sensitive GadC transporter (H. Richard & Foster, 2004). The symporters GltP, GltS and the ABC transporter GltIJKL (Schellenberg & Furlong, 1977). Collectively these transporters are regulated by the action of Lrp (Cho, Federowicz, Park, Zengler, & Palsson, 2012) that has been discussed previously in this chapter.

DM was optimised during development to maintain a suitable pH for bacterial growth (Helliwell, 2013). It is unlikely reduced uptake is in response to pH change from the

removal of 0.9 mM of glycine as the acid response is upregulated in conditions of pH <4.0 (De Biase & Lund, 2015). Due to the role of glutamate, lysine and arginine in central metabolism and regulation by Lrp, it is likely the reduced uptake is in response to nutrient stress from both the change to 1CM by SMX and removal of an important source of glycine.

Figure 5.11 also shows a significant reduction in uptake of methionine for WTK and WTK treated with SMX when glycine is absent from DM. Under normal DM conditions SMX appears to reduce uptake but not significantly. Here it can be seen that uptake by both the control and SMX conditions are reduced at almost identical levels. De-novo methionine biosynthesis is dependent on the availability of the folate 5,10-met THF that is a product of the interconversion of serine to glycine by SHMT and the GCV system degradation of glycine (Grundy & Henkin, 2001). Uptake of external methionine is by the high affinity MetNIQ transporter (R. J. Kadner, 1974; R J Kadner, 1977). It is regulated by the internal pool of methionine by transinhibition (J. G. Yang & Rees, 2015). High internal methionine represses transport from external supply allowing maintenance of intracellular concentration at a low energy cost to the bacteria (J. G. Yang & Rees, 2015).

The changes in uptake may be attributed to an increase in the internal pool of methionine driving repression of transport. This may be unlikely as SMX and the absence of glycine reduce the availability of key 1C substrates to synthesise 5,10-met THF that is integral to methionine synthesis (Y. K. Kwon et al., 2010). The attenuation of methionine biosynthesis would result in low endogenous concentrations that would promote transporter activity (R. J. Kadner, 1974; ROBERT J Kadner, 1975). The wider mechanisms of methionine metabolism and regulation in *E. coli* has still not been fully elucidated in particular under conditions of stress (Hondorp, Matthews, & Stewart, 2006). Further work would be needed to determine if changes seen here are the result of novel regulatory and metabolic pathways or a product of experimental bias.

The absence of glycine in DM had a significant effect on alanine uptake of WTK treated with SMX. Figure 5.13 demonstrates that uptake of alanine WTK control remained unchanged when glycine was removed whilst the SMX condition had a rapid and sustained uptake of the amino acid. SMX is found to reduce uptake of alanine under normal DM

conditions. The change seen here suggests glycine may have a role in regulating alanine transport.

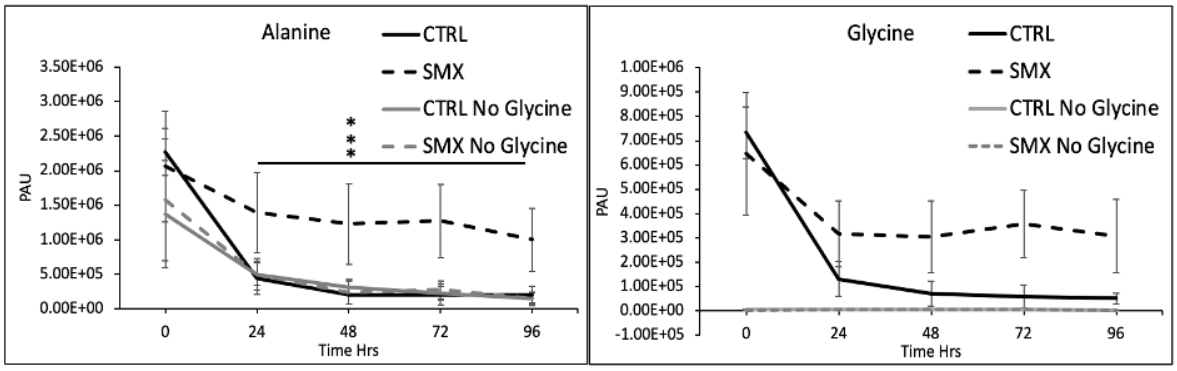


**Figure 5.13 Graph showing the absence of exogenous glycine in DM changes the WTK + SMX amino acid exometabolome of alanine.** Samples were obtained from the full depth of the agar beneath the centre of bacterial lawns seeded on DM agar +/- 11.53 µg/ml glycine and +/- 128 µg/ml SMX. Plates were incubated at 25 °C. CTRL = WTK; SMX = WTK + 128 µg/ml SMX. Alanine shows a significant difference between all conditions at 24, 48, 72 and 96 hours. Glycine data has been previously discussed but is included here for reference. Error bars represent SD. PAU, peak area under the curve. Asterisks represent the results of Student's t-Test Two-Sample Assuming Unequal Variances. *=P<0.05; **=P<0.005; ***=P<0.001.

SMX treated WTK reduces glycine uptake that suggests attenuation of folate synthesis has a direct impact on glycine metabolism limiting the reduction in exogenous glycine and alanine. Alanine uptake is by two pathways, CycA that is shared with glycine but in its absence is found to have a minor effect on alanine transport (Robert J Wargel, Shadur, & Neuhaus, 1971) and the LIV-I transport system that is regulated by Lrp (Reitzer, 2004).

It has previously been reported that accumulation of glycine inhibits alanine transport by up to 30% (R. J. Wargel, Hadur, & Neuhaus, 1971). Leucine and glycine have also been reported to have an additive effect completely inhibiting alanine uptake (Robbins & Oxender, 1973). The absence of glycine in the DM may be increasing the effect of SMX on endogenous glycine levels by removing an exogenous source that may be contributing to the internal pool or inhibiting glycine transport.

### 5.3.10 The absence of exogenous glycine slows *C. elegans* ageing

Lifespan assays were planned to investigate if reduced uptake of glycine or, the presence of higher exogenous glycine in the DM correlates with the extended lifespan phenotype of

SMX. Due to time constraints, it was not possible to conduct lifespan assays to fully explore the relationship between glycine and lifespan. The services of Magnitude Biosciences Ltd, a specialist contract research organisation was offered. The company has a novel automated technology for measuring healthspan as opposed to lifespan in *C. elegans.* The protocol used by Magnitude Biosciences Ltd for their healthspan assays mirrors our lifespan protocol described in chapter 2 of this thesis. The benefit of the healthspan assay is reduced setup time and provision of data within two weeks, significantly reducing workload and optimising investigation time.

The healthspan analysis uses an automated non-invasive system of cameras to capture *C. elegans* movement on DM agar seeded with a bacterial lawn. Unlike a lifespan assay where worms are counted as either alive, dead or censured the healthspan assay relies on movement as a biomarker for age. The system captures images of the worms every 0.8 seconds for 160 seconds. This process is repeated every 5 minutes for the duration of the experiment. The data is used to produce a graphical readout in the form of a healthspan curve. For the purpose of the healthspan experiment Magnitude Biosciences Ltd used OP50 *E. coli* as opposed to WTK that has been examined throughout this work. OP50 *E. coli* does not require kanamycin in the media but does have uracil supplementation in DM as this strain lacks the ability to synthesise uracil.

This chapter has reported that SMX causes glycine concentration in the DM agar to remain elevated compared to WTK during the time period of a lifespan assay. It is not known if the bacteria have attenuated glycine uptake or, are secreting the glycine as part of changes to glycine metabolic pathways by SMX. It is also not known if changes to glycine metabolism by SMX contribute to the long lived phenotype of *C. elegans* maintained on 128 μg/ml SMX.

To investigate if the no-glycine metabolic changes reported in this chapter alters *C. elegans* ageing a healthspan assay was conducted. Due to cost and time constraints it was only possible to commission a single Healthspan experiment by Magnitude Biosciences Ltd.

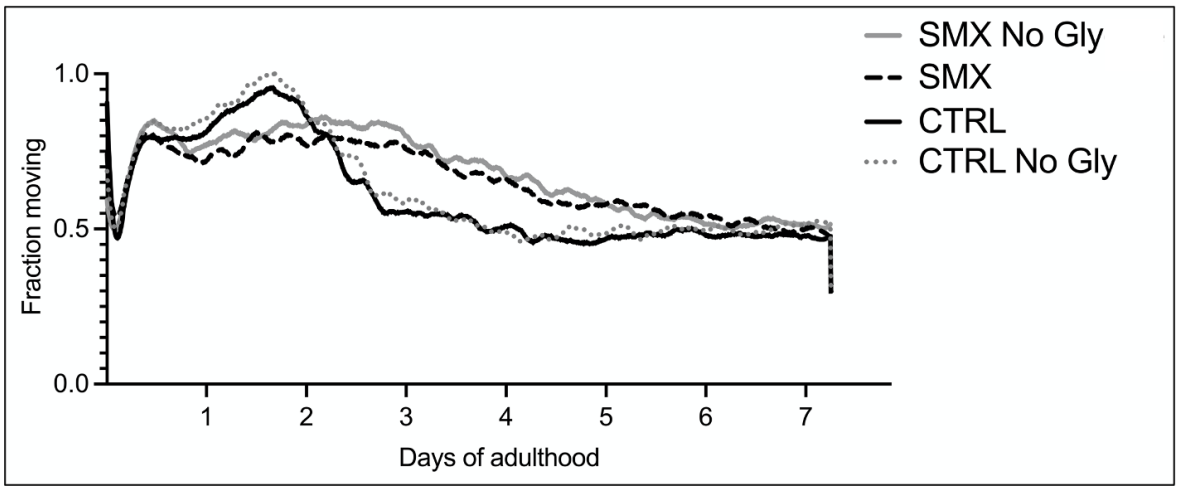


**Figure 5.14 Healthspan data demonstrating the absence of exogenous glycine slows *C. elegans* ageing.** Healthspan curve of fraction of worms moving in 160s interval. *C. elegans* were transferred at day 1 of adulthood onto OP50 *E. coli* seeded on DM agar supplemented +/- glycine and +/- 128 μg/ml SMX at 25 °C. CTRL, OP50 seeded onto DM agar plates containing glycine (n=268); CTRL No Gly, OP50 seeded onto DM agar plates free from glycine (n=210); SMX, OP50 seeded onto DM agar plates containing glycine and 128 μg/ml SMX (n=240); SMX No Gly, OP50 seeded onto DM agar plates and 128 μg/ml SMX free from glycine (n=240). Statistical analysis was conducted using one-way ANOVA.

Magnitude Biosciences Ltd provided a limited report of the healthspan and the raw data consisting of mean fraction of *C. elegans* moving at each data collection timepoint. When investigating a lifepan assay the data is used to produce a Kaplan Meir survival curve for statistical analysis. Here one-way analysis of variance was used to statistically analyse the raw data of the mean of *C. elegans* movement for each condition over the duration of the healthspan.

The data provided by Magnitude Biosciences Ltd (figure 5.14) demonstrated that the absence of exogenous glycine conferred a small but significant change to healthspan in the SMX and WTK no-glycine conditions compared to their respective glycine conditions. The effect of no-glycine on SMX and CTRL conditions shows worm movement is increased suggesting healthspan is prolonged. The ageing associated reduction in movement occurs at 48 hours for the CTRL conditions, whilst the SMX conditions have a higher proportion of the population moving over a prolonged period. In the context of the healthspan the data supports previous lifespan studies that show SMX slowing aging as early as 48 hours (Maynard, 2017; Virk, 2013; Virk et al., 2012; Virk et al., 2016).

The observed changes may not be a direct reflection of slowed ageing as they are present across all timepoints, occur early in the healthspan and remain consistent in both non-glycine conditions. The data may represent increased movement in response to nutrient stress altering behaviour as opposed to age related loss of locomotion. To fully establish if these observations correlate with the metabolomic analysis repeat healthspans will be required with the WTK strain. The healthspan should also be supported by lifespan assays to correlate loss of movement with death.

The slowing of ageing observed in the non-glycine conditions may be attributed to the exometabolomic changes reported in section 5.3.9 of this chapter. The absence of exogenous glycine attenuated the uptake of methionine, glutamic acid, arginine and lysine in both SMX and WTK conditions (figure 5.12). These results were discussed in section 5.3.9 of this chapter where it was suggested the attenuated uptake may be due to a bacterial nutrient stress response as a product of impaired 1CM and glycine metabolism. This may lead to a change in the *E. coli* nutrient profile, in particular a reduction in the availability of the essential amino acids' methionine, arginine and lysine.

*C. elegans* is able to sense nutrient depravation that can induce a dietary restriction (DR) response that extends lifespan without malnutrition (Greer & Brunet, 2009). Modulation of DR through nutrient sensing occurs through two key signalling pathways IIS (insulin/insulin-like growth factor 1) and LET-363/mTOR (mechanistic target of rapamycin) (Dall & Færgeman, 2019). The sensing of amino acids is by the LET-365/mTOR pathway (Antikainen, Driscoll, Haspel, & Dobrowolski, 2017). The mTORC complex (mTORC1) is bound to lysosomal membranes and regulates metabolic processes in the cell including autophagy in response to cellular amino acid and growth factor levels (Antikainen et al., 2017). When low nutrient levels are sensed the protein complex TSC (tuberous sclerosis 1 and 2) that receives signals from kinases on metabolic state deactivates Rheb (Ras homolog enhanced in the brain (Antikainen et al., 2017; S. Rashid, Pho, Mesbahi, & MacNeil, 2020). Deactivation of Rheb causes mTORC1 to disassociate from the lysosome preventing phosphorylation of the transcription factors DAF-16/FOXO and HLH-30/TFEB (Antikainen et al., 2017; S. Rashid et al., 2020). The two transcription factors are able to relocate to the nucleus to transcribe genes encoding autophagy components (Antikainen et al., 2017; Dall & Færgeman, 2019; S. Rashid et al., 2020).

The catabolic process of autophagy is evolutionarily conserved and prevents cellular toxicity by removal and recycling of damaged organelles and misfolded proteins (Dall & Færgeman, 2019). It is also a mechanism to provide nutrients and molecular components to maintain metabolic homeostasis during periods of cellular, environmental and nutrient starvation (Hansen et al., 2008; Kroemer, Mariño, & Levine, 2010). Autophagy has been reported to be a convergent downstream mechanism for longevity paradigms (Nakamura & Yoshimori, 2018). In long lived animals autophagy has been found to be upregulated and crucial for their increased lifespan (Gelino et al., 2016; Nakamura & Yoshimori, 2018).

The absence of glycine in the food source and rapid uptake in SMX and WTK conditions of methionine, arginine and lysine may directly affect *C. elegans* ageing. This may occur through nutrient sensing by the activity of mTORC1 independently of the mechanism of effect by SMX. In particular restriction of the essential amino acid methionine (Zečić, Dhondt, & Braeckman, 2019). Methionine restriction has previously been shown to induce a long lived phenotype in Drosophila, rats, mice and *S. cerevisiae* (Brind et al., 2011; B. C. Lee et al., 2014; R. A. Miller et al., 2005; Orentreich, Matias, DeFelice, & Zimmerman, 1993; Ruckenstuhl et al., 2014). The reduction in bacterial growth observed in section 5.3.9 of chapter 5 may also correlate with these findings suggesting changes to the amino acid profile of *C. elegans* food source may confer a limited lifespan increasing phenotype. Further work using a fecundity assay would be needed to observe if the healthspan changes seen here are a product of DR.

## 5.4 Discussion

### 5.4.1 Sulfamethoxazole reduces bacterial growth on DM agar

The effect of SMX on bacterial growth using our current DM protocol has not been fully explored over the entire timeline of a lifespan protocol. Nor has the relationship between growth and lifespan been explored. A comparison was made between NGM agar DM agar to observe if SMX affected the media in the same manner. Previous work by Virk (2013) found that SMX did not affect bacterial growth on NGM agar. Here it has been shown that over a prolonged period it significantly reduced growth after 72 hours. Possibly due to depletion of folate precursors in both the culture and agar that support growth in the presence of SMX.

Maynard (2017) evaluated the use of DM agar as an alternative nutrient source for *E. coli* and found that bacterial growth did not differ from NGM agar. The results in this chapter contradict these findings. It has been shown quite robustly that bacterial growth on DM agar is considerably less than that of NGM agar. Why the DM agar findings are different will require further examination with repeats using a larger number of replicates. The nutrient content between the media may be a causative factor due to batch differences in peptone. It is also possible that individual preparation variation may also have a contributing factor. Irrespective of the differences in bacterial growth reported here lifespan assays on these media yield similar lifespan outcomes for *C. elegans* in the reduced folate model.

The *E. coli* mutant *ΔpabA* also increases *C. elegans* lifespan via the low folate model retaining a morphology similar to WTK with a swarming zone phenotype (chapter 3 of this thesis) allowing the bacterial lawn to proliferate into the wider environment. This mutant also had a growth profile similar to SMX treated WTK that further supports the argument bacterial lawn growth does not correlate with *C. elegans* lifespan.

The data presented here shows that *ΔpabA* has growth characteristics very similar to WTK. These findings suggest that neither the presence of the swarming zone or increased growth compared to SMX bacteria correlate with the reduced *C. elegans* lifespan in our model. A final growth curve was conducted to investigate if a rescue concentration of PABA was able to recover SMX treated lawn growth to WTK levels in line with its full reversal of increased lifespan in *C. elegans*. Growth was partially but not completely recovered to WTK levels suggesting that the lifespan increase is independent of bacterial growth and proliferation.

### 5.4.2 Sulfamethoxazole alters the amino acid exometabolome of *E. coli*

The data revealed that there are significant differences in bacterial uptake of glycine, glutamic acid, proline and alanine from DM between conditions for SMX treated *E. coli*. There also appears to be a change in the pattern of uptake by the SMX conditions for phenylalanine, valine, methionine, leucine and tyrosine although this is not significant. Aspartic acid, lysine, threonine, arginine and serine remain unchanged.

As discussed previously in chapter 4, an inference cannot be drawn between differences in uptake and excretion without an accurate and robust method of quantification. The protocol allows an analysis of the patterns of change for each individual amino acid. The use of a temporal assay provides multiple data points for comparison along the time line and changes observed are restricted to comparison against the data from 0 hours that represents the amino acid concentration prior to bacterial seeding. The data provides a profile of the pattern of change between conditions.

Previous work reported that SMX lowered endogenous 5,10-met THF in *E. coli* (Maynard, 2017). The work suggested changes to 5,10-met THF may correlate with the extended lifespan phenotype of *C. elegans* when maintained on SMX treated *E. coli* (Maynard, 2017; Virk, 2013). Due to the central role of glycine in 1CM for the synthesis of 5,10-met THF and folate previously found to be reduced by SMX (Maynard, 2017) this body of work focused on glycine to investigate if changes to this amino acid correlated with exometabolome changes by SMX.

The model in section 5.3.7 of this chapter proposed that attenuation of bacterial folate synthesis decreases availability of 1C units to degrade the internal pool of glycine. As a product of this, attenuation of glycine metabolism impairs synthesis of 5,10-met THF and increases the internal pool of glycine. The pool is subsequently maintained above a threshold repressing transport of external glycine. Loss of glycine availability and attenuation to degradation pathways for 5,10-met synthesis may attenuate an underlying toxicity or, have a wider impact on amino acid metabolism to provide an anti-ageing nutrient profile that extends *C. elegans* lifespan.

Without quantifiable and endometabolomic data the changes seen can only be assumed to be in relation to uptake from the DM. There are what appears to be points of excretion where PAU increases but this is likely a product of biological variance and artifacts within the LC-MS/MS. Further work would need to be done to establish if the observed changes are a direct result of reduced bacterial folate synthesis or a product of reduced bacterial growth.

A limitation is the previously observed signal amplification in section 4.4.1 of chapter 4 preventing quantitative analysis. PAU is relative to concentration of the analyte based on a

linear standard curve of a known concentration of the same analyte. In some cases, the PAU is higher than the starting baseline. This suggests excretion may be occurring however, this conclusion cannot be drawn as there is considerable variation within samples as can be seen by the SD. Outliers within the data introduce an inherent bias skewing the results. Further work needs to be done to refine and improve the protocol to reduce variation and remove the signal amplification to allow a robust conclusion of the changes in the bacterial metabolism.

5.4.3 The absence of exogenous glycine in defined media reduced bacterial growth

*E. coli* lawns maintained on glycine free DM showed a reduction in growth for both SMX and WTK conditions. Suggesting the bacteria can compensate for reduced availability of glycine through de-novo biosynthesis but, not enough to recover growth to the same levels when availability is high. The effect of SMX on the internal glycine pool and 5,10-met THF synthesis may not impede the serine-glycine pathway and GCV system as severely as previously proposed. 1CM may still be able to function at a level to support growth. But ,as seen by the lack of recovery to control levels by WTK the reduced growth may be a product of nutrient deficiency. Supply by de-novo synthesis may not meet the demands of metabolism for normal growth. The attenuated uptake of glycine and other proteinogenic amino acids by SMX seen in the LC-MS/MS analysis may be a growth-related reduction in response to impaired folate synthesis, rather than a direct effect of changes to glycine metabolism.

A limitation to comparing bacterial growth to the metabolomic analysis data is the growth curves are produced from the entire lawn, whereas the metabolomic data is produced from a region central to the lawn. The central lawn area may no longer be in a state of exponential growth after 24 hours reducing lessening for nutrients from the agar. Chapter 3 revealed the lawns have a proliferating leading edge suggesting the majority of metabolically active bacteria are in this region, rather than the centre of the lawn. Adaptations to the growth curve method to recover bacteria, specifically from the same region as targeted by the LC-MS/MS protocol may provide a more accurate comparison of SMX and exogenous glycine effect on growth. It may also reveal if bacterial growth correlates with the increased lifespan phenotype of *C. elegans*.

5.4.4 The absence of exogenous glycine revealed similarities to the sulfamethoxazole exometabolome

WTK seeded in the absence and presence of SMX was found to have altered amino acid uptake form glycine free DM. Some of the observed changes in the non-SMX WTK conditions were similar to the amino acid exometabolome of SMX treated WTK. Whilst threonine, serine, aspartic acid and proline remained unaffected. These amino acids are key carbon sources (Mesibov & Adler, 1972) suggesting *E. coli* is still able to utilise these as carbon sources.

The data suggests that changes to glycine metabolism by SMX may have a direct effect on the metabolism of leucine, valine, phenylalanine, tyrosine, glutamic acid, arginine, lysine and methionine. These amino acids are all involved in protein synthesis and central metabolic pathways that share transport pathways (Maser et al., 2020; James Pittard & Yang, 2008; G. V. Stauffer & Stewart, 2004). Regulation of their metabolism is connected by the transcription regulator Lrp (Calvo & Matthews, 1994). Lrp is responsible for the regulation of genes involved in 1CM, amino acid catabolism and transport of nutrients along with other cellular functions (Calvo & Matthews, 1994). The glycine interconversion with threonine provides upstream substrates for BCAA and leucine biosynthesis as part of the threonine degradation pathway (laRossa, 2015; J. Q. Liu et al., 1998). Perturbations to these pathways may alter internal levels of leucine which is the key signalling substrate for Lrp. The changes seen here for uptake for uptake of these amino acids may be part of the wider Lrp nutrient stress response.

The variance within the samples is high and the presence of outliers in the data makes an accurate conclusion difficult. The glycine metabolic pathways in *E. coli* have not been fully elucidated. It will require further investigation using endometabolomics and gene expression analysis to determine the exact mechanism by which SMX alters glycine and amino acid metabolism, and if those changes correlate with the lifespan phenotype seen in *C. elegans.*

5.4.5 The absence of exogenous glycine increased healthspan

The healthspan assay revealed some small but significant changes to *C. elegans* healthspan. The worms appear to remain motile for a longer duration in the non-glycine conditions suggesting ageing is slowed. These results suggest alterations to the amino acid

profile of the bacterial food source may influence ageing. It is not clear if those changes are a product of the wider metabolic alteration or, the product of changes to a specific amino acid. *C. elegans* may sense the decreased availability of glycine or changes to the levels of the essential amino acids methionine, arginine and lysine in *E. coli*. The absence of glycine did not accelerate *C. elegans* healthspan. This suggests the worm was able to compensate by de-novo synthesis of the non-essential amino acid glycine from metabolites in its diet (Zečić et al., 2019). The alterations to the nutrient profile of the bacterial food source may induce a nutrient starvation stress response via the mTORC1 pathway (Kang & Avery, 2009) that may be responsible for the changes seen here.

# Chapter 6

# General Discussion

## 6.1 Summary of findings

This thesis aimed to improve the understanding of the interaction between *E. coli* and *C. elegans* by investigating components of the lawn that may be affected by folate synthesis and may be influencing *C. elegans* lifespan.

The investigation of this relationship began with the exploration of bacterial formaldehyde synthesis as a possible source of bacterial toxicity using a formaldehyde sensing lacZ reporter. A novel method was developed to quantify the output of the reporter in a bacterial lawn. The lifespan of *C. elegans* maintained on an *E. coli* strain that constitutively expresses the FrmA/B formaldehyde detoxification enzymes was also investigated. It was found that SMX does not reduce endogenous formaldehyde levels in *E. coli* and overexpression of formaldehyde detoxification enzymes does not increase *C. elegans* lifespan. Suggesting formaldehyde is not a source of toxicity that negatively influences worm ageing.

The method for investigating formaldehyde synthesis in chapter 3 revealed distinct differences in bacterial lawn morphology between the WTK (kanamycin resistant BW25113 strain) and SMX (WTK treated with 128 μg/ml SMX) conditions. The images generated by the formaldehyde experiments were used to produce a graphical representation of the bacterial lawn topography where LacZ output was relative to bacterial density. A comparison of morphological differences was made against low folate *E. coli* mutant strains that increase *C. elegans* lifespan. Bacterial growth of the lawn on DM was also explored comparing the effect of SMX to a previously discovered *E. coli* mutant strain. The strain has attenuated folate synthesis that increased *C. elegans* lifespan. The lifespan effect was reveresed with a rescue concentration of PABA. Assays were also conducted to determine if SMX impairs the bacterial ability to proliferate outside of the main lawn by transfer from *C. elegans* transiting through the lawn and wider agar substrate. Together the data revealed that SMX reduces bacterial growth on DM compared

to WTK and lifespan increasing mutants and, that the bacterial ability to establish new lawns and proliferate separate from a parent lawn was attenuated.

The exometabolome of the lawn was explored in chapters 4 and 5 to understand how SMX changes bacterial metabolism and if a product of that correlates with the increased lifespan phenotype of *C. elegans*. Specifically changes to the amino acid exometabolome within the DM agar. A novel method was developed to extract amino acids for analysis by LC-MS/MS. The method was able to provide qualitative data but needed further refinement to produce robust quantitative data. The LC-MS/MS analysis revealed SMX significantly altered the uptake of proline, glycine, tyrosine, alanine and glutamic acid from the DM although it was not possible to determine if these changes were also a product of excretion. The data also revealed that the changes by SMX did not correlate with the exometabolome of the reduced folate *E. coli* mutants as previously seen by NMR spectroscopy.

The LC-MS/MS method was used to explore the exometabolome temporally focusing on WTK and SMX over the duration of a lifespan assay. It was found that bacterial metabolism relating to the serine-glycine pathway was significantly altered along with several other amino acids associated with growth. Glycine-free DM was used to investigate if the absence of an external glycine source produced an exometabolomic amino acid profile that correlated with the differences seen in SMX conditions. The absence of exogenous glycine revealed changes to the exometabolome profile of SMX and WTK amino acids. Similarities and differences were seen between the conditions. A healthspan analysis of *C. elegans* maintained on bacterial lawns seeded on glycine free DM revealed exometabolomic glycine changes may correlate with an increased lifespan phenotype.

## 6.2 Implications of this work

### 6.2.1 A formaldehyde associated toxicity that reduced lifespan was not observed

The use of a novel method to quantify bacterial formaldehyde synthesis in chapter 3 revealed that SMX does not alter endogenous levels compared to WTK. It also showed that constitutive expression of *E. coli* formaldehyde detoxification enzymes do not increase *C. elegans* lifespan. The biochemistry of folate metabolism related formaldehyde synthesis is shared between eukaryotes and prokaryotes (Bourne, 2014). The methodology

here focused on bacterial formaldehyde synthesis and detoxification. Specifically, if changes to those pathways provide the link between a bacterial folate dependent toxicity that alters the lifespan phenotype of *C. elegans*.

It is unlikely bacterial folate metabolism is a source of toxic levels of formaldehyde to *C. elegans* as *E. coli* has robust detoxification mechanisms in place. The enzymes FrmA/B provide the primary mechanism of formaldehyde detoxification (Gonzalez et al., 2006). The serine hydrolase YeiG provides a secondary mechanism that is constitutively expressed in the absence of FrmB (Gonzalez et al., 2006). Together these enzymes catalyse the conversion of formaldehyde to formate that is returned to 1CM (Gonzalez et al., 2006). Formaldehyde is also sequestered by the serine-glycine pathway providing a 1C unit for the synthesis of 5,10-met THF providing a cyclical pathway of synthesis and degradation for both folate and formaldehyde (N. H. Chen et al., 2016; K. Denby et al., 2016; Gonzalez et al., 2006). Together the organism has robust pathways to prevent cytotoxic accumulation.

The attenuation of bacterial folate synthesis by SMX may reduce the overall pool of formaldehyde. Although, this maybe inconsequential as the existing pool is below a level cytotoxic to the bacteria. As can be seen by the robust growth of WTK on DM and NGM. Coupled with the volatility of formaldehyde it is unlikely the level of formaldehyde in WTK contributes to a chronic underlying toxicity in *C. elegans* sufficient to shorten lifespan.

A recent study by Morellato et al. (2021) focusing on mammalian 1CM. The study described a formaldehyde cycle that demonstrated the flux of the metabolite throughout 1CM (figure 6.1) where it is continuously synthesised and sequestered (Morellato et al., 2021). The study also proposed a mechanism of toxicity through a surplus of formaldehyde in the cells that contributes to cellular damage within the cytosol, mitochondria and nucleus (Morellato et al., 2021). In the cytoplasm and potentially the nucleus 1CM derived formaldehyde spontaneously reacts with glutathione (GSH) to form *S*-hydroxymethyl-GSH (HSMGSH) (Umansky et al., 2020; Umansky et al., 2022). In the cytosol HSMGSH is catabolised by the alcohol dehydrogenase ADH5 and a formyl-GSH hydrolase to yield formate (Burgos-Barragan et al., 2017; Morellato et al., 2021). In the mitochondria formaldehyde is catabolised by the aldehyde dehydrogenase ALDH2 to

produce formate (Burgos-Barragan et al., 2017; Morellato et al., 2021). Formate is incorporated back into 1CM and the folate cycle to yield de novo 5,10-met THF (Burgos-Barragan et al., 2017; Morellato et al., 2021). A more recent study by Umansky et al. (2022) reported that cytoxicity in *C. elegans* and human cancer cells was a product of oxidative stress from endogenous formaldehyde changing the redox balance of GSH and its oxidised form GSH disulphide (GSSG) (GSH:GSSG) by reacting with the thiol group in GSH.

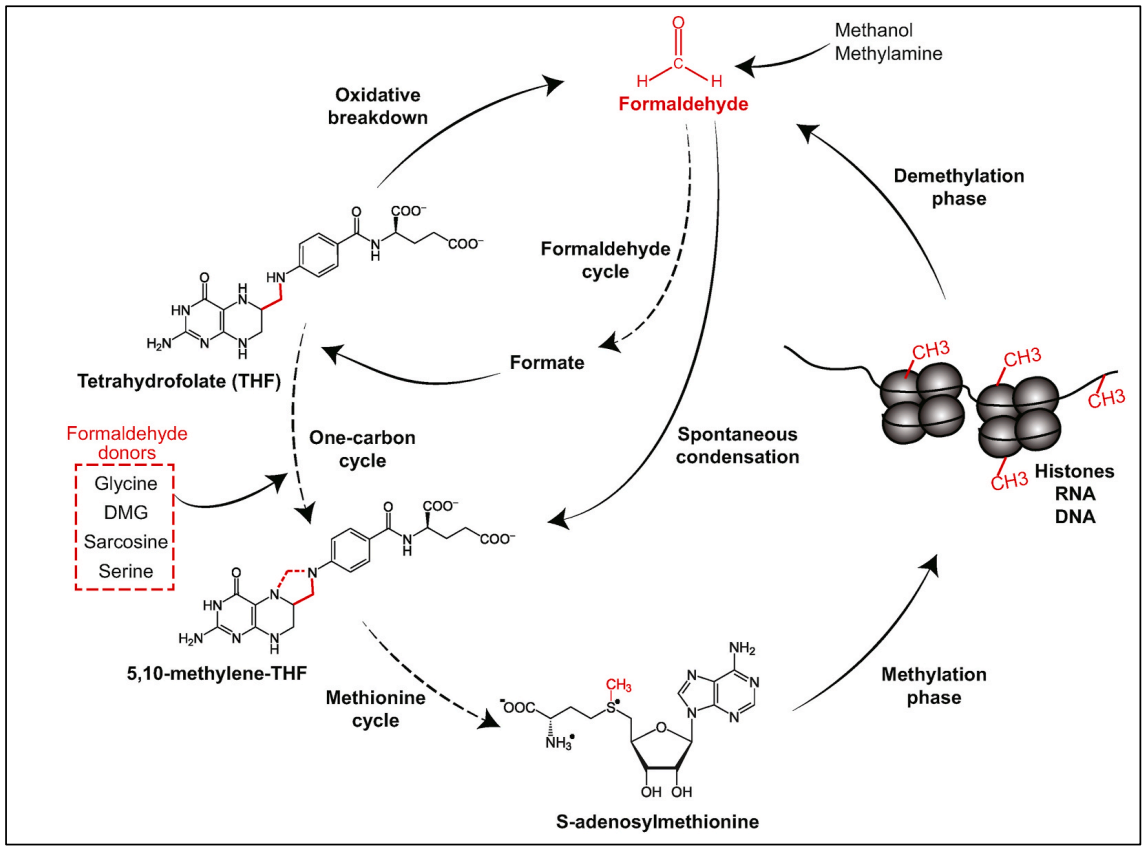


**Figure 6.1 One carbon metabolism associated formaldehyde flux in mammals.** The flux of formaldehyde in 1CM is shown here depicting the metabolic pathways involved. The cartoon demonstrates the cyclical nature of formaldehyde synthesis and utilisation to yield THF and 5,10-met THF through the introduction of formate to 1CM and donation by glycine, dimethylglycine (DMG), sarcosine and serine. The reactions of the methionine cycle to produce methyl groups for DNA and histone methylation and demethylation occurs in the mitochondria. Image adapted from (Morellato et al., 2021).

This may translate to *C. elegans* in the context of SMX as the endogenous levels of THFs were found to be reduced in worms, specifically 5,10-met THF (Maynard, 2017). Degradation of 5,10-met THF is key source of formaldehyde contributing to the cellular

pool (N. H. Chen et al., 2016; Schug, 2018). This also corresponds with findings by Annibal et al. (2021) who reported that levels of 5,10-met THF were lower in *C. elegans* long lived mutants *daf-2*, *eat-2* and *isp-1*. Attenuation of folate in the worm's diet may be reducing the pool of folates within *C. elegans* that contributes to the formaldehyde cycle. This in turn may reduce formaldehyde accumulation preventing or limiting cytoxicity by maintaining a balanced GSH:GSSG ratio that may promote lifespan extension.

Further work would be needed to explore this hypothesis by focusing on *C. elegans* formaldehyde levels and gene transcription in response to maintenance on SMX treated bacteria. Formaldehyde associated detoxification enzymes and pathways have not been fully identified in *C. elegans.* A targeted genomics analysis would be limited to ADH5. This would limit data relating to part of the formaldehyde associated mechanisms thus, not giving a full overview of transcriptional changes.

Due to the difficulties in measuring endogenous formaldehyde formate may serve as a proxy biomarker for its synthesis. Under normal conditions formate synthesis may correlate with the activities of both the ADH5 homolog (Umansky et al., 2020) and ALDH2 (a homolog currently remains unidentified) whereby a steady state of formate synthesis relative to formaldehyde synthesis/degradation may be observed.

DNA microarray technology can be used for global gene expression profiling and has successfully been applied to studying *C. elegans* (S. K. Kim et al., 2001; Lund et al., 2002; Portman, 2006; Reinke, 2002). Microarrays of PCR fragments corresponding to open reading frames can be used to study changes in transcription and reveal previously unidentified genes (DeRisi, Iyer, & Brown, 1997; S. K. Kim et al., 2001; Richmond, Glasner, Mau, Jin, & Blattner, 1999; Schembri, Kjærgaard, & Klemm, 2003; Teng & Xiao, 2009). The method allows comparison of gene expression under different environmental conditions over time, regardless of growth or genetic state (S. K. Kim et al., 2001; Richmond et al., 1999; J. Wang & Kim, 2003). In the context of our lifespan protocol a baseline of gene expression could be derived from normal worm maintenance on a bacterial lawn. Further conditions to observe changes in gene expression could be explored. The addition of exogenous formate to overexpress transcription and identify formate related gene transcription changes. The addition of SMX to observe changes to fthe identified ormate associated genes. Exogenously adding formate to the bacterial lawn

may upregulate *C. elegans* gene expression relating to ADH5. and potentially identify the ALDH2 homolog in *C. elegans*. Previous work has investigating the effect of formate on *E. coli* protein expression reported high levels of formate slows bacterial growth (Kirkpatrick et al., 2001). Before attempting a *C. elegans* assay, bacterial growth, worm lidfespan and exogenous formate should be explored. It will be necessary to identify a suitable formate concentration range that does not retard bacterial growth or kill *C. elegans* but, stimulates a transcription response in *C.elegans*.

It is hypothesised an SMX-*E. coli* induced reduction in *C. elegans* 5,10-met THF may correlate with reduced formate as a product of reduction in the formaldehyde pool linking the effect of SMX in *E. coli* to the extended lifespan phenotype in *C. elegans*.

6.2.2 Flagella and formaldehyde may not be a source of toxicity

The concept of 1CM related toxicity independent of folates led to the investigation of formaldehyde in this thesis. It was also the catalyst for exploring flagella expression as a component of bacterial proliferation and growth that may be a source of underlying toxicity (Barnhart & Chapman, 2006). The observed presence of flagella, lawn morphology and growth of reduced folate *E. coli* mutants *ΔpabA* and *ΔrpoS* corresponded with WTK as opposed to SMX treated *E. coli*. It was reported by Maynard (2017) that *C. elegans* bacterial aversion behaviour was reduced when maintained on *ΔpabA* and *ΔrpoS*.

The formaldehyde lifespan assay in section 3.3.5 of chapter 3 did not support the hypothesis that formaldehyde is a source of lifespan reducing toxicity. The lack of significant difference between conditions using a formaldehyde sensitive LacZ reporter also suggests it may not be a component that influences aversion behaviour. The proliferation assays and electron microscopy images of the bacteria also showed that whilst flagella may be absent in bacteria treated with SMX this may not be a source of toxicity. Although, a lifespan assay to investigate flagella deficient *E. coli* would be required to confirm this conclusion. Together the data suggest flagella and formaldehyde are not reducing *C. elegans* lifespan as a source of toxicity.

### 6.2.3 Aversion behaviour may not be related to bacterial toxicity

The previously observed aversion and congregation behaviour differences between worms maintained on WTK and SMX lawns were seen as a clue to indicate a possible absence of toxicity that may be increasing *C. elegans* lifespan (Maynard, 2017). This may not be a response to bacterial toxicity particularly as WTK is a non-pathogenic strain.

The aversion behaviour may be aerotaxis to avoid hyperoxic regions of the WTK lawn (A. J. Chang, Chronis, Karow, Marletta, & Bargmann, 2006). It has been previously reported that bacterial lawn growth on agar produces an oxygen gradient that is radial to the lawn edge whereby, the regions of highest bacterial concentration are also the lowest in oxygen concentration (Gray et al., 2004; Reddy, Hunter, Bhatla, Newman, & Kim, 2011). The lawn edge represents a region of low oxygen compared to the centre of the lawn (Demir, Yaman, Basaran, & Kocabas, 2020; Reddy et al., 2011). The morphology plots and lawn images discussed in this thesis show that WTK have a more diffuse radial band at the edge of the lawn. Whilst SMX treated lawns retain what appears to be a more condensed region of bacteria lacking diffusion.

Studies using the *C. elegans* wildtype strain N2 maintained on *E. coli* OP50 found that worms exhibit an aerotactic response to regions of low oxygen in their environment (Gray et al., 2004; Meisel & Kim, 2014). Bacterial lawns are typically hypoxic due to the metabolic activity of the bacteria, *C. elegans* is attracted to regions of low oxygen preferably between 2 % and 12 % as part of an aerotactic response enabling them to locate food sources in the wild (Gray et al., 2004; Meisel & Kim, 2014). Oxygen is able to diffuse rapidly through *C. elegans* and is not a limiting factor for respiration until the external concentration is reduced to < 4 % (Gray et al., 2004). Respiration is unaffected by increases in oxygen but it may cause an elevation in ROS production and oxidative damage decreasing lifespan (Gray et al., 2004; M. Zhang et al., 2020).

The original hypothesis of SMX removing an underlying low level toxicity component of the bacteria maybe incorrect. Instead, SMX may alter the lawn morphology to create a more desirable hypoxic lawn edge that reduces aversion behaviour. Prolonged exposure to a low oxygen environment may promote longer life in *C. elegans*. Conducting lifespan assays by altering the external oxygen levels of the bacterial lawns would have to be conducted with care as this might alter bacterial metabolism and produce skewed data.

Previous work by Demir et al. (2020) used fibre optic probes to measure $O_2$ concentration in bacteria and *C. elegans* accumulations on agar. This technique may be successfully adaptable to measuring $O_2$ at the bacterial lawn edge under our conditions. By using the fibre optic technique probing the specific regions of the bacterial lawn and its satellite colonies where worms aggregate may be achieved. An analysis would need to obtain data across the duration of a lifespan. For accurate analysis the probes would need to remain in situ in the lawn with minimal disruption of the plates. Removal of plates from incubators may alter $O_2$ saturation in the lawn potentially skewing the data, a method for accurate remote monitoring would need to be developed. A comparison of oxygen concentrations may be determined between WTK, SMX treated bacteria and lifespan increasing mutant strains. It may reveal similarities and differences to support this hypothesis.

### 6.2.4 SMX attenuates bacterial lawn growth

The investigation into bacterial growth in chapter 5 clearly demonstrated that SMX reduces bacterial growth. During the development of DM it was optimised for the growth of the *E. coli* WT strains OP50 and BW25113 (Helliwell, 2013) but not for use with SMX. It was also found the addition of 0.1 μM PABA was sufficient to support growth of *ΔpabA* and *ΔrpoS* without reversing the increased lifespan phenotype effect on *C. elegans* (Helliwell, 2013; Maynard, 2017).

These findings support the previous work reported by Maynard (2017) who found OP50 *E. coli* had attenuated growth on DM agar inoculated with 128 μg/ml SMX and concluded DM is not optimised for bacterial growth with SMX. The results did not support the previous work by Virk (2013); Virk et al. (2016) that SMX does not affect bacterial growth on NGM agar as it was shown not to be the case in this work. Previous work by our lab reported that 250 μM PABA added to NGM agar was sufficient to reverse the increased lifespan of *C. elegans* maintained on *E. coli* treated with 128 μg/ml SMX (Virk, 2013). The data reported here found that a concentration of 250 μM PABA was not sufficient to recover SMX treated bacterial growth to WTK levels. The results demonstrate the effectiveness of SMX as a competitive inhibitor of bacterial folate synthesis, and that whilst a lifespan increase in worms can be reversed at very low concentrations of PABA bacterial growth is still significantly affected.

To make a direct comparison between lifespan conditions that slow ageing in *C. elegans* and previous work NGM and DM need to be optimised to be able to support growth of bacteria to WTK levels. This may be problematic as it has been shown here that the minimum concentration of PABA required to reverse the SMX lifespan effect did not fully rescue bacterial growth. It was reported by Virk et al. (2012) that SMX was able to significantly increase *C. elegans* lifespan dose dependently from 2 ug/ml to 128 ug/ml. An alternative approach would be to lower the working concentration of SMX based on these findings to minimise the effect of competitive inhibition in the presence of PABA. A suitable combined working concentration for SMX and PABA may be found that produces a balance between lifespan and bacterial growth for future experimental protocols.

### 6.2.5 Bacterial lawn morphology differs between conditions

It was found in chapter 3 that the bacterial lawns contained radial regions of population density that differed between WTK, *ΔpabA*, *ΔrpoS* and SMX conditions. These findings correlated with previous work by Inoue et al. (2007); J A Shapiro (1987) that explored the structure of bacterial colonies on agar under the context of biofilm formation and development. It is not fully understood what the differences reported in this body of work represent in terms of metabolic activity and growth. The use of LacZ proved a useful tool for visualising the morphology of the lawn but the output was ineffective for identifying boundary limits. This was due to colour leeching and saturation over time and did not reveal the vertical stratification of the lawn

A more accurate understanding for comparison would be to investigate lawn growth regionally. Separating the lawn into specific regions of growth based on the geography of the population density. This may identify what growth state the radial regions of the lawn are in and how that relates to the proportion of metabolic activity in the total lawn. Development of a method to observe lawn stratification vertically would allow an investigation of changes to the composition of the bacteria directly associated with the agar or surface environment.

The limitation to segregating lawns by specific regions would be determining the boundary between the outer perimeter and the central region and how to separate those regions without mixing or initiating a bacterial stress response that could alter morphology such as freezing and thawing.

6.2.6 SMX prevents bacterial proliferation of satellite colonies to the parent lawn

This work in chapter 3 found that SMX prevented the expansion of individually seeded 2 µl mini lawns on NGM. Proliferation in terms of growth of population was not measured and an accurate conclusion on motility driven lawn expansion could not be made.

These findings correlate with previous work in our lab by Pefani (2019) who found SMX prevented bacterial accumulation by transfer from a parent lawn by *C. elegans* on NGM. The results are difficult to compare directly as Pefani (2019) used GFP expression to measure growth as a product of physical transfer by the worms in the context of adhesion. Whereas the work here used surface area change to focus specifically on the expansion and proliferation of manually seeded bacteria. The manually seeded mini lawns were used at a volume and concertation that had already been established to grow on NGM whilst there was no means to control the concentration of bacteria transferred by worms.

Further work would need to determine what components of the mini lawn are driving the surface area increase, when and if they are expressed by SMX to inhibit lawn expansion. It would also need to be determined if this translates to the morphological differences seen in 100 µl lawns used for lifespan assays. An expansion and adaptation of the previously reported electron microscopy work in chapter 3 of this thesis may provide visual analysis of mini lawn morphology. The technique would need improvement to accurately target specific points of the mini lawn without the need for destructive removal and homogenisation.

An appropriate method for producing growth curves of the mini lawns would also establish if surface area change is a product of impaired bacterial growth or, loss of the ability to exploit the surrounding agar through motile mechanisms. Removal of the parent lawn by scraper as demonstrated in chapter 4 of this thesis would leave the mini lawns undisturbed. They could then be removed via low volume washing with M9 and a protocol for $OD_{600}$ analysis could be followed (chapter 2 of this thesis). It has also not been established what the minimum threshold of bacterial concentration is required to successfully seed a mini lawn on SMX treated agar and if that differs between media. There would also need to be a deeper understanding of the bacterial dynamics within a small population that may

impair growth when 1CM is inhibited but a sufficient rescue concentration of PABA is present.

### 6.2.7 An agar nutrient gradient

The data suggested the presence of a larger more densely populated lawn in the proximity of satellite lawns maybe competing for nutrients in the agar. These findings may be supported by evidence presented in a review by Douglas (2020). It reported on metabolite transfer and cross feeding between the microbiota other microbes in the community and the host (Douglas, 2020). The review revealed mutualistic relationships between separate bacterial communities (Douglas, 2020). Secreted metabolites were found to rescue growth of substrate deficient strains in both liquid culture and semi solid media (Douglas, 2020; Kelly, Fischer, & Collins, 2021; Lubbe, Bowen, & Northen, 2017).

An appropriate assay would need to be developed to support the conclusion of the presence of nutrient gradients within the agar that may influence bacterial growth. To the best of our knowledge bacterial lawn derived nutrient gradients within the agar substrate has not been explored and reported on in the literature. The gradient would need to be investigated across the entire three dimensional structure of the agar, as opposed to a vertical observation of the surface. It would need to be established if the nutrients contained within the media form concentration gradients through diffusion in the agar in response to consumption by a bacteria lawn. And if the bacterial lawn contributes nutrients to the agar through excretion and secretion as products of metabolism and bacterial turnover. It would also need to be ascertained if the bacterial contribution of nutrients creates an antagonistic or synergistic gradient and how that influences nutrient flux within the agar.

The metabolite profile of *E. coli* is complex and diverse containing 995 known compounds (Mackie, Keseler, Nolan, Karp, & Paulsen, 2013). The scale of monitoring each metabolite would be prohibitive for an accurate assessment of flux within the agar. Any investigation should be limited to nutrients required for growth found in both the agar and bacteria. Because there is the possibility of bidirectional flux separate labelling maybe required. A complication to this is developing a protocol that allows for easy identification, separation and imaging of agar metabolites and de-novo synthesised metabolites secreted or excreted into the agar along horizontal and vertical planes.

A potential method would be to adapt the LC-MS/MS method developed in chapter 3 of this thesis. Samples could be extracted from the agar across its width and each sample halved or quartered to analyse the stratification within the plate. The LC-MS/MS analysis could focus specifically on DM reagents by use of appropriate standards. The data from each sample could be plotted into a three dimensional concentration plot to reveal the lateral and vertical gradients within the agar. An obvious limitation to this approach is the sheer volume of samples required may make the method unworkable. In addition, the protocol would need considerable refinement and improvement for any quantification analysis as discussed in section 6.2.10 of this chapter.

A basic understanding of nutrient diffusion through agar may be achieved through the use of fluorophores or dyes to observe the rate, pattern and distribution in a lawn free agar plate (Katritzky & Narindoshvili, 2009). By adding markers that can be easily imaged during preparation of the media distribution can be imaged and analysed over time. This will remove the need for destructive and invasive protocols to obtain analytes and follow the pattern of change in the media from liquid to semi-solid. The markers could also be added to the surface of the agar in a range of concentrations to the surface of the agar to replicate bacterial secretion over time. A limitation is that dye and fluorophore compounds are typically higher in molecular weight than metabolites, the ionic state of dyes may have differing interactions with the agar and reagents contained within the media (Gurr, 2012; Stewart, 1981; Y. Yang et al., 2008). The outcome would be a specific diffusion pattern and rate that does not correlate with nutrient metabolites but, may give some indication of how metabolites behave in the media over time.

### 6.2.8 LC-MS/MS protocol to analyse amino acid changes in Defined media agar

The results in chapter 4 demonstrate a robustly reproducible method for analysing amino acids extracted from DM agar using LC-MS/MS. It was found that the data had an unusually high amplification of the analyte signal and was thought that the amplification was a product of a matrix effect. A considerable amount of QC work was conducted that ruled out a matrix effect but, was not able to resolve the anomaly limiting the analysis to qualitative data rather than quantitative data. Optimisation of the protocol may improve analyte variance and accuracy. In addition, it will be necessary to identify and remedy the source of amplification. Analyte recovery that is comparable to a known baseline will allow for quantitative analysis between conditions.

A shotgun analysis may reveal additional metabolites that can be extracted from the agar with this protocol widening the application of this method. A study by E. D. Smith et al. (2008) reported a diffusible metabolite from *E. coli* may limit *C. elegans* lifespan. The metabolite was able to diffuse through agar to negatively influence the worm's lifespan suggesting it was part of the bacterial exometabolome but was not identified (E. D. Smith et al., 2008). The protocol developed here may serve as a tool to extract and analyse unidentified metabolites directly from the agar during lifespan assay conditions. This may add to the current body of knowledge of the *E. coli* exometabolome in agar and the relationship with host organisms.

6.2.9 Changes to exometabolomic amino acids in defined media agar

In chapter 4 an LC-MS/MS analysis of amino acids in DM agar after 48 hours of growth found that SMX significantly changed the amino acid exometabolome in DM agar. The results were consistently reproducible. The data revealed that the SMX amino acid exometabolome did not correlate with the amino acid exometabolome of *ΔpabA* and *ΔrpoS* at 48 hours.

The results did not directly support previously reported serine and glycine changes of *ΔpabA* using NMR by Helliwell (2013). It was previously reported that after 20 hours of growth exogenous glycine remained high in the *ΔpabA* condition (Helliwell, 2013). It was also reported that glycine was completely consumed in the CTRL condition whilst serine was completely consumed in both conditions (Helliwell, 2013). Here it was found a similar pattern occurred but the changes were seen in the SMX condition only. The lack of correlation between the folate deficient mutants and SMX may be attributed to the mutants compensating for disruption to folate synthesis more efficiently than *E. coli* treated with SMX. It has previously been reported that OP50 bacterial folate levels are severely diminished in SMX treated bacteria compared to *ΔpabA* and WT *E. coli* (Maynard, 2017).

The work here correlates with work by Maynard (2017). SMX has an increased negative effect on *E. coli* metabolism. SMX competitively inhibits exogenous PABA for folate synthesis, whilst *ΔpabA* only requires nanomolar concentrations of PABA for recovery. Without a temporal analysis of the *ΔpabA* and *ΔrpoS* exometabolome it is not possible to

determine if temporal amino acid changes match the SMX condition as exogenous PABA is depleted.

Further work would need to analyse WTK folate levels under these conditions to observe if they correlate with the previously reported results in OP50. Optimisation of DM for bacterial growth with SMX may rescue folate synthesis. It may reveal similarities with *ΔpabA* in both bacterial folate and amino acid exometabolomic data. These changes may also correspond with the rescue of bacterial growth. Further supporting the data that bacterial growth does not correlate with lifespan.

6.2.10 Temporal changes to exometabolomic amino acids in defined media agar

In chapter 5 It was demonstrated by LC-MS/MS that SMX significantly altered amino acids in DM agar over the duration of 5 days. Because no differences were seen in the previous *ΔpabA* 48 hour data it was decided to focus on SMX and WTK conditions only over the duration of a lifespan timeline. By reducing the investigation to two conditions over a longer time it allowed for appropriate management for scale to maintain accuracy and reproducibility.

It was established that consumption of the amino acids was occurring by comparing the starting 0 hours data against the data at each time point over the duration of the temporal study. The pattern of change observed for each amino acid was robustly reproducible and matched the observations previously seen in the 48 hour study in chapter 4. It was not possible to determine if secretion was occurring from the bacteria. This was due to the lack of accurate quantification against the known starting amino acid concentration within the agar. Amplification of the analyte signal also prevented an accurate baseline being established. In addition, outliers from sample variance may have skewed the data disguising if the increase in mean PAU output for each amino acid was a product of secretion. Further work required to improve the efficiency of the LC-MS/MS protocol is discussed in section 6.2.4i of this chapter and section 4.4.1 of chapter 4.

Due to the novelty of this work the results cannot be directly compared to work within the field. A thorough search of the literature did not reveal any studies that investigated the bacterial lawn exometabolome in agar or, the changes that may be incurred by treatment

with SMX. The results in section 5.3.6 of chapter 5 provide an insight into the changes in amino acid concentrations within agar as a product of bacterial metabolism over time. These results may correlate with investigations exploring bacterial supernatant from liquid culture that may show a conserved pattern of amino acid uptake across conditions. The conserved pattern of uptake is dependent upon the metabolic cost of amino acids (figure 6.2) in relation to availability and biosynthetic demand (Akashi & Gojobori, 2002). In conditions of low availability and energy limitation preference for uptake may be skewed towards metabolically cheap amino acids and vice versa in conditions of high availability and low energy demand (Akashi & Gojobori, 2002). Thus maintaining energy efficiency for reproduction and growth (Akashi & Gojobori, 2002).

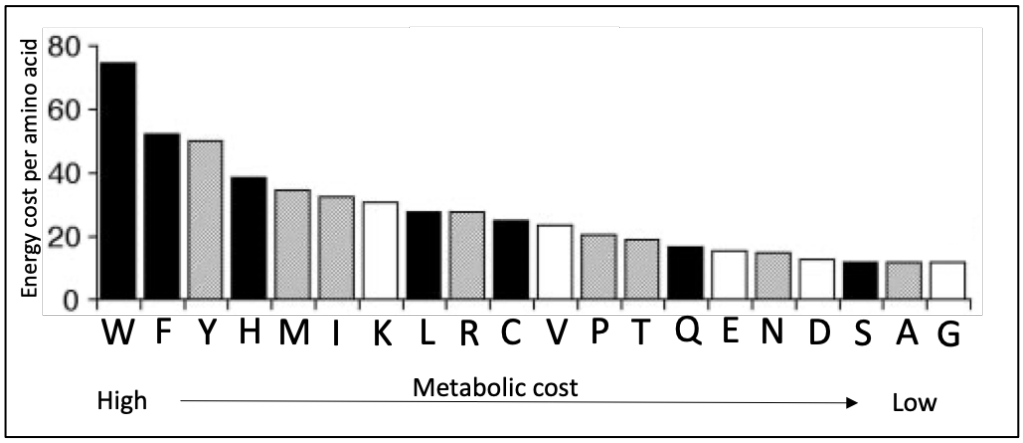


**Figure 6.2 Graph showing metabolic value of individual amino acids in *E. coli*.** Amino acids are arranged in order of decreasing metabolic cost from left to right. A, alanine; C, cystine; D, aspartate; E, glutamate; F, phenylalanine; G, glycine; H, histidine; I, isoleucine; K, lysine; L, leucine; M, methionine; N, asparagine; P, proline; Q, glutamine; R, arginine; S, serine; T, threonine; V, valine; W, tryptophan; Y, tyrosine. Image adapted from (Akashi & Gojobori, 2002)

Zampieri et al. (2019) investigated amino acid concentrations in bacterial supernatant of *E. coli* grown in liquid culture of media with glucose, supplemented with Casamino acids at 37 °C. The study was conducted over 12 hours comparing analyte concentration with $OD_{600}$ measurements of bacterial growth (Zampieri et al., 2019). The rapid consumption of the degradable (low cost) amino acids serine, glycine, threonine, aspartate and glutamate was reported to provide the majority of carbon and nitrogen during rapid exponential growth (Zampieri et al., 2019). The amino acids isoleucine, leucine, histidine, methionine, phenylalanine, tyrosine and valine lack degradation pathways (Keseler, 2021; Maser et al., 2020). They were also reported to have lower uptake in relation to growth and uptake is

tightly regulated by internal feedback loops to prevent cellular accumulation (Zampieri et al., 2019).

Maser et al. (2020) also conducted an LC-MS/MS investigation into amino acid utilisation by *E. coli* in liquid culture. Bacterial cultures were prepared in a minimal media containing glucose, trace metals and 20 amino acids with the concentration matched to biomass and grown at 37 °C (Maser et al., 2020). It was reported that serine, aspartate and glutamine were rapidly consumed with serine being the most consumed for ATP synthesis and a source of nitrogen (Maser et al., 2020). It was also observed that the amino acids serine, aspartate, cystine, and glutamine were over consumed relative to protein synthesis to meet the demands of the TCA cycle and glycolysis (Maser et al., 2020). The non-degradable amino acids histidine, valine, isoleucine, leucine, methionine, phenylalanine, tryptophan and tyrosine were also found to be consumed close to the requirements for protein synthesis (Maser et al., 2020).

The results in chapters 4 and 5 of this thesis reported rapid and complete uptake of serine and aspartate by 48 hours. This supported the previous the findings reported by Akashi and Gojobori (2002); Maser et al. (2020); Zampieri et al. (2019) that *E. coli* has a preference for serine. Contrary to the previous work that reported the presence of serine prevented glycine uptake (Maser, Peebo, & Nahku, 2019; Maser et al., 2020; Zampieri et al., 2019) the WTK conditions observed here had complete and rapid uptake of glycine. This may correlate with the observation that glycine is a low cost amino acid (Akashi & Gojobori, 2002) and is present in high concentrations in DM. A comparison of $OD_{600}$ of bacterial growth on DM agar and LC-MS/MS data at the respective time point from the temporal assays in chapter 5 also reveals a similar pattern of uptake to those reported by Zampieri et al. (2019). The results in chapters 4 and 5 correlate with these findings and those of Maser et al. (2020). It was found that the non-degradable high cost (Akashi & Gojobori, 2002) amino acids phenylalanine, methionine, leucine, isoleucine, valine, tyrosine and histidine were not consumed as completely or as rapidly as the other low cost (Akashi & Gojobori, 2002) amino acids. The SMX conditions also supported the previous findings discussed here. It was shown in section 5.3.3 of chapter 5 to have attenuated bacterial growth. This was reflected in the further reduced uptake of non-degradable amino acids compared to WTK.

There were clear differences between the two media used for the studies discussed here (Maser et al., 2020; Zampieri et al., 2019) and DM used for this work. Yet, the patterns of amino acid consumption between DM agar bacterial lawns and liquid cultures in a glucose supplemented media were strikingly similar. Together these findings support the observation that *E. coli* has a regulated and robust hierarchical uptake of amino acids. Uptake is based on metabolic cost to meet biosynthetic demand that may only be partially influenced by perturbations to folate synthesis. This may enable *E. coli* to manage energy efficiency to support growth that is conserved across differing backgrounds of nutrient availability (Maser et al., 2019; Zampieri et al., 2019). Further work is needed to investigate if the absence of serine in the media alters glycine uptake under the conditions used in this thesis. A repeat of the no-glycine experiments conducted in this work using a no-serine condition could be used to explore this question further. In addition, LC-MS/MS analysis of *E. coli* in liquid DM culture may further support these findings and provide an understanding of why a rapid uptake of glycine from the agar occurred.

### 6.2.11 An absence of exogenous glycine slows bacterial growth and alters the exometabolome

Section 5.3.9 and 5.3.10 of Chapter 5 investigated the effect of removal of exogenous glycine in DM agar on bacterial growth and the amino acid exometabolome. It was found that removal of glycine from the media attenuated growth of the *E. coli* bacterial lawn in all conditions. The LC-MS/MS analysis revealed that absence of exogenous glycine altered the WTK exometabolome but, not to one that was similar to treatment with SMX. Without endometabolomic data it is not possible to conclusively determine what metabolic changes are occurring within the bacteria. Endometablomic data may provide further insight to why growth was reduced and the observed changes to uptake of exogenous amino acids.

A previous study by Yun Kyung Kwon, Meytal B Higgins, and Joshua D Rabinowitz (2010) investigated the depletion of intracellular glycine by inhibition of bacterial folates synthesis in *E. coli* with the antifolate trimethoprim. Trimethoprim targets down stream of SMX where it inhibits the enzyme dihydrofolate reductase (DHFR), preventing conversion of DHF to the active form THF (Y. K. Kwon et al., 2010). The study observed bacterial growth and used LC-MS/MS to explore the bacterial endometabolome (Y. K. Kwon et al., 2010). It was reported that depletion of intracellular glycine depletes cellular purine levels

initiating a stationary phase that prolongs survival known as the stringent response (Y. K. Kwon et al., 2010). The stringent response occurs when starvation of one or more amino acids upregulate uncharged tRNAs and stalled ribosomes (Wendrich, Blaha, Wilson, Marahiel, & Nierhaus, 2002). These signal RelA to synthesise the alarmones ppGpp and pppGpp (guanosine 5',3' bispyrophosphate and guanosine pentaphosphate) (Durfee et al., 2008). The alarmones ppGpp and pppGpp bind to the ribosomal A site preventing transcription of transfer and ribosomal RNAs regulating gene expression to ensure cell survival (Aurélia Battesti & Bouveret, 2009; Durfee et al., 2008; Gentry & Cashel, 1996; Magnusson et al., 2005; Wendrich et al., 2002). These findings were also discussed in section 3.3.6ii of chapter 3 as a possible mechanism to explain the morphological and proliferation changes observed in SMX treated *E. coli.*

The reported changes in bacterial lawn growth in section 5.5.9 of chapter 5 may correlate with investigations discussed here. Further work would be needed to determine if the observed changes in both WTK and SMX conditions are a product of nutrient deficiency due to the absence of sufficient glycine to support growth. This could be achieved through use of LC-MS/MS to explore the bacterial endometabolome specifically, amino acid and ppGpp levels. Obtaining these metabolites from a bacterial lawn has not been previously attempted. During the course of this work protocols were explored to attempt endometabolomics. A protocol by Smart et al. (2010) may be a suitable starting point if the difficulties and technicalities of quenching and lawn extraction could be overcome. Coupling an adaptation of this method with the methods for ppGpp analysis by D. Ito et al. (2020) may prove successful to understand if SMX and the absence of exogenous glycine is triggering a stringent response in *E. coli*. In addition, the use of RNAseq to profile the transcription response of RelA to SMX and absence of external glycine may provide further evidence to understand the mechanisms reported here. This kind of analysis for RelA has successfully been achieved in work by Durfee et al. (2008). Although, some adaptation would be required to extract RNA from a bacterial lawn on DM agar as opposed to in liquid culture.

### 6.2.12 The absence of exogenous glycine and *C. elegans* Healthspan

The effect of the absence of exogenous glycine in the agar on the healthspan of *C. elegans* was investigated in section 5.3.10 of chapter 5. It was found that maintaining *C. elegans* on OP50 *E. coli* grown on glycine free DM agar conferred a small but significant increase

to the worms healthspan. The change to healthspan was observed in both SMX and WTK conditions suggesting it was independent of the changes to 1CM by SMX. It was proposed that the results may be a product of DR but without fecundity assays to confirm or rule out DR and endometabolomic data from both *C. elegans* and *E. coli* it is not possible to make a robust conclusion to support this hypothesis.

The work presented in this thesis is not directly comparable to previous studies by Edwards et al. (2015); Y. J. Liu et al. (2019) discussed here. These studies used UV killed OP50 *E. coli* treated with the antibiotic carbenicillin supplemented with glycine and serine. As opposed to this body of work where *C. elegans* was exposed to live *E. coli* in the complete absence of glycine supplementation. The healthspan effect was investigated as a product of bacterial metabolism rather than a direct effect of supplementation of specific amino acids on a background of metabolically inactive bacteria. An increase in dietary glycine may decelerate *C. elegans* ageing but the metabolic demand of the UV killed bacteria will differ from live *E. coli* (Villarino, Rager, Grimont, & Bouvet, 2003) which are still able to proliferate and grow. This may produce differing nutrient profiles that contribute to *C. elegans* metabolism and ageing.

Recent work revealed the relationship between the glycine and methionine metabolic pathways in *C. elegans*. It was reported that glycine accumulates in ageing worms and supplementation with glycine significantly increases *C. elegans* lifespan by reversing age induced repression of 1CM and purine metabolism genes (Y. J. Liu et al., 2019). Increased endogenous glycine levels were also reported in the long lived *C. elegans* mutants *daf-2* and *eat-2* where the metabolism of methionine, glycine and THF dependant 1CM was upregulated (Edwards et al., 2015; Y. J. Liu et al., 2019). It was also reported that supplementation of serine or glycine was required during the first 72 hours of adulthood to confer a beneficial effect. The temporal requirement corresponded with the worm's reproductive period suggesting possible crosstalk between longevity and the reproductive pathway (A. W. Gao et al., 2017; Y. J. Liu et al., 2019). The temporality of these findings may also correlate with the pattern of amino acid uptake reported in this thesis and the temporal window for SMX reported by Maynard (2017)

The study by Y. J. Liu et al. (2019) also reported that serine and glycine induced longevity was dependant on the methionine cycle and consistently found methionine levels decreased

with ageing in *C. elegans* as part of the ageing phenotype. Both serine and glycine feed into the methionine cycle by providing THF one carbon donors for the biosynthesis of methionine and the methyl donor S-adenosylmethionine (Grundy & Henkin, 2001). In *C. elegans* and higher organisms these 1CM metabolites maintain the methyl pool for numerous biological pathways (Locasale, 2013). Several methylation and de-methylation enzymes and mutations to the methionine cycle in *C. elegans* have been implicate in regulation of longevity coupling 1CM to the ageing process (Greer et al., 2010; Jin et al., 2011; Y. J. Liu et al., 2019; Merkwirth et al., 2016).

The bacterial exometabolome changes reported in chapter 5 do not directly correlate with the data reported in these prior studies as the metabolomic data is from *C. elegans* not agar or bacteria. Attenuated methionine uptake observed in glycine free media and attenuation of glycine uptake seen in DM agar containing glycine and supplemented with SMX, may correlate with the reported relationship between 1CM and ageing in *C. elegans*. In both instances it may indicate an accumulation in the bacteria that may confer a supplementary effect to the worm (discussed in chapter 5.3.9) that is independent of bacterial or host folate status as reported by Virk et al. (2016). In the case of methionine, the mechanism of action may differ as previously discussed in section 5.3.10 due do to the effect being independent of SMX (and glycine uptake attenuation discussed in section 5.3.9). This suggests DR is the likely mechanism and does not correlate with the work reported here.

As described in section 5.3.10 in chapter 5 of this thesis further work would need to repeat the no-glycine healthspan assay with the WTK bacterial strain used in this work. Additional manual lifespan assays would also provide evidence of robust reproducibility to demonstrate the accuracy of worm motility correlating with ageing. Together they will determine if the observed changes are a product of an alteration to the bacterial amino acid metabolome or a product of biological variability amongst the worm population. In addition, investigation of both the *C. elegans* and *E. coli* endometabolome may reveal if an accumulation of individual amino acids are occurring and if they correlate with an extended lifespan phenotype.

## 6.3 Sulfamethoxazole, bacterial toxicity and host health

This thesis set out to uncover the mechanism by which SMX treated *E. coli* increased the lifespan of *C. elegans*. It was hypothesised that WTK *E. coli* shortens the lifespan of *C. elegans* by a chronic low level toxicity. It was also hypothesised that treatment with SMX at a concentration that alters bacterial biochemistry without effecting growth (sub-mic), removes a toxicity extending lifespan. This thesis did not reveal evidence of an underlying folate dependant toxicity. It did show through the use of a novel LC-MS/MS protocol that bacterial amino acid metabolism is significantly altered. It also demonstrated the current lifespan protocol for investigating *C. elegans* ageing using DM is not optimised for bacterial growth with SMX. Optimisation of growth would be needed to conduct an accurate LC-MS/MS analysis of the metabolome.

It is hypothesised here that SMX beneficially alters the nutrient profile of bacteria to reflect a pro-health metabolome for the host. This may include an increase in the availability of amino acids, a reduction in ROS and biosynthesis of antioxidant metabolites. Evidence supporting a link between SMX and metabolites that promote host health has been reported by H. B. Park et al. (2020). The study found sub-inhibitory concentrations (200 μg/ml) of SMX upregulated a previously undiscovered group of metabolites named colipterins. The colipterins were found to have antioxidant properties that promoted immunological activity in human tissues, upregulated the anti-inflammatory cytokine interleukin-10 and improved the symptoms of colitis in mice (H. B. Park et al., 2020). Investigating how sub-mic concentrations of SMX modulate bacterial metabolism may increase understanding of the changes conferred, and how that translates to ageing in higher organisms. This may identify novel metabolites and novel metabolic pathways that can be targeted to alleviate disease states. In addition, SMX investigations would need to include the wider folate synthesising bacterial community.

By exploring the effect of SMX on the complex environment of the gut microbiota in higher organisms' therapies maybe derived. These novel therapeutic interventions could be developed to specifically target gut bacteria without directly effecting host physiology.

# Appendix A:

## Supplementary Amino acid data for LC-MS/MS repeats

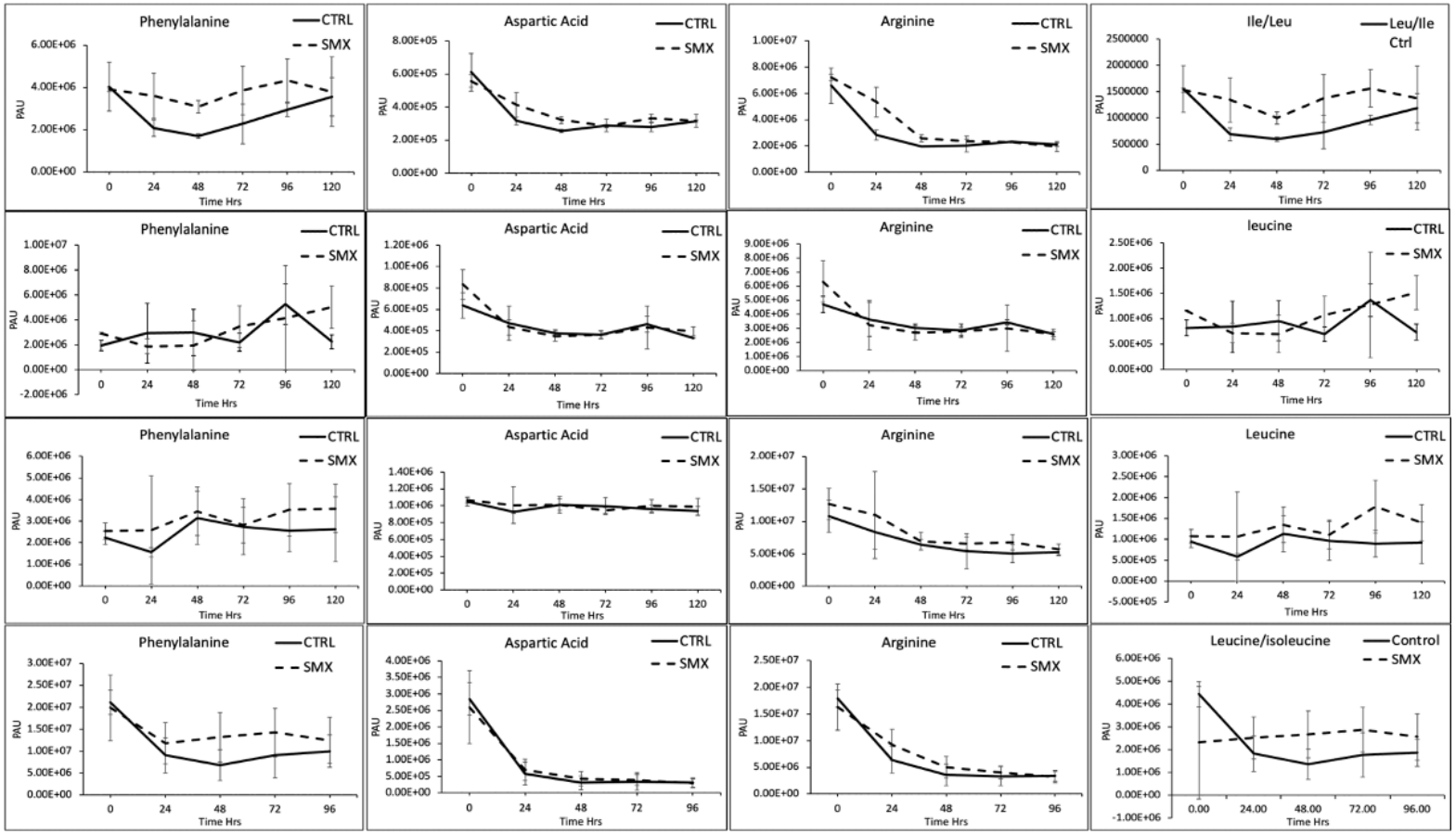

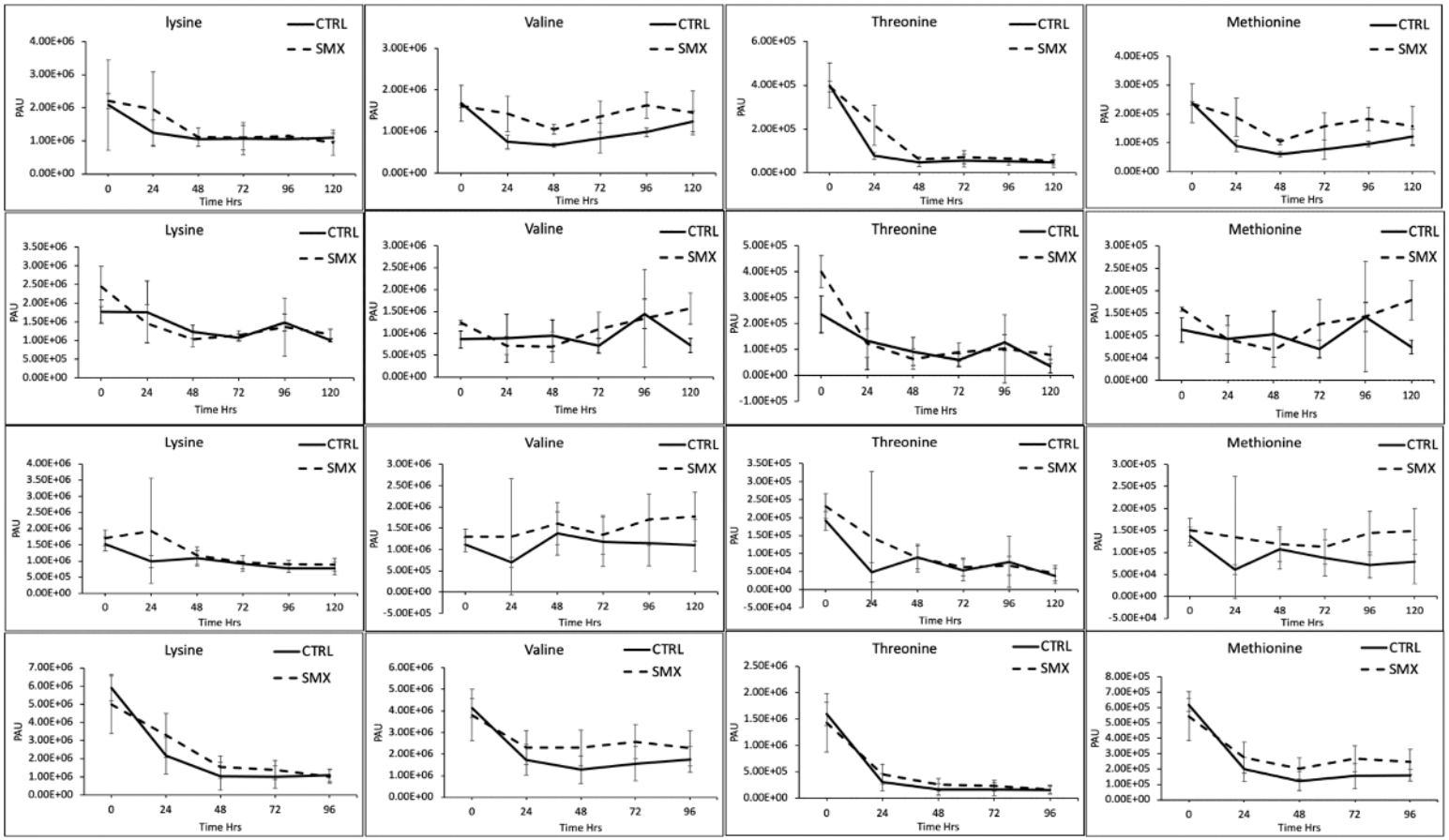
lysine
Valine
Threonine
Methionine
Lysine
Valine
Threonine
Methionine
Lysine
Valine
Threonine
Methionine
Lysine
Valine
Threonine
Methionine
CTRL
SMX
PAU
Time Hrs

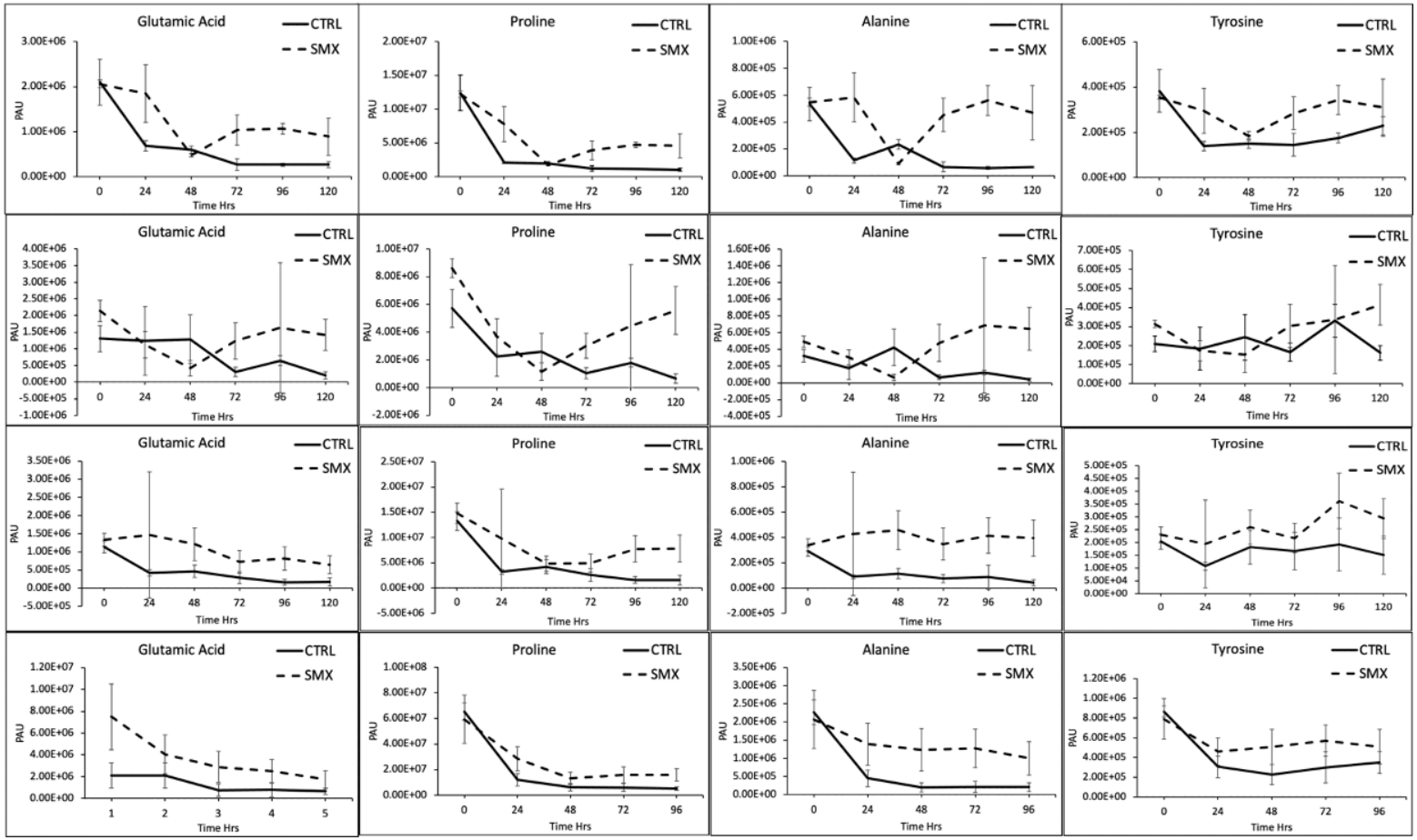
Glutamic Acid
Proline
Alanine
Tyrosine
CTRL
SMX
PAU
Time Hrs

# References


Aballay, A., & Ausubel, F. M. (2001). Programmed cell death mediated by ced-3 and ced-4 protects Caenorhabditis elegans from Salmonella typhimurium-mediated killing. *Proceedings of the National Academy of Sciences, 98*(5), 2735-2739.

Adams, J. B., Johansen, L. J., Powell, L. D., Quig, D., & Rubin, R. A. (2011). Gastrointestinal flora and gastrointestinal status in children with autism–comparisons to typical children and correlation with autism severity. *BMC gastroenterology, 11*(1), 1-13.

Agus, A., Planchais, J., & Sokol, H. (2018). Gut microbiota regulation of tryptophan metabolism in health and disease. *Cell host & microbe, 23*(6), 716-724.

Akashi, H., & Gojobori, T. (2002). Metabolic efficiency and amino acid composition in the proteomes of Escherichia coli and Bacillus subtilis. *Proceedings of the National Academy of Sciences, 99*(6), 3695-3700.

Aledo, J. C. (2019). Methionine in proteins: The Cinderella of the proteinogenic amino acids. *Protein Science, 28*(10), 1785-1796.

Alkhalaf, L. M., & Ryan, K. S. (2015). Biosynthetic manipulation of tryptophan in bacteria: pathways and mechanisms. *Chemistry & biology, 22*(3), 317-328.

Allison, C., & Hughes, C. (1991). Bacterial swarming: an example of prokaryotic differentiation and multicellular behaviour. *Science Progress (1933- ), 75*(3/4 (298)), 403-422. Retrieved from http://www.jstor.org/stable/43421281

Allocati, N., Masulli, M., Di Ilio, C., & De Laurenzi, V. (2015). Die for the community: an overview of programmed cell death in bacteria. *Cell death & disease, 6*(1), e1609-e1609.

Alvarez, Y., Glotfelty, L. G., Blank, N., Dohnalová, L., & Thaiss, C. A. (2020). The microbiome as a circadian coordinator of metabolism. *Endocrinology, 161*(6), bqaa059.

Ambagaspitiye, S., Sudarshan, S., Hogins, J., McDill, P., De Nisco, N. J., Zimmern, P. E., & Reitzer, L. (2019). Fimbriae and flagella mediated surface motility and the effect of glucose on nonpathogenic and uropathogenic Escherichia coli. *Biorxiv*, 840991.

An, R., Wilms, E., Masclee, A. A., Smidt, H., Zoetendal, E. G., & Jonkers, D. (2018). Age-dependent changes in GI physiology and microbiota: time to reconsider? *Gut, 67*(12), 2213-2222.

Andrews, A. E., Lawley, B., & Pittard, A. J. (1991). Mutational analysis of repression and activation of the tyrP gene in Escherichia coli. *J Bacteriol, 173*(16), 5068-5078. doi:10.1128/jb.173.16.5068-5078.1991

Angier, R. B., Stokstad, E., Mowat, J. H., Hutchings, B. L., Boothe, J. H., Waller, C. W., . . . Fahrenbach, M. (1948). Synthesis of pteroylglutamic acid. III. *Journal of the American Chemical Society, 70*(1), 25-26.

Annibal, A., Tharyan, R. G., Schonewolff, M. F., Tam, H., Latza, C., Auler, M. M. K., . . . Antebi, A. (2021). Regulation of the one carbon folate cycle as a shared metabolic signature of longevity. *Nature communications, 12*(1), 1-14.

Antikainen, H., Driscoll, M., Haspel, G., & Dobrowolski, R. (2017). TOR-mediated regulation of metabolism in aging. *Aging cell, 16*(6), 1219-1233.

Aronson, J. K. (2015). *Meyler's side effects of drugs: the international encyclopedia of adverse drug reactions and interactions*: Elsevier.

Arpaia, N., Campbell, C., Fan, X., Dikiy, S., van der Veeken, J., deRoos, P., . . . Rudensky, A. Y. (2013). Metabolites produced by commensal bacteria promote peripheral regulatory T-cell generation. *Nature, 504*(7480), 451-455. doi:10.1038/nature12726

Baba, T., Ara, T., Hasegawa, M., Takai, Y., Okumura, Y., Baba, M., . . . Mori, H. (2006). Construction of Escherichia coli K-12 in-frame, single-gene knockout mutants: the Keio collection. *Molecular systems biology, 2*(1), 2006.0008.

Bachem, A., Makhlouf, C., Binger, K. J., de Souza, D. P., Tull, D., Hochheiser, K., . . . Kastenmüller, W. (2019). Microbiota-derived short-chain fatty acids promote the memory potential of antigen-activated CD8+ T cells. *Immunity, 51*(2), 285-297. e285.

Bachman, M. A., & Swanson, M. S. (2001). RpoS co-operates with other factors to induce Legionella pneumophila virulence in the stationary phase. *Molecular microbiology, 40*(5), 1201-1214.

Backes, C., Martinez-Martinez, D., & Cabreiro, F. (2021). C. elegans: A biosensor for host–microbe interactions. *Lab Animal, 50*(5), 127-135. doi:10.1038/s41684-021-00724-z

Badal, V. D., Vaccariello, E. D., Murray, E. R., Yu, K. E., Knight, R., Jeste, D. V., & Nguyen, T. T. (2020). The gut microbiome, aging, and longevity: a systematic review. *Nutrients, 12*(12), 3759.

Bae, H., Gurinovich, A., Malovini, A., Atzmon, G., Andersen, S. L., Villa, F., . . . Sebastiani, P. (2018). Effects of FOXO3 polymorphisms on survival to extreme longevity in four centenarian studies. *The Journals of Gerontology: Series A, 73*(11), 1439-1447.

Bai, Y., & Mansell, T. J. (2020). Production and Sensing of Butyrate in a Probiotic E. coli Strain. *International Journal of Molecular Sciences, 21*(10), 3615. Retrieved from https://www.mdpi.com/1422-0067/21/10/3615

Bailey, L. B., Stover, P. J., McNulty, H., Fenech, M. F., Gregory, J. F., III, Mills, J. L., . . . Raiten, D. J. (2015). Biomarkers of Nutrition for Development—Folate Review. *The Journal of nutrition, 145*(7), 1636S-1680S. doi:10.3945/jn.114.206599

Barber, T. M., Kabisch, S., Pfeiffer, A. F. H., & Weickert, M. O. (2020). The Health Benefits of Dietary Fibre. *Nutrients, 12*(10), 3209. Retrieved from https://www.mdpi.com/2072-6643/12/10/3209

Barcik, W., Wawrzyniak, M., Akdis, C. A., & O'Mahony, L. (2017). Immune regulation by histamine and histamine-secreting bacteria. *Current opinion in immunology, 48*, 108-113.

Barnhart, M. M., & Chapman, M. R. (2006). Curli Biogenesis and Function. *Annual Review of Microbiology, 60*(1), 131-147. doi:10.1146/annurev.micro.60.080805.142106

Battesti, A., & Bouveret, E. (2009). Bacteria possessing two RelA/SpoT-like proteins have evolved a specific stringent response involving the acyl carrier protein-SpoT interaction. *Journal of bacteriology, 191*(2), 616-624.

Battesti, A., Majdalani, N., & Gottesman, S. (2011). The RpoS-mediated general stress response in Escherichia coli. *Annual Review of Microbiology, 65*, 189-213.

Baugh, C., Krumdieck, C., Baker, H., & Butterworth, C. (1971). Studies on the absorption and metabolism of folic acid: I. Folate absorption in the dog after exposure of isolated intestinal segments to synthetic pteroylpolyglutamates of various chain lengths. *The Journal of clinical investigation, 50*(10), 2009-2021.

Bayne-Jones, S. (1936). The effect of carbohydrates on bacterial growth and development of infection. *Bulletin of the New York Academy of Medicine, 12*(5), 278.

Beanan, M. J., & Strome, S. (1992). Characterization of a germ-line proliferation mutation in C. elegans. *Development, 116*(3), 755-766.

Bennett, B. D., Kimball, E. H., Gao, M., Osterhout, R., Van Dien, S. J., & Rabinowitz, J. D. (2009). Absolute metabolite concentrations and implied enzyme active site occupancy in Escherichia coli. *Nature chemical biology, 5*(8), 593-599. doi:10.1038/nchembio.186

Berg, M., Stenuit, B., Ho, J., Wang, A., Parke, C., Knight, M., . . . Shapira, M. (2016). Assembly of the Caenorhabditis elegans gut microbiota from diverse soil microbial environments. *The ISME journal, 10*(8), 1998-2009.

Bhatt, A. P., Redinbo, M. R., & Bultman, S. J. (2017). The role of the microbiome in cancer development and therapy. *CA: a cancer journal for clinicians, 67*(4), 326-344.

Bhattacharya, T., Ghosh, T. S., & Mande, S. S. (2015). Global profiling of carbohydrate active enzymes in human gut microbiome. *PloS one, 10*(11), e0142038.

Biotechnology, G. (2021). 20 mg/ml X-Gal Stock Solution. Retrieved from https://www.goldbio.com/uploads/documents/c81e12c041a332624122ee0f8acf42c2.pdf

Bishehsari, F., Engen, P. A., Preite, N. Z., Tuncil, Y. E., Naqib, A., Shaikh, M., . . . Hamaker, B. R. (2018). Dietary fiber treatment corrects the composition of gut microbiota, promotes SCFA production, and suppresses colon carcinogenesis. *Genes, 9*(2), 102.

Blackwell, T. K., Steinbaugh, M. J., Hourihan, J. M., Ewald, C. Y., & Isik, M. (2015). SKN-1/Nrf, stress responses, and aging in Caenorhabditis elegans. *Free radical biology and medicine, 88*, 290-301.

Blakely, R. L. (1987). Nomenclature and symbols for folic acid and related compounds: recommendations 1986. *European journal of biochemistry, 168*(2), 251-253.

Blander, J. M., Longman, R. S., Iliev, I. D., Sonnenberg, G. F., & Artis, D. (2017). Regulation of inflammation by microbiota interactions with the host. *Nature immunology, 18*(8), 851-860.

Blaser, M. J., & Dominguez-Bello, M. G. (2016). The human microbiome before birth. *Cell host & microbe, 20*(5), 558-560.

Blüher, M., Kahn, B. B., & Kahn, C. R. (2003). Extended longevity in mice lacking the insulin receptor in adipose tissue. *Science, 299*(5606), 572-574.

Bolten, C. J., Kiefer, P., Letisse, F., Portais, J.-C., & Wittmann, C. (2007). Sampling for metabolome analysis of microorganisms. *Analytical Chemistry, 79*(10), 3843-3849.

Booth, I. R., Kleppang, K. E., & Kempsell, K. E. (1989). A genetic locus for the GltII-glutamate transport system in Escherichia coli. *J Gen Microbiol, 135*(10), 2767-2774. doi:10.1099/00221287-135-10-2767

Bordag, N., Janakiraman, V., Nachtigall, J., González Maldonado, S., Bethan, B., Laine, J.-P., & Fux, E. (2016). Fast filtration of bacterial or mammalian suspension cell cultures for optimal metabolomics results. *PloS one, 11*(7), e0159389.

Bourne, C. R. (2014). Utility of the biosynthetic folate pathway for targets in antimicrobial discovery. *Antibiotics, 3*(1), 1-28.

Bowden, N. A., Sanders, J. P., & Bruins, M. E. (2018). Solubility of the proteinogenic α-amino acids in water, ethanol, and ethanol–water mixtures. *Journal of Chemical & Engineering Data, 63*(3), 488-497.

Braniste, V., Al-Asmakh, M., Kowal, C., Anuar, F., Abbaspour, A., Tóth, M., . . . Kundu, P. (2014). The gut microbiota influences blood-brain barrier permeability in mice. *Science translational medicine, 6*(263), 263ra158-263ra158.

Brenner, S. (1974). The genetics of Caenorhabditis elegans. *Genetics, 77*(1), 71-94.

Brind, J., Malloy, V., Augie, I., Caliendo, N., Vogelman, J. H., Zimmerman, J. A., & Orentreich, N. (2011). Dietary glycine supplementation mimics lifespan extension by dietary methionine restriction in Fisher 344 rats. In: Wiley Online Library.

Brito, I. L. (2021). The comings and goings of the healthy human gut microbiota. *Cell host & microbe, 29*(7), 1163-1164.

Brown, J. P., Davidson, G. E., & Scott, J. M. (1974). The identification of the forms of folate found in the liver, kidney and intestine of the monkey and their biosynthesis from exogenous pteroylglutamate (folic acid). *Biochimica et Biophysica Acta (BBA)-General Subjects, 343*(1), 78-88.

Brown, K. D. (1970). Formation of Aromatic Amino Acid Pools in Escherichia coli K-12. *Journal of bacteriology, 104*(1), 177-188. doi:doi:10.1128/jb.104.1.177-188.1970

Browning, D. F., Wells, T. J., França, F. L., Morris, F. C., Sevastsyanovich, Y. R., Bryant, J. A., . . . Hobman, J. L. (2013). Laboratory adapted E scherichia coli K-12 becomes a pathogen of C aenorhabditis elegans upon restoration of O antigen biosynthesis. *Molecular microbiology, 87*(5), 939-950.

Burchall, J. J. (1973). Mechanism of action of trimethoprim-sulfamethoxazole—II. *Journal of Infectious Diseases, 128*(Supplement_3), S437-S441.

Burgos-Barragan, G., Wit, N., Meiser, J., Dingler, F. A., Pietzke, M., Mulderrig, L., . . . Cordell, R. L. (2017). Mammals divert endogenous genotoxic formaldehyde into one-carbon metabolism. *Nature, 548*(7669), 549-554.

Burokas, A., Arboleya, S., Moloney, R. D., Peterson, V. L., Murphy, K., Clarke, G., . . . Cryan, J. F. (2017). Targeting the microbiota-gut-brain axis: prebiotics have anxiolytic and antidepressant-like effects and reverse the impact of chronic stress in mice. *Biological psychiatry, 82*(7), 472-487.

Bussiere, D. E., Xie, L., Srinivas, H., Shu, W., Burke, A., Be, C., . . . Karki, R. G. (2020). Structural basis of indisulam-mediated RBM39 recruitment to DCAF15 E3 ligase complex. *Nature chemical biology, 16*(1), 15-23.

Cabreiro, F., Au, C., Leung, K.-Y., Vergara-Irigaray, N., Cochemé, H. M., Noori, T., . . . Gems, D. (2013). Metformin retards aging in C. elegans by altering microbial folate and methionine metabolism. *Cell, 153*(1), 228-239.

Cabreiro, F., & Gems, D. (2013). Worms need microbes too: microbiota, health and aging in Caenorhabditis elegans. *EMBO molecular medicine, 5*(9), 1300-1310.

Calvo, J. M., & Matthews, R. G. (1994). The leucine-responsive regulatory protein, a global regulator of metabolism in Escherichia coli. *Microbiol Rev, 58*(3), 466-490. doi:10.1128/mr.58.3.466-490.1994

Camakaris, H., & Pittard, J. (1982). Autoregulation of the tyrR gene. *Journal of bacteriology, 150*(1), 70-75.

Canfield, C.-A., & Bradshaw, P. C. (2019). Amino acids in the regulation of aging and aging-related diseases. *Translational Medicine of Aging, 3*, 70-89.

Canfora, E. E., van der Beek, C. M., Jocken, J. W., Goossens, G. H., Holst, J. J., Damink, S. W. O., . . . Blaak, E. E. (2017). Colonic infusions of short-chain fatty acid mixtures promote energy metabolism in overweight/obese men: a randomized crossover trial. *Scientific Reports, 7*(1), 1-12.

Cani, P. D. (2018). Human gut microbiome: hopes, threats and promises. *Gut, 67*(9), 1716-1725.

Cantin, L. (2010). An Experimental Primer on High-Performance Liquid Chromatography (HPLC).

Carter, E. L., Jager, L., Gardner, L., Hall, C. C., Willis, S., & Green, J. M. (2007). Escherichia coli abg genes enable uptake and cleavage of the folate catabolite p-aminobenzoyl-glutamate. *Journal of bacteriology, 189*(9), 3329-3334.

Castanie-Cornet, M.-P., Penfound, T. A., Smith, D., Elliott, J. F., & Foster, J. W. (1999). Control of Acid Resistance inEscherichia coli. *Journal of bacteriology, 181*(11), 3525-3535. doi:doi:10.1128/JB.181.11.3525-3535.1999

Catterson, J. H., Khericha, M., Dyson, M. C., Vincent, A. J., Callard, R., Haveron, S. M., . . . Partridge, L. (2018). Short-term, intermittent fasting induces long-lasting gut health and TOR-independent lifespan extension. *Current biology, 28*(11), 1714-1724. e1714.

Chang, A. J., Chronis, N., Karow, D. S., Marletta, M. A., & Bargmann, C. I. (2006). A distributed chemosensory circuit for oxygen preference in C. elegans. *PLoS biology, 4*(9), e274.

Chang, D. E., Smalley, D. J., & Conway, T. (2002). Gene expression profiling of Escherichia coli growth transitions: an expanded stringent response model. *Molecular microbiology, 45*(2), 289-306.

Chanotiya, C., Pragadhessh, V., & Uniyal, G. (2013). Avoiding interferences and contaminants using Eppendorf Safe-Lock Tubes in mass spectrometry studies of natural products. *Eppendorf Application Note, 282*.

Charlier, D., & Glansdorff, N. (2004). Biosynthesis of arginine and polyamines. *EcoSal Plus, 1*(1).

Chen, M.-m., Li, A.-l., Sun, M.-c., Feng, Z., Meng, X.-c., & Wang, Y. (2014). Optimization of the quenching method for metabolomics analysis of Lactobacillus bulgaricus. *Journal of Zhejiang University SCIENCE B, 15*(4), 333-342.

Chen, N. H., Djoko, K. Y., Veyrier, F. J., & McEwan, A. G. (2016). Formaldehyde stress responses in bacterial pathogens. *Frontiers in microbiology, 7*, 257.

Cherbut, C., Ferrier, L., Rozé, C., Anini, Y., Blottière, H., Lecannu, G., & Galmiche, J.-P. (1998). Short-chain fatty acids modify colonic motility through nerves and polypeptide YY release in the rat. *American Journal of Physiology-Gastrointestinal and Liver Physiology, 275*(6), G1415-G1422.

Chevalier, A. C., & Rosenberger, T. A. (2017). Increasing acetyl-coa metabolism attenuates injury and alters spinal cord lipid content in mice subjected to experimental autoimmune encephalomyelitis. *Journal of neurochemistry, 141*(5), 721-737.

Chiang, C.-J., Lin, Y.-L., Hu, M.-C., & Chao, Y.-P. (2021). Understanding and harnessing the glutamate metabolism in Escherichia coli. *Journal of the Taiwan Institute of Chemical Engineers, 121*, 115-121.

Cho, B.-K., Federowicz, S., Park, Y.-S., Zengler, K., & Palsson, B. Ø. (2012). Deciphering the transcriptional regulatory logic of amino acid metabolism. *Nature chemical biology, 8*(1), 65-71. doi:10.1038/nchembio.710

Choi, H., Cho, S. C., Ha, Y. W., Ocampo, B., Park, S., Chen, S., . . . Kaeberlein, M. (2019). DDS promotes longevity through a microbiome-mediated starvation signal. *Translational Medicine of Aging, 3*, 64-69. doi:https://doi.org/10.1016/j.tma.2019.07.001

Choi, H. S., Bhat, A., Howington, M. B., Schaller, M. L., Cox, R., Huang, S., . . . Mecano, J. (2021). FMO rewires metabolism to promote longevity through tryptophan and one carbon metabolism. *Biorxiv*.

Chung, H., Bang, W., & Drake, M. (2006). Stress response of Escherichia coli. *Comprehensive reviews in food science and food safety, 5*(3), 52-64.

Claesson, M. J., Jeffery, I. B., Conde, S., Power, S. E., O'connor, E. M., Cusack, S., . . . O'Sullivan, O. (2012). Gut microbiota composition correlates with diet and health in the elderly. *Nature, 488*(7410), 178-184.

Clancy, D. J., Gems, D., Harshman, L. G., Oldham, S., Stocker, H., Hafen, E., . . . Partridge, L. (2001). Extension of life-span by loss of CHICO, a Drosophila insulin receptor substrate protein. *Science, 292*(5514), 104-106.

Claret, L., & Hughes, C. (2002). Interaction of the atypical prokaryotic transcription activator FlhD2C2 with early promoters of the flagellar gene hierarchy. *Journal of molecular biology, 321*(2), 185-199.

Clark, R. I., & Walker, D. W. (2018). Role of gut microbiota in aging-related health decline: insights from invertebrate models. *Cellular and Molecular Life Sciences, 75*(1), 93-101. doi:10.1007/s00018-017-2671-1

Clausznitzer, D., Oleksiuk, O., Løvdok, L., Sourjik, V., & Endres, R. G. (2010). Chemotactic response and adaptation dynamics in Escherichia coli. *PLoS computational biology, 6*(5), e1000784.

Colin, R., & Sourjik, V. (2017). Emergent properties of bacterial chemotaxis pathway. *Current opinion in microbiology, 39*, 24-33.

Connor, E. E. (1998). Sulfonamide antibiotics. *Primary care update for ob/gyns, 5*(1), 32-35.

Cosgriff, A. J., Brasier, G., Pi, J., Dogovski, C., Sarsero, J. P., & Pittard, A. J. (2000). A study of AroP-PheP chimeric proteins and identification of a residue involved in tryptophan transport. *J Bacteriol, 182*(8), 2207-2217. doi:10.1128/jb.182.8.2207-2217.2000

Crider, K. S., Yang, T. P., Berry, R. J., & Bailey, L. B. (2012). Folate and DNA methylation: a review of molecular mechanisms and the evidence for folate's role. *Advances in nutrition, 3*(1), 21-38.

Crittenden, R., Martinez, N., & Playne, M. (2003). Synthesis and utilisation of folate by yoghurt starter cultures and probiotic bacteria. *International journal of food microbiology, 80*(3), 217-222.

Cryan, J. F., O'Riordan, K. J., Cowan, C. S., Sandhu, K. V., Bastiaanssen, T. F., Boehme, M., . . . Golubeva, A. V. (2019). The microbiota-gut-brain axis. *Physiological reviews*.

Csonka, L. N., & Leisinger, T. (2007). Biosynthesis of Proline. *EcoSal Plus, 2*(2). doi:10.1128/ecosalplus.3.6.1.4

Cummings, J., & Macfarlane, G. (1991). The control and consequences of bacterial fermentation in the human colon. *Journal of Applied Bacteriology, 70*(6), 443-459.

Cummings, J. H., Pomare, E. W., Branch, W. J., Naylor, C. P., & Macfarlane, G. T. (1987). Short chain fatty acids in human large intestine, portal, hepatic and venous blood. *Gut, 28*(10), 1221. doi:10.1136/gut.28.10.1221

Dall, K. B., & Færgeman, N. J. (2019). Metabolic regulation of lifespan from a C. elegans perspective. *Genes & Nutrition, 14*(1), 1-12.

Dawadi, S., Kordus, S. L., Baughn, A. D., & Aldrich, C. C. (2017). Synthesis and analysis of bacterial folate metabolism intermediates and antifolates. *Organic letters, 19*(19), 5220-5223.

De Biase, D., & Lund, P. A. (2015). The Escherichia coli acid stress response and its significance for pathogenesis. *Advances in applied microbiology, 92*, 49-88.

De Vadder, F., Kovatcheva-Datchary, P., Goncalves, D., Vinera, J., Zitoun, C., Duchampt, A., . . . Mithieux, G. (2014). Microbiota-generated metabolites promote metabolic benefits via gut-brain neural circuits. *Cell, 156*(1-2), 84-96.

DeJong, E. N., Surette, M. G., & Bowdish, D. M. (2020). The gut microbiota and unhealthy aging: disentangling cause from consequence. *Cell host & microbe, 28*(2), 180-189.

Del Campo, C. P., Garde-Cerdán, T., Sánchez, A. M., Maggi, L., Carmona, M., & Alonso, G. L. (2009). Determination of free amino acids and ammonium ion in saffron (Crocus sativus L.) from different geographical origins. *Food Chemistry, 114*(4), 1542-1548.

Demir, E., Yaman, Y. I., Basaran, M., & Kocabas, A. (2020). Dynamics of pattern formation and emergence of swarming in Caenorhabditis elegans. *Elife, 9*, e52781.

Den Besten, G., Van Eunen, K., Groen, A. K., Venema, K., Reijngoud, D.-J., & Bakker, B. M. (2013). The role of short-chain fatty acids in the interplay between diet, gut microbiota, and host energy metabolism. *Journal of lipid research, 54*(9), 2325-2340.

Denby, K., Iwig, J., Westwood, B., Rolfe, J., Sedelnikova, M., Svetlana, E., . . . Green, J. (2016). The mechanism of a formaldehyde-sensing transcriptional regulator. *Scientific Reports, 6*(1), 38879. doi:10.1038/srep38879

Denby, K. J., Iwig, J., Bisson, C., Westwood, J., Rolfe, M. D., Sedelnikova, S. E., . . . Chivers, P. T. (2016). The mechanism of a formaldehyde-sensing transcriptional regulator. *Scientific Reports, 6*(1), 1-15.

Deng, F.-L., Pan, J.-X., Zheng, P., Xia, J.-J., Yin, B.-M., Liang, W.-W., . . . Wu, Q.-Y. (2019). Metabonomics reveals peripheral and central short-chain fatty acid and amino acid dysfunction in a naturally occurring depressive model of macaques. *Neuropsychiatric disease and treatment, 15*, 1077.

Denko, C., Grundy, W., Wheeler, N., Henderson, C., Berryman, G., Friedemann, T., & Youmans, J. (1946). The excretion of B-complex vitamins by normal adults on a restricted intake. *Arch. Biochem., 11*, 109-117.

DeRisi, J. L., Iyer, V. R., & Brown, P. O. (1997). Exploring the metabolic and genetic control of gene expression on a genomic scale. *Science, 278*(5338), 680-686.

Desai, M. S., Seekatz, A. M., Koropatkin, N. M., Kamada, N., Hickey, C. A., Wolter, M., . . . Muller, A. (2016). A dietary fiber-deprived gut microbiota degrades the colonic mucus barrier and enhances pathogen susceptibility. *Cell, 167*(5), 1339-1353. e1321.

Devlin, A. S., Marcobal, A., Dodd, D., Nayfach, S., Plummer, N., Meyer, T., . . . Fischbach, M. A. (2016). Modulation of a circulating uremic solute via rational genetic manipulation of the gut microbiota. *Cell host & microbe, 20*(6), 709-715.

Di Lorenzo, F., De Castro, C., Silipo, A., & Molinaro, A. (2019). Lipopolysaccharide structures of Gram-negative populations in the gut microbiota and effects on host interactions. *FEMS microbiology reviews, 43*(3), 257-272.

Diaz Ricci, J. C., & Hernández, M. E. (2000). Plasmid effects on Escherichia coli metabolism. *Critical reviews in biotechnology, 20*(2), 79-108.

Diez-Gonzalez, F., Bond, D. R., Jennings, E., & Russell, J. B. (1999). Alternative schemes of butyrate production in Butyrivibrio fibrisolvens and their relationship to acetate utilization, lactate production, and phylogeny. *Archives of Microbiology, 171*(5), 324-330. doi:10.1007/s002030050717

Diez-Gonzalez, F., & Karaibrahimoglu, Y. (2004). Comparison of the glutamate-, arginine-and lysine-dependent acid resistance systems in Escherichia coli O157: H7. *Journal of applied microbiology, 96*(6), 1237-1244.

Dingler, F. A., Wang, M., Mu, A., Millington, C. L., Oberbeck, N., Watcham, S., . . . Nadler, C. (2020). Two aldehyde clearance systems are essential to prevent lethal formaldehyde accumulation in mice and humans. *Molecular cell, 80*(6), 996-1012. e1019.

Dirksen, P., Marsh, S. A., Braker, I., Heitland, N., Wagner, S., Nakad, R., . . . Rosenstiel, P. (2016). The native microbiome of the nematode Caenorhabditis elegans: gateway to a new host-microbiome model. *BMC Biology, 14*(1), 1-16.

Domagk, G. (1957). TWENTY-FIVE YEARS OF SULFONAMIDE THERAPY. *Annals of the New York Academy of Sciences, 69*(3), 380-384.

Donaldson, G. P., Lee, S. M., & Mazmanian, S. K. (2016). Gut biogeography of the bacterial microbiota. *Nature Reviews Microbiology, 14*(1), 20-32.

Dong, T., Coombes, B. K., & Schellhorn, H. E. (2009). Role of RpoS in the virulence of Citrobacter rodentium. *Infection and immunity, 77*(1), 501-507.

Dong, T., Kirchhof, M. G., & Schellhorn, H. E. (2008). RpoS regulation of gene expression during exponential growth of Escherichia coli K12. *Molecular Genetics and Genomics, 279*(3), 267-277.

Douglas, A. E. (2020). The microbial exometabolome: ecological resource and architect of microbial communities. *Philosophical Transactions of the Royal Society B, 375*(1798), 20190250.

Ducker, G. S., & Rabinowitz, J. D. (2017). One-carbon metabolism in health and disease. *Cell metabolism, 25*(1), 27-42.

Dudzik, D., Barbas-Bernardos, C., García, A., & Barbas, C. (2018). Quality assurance procedures for mass spectrometry untargeted metabolomics. a review. *Journal of pharmaceutical and biomedical analysis, 147*, 149-173.

Durfee, T., Hansen, A.-M., Zhi, H., Blattner, F. R., & Jin, D. J. (2008). Transcription profiling of the stringent response in Escherichia coli. *Journal of bacteriology, 190*(3), 1084-1096.

Edwards, C., Canfield, J., Copes, N., Brito, A., Rehan, M., Lipps, D., . . . Bradshaw, P. C. (2015). Mechanisms of amino acid-mediated lifespan extension in Caenorhabditis elegans. *BMC Genet, 16*(1), 8. doi:10.1186/s12863-015-0167-2

Egan, M. G., Sirlin, S., Rumberger, B. G., Garrow, T. A., Shane, B., & Sirotnak, F. M. (1995). Rapid Decline in Folylpolyglutamate Synthetase Activity and Gene Expression during Maturation of HL-60 Cells: Nature OF THE EFFECT, IMPACT ON FOLATE COMPOUND POLYGLUTAMATE POOLS, AND EVIDENCE FOR PROGRAMMED DOWN-REGULATION DURING MATURATION (∗). *Journal of biological chemistry, 270*(10), 5462-5468.

El Kaoutari, A., Armougom, F., Gordon, J. I., Raoult, D., & Henrissat, B. (2013). The abundance and variety of carbohydrate-active enzymes in the human gut microbiota. *Nat Rev Microbiol, 11*(7), 497-504. doi:10.1038/nrmicro3050

Eliopoulos, G. M., & Huovinen, P. (2001). Resistance to Trimethoprim-Sulfamethoxazole. *Clinical Infectious Diseases, 32*(11), 1608-1614. doi:10.1086/320532

Fei, N., & Zhao, L. (2013). *An opportunistic pathogen isolated from the gut of an obese human causes obesity in germfree mice*.

Félix, M.-A., & Braendle, C. (2010). The natural history of Caenorhabditis elegans. *Current biology, 20*(22), R965-R969.

Félix, M.-A., & Duveau, F. (2012). Population dynamics and habitat sharing of natural populations of Caenorhabditis elegans and C. briggsae. *BMC Biology, 10*(1), 1-19.

Ferla, M. P., & Patrick, W. M. (2014). Bacterial methionine biosynthesis. *Microbiology (Reading), 160*(Pt 8), 1571-1584. doi:10.1099/mic.0.077826-0

Ferone, R. (1977). Folate metabolism in malaria. *Bull World Health Organ, 55*(2-3), 291-298.

Ferreira, J. L., Gao, F. Z., Rossmann, F. M., Nans, A., Brenzinger, S., Hosseini, R., . . . Rosenthal, P. B. (2019). γ-proteobacteria eject their polar flagella under nutrient depletion, retaining flagellar motor relic structures. *PLoS biology, 17*(3), e3000165.

Flint, H. J., Scott, K. P., Louis, P., & Duncan, S. H. (2012). The role of the gut microbiota in nutrition and health. *Nature reviews Gastroenterology & hepatology, 9*(10), 577-589. doi:10.1038/nrgastro.2012.156

Frank, L., & Ranhand, B. (1964). PROLINE METABOLISM IN ESCHERICHIA COLI. 3. THE PROLINE CATABOLIC PATHWAY. *Arch Biochem Biophys, 107*, 325-331. doi:10.1016/0003-9861(64)90338-8

Franklin, F. C., & Venables, W. A. (1976). Biochemical, genetic, and regulatory studies of alanine catabolism in Escherichia coli K12. *Mol Gen Genet, 149*(2), 229-237. doi:10.1007/bf00332894

Fraser, G. M., & Hughes, C. (1999). Swarming motility. *Current opinion in microbiology, 2*(6), 630-635.

Fraser, J., & Newman, E. (1975). Derivation of glycine from threonine in Escherichia coli K-12 mutants. *Journal of bacteriology, 122*(3), 810-817.

Freilich, S., Zarecki, R., Eilam, O., Segal, E. S., Henry, C. S., Kupiec, M., . . . Ruppin, E. (2011). Competitive and cooperative metabolic interactions in bacterial communities. *Nature communications, 2*(1), 1-7.

Friedman, D. B., & Johnson, T. E. (1988). A mutation in the age-1 gene in Caenorhabditis elegans lengthens life and reduces hermaphrodite fertility. *Genetics, 118*(1), 75-86.

Fukuda, S., Toh, H., Hase, K., Oshima, K., Nakanishi, Y., Yoshimura, K., . . . Ohno, H. (2011). Bifidobacteria can protect from enteropathogenic infection through production of acetate. *Nature, 469*(7331), 543-547. doi:10.1038/nature09646

Furey, A., Moriarty, M., Bane, V., Kinsella, B., & Lehane, M. (2013). Ion suppression; a critical review on causes, evaluation, prevention and applications. *Talanta, 115*, 104-122.

Gamon, L. F., Guo, C., He, J., Hägglund, P., Hawkins, C. L., & Davies, M. J. (2020). Absolute quantitative analysis of intact and oxidized amino acids by LC-MS without prior derivatization. *Redox biology, 36*, 101586.

Gao, A. W., Chatzispyrou, I. A., Kamble, R., Liu, Y. J., Herzog, K., Smith, R. L., . . . Luyf, A. C. (2017). A sensitive mass spectrometry platform identifies metabolic changes of life history traits in C. elegans. *Scientific Reports, 7*(1), 1-14.

Gao, C., Cao, T., Martin, R., Keenan, M., Greenway, F., Finley, J., . . . Zheng, J. (2014). Butyrate increased lifespan in C. elegans (1025.13). *The FASEB Journal, 28*, 1025.1013.

Gao, P., & Xu, G. (2015). Mass-spectrometry-based microbial metabolomics: recent developments and applications. *Analytical and bioanalytical chemistry, 407*(3), 669-680.

Gao, Z., Yin, J., Zhang, J., Ward, R. E., Martin, R. J., Lefevre, M., . . . Ye, J. (2009). Butyrate improves insulin sensitivity and increases energy expenditure in mice. *Diabetes, 58*(7), 1509-1517.

Garigan, D., Hsu, A.-L., Fraser, A. G., Kamath, R. S., Ahringer, J., & Kenyon, C. (2002). Genetic analysis of tissue aging in Caenorhabditis elegans: a role for heat-shock factor and bacterial proliferation. *Genetics, 161*(3), 1101-1112.

Gaudier, E., Jarry, A., Blottiere, H., de Coppet, P., Buisine, M., Aubert, J., . . . Hoebler, C. (2004). Butyrate specifically modulates MUC gene expression in intestinal epithelial goblet cells deprived of glucose. *American Journal of Physiology-Gastrointestinal and Liver Physiology, 287*(6), G1168-G1174.

Gelino, S., Chang, J. T., Kumsta, C., She, X., Davis, A., Nguyen, C., . . . Hansen, M. (2016). Intestinal autophagy improves healthspan and longevity in C. elegans during dietary restriction. *PLoS genetics, 12*(7), e1006135.

Gems, D., & Riddle, D. L. (2000). Genetic, behavioral and environmental determinants of male longevity in Caenorhabditis elegans. *Genetics, 154*(4), 1597-1610.

Gentry, D. R., & Cashel, M. (1996). Mutational analysis of the Escherichia coli spoT gene identifies distinct but overlapping regions involved in ppGpp synthesis and degradation. *Molecular microbiology, 19*(6), 1373-1384.

Ghrist, A. C., & Stauffer, G. V. (1995). The Escherichia coli glycine transport system and its role in the regulation of the glycine cleavage enzyme system. *Microbiology, 141*(1), 133-140. doi:https://doi.org/10.1099/00221287-141-1-133

Gilbert, J. A., Blaser, M. J., Caporaso, J. G., Jansson, J. K., Lynch, S. V., & Knight, R. (2018). Current understanding of the human microbiome. *Nature medicine, 24*(4), 392-400.

Goesele, M. (2004). *New acquisition techniques for real objects and light sources in computer graphics*: Books on Demand.

Goldstein, B. (2016). Sydney Brenner on the Genetics of Caenorhabditis elegans. *Genetics, 204*(1), 1-2.

Gomes, C. C., & Preto, S. (2015). Blue light: A blessing or a curse? *Procedia Manufacturing, 3*, 4472-4479.

Gomez, F., Monsalve, G. C., Tse, V., Saiki, R., Weng, E., Lee, L., . . . Clarke, C. F. (2012). Delayed accumulation of intestinal coliform bacteria enhances life span and stress resistance in Caenorhabditis elegans fed respiratory deficient E. coli. *BMC Microbiol, 12*, 300. doi:10.1186/1471-2180-12-300

Gómez-Gómez, J.-M., Manfredi, C., Alonso, J.-C., & Blázquez, J. (2007). A novel role for RecA under non-stress: promotion of swarming motility in Escherichia coli K-12. *BMC Biology, 5*(1), 1-15.

Gonzalez, C. F., Proudfoot, M., Brown, G., Korniyenko, Y., Mori, H., Savchenko, A. V., & Yakunin, A. F. (2006). Molecular basis of formaldehyde detoxification: characterization of two S-formylglutathione hydrolases from Escherichia coli, FrmB and YeiG. *Journal of biological chemistry, 281*(20), 14514-14522.

Gottesman, S. (2019). Trouble is coming: Signaling pathways that regulate general stress responses in bacteria. *J Biol Chem, 294*(31), 11685-11700. doi:10.1074/jbc.REV119.005593

Gray, J. M., Karow, D. S., Lu, H., Chang, A. J., Chang, J. S., Ellis, R. E., . . . Bargmann, C. I. (2004). Oxygen sensation and social feeding mediated by a C. elegans guanylate cyclase homologue. *Nature, 430*(6997), 317-322. doi:10.1038/nature02714

Green, J. M., & Matthews, R. G. (2007). Folate Biosynthesis, Reduction, and Polyglutamylation and the Interconversion of Folate Derivatives. *EcoSal Plus, 2*(2). doi:10.1128/ecosalplus.3.6.3.6

Greer, E. L., & Brunet, A. (2009). Different dietary restriction regimens extend lifespan by both independent and overlapping genetic pathways in C. elegans. *Aging cell, 8*(2), 113-127.

Greer, E. L., Maures, T. J., Hauswirth, A. G., Green, E. M., Leeman, D. S., Maro, G. S., . . . Brunet, A. (2010). Members of the H3K4 trimethylation complex regulate lifespan in a germline-dependent manner in C. elegans. *Nature, 466*(7304), 383-387.

Gruber, J., & Kennedy, B. K. (2017). Microbiome and longevity: gut microbes send signals to host mitochondria. *Cell, 169*(7), 1168-1169.

Grundy, F. J., & Henkin, T. M. (2001). Synthesis of serine, glycine, cysteine, and methionine. *Bacillus subtilis and its closest relatives: From genes to cells*, 245-254.

Grzeskowiak, R., & Eppendorf, A. Extractables and Leachables in Microcentrifuge Tubes–Extensive HPLC/GC/MS Analysis.

Gude, S., Pinçe, E., Taute, K. M., Seinen, A.-B., Shimizu, T. S., & Tans, S. J. (2020). Bacterial coexistence driven by motility and spatial competition. *Nature, 578*(7796), 588-592.

Guide, T. R. (2019). Technical Reference Guide: Peptones, Supplements, and Feeds. Retrieved from https://assets.thermofisher.com/TFS-Assets/BPD/brochures/peptones-supplements-feeds-technical-reference-guide.pdf

Gurr, E. (2012). *Synthetic dyes in biology, medicine and chemistry*: Elsevier.

Gusarov, I., Gautier, L., Smolentseva, O., Shamovsky, I., Eremina, S., Mironov, A., & Nudler, E. (2013). Bacterial nitric oxide extends the lifespan of C. elegans. *Cell, 152*(4), 818-830.

Hackmann, C. (1958). Possibility of influencing signs of age in experimental animals by oral administration of compounds of 2-(p-aminobenzenesulphonamido)-pyrimidine. *Munchener Medizinische Wochenschrift, 100*, 1814-1817.

Han, B., Sivaramakrishnan, P., Lin, C.-C. J., Neve, I. A., He, J., Tay, L. W. R., . . . Wang, J. (2017). Microbial genetic composition tunes host longevity. *Cell, 169*(7), 1249-1262. e1213.

Haney, S. A., Platko, J. V., Oxender, D. L., & Calvo, J. M. (1992). Lrp, a leucine-responsive protein, regulates branched-chain amino acid transport genes in Escherichia coli. *J Bacteriol, 174*(1), 108-115. doi:10.1128/jb.174.1.108-115.1992

Hansen, M., Chandra, A., Mitic, L. L., Onken, B., Driscoll, M., & Kenyon, C. (2008). A role for autophagy in the extension of lifespan by dietary restriction in C. elegans. *PLoS genetics, 4*(2), e24.

Harshey, R. M. (2003). Bacterial motility on a surface: many ways to a common goal. *Annual Reviews in Microbiology, 57*(1), 249-273.

Hartsough, L. A., Park, M., Kotlajich, M. V., Lazar, J. T., Han, B., Lin, C.-C. J., . . . Tabor, J. J. (2020). Optogenetic control of gut bacterial metabolism to promote longevity. *Elife, 9*, e56849.

Heiss, C. N., & Olofsson, L. E. (2018). Gut microbiota-dependent modulation of energy metabolism. *Journal of innate immunity, 10*(3), 163-171.

Helliwell, N. (2013). *The interaction between C. elegans and E. coli and how it influences ageing.* (Masters by Research). Durham University,

Herndon, L. A. (2012a). Anatomy of an adult haemaphrodite. In. https://www.wormatlas.org/hermaphrodite/introduction/Introframeset.html.

Herndon, L. A. (2012b). Life cycle of *C. elegans* at 25 degrees centigrade. In. https://www.wormatlas.org/hermaphrodite/introduction/Introframeset.html.

Hetzel, M., Brock, M., Selmer, T., Pierik, A. J., Golding, B. T., & Buckel, W. (2003). Acryloyl-CoA reductase from Clostridium propionicum: An enzyme complex of propionyl-CoA dehydrogenase and electron-transferring flavoprotein. *European journal of biochemistry, 270*(5), 902-910.

Hitchings, G. H. (1973). Mechanism of action of trimethoprim-sulfamethoxazole—I. *Journal of Infectious Diseases, 128*(Supplement_3), S433-S436.

Ho, L., Ono, K., Tsuji, M., Mazzola, P., Singh, R., & Pasinetti, G. M. (2018). Protective roles of intestinal microbiota derived short chain fatty acids in Alzheimer's disease-type beta-amyloid neuropathological mechanisms. *Expert review of neurotherapeutics, 18*(1), 83-90.

Hondorp, E. R., Matthews, R. G., & Stewart, V. (2006). Methionine. *EcoSal Plus, 2*(1). doi:doi:10.1128/ecosalplus.3.6.1.7

Hopkinson, R. J., & Schofield, C. J. (2018). Deciphering functions of intracellular formaldehyde: linking cancer and aldehyde metabolism. In: ACS Publications.

Hosono, R., Nishimoto, S., & Kuno, S. (1989). Alterations of life span in the nematode Caenorhabditis elegans under monoxenic culture conditions. *Experimental gerontology, 24*(3), 251-264.

Hosseini, E., Grootaert, C., Verstraete, W., & Van de Wiele, T. (2011). Propionate as a health-promoting microbial metabolite in the human gut. *Nutrition reviews, 69*(5), 245-258.

Hounoum, B. M., Blasco, H., Emond, P., & Mavel, S. (2016). Liquid chromatography–high-resolution mass spectrometry-based cell metabolomics: Experimental design, recommendations, and applications. *TrAC Trends in Analytical Chemistry, 75*, 118-128.

How, Z. T., Busetti, F., Linge, K. L., Kristiana, I., Joll, C. A., & Charrois, J. W. (2014). Analysis of free amino acids in natural waters by liquid chromatography–tandem mass spectrometry. *Journal of Chromatography A, 1370*, 135-146.

Hussein, M. J., Green, J. M., & Nichols, B. P. (1998). Characterization of mutations that allow p-aminobenzoyl-glutamate utilization by Escherichia coli. *Journal of bacteriology, 180*(23), 6260-6268.

Hutchings, B., Bohonos, N., Hegsted, D. M., Elvehjem, C., & Peterson, W. (1941). Relation of a growth factor required by Lactobacillus casei a to the nutrition of the chick. *Journal of biological chemistry, 140*, 681-682.

Hutchings, M. I., Truman, A. W., & Wilkinson, B. (2019). Antibiotics: past, present and future. *Current opinion in microbiology, 51*, 72-80.

Inoue, T., Shingaki, R., Hirose, S., Waki, K., Mori, H., & Fukui, K. (2007). Genome-wide screening of genes required for swarming motility in Escherichia coli K-12. *Journal of bacteriology, 189*(3), 950-957.

Iriarte, M., Stainier, I., & Cornelis, G. R. (1995). The rpoS gene from Yersinia enterocolitica and its influence on expression of virulence factors. *Infection and immunity, 63*(5), 1840-1847.

Ito, A., May, T., Kawata, K., & Okabe, S. (2008). Significance of rpoS during maturation of Escherichia coli biofilms. *Biotechnology and Bioengineering, 99*(6), 1462-1471.

Ito, D., Kawamura, H., Oikawa, A., Ihara, Y., Shibata, T., Nakamura, N., . . . Masuda, S. (2020). ppGpp functions as an alarmone in metazoa. *Communications biology, 3*(1), 1-11.

Ito, M., Baba, T., Mori, H., & Mori, H. (2005). Functional analysis of 1440 Escherichia coli genes using the combination of knock-out library and phenotype microarrays. *Metabolic Engineering, 7*(4), 318-327. doi:https://doi.org/10.1016/j.ymben.2005.06.004

Itzkowitz, S. H., & Harpaz, N. (2004). Diagnosis and management of dysplasia in patients with inflammatory bowel diseases. *Gastroenterology, 126*(6), 1634-1648.

Jägerstad, M., & Jastrebova, J. (2014). 5, 10-Methylene-tetrahydrofolate dissociates into tetrahydrofolate and formaldehyde at physiological pH and acidic pH, typical conditions used during sample extraction and LC-MS/MS analysis of biological samples. *Biomedical Chromatography, 28*(7), 1041-1042.

Jandhyala, S. M., Talukdar, R., Subramanyam, C., Vuyyuru, H., Sasikala, M., & Nageshwar Reddy, D. (2015). Role of the normal gut microbiota. *World journal of gastroenterology, 21*(29), 8787-8803. doi:10.3748/wjg.v21.i29.8787

Jin, C., Li, J., Green, C. D., Yu, X., Tang, X., Han, D., . . . Cao, X. (2011). Histone demethylase UTX-1 regulates C. elegans life span by targeting the insulin/IGF-1 signaling pathway. *Cell metabolism, 14*(2), 161-172.

Johansson, M. E., Sjövall, H., & Hansson, G. C. (2013). The gastrointestinal mucus system in health and disease. *Nature reviews Gastroenterology & hepatology, 10*(6), 352-361.

Juers, D. H., Matthews, B. W., & Huber, R. E. (2012). LacZ β-galactosidase: structure and function of an enzyme of historical and molecular biological importance. *Protein Sci, 21*(12), 1792-1807. doi:10.1002/pro.2165

Jukes, T., & Stokstad, E. (1948). Pteroylglutamic acid and related compounds. *Physiological reviews, 28*(1), 51-106.

Kadaba, N. S., Kaiser, J. T., Johnson, E., Lee, A., & Rees, D. C. (2008). The high-affinity E. coli methionine ABC transporter: structure and allosteric regulation. *Science, 321*(5886), 250-253. doi:10.1126/science.1157987

Kadner, R. J. (1974). Transport systems for L-methionine in Escherichia coli. *J Bacteriol, 117*(1), 232-241. doi:10.1128/jb.117.1.232-241.1974

Kadner, R. J. (1975). Regulation of methionine transport activity in Escherichia coli. *Journal of bacteriology, 122*(1), 110-119.

Kadner, R. J. (1977). Transport and utilization of D-methionine and other methionine sources in Escherichia coli. *Journal of bacteriology, 129*(1), 207-216. doi:doi:10.1128/jb.129.1.207-216.1977

Kaeberlein, T. L., Smith, E. D., Tsuchiya, M., Welton, K. L., Thomas, J. H., Fields, S., . . . Kaeberlein, M. (2006). Lifespan extension in Caenorhabditis elegans by complete removal of food. *Aging cell, 5*(6), 487-494.

Kailasam, S. (2021). LC-MS – What Is LC-MS, LC-MS Analysis and LC-MS/MS. Retrieved from https://www.technologynetworks.com/analysis/articles/lc-ms-what-is-lc-ms-lc-ms-analysis-and-lc-msms-348238

Kaletta, T., & Hengartner, M. O. (2006). Finding function in novel targets: C. elegans as a model organism. *Nature reviews Drug discovery, 5*(5), 387-399.

Kandasamy, V., Vaidyanathan, H., Djurdjevic, I., Jayamani, E., Ramachandran, K. B., Buckel, W., . . . Ramalingam, S. (2013). Engineering Escherichia coli with acrylate pathway genes for propionic acid synthesis and its impact on mixed-acid fermentation. *Applied Microbiology and Biotechnology, 97*(3), 1191-1200. doi:10.1007/s00253-012-4274-y

Kang, C., & Avery, L. (2009). Systemic regulation of starvation response in Caenorhabditis elegans. *Genes & development, 23*(1), 12-17.

Kapahi, P., Chen, D., Rogers, A. N., Katewa, S. D., Li, P. W.-L., Thomas, E. L., & Kockel, L. (2010). With TOR, less is more: a key role for the conserved nutrient-sensing TOR pathway in aging. *Cell metabolism, 11*(6), 453-465.

Kapahi, P., Zid, B. M., Harper, T., Koslover, D., Sapin, V., & Benzer, S. (2004). Regulation of lifespan in Drosophila by modulation of genes in the TOR signaling pathway. *Current biology, 14*(10), 885-890.

Katritzky, A. R., & Narindoshvili, T. (2009). Fluorescent amino acids: advances in protein-extrinsic fluorophores. *Organic & biomolecular chemistry, 7*(4), 627-634.

KEGG. (2021). KEGG Pathway Database

Wiring diagrams of molecular interactions, reactions and relations. Retrieved from https://www.genome.jp/kegg/brite.html

Kelly, E. E., Fischer, A. M., & Collins, C. H. (2021). Drawing up a collaborative contract: Amino acid cross-feeding between interspecies bacterial pairs. *Biotechnology and Bioengineering, 118*(8), 3138-3149.

Kennedy, B. K. (2018). Ageing and the microbiome: An avenue for intervention. *Old Herborn University Seminar Monograph*(32), 25-31.

Kenyon, C., Chang, J., Gensch, E., Rudner, A., & Tabtiang, R. (1993). A C. elegans mutant that lives twice as long as wild type. *Nature, 366*(6454), 461-464.

Kenyon, C. J. (2010). The genetics of ageing. *Nature, 464*(7288), 504-512.

Keseler, I. M., Gama-Castro, S., Mackie, A., Billington, R., Billington, R., Caspi, R., Kothari, A., Krummenacker, M., Midford, P., Muñiz-Rascado, L., Ong, W., Paley, S., Santos-Zavaleta, A., Subhraveti, P., Tierrafria, V., Wolfe, A., Collado-Vides, J., Paulsen, I., and Karp, P.D., . (2021). The EcoCyc database in 2021 Escherichia coli K-12. Retrieved from https://ecocyc.org

Kim, S. K., Lund, J., Kiraly, M., Duke, K., Jiang, M., Stuart, J. M., . . . Davidson, G. S. (2001). A gene expression map for Caenorhabditis elegans. *Science, 293*(5537), 2087-2092.

Kim, T. H., Yang, J., Darling, P. B., & O'Connor, D. L. (2004). A Large Pool of Available Folate Exists in the Large Intestine of Human Infants and Piglets. *The Journal of nutrition, 134*(6), 1389-1394. doi:10.1093/jn/134.6.1389

Kim, Y.-M., Ogawa, W., Tamai, E., Kuroda, T., Mizushima, T., & Tsuchiya, T. (2002). Purification, Reconstitution, and Characterization of Na+/Serine Symporter, SstT,

of Escherichia coli1. *The Journal of Biochemistry, 132*(1), 71-76. doi:10.1093/oxfordjournals.jbchem.a003201

Kirkpatrick, C., Maurer, L. M., Oyelakin, N. E., Yoncheva, Y. N., Maurer, R., & Slonczewski, J. L. (2001). Acetate and formate stress: opposite responses in the proteome of Escherichia coli. *Journal of bacteriology, 183*(21), 6466-6477.

Kirkwood, T. B. (2005). Understanding the odd science of aging. *Cell, 120*(4), 437-447.

Kirkwood, T. B., & Finch, C. E. (2002). The old worm turns more slowly. *Nature, 419*(6909), 794-795.

Klass, M. R. (1977). Aging in the nematode Caenorhabditis elegans: major biological and environmental factors influencing life span. *Mechanisms of ageing and development, 6*, 413-429.

Klass, M. R. (1983). A method for the isolation of longevity mutants in the nematode Caenorhabditis elegans and initial results. *Mechanisms of ageing and development, 22*(3-4), 279-286.

Klipstein, F. A. (1967). Intestinal folate conjugase activity in tropical sprue. *The American journal of clinical nutrition, 20*(9), 1004-1009.

Knorr, S., Sinn, M., Galetskiy, D., Williams, R. M., Wang, C., Müller, N., . . . Hartig, J. S. (2018). Widespread bacterial lysine degradation proceeding via glutarate and L-2-hydroxyglutarate. *Nature communications, 9*(1), 5071-5071. doi:10.1038/s41467-018-07563-6

Kobayashi, J. (2018). Effect of diet and gut environment on the gastrointestinal formation of N-nitroso compounds: a review. *Nitric Oxide, 73*, 66-73.

Koch, A. L. (1999). Diffusion through agar blocks of finite dimensions: a theoretical analysis of three systems of practical significance in microbiology. *Microbiology, 145*(3), 643-654.

Koh, A., De Vadder, F., Kovatcheva-Datchary, P., & Bäckhed, F. (2016). From dietary fiber to host physiology: short-chain fatty acids as key bacterial metabolites. *Cell, 165*(6), 1332-1345.

Koh, A., Molinaro, A., Ståhlman, M., Khan, M. T., Schmidt, C., Mannerås-Holm, L., . . . Olofsson, L. E. (2018). Microbially produced imidazole propionate impairs insulin signaling through mTORC1. *Cell, 175*(4), 947-961. e917.

Kolter, R., Siegele, D. A., & Tormo, A. (1993). The stationary phase of the bacterial life cycle. *Annual Review of Microbiology, 47*(1), 855-874.

Koyanagi, T., Katayama, T., Suzuki, H., & Kumagai, H. (2004). Identification of the LIV-I/LS system as the third phenylalanine transporter in Escherichia coli K-12. *J Bacteriol, 186*(2), 343-350. doi:10.1128/jb.186.2.343-350.2004

Krautkramer, K. A., Fan, J., & Bäckhed, F. (2021). Gut microbial metabolites as multi-kingdom intermediates. *Nature Reviews Microbiology, 19*(2), 77-94.

Kriner, M. A., & Subramaniam, A. R. (2020). The serine transporter SdaC prevents cell lysis upon glucose depletion in Escherichia coli. *Microbiologyopen, 9*(2), e960.

Kroemer, G., Mariño, G., & Levine, B. (2010). Autophagy and the integrated stress response. *Molecular cell, 40*(2), 280-293.

Kroner, G. M., Wolfe, M. B., Freddolino, P. L., & DiRita, V. J. (2019). Escherichia coli Lrp Regulates One-Third of the Genome via Direct, Cooperative, and Indirect Routes. *Journal of bacteriology, 201*(3), e00411-00418. doi:doi:10.1128/JB.00411-18

Kumar, S., Egan, B. M., Kocsisova, Z., Schneider, D. L., Murphy, J. T., Diwan, A., & Kornfeld, K. (2019). Lifespan Extension in C. elegans Caused by Bacterial Colonization of the Intestine and Subsequent Activation of an Innate Immune Response. *Dev Cell, 49*(1), 100-117.e106. doi:10.1016/j.devcel.2019.03.010

Kumar, T., & Verma, K. (2010). A Theory Based on Conversion of RGB image to Gray image. *International Journal of Computer Applications, 7*(2), 7-10.

Kundu, P., Blacher, E., Elinav, E., & Pettersson, S. (2017). Our gut microbiome: the evolving inner self. *Cell, 171*(7), 1481-1493.

Kwon, Y. K., Higgins, M. B., & Rabinowitz, J. D. (2010). Antifolate-induced depletion of intracellular glycine and purines inhibits thymineless death in E. coli. *ACS Chem Biol, 5*(8), 787-795. doi:10.1021/cb100096f

Kwon, Y. K., Higgins, M. B., & Rabinowitz, J. D. (2010). Antifolate-induced depletion of intracellular glycine and purines inhibits thymineless death in E. coli. *ACS Chemical Biology, 5*(8), 787-795.

Lacour, S., & Landini, P. (2004). σ<sup>S</sup>-Dependent Gene Expression at the Onset of Stationary Phase in Escherichia coli: Function of σ<sup>S</sup>-Dependent Genes and Identification of Their Promoter Sequences. *Journal of bacteriology, 186*(21), 7186-7195. doi:doi:10.1128/JB.186.21.7186-7195.2004

Lane, M. C., Simms, A. N., & Mobley, H. L. (2007). Complex interplay between type 1 fimbrial expression and flagellum-mediated motility of uropathogenic Escherichia coli. *Journal of bacteriology, 189*(15), 5523-5533.

Lapierre, L. R., & Hansen, M. (2012). Lessons from C. elegans: signaling pathways for longevity. *Trends Endocrinol Metab, 23*(12), 637-644. doi:10.1016/j.tem.2012.07.007

laRossa, R. (2015). Escherichia coli K-12 substr. MG1655 Pathway: superpathway of branched chain amino acid biosynthesis.

Larsen, P. E., & Dai, Y. (2015). Metabolome of human gut microbiome is predictive of host dysbiosis. *Gigascience, 4*(1), s13742-13015-10084-13743.

Larsen, P. L., & Clarke, C. F. (2002). Extension of life-span in Caenorhabditis elegans by a diet lacking coenzyme Q. *Science, 295*(5552), 120-123.

Lascelles, J., & Woods, D. (1952). The synthesis of "folic acid" by Bacterium coli and Staphylococcus aureus and its inhibition by sulphonamides. *British journal of experimental pathology, 33*(3), 288.

Le Couteur, D. G., Solon-Biet, S. M., Cogger, V. C., Ribeiro, R., de Cabo, R., Raubenheimer, D., . . . Simpson, S. J. (2020). Branched chain amino acids, aging and age-related health. *Ageing research reviews, 64*, 101198. doi:https://doi.org/10.1016/j.arr.2020.101198

LeBlanc, J. G., Milani, C., De Giori, G. S., Sesma, F., Van Sinderen, D., & Ventura, M. (2013). Bacteria as vitamin suppliers to their host: a gut microbiota perspective. *Current opinion in biotechnology, 24*(2), 160-168.

Lee, B. C., Kaya, A., Ma, S., Kim, G., Gerashchenko, M. V., Yim, S. H., . . . Gladyshev, V. N. (2014). Methionine restriction extends lifespan of Drosophila melanogaster under conditions of low amino-acid status. *Nature communications, 5*(1), 1-12.

Lee, G. D., Wilson, M. A., Zhu, M., Wolkow, C. A., De Cabo, R., Ingram, D. K., & Zou, S. (2006). Dietary deprivation extends lifespan in Caenorhabditis elegans. *Aging cell, 5*(6), 515-524.

Lee, K., & Mylonakis, E. (2017). An intestine-derived neuropeptide controls avoidance behavior in Caenorhabditis elegans. *Cell reports, 20*(10), 2501-2512.

Lenaerts, I., Walker, G. A., Van Hoorebeke, L., Gems, D., & Vanfleteren, J. R. (2008). Dietary restriction of Caenorhabditis elegans by axenic culture reflects nutritional requirement for constituents provided by metabolically active microbes. *The Journals of Gerontology Series A: Biological Sciences and Medical Sciences, 63*(3), 242-252.

Levy, M., Blacher, E., & Elinav, E. (2017). Microbiome, metabolites and host immunity. *Current opinion in microbiology, 35*, 8-15. doi:https://doi.org/10.1016/j.mib.2016.10.003

Li, W., Wu, X., Hu, X., Wang, T., Liang, S., Duan, Y., . . . Qin, B. (2017). Structural changes of gut microbiota in Parkinson's disease and its correlation with clinical features. *Science China Life Sciences, 60*(11), 1223-1233.

Limoli, D. H., Warren, E. A., Yarrington, K. D., Donegan, N. P., Cheung, A. L., & O'Toole, G. A. (2019). Interspecies interactions induce exploratory motility in Pseudomonas aeruginosa. *Elife, 8*, e47365.

Lin, H. V., Frassetto, A., Kowalik Jr, E. J., Nawrocki, A. R., Lu, M. M., Kosinski, J. R., . . . Forrest, G. (2012). Butyrate and propionate protect against diet-induced obesity and regulate gut hormones via free fatty acid receptor 3-independent mechanisms. *PloS one, 7*(4), e35240.

Link, H., Anselment, B., & Weuster-Botz, D. (2008). Leakage of adenylates during cold methanol/glycerol quenching of Escherichia coli. *Metabolomics, 4*(3), 240-247.

Liu, J. Q., Dairi, T., Itoh, N., Kataoka, M., Shimizu, S., & Yamada, H. (1998). Gene cloning, biochemical characterization and physiological role of a thermostable low-specificity L-threonine aldolase from Escherichia coli. *European journal of biochemistry, 255*(1), 220-226.

Liu, K., Bittner, A. N., & Wang, J. D. (2015). Diversity in (p) ppGpp metabolism and effectors. *Current opinion in microbiology, 24*, 72-79.

Liu, X., & Locasale, J. W. (2017). Metabolomics: a primer. *Trends in biochemical sciences, 42*(4), 274-284.

Liu, Y. J., Janssens, G. E., McIntyre, R. L., Molenaars, M., Kamble, R., Gao, A. W., . . . Houtkooper, R. H. (2019). Glycine promotes longevity in Caenorhabditis elegans in a methionine cycle-dependent fashion. *PLoS genetics, 15*(3), e1007633.

Locasale, J. W. (2013). Serine, glycine and one-carbon units: cancer metabolism in full circle. *Nature Reviews Cancer, 13*(8), 572-583.

Lodish, H., Berk, A., Zipursky, S. L., Matsudaira, P., Baltimore, D., & Darnell, J. (2000). DNA cloning with plasmid vectors. In *Molecular Cell Biology. 4th edition*: WH Freeman.

Louis, P., & Flint, H. J. (2017). Formation of propionate and butyrate by the human colonic microbiota. *Environmental microbiology, 19*(1), 29-41.

Lu, C.-D. (2006). Pathways and regulation of bacterial arginine metabolism and perspectives for obtaining arginine overproducing strains. *Applied Microbiology and Biotechnology, 70*(3), 261-272.

Lu, W., Su, X., Klein, M. S., Lewis, I. A., Fiehn, O., & Rabinowitz, J. D. (2017). Metabolite measurement: pitfalls to avoid and practices to follow. *Annual review of biochemistry, 86*, 277-304.

Luan, H., Wang, X., & Cai, Z. (2019). Mass spectrometry-based metabolomics: Targeting the crosstalk between gut microbiota and brain in neurodegenerative disorders. *Mass spectrometry reviews, 38*(1), 22-33.

Lubbe, A., Bowen, B. P., & Northen, T. (2017). Exometabolomic analysis of cross-feeding metabolites. *Metabolites, 7*(4), 50.

Lund, J., Tedesco, P., Duke, K., Wang, J., Kim, S. K., & Johnson, T. E. (2002). Transcriptional profile of aging in C. elegans. *Current biology, 12*(18), 1566-1573.

Mackie, A., Keseler, I. M., Nolan, L., Karp, P. D., & Paulsen, I. T. (2013). Dead end metabolites-defining the known unknowns of the E. coli metabolic network. *PloS one, 8*(9), e75210.

Maddocks, O. D., Athineos, D., Cheung, E. C., Lee, P., Zhang, T., van den Broek, N. J., . . . Kruiswijk, F. (2017). Modulating the therapeutic response of tumours to dietary serine and glycine starvation. *Nature, 544*(7650), 372-376.

Magnúsdóttir, S., Ravcheev, D., de Crécy-Lagard, V., & Thiele, I. (2015). Systematic genome assessment of B-vitamin biosynthesis suggests co-operation among gut microbes. *Frontiers in genetics, 6*, 148.

Magnusson, L. U., Farewell, A., & Nyström, T. (2005). ppGpp: a global regulator in Escherichia coli. *Trends in microbiology, 13*(5), 236-242.

Makki, K., Deehan, E. C., Walter, J., & Bäckhed, F. (2018). The impact of dietary fiber on gut microbiota in host health and disease. *Cell host & microbe, 23*(6), 705-715.

Mangiola, F., Nicoletti, A., Gasbarrini, A., & Ponziani, F. (2018). Gut microbiota and aging. *Eur Rev Med Pharmacol Sci, 22*(21), 7404-7413.

Mansfeld, J., Urban, N., Priebe, S., Groth, M., Frahm, C., Hartmann, N., . . . Schmeisser, S. (2015). Branched-chain amino acid catabolism is a conserved regulator of physiological ageing. *Nature communications, 6*(1), 1-12.

Marcus, M., & Halpern, Y. S. (1969). The metabolic pathway of glutamate in escherichia coli K-12. *Biochimica et Biophysica Acta (BBA) - General Subjects, 177*(2), 314-320. doi:https://doi.org/10.1016/0304-4165(69)90141-X

Marriott, B. P., Birt, D. F., Stalling, V. A., & Yates, A. A. (2020). *Present Knowledge in Nutrition: Basic Nutrition and Metabolism*: Academic Press.

Maser, A., Peebo, K., & Nahku, R. (2019). Avoiding amino acid depletion in a complex medium results in improved Escherichia coli BW25113 growth. *Microbiology, 165*(1), 37-46.

Maser, A., Peebo, K., Vilu, R., & Nahku, R. (2020). Amino acids are key substrates to Escherichia coli BW25113 for achieving high specific growth rate. *Research in microbiology, 171*(5-6), 185-193.

Mashego, M. R., Rumbold, K., De Mey, M., Vandamme, E., Soetaert, W., & Heijnen, J. J. (2007). Microbial metabolomics: past, present and future methodologies. *Biotechnology letters, 29*(1), 1-16.

Masters, P. A., O'Bryan, T. A., Zurlo, J., Miller, D. Q., & Joshi, N. (2003). Trimethoprim-sulfamethoxazole revisited. *Arch Intern Med, 163*(4), 402-410. doi:10.1001/archinte.163.4.402

Masters, P. A., O'Bryan, T. A., Zurlo, J., Miller, D. Q., & Joshi, N. (2003). Trimethoprim-sulfamethoxazole revisited. *Archives of internal medicine, 163*(4), 402-410.

Matin, A., Auger, E., Blum, P., & Schultz, J. (1989). Genetic basis of starvation survival in nondifferentiating bacteria. *Annual Review of Microbiology, 43*(1), 293-314.

Maynard, C. (2017). *Factors That Influence E. Coli Folate Synthesis And Their Impact on C. Elegans Ageing.* (PhD). Durham University,

Maynard, C., Cummins, I., Green, J., & Weinkove, D. (2018). A bacterial route for folic acid supplementation. *BMC Biology, 16*(1), 1-10.

Maynard, C., & Weinkove, D. (2020). Bacteria increase host micronutrient availability: mechanisms revealed by studies in C. elegans. *Genes & Nutrition, 15*(1), 4. doi:10.1186/s12263-020-00662-4

McGee, M. D., Weber, D., Day, N., Vitelli, C., Crippen, D., Herndon, L. A., . . . Melov, S. (2011). Loss of intestinal nuclei and intestinal integrity in aging C. elegans. *Aging cell, 10*(4), 699-710.

McMaster, M. C. (2005). *LC/MS: a practical user's guide*: John Wiley & Sons.

McNabney, S. M., & Henagan, T. M. (2017). Short chain fatty acids in the colon and peripheral tissues: a focus on butyrate, colon cancer, obesity and insulin resistance. *Nutrients, 9*(12), 1348.

Meisel, J. D., & Kim, D. H. (2014). Behavioral avoidance of pathogenic bacteria by Caenorhabditis elegans. *Trends in immunology, 35*(10), 465-470.

Mellies, J., Wise, A., & Villarejo, M. (1995). Two different Escherichia coli proP promoters respond to osmotic and growth phase signals. *Journal of bacteriology, 177*(1), 144-151. doi:doi:10.1128/jb.177.1.144-151.1995

Melo, J. A., & Ruvkun, G. (2012). Inactivation of conserved C. elegans genes engages pathogen-and xenobiotic-associated defenses. *Cell, 149*(2), 452-466.

Merkwirth, C., Jovaisaite, V., Durieux, J., Matilainen, O., Jordan, S. D., Quiros, P. M., . . . Tronnes, S. U. (2016). Two conserved histone demethylases regulate mitochondrial stress-induced longevity. *Cell, 165*(5), 1209-1223.

Mesibov, R., & Adler, J. (1972). Chemotaxis toward amino acids in Escherichia coli. *Journal of bacteriology, 112*(1), 315-326.

Miller, B., & Newman, E. (1974). Control of serine transhydroxymethylase synthesis in Escherichia coli K12. *Canadian journal of microbiology, 20*(1), 41-47.

Miller, R. A., Buehner, G., Chang, Y., Harper, J. M., Sigler, R., & Smith-Wheelock, M. (2005). Methionine-deficient diet extends mouse lifespan, slows immune and lens aging, alters glucose, T4, IGF-I and insulin levels, and increases hepatocyte MIF levels and stress resistance. *Aging cell, 4*(3), 119-125.

Mills, S., Stanton, C., Lane, J. A., Smith, G. J., & Ross, R. P. (2019). Precision nutrition and the microbiome, part I: Current state of the science. *Nutrients, 11*(4), 923.

Mischke, M., & Plösch, T. (2016). The gut microbiota and their metabolites: potential implications for the host epigenome. *Microbiota of the Human Body*, 33-44.

Mitchell, H. K., Snell, E. E., & Williams, R. J. (1941). The concentration of "folic acid". *Journal of the American Chemical Society, 63*(8), 2284-2284.

Mo, Y., Dang, L., & Wei, H. (2011). Solubility of α-form and β-form of l-glutamic acid in different aqueous solvent mixtures. *Fluid Phase Equilibria, 300*(1-2), 105-109.

Moldoveanu, S. C., Zhu, J., & Qian, N. (2015). Free amino acids analysis by liquid chromatography with tandem mass spectrometry in several botanicals with antioxidant character. *Journal of separation science, 38*(13), 2208-2222.

Monson, R., Foulds, I., Foweraker, J., Welch, M., & Salmond, G. P. (2011). The Pseudomonas aeruginosa generalized transducing phage φPA3 is a new member of the φKZ-like group of 'jumbo'phages, and infects model laboratory strains and clinical isolates from cystic fibrosis patients. *Microbiology, 157*(3), 859-867.

Morellato, A. E., Umansky, C., & Pontel, L. B. (2021). The toxic side of one-carbon metabolism and epigenetics. *Redox biology, 40*, 101850. doi:https://doi.org/10.1016/j.redox.2020.101850

Naderi, N., & House, J. D. (2018). Chapter Five - Recent Developments in Folate Nutrition. In N. A. M. Eskin (Ed.), *Advances in Food and Nutrition Research* (Vol. 83, pp. 195-213): Academic Press.

Nagpal, R., Mainali, R., Ahmadi, S., Wang, S., Singh, R., Kavanagh, K., . . . Yadav, H. (2018). Gut microbiome and aging: Physiological and mechanistic insights. *Nutrition and Healthy Aging, 4*, 267-285. doi:10.3233/NHA-170030

Naja, S., Makhlouf, M., & Chehab, M. A. H. (2017). An ageing world of the 21st century: a literature review. *Int J Community Med Public Health, 4*(12), 4363-4369.

Nakamura, S., & Yoshimori, T. (2018). Autophagy and longevity. *Molecules and cells, 41*(1), 65.

Nakao, T., Yamato, I., & Anraku, Y. (1988). Mapping of the multiple regulatory sites for putP and putA expression in the putC region of Escherichia coli. *Molecular and General Genetics MGG, 214*(3), 379-388. doi:10.1007/BF00330470

Nakayasu, E. S., Burnet, M. C., Walukiewicz, H. E., Wilkins, C. S., Shukla, A. K., Brooks, S., . . . Finkel, S. (2017). Ancient Regulatory Role of Lysine Acetylation in Central Metabolism. *mBio, 8*(6), e01894-01817. doi:doi:10.1128/mBio.01894-17

Navarro Llorens, J. M., Tormo, A., & Martínez-García, E. (2010). Stationary phase in gram-negative bacteria. *FEMS microbiology reviews, 34*(4), 476-495.

Nemkov, T., D'Alessandro, A., & Hansen, K. C. (2015). Three-minute method for amino acid analysis by UHPLC and high-resolution quadrupole orbitrap mass spectrometry. *Amino Acids, 47*(11), 2345-2357.

Nichols, B. P., Seibold, A. M., & Doktor, S. Z. (1989). para-aminobenzoate synthesis from chorismate occurs in two steps. *J Biol Chem, 264*(15), 8597-8601.

Nichols, R. J., Sen, S., Choo, Y. J., Beltrao, P., Zietek, M., Chaba, R., . . . Gross, C. A. (2011). Phenotypic Landscape of a Bacterial Cell. *Cell, 144*(1), 143-156. doi:https://doi.org/10.1016/j.cell.2010.11.052

Nowak, A., & Libudzisz, Z. (2006). Influence of phenol, p-cresol and indole on growth and survival of intestinal lactic acid bacteria. *Anaerobe, 12*(2), 80-84.

O'Hara, A. M., & Shanahan, F. (2006). The gut flora as a forgotten organ. *EMBO reports, 7*(7), 688-693.

O'Keefe, S. J., Ou, J., Aufreiter, S., O'Connor, D., Sharma, S., Sepulveda, J., . . . Mawhinney, T. (2009). Products of the colonic microbiota mediate the effects of diet on colon cancer risk. *The Journal of nutrition, 139*(11), 2044-2048.

O'Toole, G., Kaplan, H. B., & Kolter, R. (2000). Biofilm formation as microbial development. *Annual Reviews in Microbiology, 54*(1), 49-79.

Ohata, J., Bruemmer, K. J., & Chang, C. J. (2019). Activity-Based Sensing Methods for Monitoring the Reactive Carbon Species Carbon Monoxide and Formaldehyde in Living Systems. *Accounts of Chemical Research, 52*(10), 2841-2848. doi:10.1021/acs.accounts.9b00386

Oliphant, K., & Allen-Vercoe, E. (2019). Macronutrient metabolism by the human gut microbiome: major fermentation by-products and their impact on host health. *Microbiome, 7*(1), 91. doi:10.1186/s40168-019-0704-8

Onken, B., & Driscoll, M. (2010). Metformin induces a dietary restriction–like state and the oxidative stress response to extend C. elegans healthspan via AMPK, LKB1, and SKN-1. *PloS one, 5*(1), e8758.

Orentreich, N., Matias, J. R., DeFelice, A., & Zimmerman, J. A. (1993). Low methionine ingestion by rats extends life span. *The Journal of nutrition, 123*(2), 269-274.

P. Stoodley, K. Sauer, D. G. Davies, & Costerton, J. W. (2002). Biofilms as Complex Differentiated Communities. *Annual Review of Microbiology, 56*(1), 187-209. doi:10.1146/annurev.micro.56.012302.160705

Palecz, B., Piekarski, H., & Romanowski, S. (2000). Studies on homogeneous interactions between zwitterions of severall-α-amino acids in water at a temperature of 298.15 K. *Journal of Molecular Liquids, 84*(3), 279-288. doi:https://doi.org/10.1016/S0167-7322(99)00194-4

Parada Venegas, D., De la Fuente, M. K., Landskron, G., González, M. J., Quera, R., Dijkstra, G., . . . Hermoso, M. A. (2019). Short Chain Fatty Acids (SCFAs)-Mediated Gut Epithelial and Immune Regulation and Its Relevance for Inflammatory Bowel Diseases. *Frontiers in Immunology, 10*(277). doi:10.3389/fimmu.2019.00277

Park, C.-H., Park, C.-H., Lee, Y.-J., Lee, S.-Y., Oh, H.-B., & Lee, J.-W. (2011). Determination of the intracellular concentrations of metabolites in Escherichia coli collected during the exponential and stationary growth phases using liquid chromatography-mass spectrometry. *Bulletin of the Korean Chemical Society, 32*(2), 524-530.

Park, H. B., Wei, Z., Oh, J., Xu, H., Kim, C. S., Wang, R., . . . Crawford, J. M. (2020). Sulfamethoxazole drug stress upregulates antioxidant immunomodulatory metabolites in Escherichia coli. *Nature microbiology, 5*(11), 1319-1329.

Parker, D. J., Demetci, P., & Li, G.-W. (2019). Rapid accumulation of motility-activating mutations in resting liquid culture of Escherichia coli. *Journal of bacteriology, 201*(19), e00259-00219.

Parkinson, J. S., Hazelbauer, G. L., & Falke, J. J. (2015). Signaling and sensory adaptation in Escherichia coli chemoreceptors: 2015 update. *Trends in microbiology, 23*(5), 257-266.

Patejko, M., Jacyna, J., & Markuszewski, M. J. (2017). Sample preparation procedures utilized in microbial metabolomics: An overview. *Journal of Chromatography B, 1043*, 150-157.

Pefani, I. (2019). *Exploring how inhibition of bacterial folate synthesis increases lifespan in the C. elegans: E. coli aging model.* (BSc Biological Sciences). Durham University,

Perez, E. R., Knapp, J. A., Horn, C. K., Stillman, S. L., Evans, J. E., & Arfsten, D. P. (2016). Comparison of LC–MS-MS and GC–MS analysis of benzodiazepine compounds included in the drug demand reduction urinalysis program. *Journal of analytical toxicology, 40*(3), 201-207.

Petri, W. (2011). Sulfonamides, trimethoprim-sulfamethoxazole, quinolones, and agents for urinary tract infections. *Goodman & Gilman's The Pharmacological Basis of Therapeutics. 12th. New York: McGraw-Hill*, 1463-1476.

Pittard, J., Camakaris, H., & Yang, J. (2005). The TyrR regulon. *Mol Microbiol, 55*(1), 16-26. doi:10.1111/j.1365-2958.2004.04385.x

Pittard, J., & Yang, J. (2008). Biosynthesis of the aromatic amino acids. *EcoSal Plus, 3*(1).

Pittard, J., Yang, J., & Stewart, V. (2008). Biosynthesis of the Aromatic Amino Acids. *EcoSal Plus, 3*(1). doi:doi:10.1128/ecosalplus.3.6.1.8

Pizer, L. I. (1965). Glycine Synthesis and Metabolism in Escherichia coli. *Journal of bacteriology, 89*(4), 1145-1150. doi:doi:10.1128/jb.89.4.1145-1150.1965

Pizer, L. I. (1965). GLYCINE SYNTHESIS AND METABOLISM IN ESCHERICHIA COLI. *J Bacteriol, 89*(4), 1145-1150. doi:10.1128/jb.89.4.1145-1150.1965

Pletnev, P., Osterman, I., Sergiev, P., Bogdanov, A., & Dontsova, O. (2015). Survival guide: Escherichia coli in the stationary phase. *Acta Naturae (англоязычная версия), 7*(4 (27)).

Popkes, M., & Valenzano, D. R. (2020). Microbiota–host interactions shape ageing dynamics. *Philosophical Transactions of the Royal Society B, 375*(1808), 20190596.

Portal-Celhay, C., Bradley, E. R., & Blaser, M. J. (2012). Control of intestinal bacterial proliferation in regulation of lifespan in Caenorhabditis elegans. *BMC Microbiology, 12*(1), 49. doi:10.1186/1471-2180-12-49

Portman, D. S. (2006). Profiling C. elegans gene expression with DNA microarrays. *WormBook: The Online Review of C. elegans Biology [Internet]*.

Possemato, R., Marks, K. M., Shaul, Y. D., Pacold, M. E., Kim, D., Birsoy, K., . . . Jha, A. K. (2011). Functional genomics reveal that the serine synthesis pathway is essential in breast cancer. *Nature, 476*(7360), 346-350.

Pradhan, A. A., & Vera, J. H. (1998). Effect of acids and bases on the solubility of amino acids. *Fluid Phase Equilibria, 152*(1), 121-132.

Prüss, B., Nelms, J. M., Park, C., & Wolfe, A. J. (1994). Mutations in NADH: ubiquinone oxidoreductase of Escherichia coli affect growth on mixed amino acids. *Journal of bacteriology, 176*(8), 2143-2150.

Pryde, S. E., Duncan, S. H., Hold, G. L., Stewart, C. S., & Flint, H. J. (2002). The microbiology of butyrate formation in the human colon. *FEMS Microbiology Letters, 217*(2), 133-139. doi:10.1111/j.1574-6968.2002.tb11467.x

Pryor, R., Norvaisas, P., Marinos, G., Best, L., Thingholm, L. B., Quintaneiro, L. M., . . . Lujan, C. (2019). Host-microbe-drug-nutrient screen identifies bacterial effectors of metformin therapy. *Cell, 178*(6), 1299-1312. e1229.

Pulvermacher, S. C., Stauffer, L. T., & Stauffer, G. V. (2009). Role of the sRNA GcvB in regulation of cycA in Escherichia coli. *Microbiology (Reading), 155*(Pt 1), 106-114. doi:10.1099/mic.0.023598-0

Qi, H., Atkinson, I., Xiao, S., Choi, Y.-J., Tobimatsu, T., & Shane, B. (1999). Folylpoly-gamma-glutamate synthetase: generation of isozymes and the role in one carbon metabolism and antifolate cytotoxicity. *Advances in enzyme regulation, 39*, 263-273.

Ragsdale, S. W., & Pierce, E. (2008). Acetogenesis and the Wood–Ljungdahl pathway of CO2 fixation. *Biochimica et Biophysica Acta (BBA)-Proteins and Proteomics, 1784*(12), 1873-1898.

Rahman, M., Hasan, M. R., Oba, T., & Shimizu, K. (2006). Effect of rpoS gene knockout on the metabolism of Escherichia coli during exponential growth phase and early stationary phase based on gene expressions, enzyme activities and intracellular metabolite concentrations. *Biotechnology and Bioengineering, 94*(3), 585-595.

Rahmanian, M., Claus, D. R., & Oxender, D. L. (1973). Multiplicity of Leucine Transport Systems in Escherichia coli K-12. *Journal of bacteriology, 116*(3), 1258-1266. doi:doi:10.1128/jb.116.3.1258-1266.1973

Rashid, F. Z. M., Chaurasiya, K. R., Brocken, D. J., & Dame, R. T. (2021). Regulation of Provwx Transcription By Local Chromatin Remodelling. *Biophysical Journal, 120*(3), 317a.

Rashid, S., Pho, K. B., Mesbahi, H., & MacNeil, L. T. (2020). Nutrient sensing and response drive developmental progression in Caenorhabditis elegans. *Bioessays, 42*(3), 1900194.

Ratzke, C., & Gore, J. (2018). Modifying and reacting to the environmental pH can drive bacterial interactions. *PLoS biology, 16*(3), e2004248.

Reddy, K. C., Hunter, R. C., Bhatla, N., Newman, D. K., & Kim, D. H. (2011). Caenorhabditis elegans NPR-1–mediated behaviors are suppressed in the presence of mucoid bacteria. *Proceedings of the National Academy of Sciences, 108*(31), 12887-12892.

Reinke, V. (2002). Functional exploration of the C. elegans genome using DNA microarrays. *nature genetics, 32*(4), 541-546.

Reitzer, L. (2003). Nitrogen assimilation and global regulation in Escherichia coli. *Annu Rev Microbiol, 57*, 155-176. doi:10.1146/annurev.micro.57.030502.090820

Reitzer, L. (2004). Biosynthesis of glutamate, aspartate, asparagine, L-alanine, and D-alanine. *EcoSal Plus, 1*(1).

Rera, M., Azizi, M. J., & Walker, D. W. (2013). Organ-specific mediation of lifespan extension: more than a gut feeling? *Ageing research reviews, 12*(1), 436-444.

Riccio, P., & Rossano, R. (2020). The human gut microbiota is neither an organ nor a commensal. *FEBS letters, 594*(20), 3262-3271.

Richard, H., & Foster, J. W. (2004). Escherichia coli glutamate- and arginine-dependent acid resistance systems increase internal pH and reverse transmembrane potential. *J Bacteriol, 186*(18), 6032-6041. doi:10.1128/jb.186.18.6032-6041.2004

Richard, H. T., & Foster, J. W. (2003). Acid resistance in Escherichia coli. *Adv Appl Microbiol, 52*, 167-186. doi:10.1016/s0065-2164(03)01007-4

Richards, T. A., Dacks, J. B., Campbell, S. A., Blanchard, J. L., Foster, P. G., McLeod, R., & Roberts, C. W. (2006). Evolutionary origins of the eukaryotic shikimate pathway: gene fusions, horizontal gene transfer, and endosymbiotic replacements. *Eukaryot Cell, 5*(9), 1517-1531. doi:10.1128/ec.00106-06

Richey, D. P., & Brown, G. M. (1969). The Biosynthesis of Folic Acid: IX. Purification and properties of the enzymes required for the formation of dihydropteroic acid. *Journal of biological chemistry, 244*(6), 1582-1592.

Richmond, C. S., Glasner, J. D., Mau, R., Jin, H., & Blattner, F. R. (1999). Genome-wide expression profiling in Escherichia coli K-12. *Nucleic acids research, 27*(19), 3821-3835.

Riley M, C. R., Fulcher C,. (2007). Escherichia coli K-12 substr. MG1655 Pathway: glycine cleavage. Retrieved from https://ecocyc.org/ECOLI/NEW-IMAGE?type=PATHWAY&object=GLYCLEAV-PWY

Rinninella, E., Raoul, P., Cintoni, M., Franceschi, F., Miggiano, G. A. D., Gasbarrini, A., & Mele, M. C. (2019). What is the Healthy Gut Microbiota Composition? A Changing Ecosystem across Age, Environment, Diet, and Diseases. *Microorganisms, 7*(1). doi:10.3390/microorganisms7010014

Robbins, J. C., & Oxender, D. L. (1973). Transport systems for alanine, serine, and glycine in Escherichia coli K-12. *J Bacteriol, 116*(1), 12-18. doi:10.1128/jb.116.1.12-18.1973

Rosen, B. P. (1971). Basic amino acid transport in Escherichia coli. *Journal of biological chemistry, 246*(11), 3653-3662.

Ross, A. C., Caballero, B., Cousins, R. J., Tucker, K. L., & Ziegler, T. R. (2012). *Modern nutrition in health and disease*: Lippincott Williams & Wilkins.

Rossi, M., Amaretti, A., & Raimondi, S. (2011). Folate production by probiotic bacteria. *Nutrients, 3*(1), 118-134.

Round, J. L., & Mazmanian, S. K. (2009). The gut microbiota shapes intestinal immune responses during health and disease. *Nature reviews immunology, 9*(5), 313-323.

Roux, B., & Walsh, C. T. (1992). p-aminobenzoate synthesis in Escherichia coli: kinetic and mechanistic characterization of the amidotransferase PabA. *Biochemistry, 31*(30), 6904-6910.

Ruckenstuhl, C., Netzberger, C., Entfellner, I., Carmona-Gutierrez, D., Kickenweiz, T., Stekovic, S., . . . Sorgo, A. G. (2014). Lifespan extension by methionine restriction requires autophagy-dependent vacuolar acidification. *PLoS genetics, 10*(5), e1004347.

Said, H. M., Chatterjee, N., Haq, R. U., Subramanian, V. S., Ortiz, A., Matherly, L. H., . . . Rubin, S. A. (2000). Adaptive regulation of intestinal folate uptake: effect of dietary folate deficiency. *American Journal of Physiology-Cell Physiology, 279*(6), C1889-C1895. doi:10.1152/ajpcell.2000.279.6.C1889

Saiki, R., Lunceford, A. L., Bixler, T., Dang, P., Lee, W., Furukawa, S., . . . Clarke, C. F. (2008). Altered bacterial metabolism, not coenzyme Q content, is responsible for the lifespan extension in Caenorhabditis elegans fed an Escherichia coli diet lacking coenzyme Q. *Aging cell, 7*(3), 291-304.

Salazar, N., González, S., Nogacka, A. M., Rios-Covián, D., Arboleya, S., Gueimonde, M., & de Los Reyes-Gavilán, C. G. (2020). Microbiome: Effects of ageing and diet. *Current issues in molecular biology, 36*(1), 33-62.

Samuel, B. S., Rowedder, H., Braendle, C., Félix, M.-A., & Ruvkun, G. (2016). Caenorhabditis elegans responses to bacteria from its natural habitats. *Proceedings of the National Academy of Sciences, 113*(27), E3941-E3949.

Sánchez-Blanco, A., Rodríguez-Matellán, A., González-Paramás, A., González-Manzano, S., Kim, S. K., & Mollinedo, F. (2016). Dietary and microbiome factors determine longevity in Caenorhabditis elegans. *Aging (Albany NY), 8*(7), 1513.

Sawers, G. (1998). The anaerobic degradation of L-serine and L-threonine in enterobacteria: networks of pathways and regulatory signals. *Arch Microbiol, 171*(1), 1-5. doi:10.1007/s002030050670

Schellenberg, G. D., & Furlong, C. E. (1977). Resolution of the multiplicity of the glutamate and aspartate transport systems of Escherichia coli. *J Biol Chem, 252*(24), 9055-9064.

Schembri, M. A., Kjærgaard, K., & Klemm, P. (2003). Global gene expression in Escherichia coli biofilms. *Molecular microbiology, 48*(1), 253-267.

Schilling, B., Basisty, N., Christensen, D. G., Sorensen, D., Orr, J. S., Wolfe, A. J., & Rao, C. V. (2019). Global lysine acetylation in Escherichia coli results from growth conditions that favor acetate fermentation. *Journal of bacteriology, 201*(9), e00768-00718.

Schirch, V., & Strong, W. B. (1989). Interaction of folylpolyglutamates with enzymes in one-carbon metabolism. *Archives of biochemistry and biophysics, 269*(2), 371-380.

Schneider, B. L., Kiupakis, A. K., & Reitzer, L. J. (1998). Arginine Catabolism and the Arginine Succinyltransferase Pathway in Escherichia coli. *Journal of bacteriology, 180*(16), 4278-4286. doi:doi:10.1128/JB.180.16.4278-4286.1998

Schubert, C., Winter, M., Ebert-Jung, A., Kierszniowska, S., Nagel-Wolfrum, K., Schramm, T., . . . Unden, G. (2021). C4-dicarboxylates and l-aspartate utilization by Escherichia coli K-12 in the mouse intestine: l-aspartate as a major substrate for fumarate respiration and as a nitrogen source. *Environ Microbiol, 23*(5), 2564-2577. doi:10.1111/1462-2920.15478

Schug, Z. T. (2018). Formaldehyde Detoxification Creates a New Wheel for the Folate-Driven One-Carbon "Bi"-cycle. *Biochemistry, 57*(6), 889-890. doi:10.1021/acs.biochem.7b01261

Scott, K. P., Martin, J. C., Campbell, G., Mayer, C.-D., & Flint, H. J. (2006). Whole-genome transcription profiling reveals genes up-regulated by growth on fucose in the human gut bacterium "Roseburia inulinivorans". *Journal of bacteriology, 188*(12), 4340-4349.

Scozzafava, A., Owa, T., Mastrolorenzo, A., & Supuran, C. T. (2003). Anticancer and antiviral sulfonamides. *Current medicinal chemistry, 10*(11), 925-953.

Sébédio, J.-L. (2017). Metabolomics, nutrition, and potential biomarkers of food quality, intake, and health status. In *Advances in Food and Nutrition Research* (Vol. 82, pp. 83-116): Elsevier.

Selvarasu, S., Ow, D. S., Lee, S. Y., Lee, M. M., Oh, S. K., Karimi, I. A., & Lee, D. Y. (2009). Characterizing Escherichia coli DH5alpha growth and metabolism in a complex medium using genome-scale flux analysis. *Biotechnol Bioeng, 102*(3), 923-934. doi:10.1002/bit.22119

Sender, R., Fuchs, S., & Milo, R. (2016). Are we really vastly outnumbered? Revisiting the ratio of bacterial to host cells in humans. *Cell, 164*(3), 337-340.

Seydel, J. K. (1968). Sulfonamides, Structure-Activity Relationship, and Mode of Action: Structural Problems of the Antibacterial Action of 4-Aminobenzoic Acid (PABA) Antagonists. *Journal of Pharmaceutical Sciences, 57*(9), 1455-1478. doi:https://doi.org/10.1002/jps.2600570902

Shane, B., & Stokstad, E. (1985). Vitamin B12-folate interrelationships. *Annual review of nutrition, 5*, 115-141.

Shapiro, B., & Stadtman, E. (1970). The regulation of glutamine synthesis in microorganisms. *Annual Reviews in Microbiology, 24*(1), 501-524.

Shapiro, J. A. (1987). Organization of developing Escherichia coli colonies viewed by scanning electron microscopy. *Journal of bacteriology, 169*(1), 142-156. doi:doi:10.1128/jb.169.1.142-156.1987

Shapiro, J. A. (1998). Thinking about bacterial populations as multicellular organisms. *Annual Review of Microbiology, 52*(1), 81-104.

Shetty, S., & Varshney, U. (2021). Regulation of translation by one-carbon metabolism in bacteria and eukaryotic organelles. *Journal of biological chemistry, 296*.

Shin, M.-G., Lee, J.-W., Han, J.-S., Lee, B., Jeong, J.-H., Park, S.-H., . . . Kim, S.-Y. (2020). Bacteria-derived metabolite, methylglyoxal, modulates the longevity of C. elegans through TORC2/SGK-1/DAF-16 signaling. *Proceedings of the National Academy of Sciences, 117*(29), 17142-17150.

Shoeman, R., Redfield, B., Coleman, T., Greene, R. C., Smith, A. A., Brot, N., & Weissbach, H. (1985). Regulation of methionine synthesis in <em>Escherichia coli</em>: Effect of <em>metJ</em> gene product and <em>S</em>-adenosylmethionine on the expression of the <em>metF</em> gene. *Proceedings of the National Academy of Sciences, 82*(11), 3601. doi:10.1073/pnas.82.11.3601

Silva, Y. P., Bernardi, A., & Frozza, R. L. (2020). The Role of Short-Chain Fatty Acids From Gut Microbiota in Gut-Brain Communication. *Frontiers in Endocrinology, 11*(25). doi:10.3389/fendo.2020.00025

Simanshu, D. K., Chittori, S., Savithri, H. S., & Murthy, M. R. (2007). Structure and function of enzymes involved in the anaerobic degradation of L-threonine to propionate. *J Biosci, 32*(6), 1195-1206. doi:10.1007/s12038-007-0121-1

Smart, K. F., Aggio, R. B., Van Houtte, J. R., & Villas-Bôas, S. G. (2010). Analytical platform for metabolome analysis of microbial cells using methyl chloroformate derivatization followed by gas chromatography–mass spectrometry. *Nature protocols, 5*(10), 1709-1729.

Smith, E. A., & Macfarlane, G. (1997). Dissimilatory amino acid metabolism in human colonic bacteria. *Anaerobe, 3*(5), 327-337.

Smith, E. A., & Macfarlane, G. T. (1996). Enumeration of human colonic bacteria producing phenolic and indolic compounds: effects of pH, carbohydrate availability and retention time on dissimilatory aromatic amino acid metabolism. *Journal of Applied Bacteriology, 81*(3), 288-302.

Smith, E. A., & Macfarlane, G. T. (1997). Dissimilatory Amino Acid Metabolism in Human Colonic Bacteria. *Anaerobe, 3*(5), 327-337. doi:https://doi.org/10.1006/anae.1997.0121

Smith, E. D., Kaeberlein, T. L., Lydum, B. T., Sager, J., Welton, K. L., Kennedy, B. K., & Kaeberlein, M. (2008). Age-and calorie-independent life span extension from dietary restriction by bacterial deprivation in Caenorhabditis elegans. *BMC developmental biology, 8*(1), 1-13.

Soenen, S., Rayner, C. K., Jones, K. L., & Horowitz, M. (2016). The ageing gastrointestinal tract. *Curr Opin Clin Nutr Metab Care, 19*(1), 12-18. doi:10.1097/mco.0000000000000238

Sommer, F., & Bäckhed, F. (2013). The gut microbiota—masters of host development and physiology. *Nature Reviews Microbiology, 11*(4), 227-238.

Son, H. G., Altintas, O., Kim, E. J. E., Kwon, S., & Lee, S. J. V. (2019). Age-dependent changes and biomarkers of aging in Caenorhabditis elegans. *Aging cell, 18*(2), e12853.

Soto, M., Herzog, C., Pacheco, J. A., Fujisaka, S., Bullock, K., Clish, C. B., & Kahn, C. R. (2018). Gut microbiota modulate neurobehavior through changes in brain insulin sensitivity and metabolism. *Molecular psychiatry, 23*(12), 2287-2301.

Soukas, A. A., Kane, E. A., Carr, C. E., Melo, J. A., & Ruvkun, G. (2009). Rictor/TORC2 regulates fat metabolism, feeding, growth, and life span in Caenorhabditis elegans. *Genes & development, 23*(4), 496-511.

Sourjik, V., & Wingreen, N. S. (2012). Responding to chemical gradients: bacterial chemotaxis. *Current opinion in cell biology, 24*(2), 262-268.

Stafford, G. P., Ogi, T., & Hughes, C. (2005). Binding and transcriptional activation of non-flagellar genes by the Escherichia coli flagellar master regulator FlhD2C2. *Microbiology (Reading, England), 151*(Pt 6), 1779.

Stauffer, G. (1996). Biosynthesis of serine, glycine, and one-carbon units. *Escherichia coli and Salmonella: cellular and molecular biology, 2nd ed. ASM Press, Washington, DC*, 506-513.

Stauffer, G. V., & Stewart, V. (2004). Regulation of Serine, Glycine, and One-Carbon Biosynthesis. *EcoSal Plus, 1*(1). doi:doi:10.1128/ecosalplus.3.6.1.2

Stewart, W. W. (1981). Lucifer dyes—highly fluorescent dyes for biological tracing. *Nature, 292*(5818), 17-21.

Stiernagle, T. (1999). Maintenance of C. elegans.

Stokstad, E., & Jukes, T. (1987). Sulfonamides and folic acid antagonists: a historical review. *The Journal of nutrition, 117*(7), 1335-1341.

Stranix, B. R., Sauvé, G., Bouzide, A., Coté, A., Sévigny, G., Yelle, J., & Perron, V. (2004). Lysine sulfonamides as novel HIV-protease inhibitors: Nε-disubstituted ureas. *Bioorganic & medicinal chemistry letters, 14*(15), 3971-3974.

Strickland, K. C., Krupenko, N. I., & Krupenko, S. A. (2013). Molecular mechanisms underlying the potentially adverse effects of folate. *Clinical chemistry and laboratory medicine, 51*(3), 607-616.

Stubbendieck, R. M., Vargas-Bautista, C., & Straight, P. D. (2016). Bacterial communities: interactions to scale. *Frontiers in microbiology, 7*, 1234.

Studier, F. W. (2005). Protein production by auto-induction in high-density shaking cultures. *Protein expression and purification, 41*(1), 207-234.

Suh, S.-J., Silo-Suh, L., Woods, D. E., Hassett, D. J., West, S. E., & Ohman, D. E. (1999). Effect of rpoS mutation on the stress response and expression of virulence factors in Pseudomonas aeruginosa. *Journal of bacteriology, 181*(13), 3890-3897.

Sun, L., Hu, C., Zheng, C., Qian, Y., Liang, Q., Lv, Z., . . . Zhang, Z. (2015). FOXO3 variants are beneficial for longevity in Southern Chinese living in the Red River Basin: A case-control study and meta-analysis. *Scientific Reports, 5*(1), 1-7.

Sun, X., Chen, W.-D., & Wang, Y.-D. (2017). DAF-16/FOXO Transcription Factor in Aging and Longevity. *Frontiers in Pharmacology, 8*(548). doi:10.3389/fphar.2017.00548

Svetlitchnaia, T., Svetlitchnyi, V., Meyer, O., & Dobbek, H. (2006). Structural insights into methyltransfer reactions of a corrinoid iron-sulfur protein involved in acetyl-CoA synthesis. *Proc Natl Acad Sci U S A, 103*(39), 14331-14336. doi:10.1073/pnas.0601420103

Swedberg, G., Fermér, C., & Sköld, O. (1993). Point mutations in the dihydropteroate synthase gene causing sulfonamide resistance. In *Chemistry and Biology of Pteridines and Folates* (pp. 555-558): Springer.

Tan, J., McKenzie, C., Potamitis, M., Thorburn, A. N., Mackay, C. R., & Macia, L. (2014). The role of short-chain fatty acids in health and disease. *Advances in immunology, 121*, 91-119.

Tang, W. W., Bäckhed, F., Landmesser, U., & Hazen, S. L. (2019). Intestinal microbiota in cardiovascular health and disease: JACC state-of-the-art review. *Journal of the American College of Cardiology, 73*(16), 2089-2105.

Taylor, P. J. (2005). Matrix effects: the Achilles heel of quantitative high-performance liquid chromatography-electrospray-tandem mass spectrometry. *Clin Biochem, 38*(4), 328-334. doi:10.1016/j.clinbiochem.2004.11.007

Taymaz-Nikerel, H., De Mey, M., Ras, C., ten Pierick, A., Seifar, R. M., Van Dam, J. C., . . . van Gulik, W. M. (2009). Development and application of a differential method for reliable metabolome analysis in Escherichia coli. *Analytical biochemistry, 386*(1), 9-19.

Teng, X., & Xiao, H. (2009). Perspectives of DNA microarray and next-generation DNA sequencing technologies. *Science in China Series C: Life Sciences, 52*(1), 7-16.

Thornalley, P. J. (1996). Pharmacology of methylglyoxal: formation, modification of proteins and nucleic acids, and enzymatic detoxification-a role in pathogenesis and antiproliferative chemotherapy. *General Pharmacology: The Vascular System, 27*(4), 565-573.

Thursby, E., & Juge, N. (2017). Introduction to the human gut microbiota. *Biochemical Journal, 474*(11), 1823-1836.

Tissenbaum, H. A. (2012). Genetics, life span, health span, and the aging process in Caenorhabditis elegans. *Journals of Gerontology Series A: Biomedical Sciences and Medical Sciences, 67*(5), 503-510.

Traxler, M. F., Summers, S. M., Nguyen, H. T., Zacharia, V. M., Hightower, G. A., Smith, J. T., & Conway, T. (2008). The global, ppGpp-mediated stringent response to amino acid starvation in Escherichia coli. *Molecular microbiology, 68*(5), 1128-1148.

Troemel, E. R., Félix, M.-A., Whiteman, N. K., Barrière, A., & Ausubel, F. M. (2008). Microsporidia are natural intracellular parasites of the nematode Caenorhabditis elegans. *PLoS biology, 6*(12), e309.

Turnbaugh, P. J., Ley, R. E., Hamady, M., Fraser-Liggett, C. M., Knight, R., & Gordon, J. I. (2007). The human microbiome project. *Nature, 449*(7164), 804-810.

Turner, F. B., Andreassi, J. L., Ferguson, J., Titus, S., Tse, A., Taylor, S. M., & Moran, R. G. (1999). Tissue-specific expression of functional isoforms of mouse folylpoly-γ-glutamate synthetase: a basis for targeting folate antimetabolites. *Cancer research, 59*(24), 6074-6079.

Tzin, V., Galili, G., & Aharoni, A. (2012). Shikimate pathway and aromatic amino acid biosynthesis. *eLS*.

Umansky, C., Morellato, A., Scheidegger, M., Rieckher, M., Martinefski, M. R., Fernandez, G. A., . . . Reingruber, H. (2020). Endogenous formaldehyde scavenges cellular glutathione resulting in cytotoxic redox disruption. *Biorxiv*.

Umansky, C., Morellato, A. E., Rieckher, M., Scheidegger, M. A., Martinefski, M. R., Fernández, G. A., . . . Bollini, M. (2022). Endogenous formaldehyde scavenges cellular glutathione resulting in redox disruption and cytotoxicity. *Nature communications, 13*(1), 1-15.

Unger, M. M., Spiegel, J., Dillmann, K.-U., Grundmann, D., Philippeit, H., Bürmann, J., . . . Schäfer, K.-H. (2016). Short chain fatty acids and gut microbiota differ between patients with Parkinson's disease and age-matched controls. *Parkinsonism & related disorders, 32*, 66-72.

Uno, M., & Nishida, E. (2016). Lifespan-regulating genes in C. elegans. *npj Aging and Mechanisms of Disease, 2*(1), 1-8.

Urbanowski, M. L., Stauffer, L. T., & Stauffer, G. V. (2000). The gcvB gene encodes a small untranslated RNA involved in expression of the dipeptide and oligopeptide transport systems in Escherichia coli. *Molecular microbiology, 37*(4), 856-868.

Vallianou, N., Stratigou, T., Christodoulatos, G. S., & Dalamaga, M. (2019). Understanding the Role of the Gut Microbiome and Microbial Metabolites in

Obesity and Obesity-Associated Metabolic Disorders: Current Evidence and Perspectives. *Current Obesity Reports, 8*(3), 317-332. doi:10.1007/s13679-019-00352-2

Van Gulik, W. M. (2010). Fast sampling for quantitative microbial metabolomics. *Current opinion in biotechnology, 21*(1), 27-34.

Vedantam, G., Guay, G. G., Austria, N. E., Doktor, S. Z., & Nichols, B. P. (1998). Characterization of mutations contributing to sulfathiazole resistance in Escherichia coli. *Antimicrobial agents and chemotherapy, 42*(1), 88-93.

Vernocchi, P., Del Chierico, F., & Putignani, L. (2016). Gut microbiota profiling: metabolomics based approach to unravel compounds affecting human health. *Frontiers in microbiology, 7*, 1144.

Vijayakumar, S. R., Kirchhof, M. G., Patten, C. L., & Schellhorn, H. E. (2004). RpoS-regulated genes of Escherichia coli identified by random lacZ fusion mutagenesis. *Journal of bacteriology, 186*(24), 8499-8507.

Villarino, A., Rager, M. N., Grimont, P. A., & Bouvet, O. M. (2003). Are UV-induced nonculturable Escherichia coli K-12 cells alive or dead? *European journal of biochemistry, 270*(12), 2689-2695.

Virk, B. (2013). *Excessive folate synthesis in Escherichia coli and its influence on Caenorhabditis ageing.* (PhD). Durham University,

Virk, B., Correia, G., Dixon, D. P., Feyst, I., Jia, J., Oberleitner, N., . . . Weinkove, D. (2012). Excessive folate synthesis limits lifespan in the C. elegans: E. coliaging model. *BMC Biology, 10*(1), 67. doi:10.1186/1741-7007-10-67

Virk, B., Jia, J., Maynard, C. A., Raimundo, A., Lefebvre, J., Richards, S. A., . . . Weinkove, D. (2016). Folate Acts in E. coli to Accelerate C. elegans Aging Independently of Bacterial Biosynthesis. *Cell Rep, 14*(7), 1611-1620. doi:10.1016/j.celrep.2016.01.051

Walker, A. C., Bhargava, R., Vaziriyan-Sani, A. S., Pourciau, C., Donahue, E. T., Dove, A. S., . . . Czyż, D. M. (2021). Colonization of the Caenorhabditis elegans gut with human enteric bacterial pathogens leads to proteostasis disruption that is rescued by butyrate. *PLoS pathogens, 17*(5), e1009510.

Walker, G., Houthoofd, K., Vanfleteren, J. R., & Gems, D. (2005). Dietary restriction in C. elegans: from rate-of-living effects to nutrient sensing pathways. *Mechanisms of ageing and development, 126*(9), 929-937.

Walsh, C. T., Liu, J., Rusnak, F., & Sakaitani, M. (1990). Molecular studies on enzymes in chorismate metabolism and the enterobactin biosynthetic pathway. *Chemical Reviews, 90*(7), 1105-1129.

Wang, J., & Kim, S. K. (2003). Global analysis of dauer gene expression in Caenorhabditis elegans.

Wang, X., Xie, Y., Gao, P., Zhang, S., Tan, H., Yang, F., . . . Xu, G. (2014). A metabolomics-based method for studying the effect of yfcC gene in Escherichia coli on metabolism. *Analytical biochemistry, 451*, 48-55.

Wargel, R. J., Hadur, C. A., & Neuhaus, F. C. (1971). Mechanism of D-cycloserine action: transport mutants for D-alanine, D-cycloserine, and glycine. *J Bacteriol, 105*(3), 1028-1035. doi:10.1128/jb.105.3.1028-1035.1971

Wargel, R. J., Shadur, C. A., & Neuhaus, F. C. (1971). Mechanism of D-cycloserine action: transport mutants for D-alanine, D-cycloserine, and glycine. *Journal of bacteriology, 105*(3), 1028-1035.

Waterman, S. R., & Small, P. (2003). The glutamate-dependent acid resistance system of Escherichia coli and Shigella flexneri is inhibited in vitro by L-trans-pyrrolidine-2, 4-dicarboxylic acid. *FEMS Microbiology Letters, 224*(1), 119-125.

Weber, H., Polen, T., Heuveling, J., Wendisch, V. F., & Hengge, R. (2005). Genome-wide analysis of the general stress response network in Escherichia coli: σS-dependent genes, promoters, and sigma factor selectivity. *Journal of bacteriology, 187*(5), 1591-1603.

Wei, Y. B., Melas, P. A., Wegener, G., Mathé, A. A., & Lavebratt, C. (2015). Antidepressant-like effect of sodium butyrate is associated with an increase in TET1 and in 5-hydroxymethylation levels in the Bdnf gene. *International Journal of Neuropsychopharmacology, 18*(2).

Weinkove, D., & Goljanek-Whysall, K. (2017). Why do we age? Insights into biology and evolution of ageing. *Biogerontology, 18*(6), 855-857. doi:10.1007/s10522-017-9734-4

Weissbach, H., & Brot, N. (1991). Regulation of methionine synthesis in Escherichia coli. *Molecular microbiology, 5*(7), 1593-1597.

Wendrich, T. M., Blaha, G., Wilson, D. N., Marahiel, M. A., & Nierhaus, K. H. (2002). Dissection of the mechanism for the stringent factor RelA. *Molecular cell, 10*(4), 779-788.

Whipp, M. J., & Pittard, A. J. (1977). Regulation of aromatic amino acid transport systems in Escherichia coli K-12. *Journal of bacteriology, 132*(2), 453-461. doi:doi:10.1128/jb.132.2.453-461.1977

Wilkinson, J. E., Burmeister, L., Brooks, S. V., Chan, C. C., Friedline, S., Harrison, D. E., . . . Wood, L. K. (2012). Rapamycin slows aging in mice. *Aging cell, 11*(4), 675-682.

Wilmanski, T., Diener, C., Rappaport, N., Patwardhan, S., Wiedrick, J., Lapidus, J., . . . Robinson, M. (2021). Gut microbiome pattern reflects healthy ageing and predicts survival in humans. *Nature metabolism, 3*(2), 274-286.

Wilmes, L., Collins, J. M., O'Riordan, K. J., O'Mahony, S. M., Cryan, J. F., & Clarke, G. (2021). Of bowels, brain and behavior: A role for the gut microbiota in psychiatric comorbidities in irritable bowel syndrome. *Neurogastroenterology & Motility, 33*(3), e14095.

Winder, C. L., Dunn, W. B., Schuler, S., Broadhurst, D., Jarvis, R., Stephens, G. M., & Goodacre, R. (2008). Global metabolic profiling of Escherichia coli cultures: an evaluation of methods for quenching and extraction of intracellular metabolites. *Analytical Chemistry, 80*(8), 2939-2948.

Windey, K., De Preter, V., & Verbeke, K. (2012). Relevance of protein fermentation to gut health. *Molecular nutrition & food research, 56*(1), 184-196.

Wolfe, A. J. (2005). The acetate switch. *Microbiology and molecular biology reviews, 69*(1), 12-50.

Wolfe, A. J., & Berg, H. C. (1989). Migration of bacteria in semisolid agar. *Proceedings of the National Academy of Sciences, 86*(18), 6973-6977.

Wolkow, C. A., Kimura, K. D., Lee, M.-S., & Ruvkun, G. (2000). Regulation of C. elegans life-span by insulinlike signaling in the nervous system. *Science, 290*(5489), 147-150.

Wood, J. M. (1988). Proline porters effect the utilization of proline as nutrient or osmoprotectant for bacteria. *The Journal of membrane biology, 106*(3), 183-202.

Wookey, P., Pittard, J., Forrest, S., & Davidson, B. (1984). Cloning of the tyrP gene and further characterization of the tyrosine-specific transport system in Escherichia coli K-12. *Journal of bacteriology, 160*(1), 169-174.

Wu, Z. A., & Wang, H. X. (2019). A Systematic Review of the Interaction Between Gut Microbiota and Host Health from a Symbiotic Perspective. *SN Comprehensive Clinical Medicine, 1*(3), 224-235. doi:10.1007/s42399-018-0033-4

Xu, S., Nilles, J. M., & Bowen Jr, K. H. (2003). Zwitterion formation in hydrated amino acid, dipole bound anions: how many water molecules are required? *The Journal of chemical physics, 119*(20), 10696-10701.

Yang, J. G., & Rees, D. C. (2015). The allosteric regulatory mechanism of the Escherichia coli MetNI methionine ATP binding cassette (ABC) transporter. *Journal of biological chemistry, 290*(14), 9135-9140.

Yang, Q., Liang, Q., Balakrishnan, B., Belobrajdic, D. P., Feng, Q.-J., & Zhang, W. (2020). Role of dietary nutrients in the modulation of gut microbiota: a narrative review. *Nutrients, 12*(2), 381.

Yang, Q., Wang, Y., Jia, A., Wang, Y., Bi, Y., & Liu, G. (2021). The crosstalk between gut bacteria and host immunity in intestinal inflammation. *Journal of Cellular Physiology, 236*(4), 2239-2254.

Yang, Y., Lowry, M., Xu, X., Escobedo, J. O., Sibrian-Vazquez, M., Wong, L., . . . Warner, I. M. (2008). Seminaphthofluorones are a family of water-soluble, low molecular weight, NIR-emitting fluorophores. *Proceedings of the National Academy of Sciences, 105*(26), 8829-8834.

Yildiz, F. H., & Schoolnik, G. K. (1998). Role of rpoS in stress survival and virulence of Vibrio cholerae. *Journal of bacteriology, 180*(4), 773-784.

Yilmaz, L. S., & Walhout, A. J. (2014). Worms, bacteria, and micronutrients: an elegant model of our diet. *Trends in Genetics, 30*(11), 496-503.

Zampieri, M., Hörl, M., Hotz, F., Müller, N. F., & Sauer, U. (2019). Regulatory mechanisms underlying coordination of amino acid and glucose catabolism in Escherichia coli. *Nature communications, 10*(1), 1-13.

Zečić, A., Dhondt, I., & Braeckman, B. P. (2019). The nutritional requirements of Caenorhabditis elegans. *Genes & Nutrition, 14*(1), 1-13.

Zhang, A., Sun, H., Wang, P., Han, Y., & Wang, X. (2012). Modern analytical techniques in metabolomics analysis. *Analyst, 137*(2), 293-300.

Zhang, J., Holdorf, A. D., & Walhout, A. J. (2017). C. elegans and its bacterial diet as a model for systems-level understanding of host–microbiota interactions. *Current opinion in biotechnology, 46*, 74-80.

Zhang, M., Li, Z., Gao, D., Gong, W., Gao, Y., & Zhang, C. (2020). Hydrogen extends Caenorhabditis elegans longevity by reducing reactive oxygen species. *PloS one, 15*(4), e0231972.

Zhang, X., El-Hajj, Z. W., & Newman, E. (2010). Deficiency in L-serine deaminase interferes with one-carbon metabolism and cell wall synthesis in Escherichia coli K-12. *Journal of bacteriology, 192*(20), 5515-5525. doi:10.1128/JB.00748-10

Zheng, Y., & Cantley, L. C. (2018). Toward a better understanding of folate metabolism in health and disease. *Journal of Experimental Medicine, 216*(2), 253-266. doi:10.1084/jem.20181965

Zhou, X., Fan, J., Li, N., Du, Z., Ying, H., Wu, J., . . . Bai, J. (2012). Solubility of l-phenylalanine in water and different binary mixtures from 288.15 to 318.15 K. *Fluid Phase Equilibria, 316*, 26-33.